RESEARCH ON ATMOSPHERIC ASSIMILATING CAPACITY AND AIR POLLUTION CONTROL SYSTEM OF INDUSTRIAL MUNICIPALITIES IN TAIWAN AREA

by

Chin-Yuan Chiang

RESEARCH ON ATMOSPHERIC ASSIMILATING CAPACITY AND AIR POLLUTION CONTROL SYSTEM OF INDUSTRIAL MUNICIPALITIES IN TAIWAN AREA

by

Chin-Yuan Chuang

PREFACE

(the point of view and goal of this study)

The economy and energy of Taiwan, R.O.C. were influenced by the worldwide economic recession and the search for substitute energy. The people of the country have realized that they must undertake a long struggle to lift the country to the level of developed countries. We should take good advantage of energy and keep on developing to bolster the country's economy. During development, it is easy to neglect the environmental problems. We would be regretful in the future if we don't immediately take up the necessary pollution control strategy to minimize the environmental damage to maintain the assimilating capacity.

The economic growth of Japan after the War has astonished the rest of the world. But her people continually berated the social benefit system. The cases of minamata disease, Itai-itai disease and Yokaichi city case brought about the attention of the people for there were so many injuries. The whole country then devoted expensive manpower and investment to fight for the environmental protection. After that, the problems were minimized. As for our situation of development and environment, they are far too analogous to that of Japan. For the time being, no matter how much is achieved in economic affairs, if some public disease should occur, do we have enough manpower and materials to fight it? This is the most serious implicit problem today.

This article will try to introduce the "assimilating capacity" concept which the leading countries such as Japan utilize day by day, and apply it to the developing country such as our country. We will try to find the best way to control pollution by air pollution study and by smoke flow spreading research.

(the structure of this study)

The author divides this study into two parts, the first part, including chapter 1 to Chapter 5, accumulates the technical base line data and the study of pollution phenomena in Taiwan. These results can provide the second part, from Chapter 6 to Chapter 7, with the data develop air pollution control strategies for maintaining assimilating capacity.

Summaries of each chapter are as following:
In Chapter 1, the author reviews the present status of pollution in Taiwan, refers to the leading countries with their trend in pollution issues and tries to settle the allowable capacity of industrial pollution for the inhabitants of industrial urban areas of the developing countries. In this Chapter I review also the present status of setting up a nation-wide air monitoring system for information, ranking of location, or some other purposes.

In Chapter 2, according to the climate records and other meteorological information in recent years, I analyze meteorolgical phenomena which govern the air pollution level of southern and northern Taiwan.

In Chapter 3, although the Analytic conclusion has already been made to go with the foregoing study of Kaohsiung area from 1975 to 1979 by the author, a comparison in made of the analogically simulant prediction results with the experimental results of tracer gas dispersion research at the same area also taken in 1981, in the hope it will help better understanding of that area.

In Chapter 4, I establish the predictive simulation of air pollution of that area with using the experimental results after modifying traditional methods such as Pasquill-Gifford chart and so on.

In Chapters 5 , I state the experimental studies for air pollution dispersion in northern Taiwan, such as Taipei area, to compare with pollution characteristics of the southern area.

Finally, in Chapter 6 and 7 I summarize the results above to set up an allowable assimilation capacity model of the Kaohsiung area, and suggest that the conclusions and the general rule of control strategy will be applied to the other areas.

CONTENTS

LIST OF TABLES

LIST OF FIGURES

PART I

ACCUMULATING THE TECHNICAL BASE LINE DATA AND THE STUDY OF POLLUTION PHENOMENA

CHAPTER 1 PRESENT STATUS OF AIR POLLUTION IN TAIWAN

1-1 The assimilating capacity of industrial cities in Taiwan area of the Republic of China

Taiwan is located within 119 to 122 degrees east longitude and 21 to 25 degrees north latitude. To the east and the south are the Pacific Ocean and the Philippines respectively. The island is separated by the Strait of Taiwan from the China mainland and is only 300 miles south-west of Okinawa.

The island is 377 Km long and about 142 Km wide. The total area measures 35,966 square kilometers in which two third belongs to the mountainous areas in the east.

The western part of the island is an open area of rich plains with very dense population (Fig. 1-1).

Taiwan belongs partly to sub-tropical and partly to tropical wheather with very warm temperature (an annual average temperature of 22 degrees centigrade) and high humidity which provide the island with abundent agricultural products. Natural resources are estimated as 226 milliontons in soft coal, 30 billion cubic meters in natural gas and 241 million cubic meters in forest production respectivly.

Economic development in Taiwan area has been so rapid and sustained during the past two decades (presently, there are about 50,000 registered factories on Taiwan) that it has become one of the most prosperous countries of the Far East. This unprecedented growth has brought with it not only the fruits of prosperity, but also

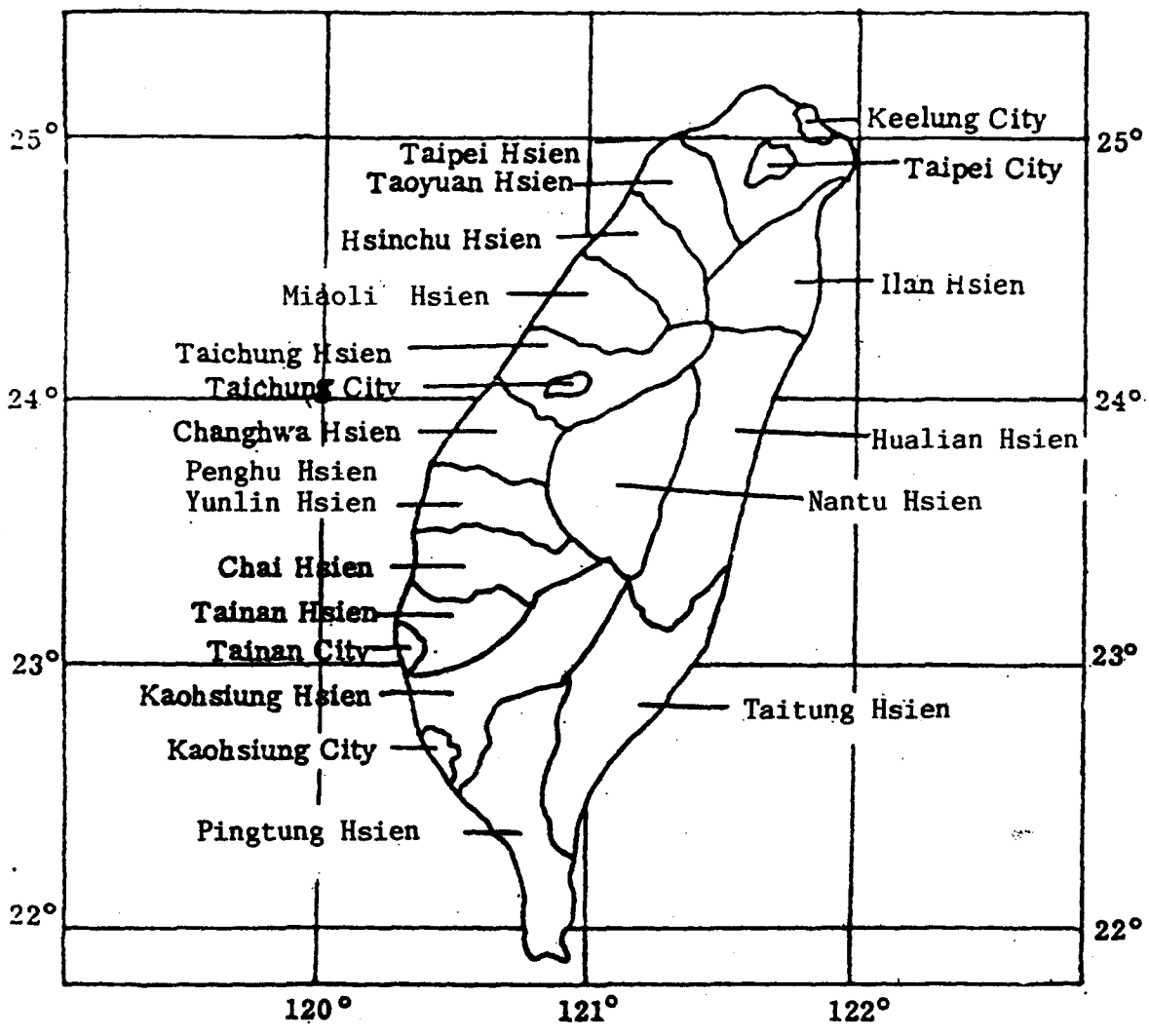

Fig. 1-1 The map of Taiwan, R.O.C.

the adverse effect of environmental pollution as a consequence of an increased population (currently, at a density of 486 persons per sq. km., the highest population density in the world), increased numbers of motor vehicles and burgeoning industrial complex with its myriad of noxious gases, particulate and liquid effluents known to be hazardous to human health. (1)

During the past two decades, there has been a steady increase in various chronic diseases, many of which have been linked with an increasingly fouled environment, notable among these are cancer, bronchial asthma and emphysema. (2)

In Fig. 1-2, the consumption of energy of Taiwan, R.O.C., has increased yearly and the environmental quality has decreased at the same time. There is some result from the "air pollution control act" which was announced by the President on May 23, 1975. But the environmental problems get more serious for the consumption of energy had reached an astonishing degree and the population of cities increasing day by day go with the other factors. (3)

In general, according to the Dec. 1, 1975 standard for environment air quality of the Taiwan area of R.O.C., it was specified that the pollution level of suspended particulates, sulfur oxides, nitrogen oxides, carbon monoxide and malodorous (offensive odor) should be limited below the allowed standard to maintain the envronment in a safe, healthy and confortable manner.(4) In our country, environmental protection is at a beginning stage. We are eager to establish a complete national system. Also, for environmental protection, we should work to prevent artificial pollution from seeping into the natural environment which causes damage in the

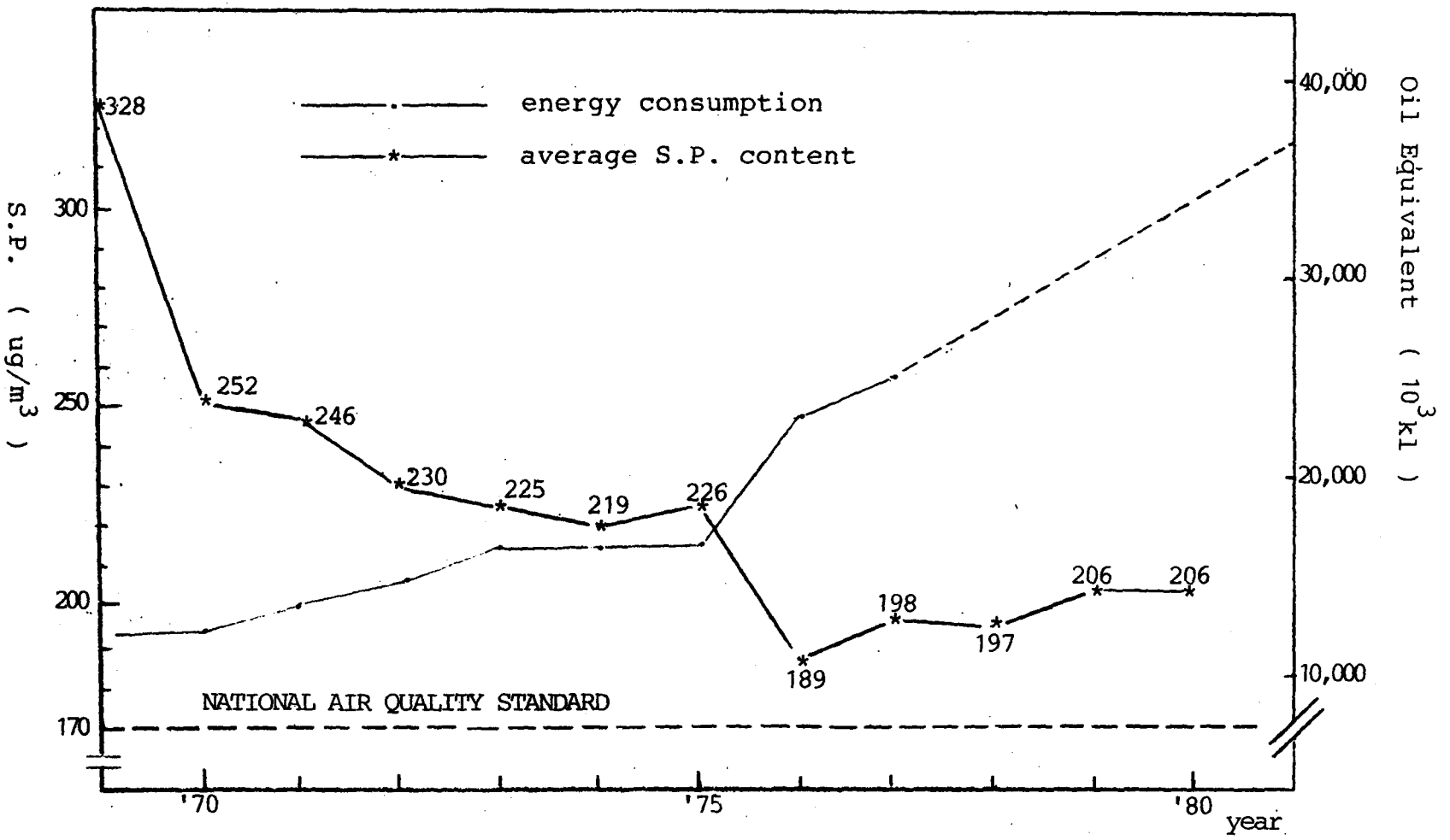

Figure 1-2 The relation between the energy consumption and the average suspended particles content.

social and economic affairs. The boundry includes human beings, animals, plants, soils and waters. We may set the maximum permissible quantity of pollutants, as the "assimilating capacity of the environment". This is a concept which has been taken by the leading countries of the world. The author will make further reference to this concept in later chapters.

Environmental assimilating capacity includes the following: the purification ability and boundry of nature, the degree of threat to mankind or animals plants and the threat of people's comfort. Generally speaking we cannot settle all the assimilating capacity under present technology. So we can only work on the serious items such as dustfalls, sulfur oxides and the nitrogen oxides. (5)

Environmental protection would be difficult if the total pollutants emission in an area is more than the purifying ability of nature. This is especially true for islands. Interior bay areas e.g. the littoral industrial parks in Taiwan, have the highest degree of danger.

In terms of "source emission concentration", the basic legal ideal is that we should be able to curb the majority of pollutors. But in practice, the control has not been satisfactory for those countries which took this route.(6) However, for island-marine climates such as Taiwan's, along with the high density of population and the high economic growth and development, the most important issues lying ahead are the balance of "developing of economics" and "protection of environment".(7) Table 1-1 shows the estimated value of air pollution for the Taiwan Area. Table 1-2 shows the comparison of pollutants and major emission source in 1978. (8)

Table 1-1 Estimated value of air pollution emitted from industry for the Taiwan Area. (1976)

Pollutants / Resources	particulates		sulphur oxides		nitrogen oxides		HC		CO	
	quantity (tons/year)	%	quantity (tons/year)	%	quantity (tons/year)	%	quantity (tons/year)	%	quantity (tons/year)	%
Thermal Generation of Electricity	1.94×10^4	29	4.9×10^5	73.4	5.4×10^4	66	2.6×10^3	8.1	3.66×10^3	6.3
petroleum treatment	2.3×10^3	3.4	4.37×10^4	6.5	6.59×10^3	8	2.23×10^4	69.5	6.66×10^3	11.6
Steel industry	3.4×10^3	5.1	3.05×10^4	4.5	3.33×10^3	4	4.53×10^2	1.4	3.87×10^2	0.7
Chemical industry	2.73×10^3	4.1	6.64×10^4	9.9	8.03×10^3	9.7	4.12×10^2	1.3	5.65×10^2	1
Cement industry	2.78×10^4	41.8	5.9×10^2	0.08	9.37×10^2	1.1	0	0	3.78×10^4	65.6
porcelain industry	4.55×10^3	6.8	1.33×10^4	1.9	3.24×10^3	3.9	2×10^3	6.2	7.79×10^3	13.5
Wood industry	4.09×10^3	6.1	1.7×10^3	0.2	2.49×10^3	3	4.5×10^2	1.4	4.55×10^2	0.8
others	2.28×10^3	3.4	2.24×10^4	3.3	3.23×10^3	3.9	3.78×10^3	11.8	3.43×10^2	0.6
Total	6.65×10^4	100	6.68×10^5	100	8.2×10^4	100	3.2×10^4	100	5.76×10^4	100

Table 1-2 The comparison of pollutants and major emission source in 1978
(Unit:metric tons/year)

Amounts \ Cities / Pollutants	Taipei Municipality				Kaohsiung Area			
	Amounts	%	Automobile	%	Amounts	%	Industry	%
Sulfur oxides	465	0.57	155	33.1	3.6×10^5	53.5	3.56×10^5	99.6
Particulates	1,513	1.84	460	30.4	5.1×10^4	7.6	4.0×10^4	79.6
Nitrogen Oxides	4,916	5.98	3,073	61.3	6.0×10^4	9.0	4.87×10^4	80.4
Hydrocarbons	17,616	21.44	16,541	88.8	4.4×10^4	6.5	2.55×10^4	58.2
Carbon Monoxides	57,645	70.17	55,109	95.6	1.6×10^5	23.4	4.05×10^4	26
Total	8.2×10^4	100	7.5×10^4	91.7	6.58×10^5	100	5.1×10^5	76.5

1-2 Air quality monitoring in Taiwan

In order to determine the severity of the pollution problem and to assess health-risk exposures to ambient toxic control strategy to maintain assimilating capacity of environment in future, it is first necessary to establish an air quality monitoring system around the whole island. Nowadays, most urban areas of Taiwan have only sporadic particulate and dustfall monitors, no more than 110. Table 1-3 shows the record of total suspended particulated during these recent years. But, a nationwide air monitoring program is in effect. Parameters to be measured at each recommended site included: SO2, CO, NO/NOx, O_3 THC, CO_2, TSP, Dustfall, and meteorolgoical data, including wind direction, wind speed, temperature and humidity. Based on the preliminary analyses and known network resource requirements, Table 1-4 indicates the recommended areas for monitoring sites and the surveillance purposes of each location.[11] In general, the monitoring data may also be used for resource allocation, ranking of location, enforcement of air quality standards, air quality trend analysis, public information and scientific research. First stage of the National Air Monitoring Network(NAMN) will consist of an Air Monitoring Center (AMC) and twenty remote monitoring stations as shown in Fig. 1-3.

AMC consists of a receiver component to handle date communication in the network. Each remote station will have a specific telephone number, and transmits the data over the phone lines in serial form. A processing component can process data from a receiver component and from external source tapes simultaneously without interruption owing to the control of real-time multi-processing operating system.

Table 1-3 The mean value of total suspended particulates ($\mu g/Nm^3$) in Taiwan area (9,10)

region \ year	1970	1971	1972	1973	1974	1975	1976	1977	1978	1979	1980
Taipei City	240	254	188	140	152	126	160	139	121	141	155
Taipei Hsien	230	272	281	280	283	272	233	250	292	284	284
Keelung City	229	216	247	221	199	236	184	187	185	228	249
Ilan Hsien	-	268	223	200	207	211	158	162	180	166	180
Taoyuan Hsien	-	180	195	201	168	187	165	195	164	182	164
Hsinchu Hsien	220	207	201	211	168	188	160	207	247	219	227
Taichung City	194	214	234	210	216	213	175	214	227	243	206
Changhwa hsien	234	251	246	251	224	246	208	218	278	282	231
Chai Hsien	269	256.	206	235	229	246	197	176	174	167	191
Tainan City	-	237	225	201	215	226	180	177	185	223	257
Tainan Hsien	-	-	186	190	208	227	218	188	190	189	179
Kaohsiung City	314	335	307	281	268	262	213	276	264	305	332
Kaohsiung Hsien		260	217	241	280	306	225	135	257	274	268
Taichung Hsien				138	172	153	156	191	208	208	224
Miaoli Hsien						197	175	200	136	132	157
Hualian Hsien						227	181	135	153	186	185
Nantu Hsien						-	197	168	158	171	174
Yunlin Hsien						-	-	171	136	126	128
Taitung Hsien						-	-	-	110	148	141
Pingtung Hsien						-	-	-	-	180	183
Penghu Hsien						-	-	-	-	-	-
Average	252	246	230	225	219	226	189	198	197	206	**206**

Table 1-4. RECOMMENDED SITING AREAS (GENERAL)

No.	City	Purpose: Primary	Purpose: Secondary
	Taipei Area		
1.	Central	Urban	
2.	WNW (Sanchung)	Receptor	Urban
3.	SW (Panchiao)	Receptor	Urban
4.	S (Yungho)	Receptor	Urban
5.	E (Sungshan)	Industrial	Receptor
6.	E (Nankang)	Industrial	Receptor
	Kaoshiung		
7.	S (shipping area)	Industrial	
8.	NE (Nantzu)	Industrial	
9.	Central	Urban	
10.	Fengshan	Receptor	Urban
11.	Ping Tung	Receptor	Urban
12.	Tainan	Urban	
13.	Keelung	Urban	
14.	Chung Li	Urban	
15.	Hsin Chu	Urban	
16.	Taichung	Urban	
17.	Chang Hwa	Urban	
18.	Hwalien	Urban	
19.	Chiayi	Urban	
20.	Mobile Monitoring*		
	a) Tao Yuan		
	b) Ilan		
	c) Miaoli		
	d) Yun Lin		
	e) Feng Yuan		
	f) Wuchi		
	g) Kangshan		
	h) Chao Chou		

*Mobile monitoring van can be used for temporary sampling at each potential site to better determine existing air quality conditions for proper prioritizing of additional sites.

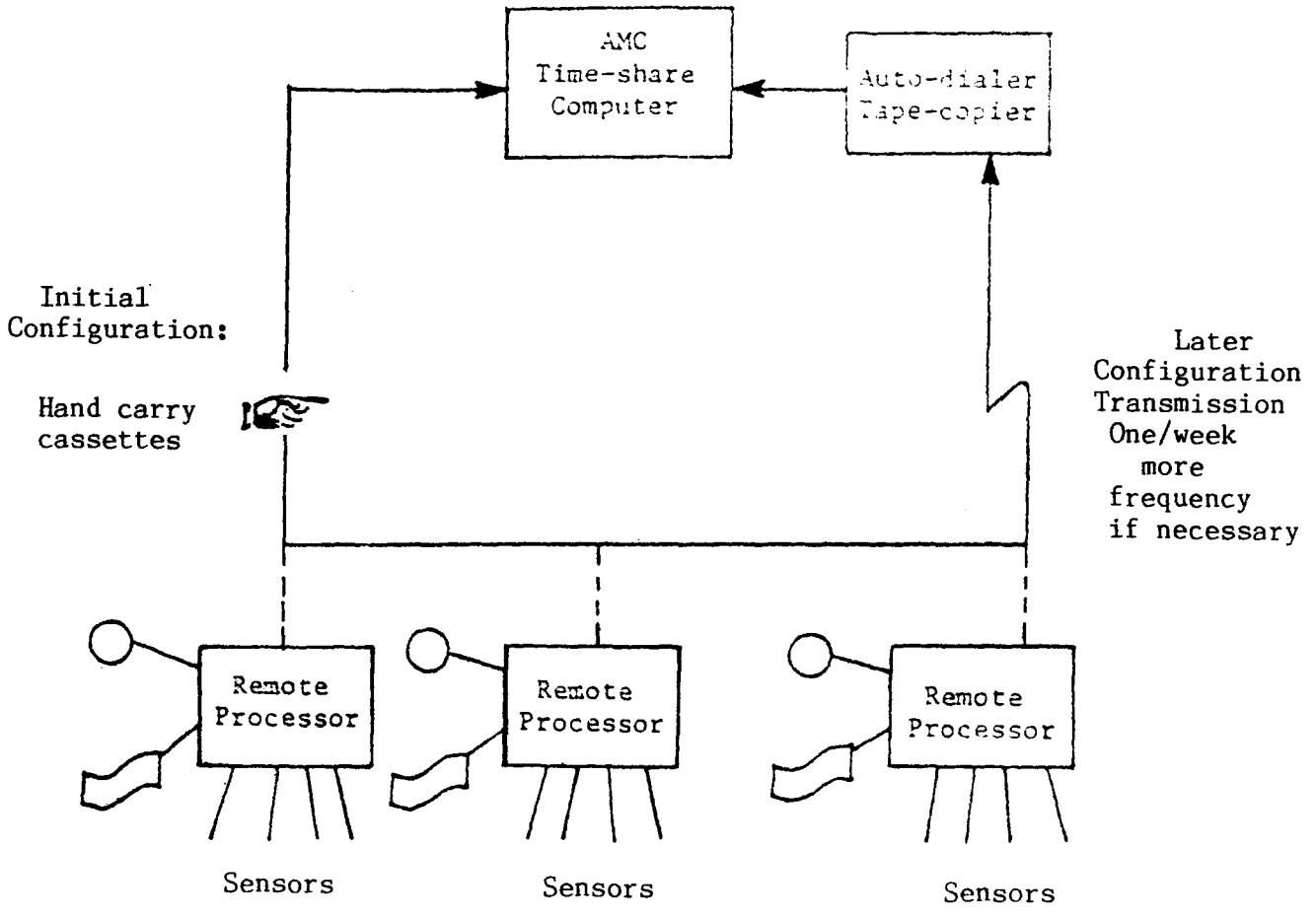

Fig. 1-3 Recommended configuration for the NAMN

CHAPTER 2 CHARACTERISTIC FEATURE OF THE METEOROLOGICAL PHENOMENA RELATING TO THE AIR POLLUTION IN TAIWAN

2-1 Meteorology in the southern area of Taiwan

2-1-1 General meteorological conditions

The climate or the Kaohsiung area belongs to the sub-tropical region. There are two seasons per year -- the dry season and the wet season. Due to the strong continental air mass, the Northeast wind crosses Taiwan from October to April. This period because of low precipitation is called the dry season. The period from May to September, because of high precipitation is called the rainy season. During May of each years, when the tropical ocean air mass develops, the direction of the wind changes. During the period from the middle part of May to the middle of June each year, the cold front of the rainy season lingers in the northern part of Taiwan. As the Kaohsiung area is located at the southern edge of the cold front, showers occur frequently. During the typhoon season, from July to September, 2-3 typhoons visit the Kaohsiung area. (12)

During the rainy season (summer) there are typhoons, thunder storms and showers which adversely effect the visibility. However this period does not usually last for very long. During the dry season (winter) the seasonal northeast wind prevails in Taiwan. As Kaohsiung is located on the north face of the Taiwan mountain range and is exposed to the wind, downwashes can easily occur there. Therefore, generally speaking, the visibility during the dry season is slightly worse than during the rainy season. At the same time there is a high occurance of heavy fog, 60% of which occurs in December, January and February and always

last for only a few days. 72% of the thunder storms occur in July, August and September. The thunder storms result in poor visibility and low cloud cover. However this type of weather does not last long and also helps to wash out the pollution from the air .

Advanced discussion of the meteorological conditions will be made in Chapter 3.

2-2 Characteristics of wind direction

During this season when the northeast wind prevails and typhoons are common, it is generally impossible to ascertain wind direction. However during the rainy season (spring and autumn) the wind system weakens and the daily wind direction can be determined.

As a result, refer to Table 2-1 and Table 2-2, the general considerations are as follows:

(1) Winter (December, January and February)
During the winter when the Taiwan area is under the influence of the continental cold air mass, a northeast wind (NNE-NNW) prevails (42.1%) in the Kaohsiung area. When the northeast wind weakens during the day due to the effect of the ocean wind, a west, northwest-west or northwest wind prevails. The occurance of calm winds is only 15.8%.

(2) Spring (March, April and May)
During the spring, the air pressure system and the northeast wind weakens and the west wind becomes strongs. Calm winds occur 18.8%, which is the highest percentage during the entire year. From May on the south wind system (SSE-SSW) grows strong gradually and the air mass changes to a tropical air mass.

(3) Summer (June, July and August)

The predominate wind system during the summer is formed by the tropical ocean air mass. During this season the south wind and west wind systems become strong. Because of this the rate of the appearance of all wind directions is more even.

(4) Autumn (September, October and November)

During autumn, the wind direction is the opposite of that in spring. The south wind system weakens and is replaced by the north wind system. Calm winds constitute 17.5%.

From Table 2-1-a we can understand in one year from May to September, the seabreeze time is longer than other months.

2-1-3 The characteristics of wind velocity

The variation of wind velocity daily in southern Taiwan is regular. As a rule the wind velocity reaches its high point around 2:00 PM, the average wind velocity is 5.3m/s. The average wind velocity during the night decreases to 2.3 m/s. After 6:00 AM the wind velocity becomes stronger and after 9:00 AM goes up drastically.

Table 2-1-a Period of sea-breeze occured during a day (1981-1982), in Kaohsiung littoral area.

hr. / NO. month	1	2	3	4	5	6	7	8	9	10	11	12	13	14	15	16	17	18	19	20	21	22	23	24
1981 Sept.	11	9	10	9	8	5	8	6	(11)	21	24	25	24	22	20	21	20	16	(13)	9	8	8	7	5
Oct.	0	1	1	2	1	3	0	1	(12)	25	29	30	30	28	29	30	25	17	(14)	10	6	5	6	1
Nov.	0	2	1	0	0	0	1	1	3	(18)	21	21	22	21	23	21	19	(13)	6	9	4	1	0	0
Dec.	0	2	1	0	0	1	0	0	1	3	(12)	18	20	20	23	25	18	(12)	6	2	2	1	0	0
1982 Jan.	0	1	0	0	0	0	0	0	1	(10)	19	24	28	29	28	29	22	14	(11)	4	3	3	0	3
Feb.	0	4	5	1	0	0	0	1	3	(11)	19	21	25	24	25	22	22	16	11	(10)	5	3	1	1
Mar.	2	2	2	2	2	3	2	2	6	(19)	24	26	27	28	27	27	25	19	14	(12)	5	7	4	0
Apr.	3	1	2	1	2	1	1	3	(11)	18	24	29	29	29	27	25	22	20	15	(15)	9	8	8	8
May	7	5	2	2	2	2	2	5	(17)	21	23	23	25	28	28	29	27	25	24	19	20	18	14	(12)
June	11	7	2	3	1	0	2	6	(14)	22	21	23	24	23	24	23	26	23	21	18	11	(11)	8	8
July	10	5	6	4	5	5	3	5	(11)	22	24	25	24	25	26	26	26	25	22	18	20	14	13	(12)
Aug.	9	9	8	8	7	6	4	5	(12)	23	24	24	24	27	24	26	21	17	17	16	15	14	10	(11)
Sept.	1	1	2	1	1	2	2	1	(14)	21	24	26	27	28	27	28	23	18	12	12	(11)	8	6	4

Note: Define wind direction No.8-14 as seabreeze, numbers in table mean the frequency of seabreeze i.e. total days in that month.

Table 2-1-b Annual wind direction freq. in southern Taiwan (%)

Direction \ Month No.	1	2	3	4	5	6	7	8	9	10	11	12	mean
C	15.2	16.3	15.7	20.3	20.5	15.5	12.2	10.6	13.7	18.7	20.2	16.0	16.2
N	13.7	11.3	9.2	5.4	4.1	3.9	3.5	5.2	6.5	7.8	10.0	13.7	7.8
NNE	15.8	12.9	9.7	6.0	4.3	3.8	3.9	5.4	6.0	8.2	13.0	15.4	8.5
NE	3.8	3.9	3.8	3.1	3.7	4.5	5.1	4.7	4.7	4.7	5.4	5.1	4.4
ENE	4.0	5.3	6.0	5.1	6.6	10.1	8.0	11.1	10.0	7.7	6.0	4.5	7.1
E	2.4	2.9	3.0	2.7	3.3	4.9	4.9	5.1	5.2	4.1	2.6	2.1	3.6
ESE	2.1	1.6	3.3	3.4	4.4	7.4	9.0	5.5	5.0	4.1	2.8	1.5	4.1
SE	1.0	1.3	1.6	2.2	2.7	4.7	4.8	3.0	2.4	1.3	0.7	0.8	2.2
SSE	1.0	1.2	2.5	3.8	4.7	6.5	7.7	4.9	3.1	1.2	0.7	0.5	3.2
S	0.7	0.9	1.6	2.4	3.1	4.6	4.3	3.2	2.3	0.8	0.5	0.7	2.1
SSW	0.3	0.5	1.1	1.7	3.0	5.0	4.1	2.9	2.7	0.8	0.2	0.2	2.0
SW	0.2	0.6	0.6	1.2	2.4	2.7	2.7	2.2	1.2	1.5	0.3	0.2	1.4
WSW	0.4	0.9	1.3	2.3	4.7	4.3	5.1	5.2	4.7	4.0	1.1	0.7	2.9
W	1.5	1.4	2.0	1.9	3.5	3.0	3.6	3.4	3.3	3.0	2.1	1.6	2.6
WNW	5.5	5.5	5.7	7.2	6.1	4.8	5.9	6.0	6.6	7.5	5.5	4.3	5.9
NW	18.6	20.4	19.5	17.4	13.6	6.7	7.6	10.4	10.2	11.1	13.1	14.6	13.5
NNW	13.7	13.3	13.2	13.5	9.1	7.5	6.9	10.7	11.9	13.1	15.6	17.0	12.1

Table 2-2 Variety of wind direction frequency in southern Taiwan (%)

Direction / Season	NNE-NNW	WNW-WSW	SSW-SSE	ENE-ESE
winter	42.1	7.3	2.0	8.9
spring	24.8	11.6	8.0	12.6
summer	17.0	13.7	14.4	22.0
autumn	30.7	12.9	4.1	15.7

Table 2-3 Variety of wind velocity frequency in southern Taiwan (%)

Wind velocity	0-1.7	1.8-3.5	3.6-5.7	5.8-
%	24.82	36.7	25.1	13.37

There are two high points and two low points in the annual wind velocity changes. In January when the strongest cold weather occurs, the highest wind velocity is 3.5 m/s. In May which is between spring and autumn, the average wind velocity is 3.0 m/s, the lowest during the entire year. During this period typhoons occur very often, causing the second high point of average wind velocity, 5.3 m/s to appear. In October the second low point (average wind of 2.9 m/s) which is similiar to that of May appears. Table 2-3 shows the variation of wind volocity frequency in average. (use date of Central Weather Bureau in 1970)

2-1-4 Characteristics of sea-land wind

In southern Taiwan, in addition to the typhoons in the summer and the northeast trade wind in the winter, the sea-land breeze appears daily. Here I will analyze and compare the sea-land wind in the summer and winter. For convenience sake, 1400L will represent the observation data used for the sea wind and 0500L for the land wind.

(1) Summer land wind: In the summer, under the influence of the tropical ocean air mass and the equatorial ocean air mass, the sea and land breeze are very evident in Taiwan. In the Kaohsiung region in the morning, the 0500L is usually calm or there is a light wind. Over 65% of the time it is calm and 15% of the time the velocity is 3 m/s or more. The land wind direction is usually northeast, northeast-east or east (14%).

(2) Summer sea wind: In summer because of solar radiation, the temperature increases and the air pressure on the surface of the land becomes thin. From the beginning of the 0830L, the air moves from the sea to the land forming the sea wind, 43% of which are southeast or

west winds with a velocity of 8 m/s or less. The sea wind velocity of 8 m/s at 1400L is the strongest. When reaching the high point of 8 m/s at 1400L the occurance of calm winds is only 4%.

(3) Winter land wind: During winter in the Taiwan area, under the influence of the continental air mass, the northeast wind prevails. In southern Taiwan, due to the influence of the Taiwan mountain range, the northeast wind changes into a north wind. The average velocity of 4 m/s is quite high. However during the night, the volocity of the north wind becomes as weak as the velocity during the day. Therefore it is impossible to see the land wind in the kaohsiung region during the winter 42% of the time the north wind prevails and 19% of the time the NNE wind prevails.

(4) Winter sea wind: When the cold front comes it is cloudy in the southern Taiwan region. However due to the prevailing north wind, the velocity is also high. When the north wind weakens and the sunlight is strong the sea wind is formed. It begins rather late around 10:00 AM. The sea wind in Taiwan, the southern part, is for the most part a west wind. Under the influence of the north wind, the direction and volume of the two change into a northwest NNW wind. This occurs 43% of the time. If the north wind dies down, the sea wind will rise as a northwest, west or southern wind, 39% of the time. During this season, the rate of the appearance of calm winds is the lowest, only 3% with a velocity below 8 m/s.

2-1-5 Atmospheric stability in southern Taiwan

The atmospheric stability in southern is analized and shown in Table 2-4 according to weather information in 1980. B,C and D class prevail always during daytime through whole year. (13)

Table 2-4 The probability of the atmospheric stability in Kaohsiung area (1980)

P-G CLASS	A	B	C	D	E	F
Spring	2.30	16.92	22.60	20.28	7.14	30.76
Summer	2.75	15.76	20.50	25.11	4.93	30.94
Autumn	3.10	15.96	23.49	12.45	6.26	38.74
Winter	1.84	10.44	25.99	17.56	11.01	33.16
Average	2.50	14.78	23.14	18.87	7.33	33.38

2-2 Meteorology in the northern area of Taiwan

2-2-1 General meteorological conditions

Due to the weak surface mean circulation, low velocity and uncertain wind direction in April, the potential air pollution may be high. In this arid month the mean temperature difference in the coastal area, terrace region and inland area of Taoyuan is not high and decreases gradually as one moves from the sea to the land, indicating a strong effect. However, the absolute maximum temperature appears as the opposite, decreasing from the Lungton seashore to the Taoyuan seashore. This temperature degree, when the air pollution disperses from the seashore toward the inland causes the sea wind to be quite important. When the maximum temperature appears, the prevailing wind is usually light. The absolute temperature distribution in July is similiar to that in April; it is lower at the seashore than at the inland area. However the difference is not as high as that in April. The rain can remove the pollutants suspended in the air. Around the Taoyuan seashore area, rainy days with a minimum value of percipitation appear in July. The mean weak surface circulation in July is lower than only that in April. Therefore, there is potential air pollution in July. The primary conclusion provided by the foregoing analysis of the climate in the Taoyuan seashore area indicates that there is potential air pollution mainly in spring followed by the summer. Winter is the season with the least pollution.

2-2-2 Characteristics of wind direction and velocity

(1) Winter: The northeast wind prevails in northern Taiwan (70%). However, when the high air pressure leaves for the sea, the southeast wind prevails (20%). Before the cold front passes a southwest wind prevails and after the front passes a northwest wind prevails (10%)

(2) Spring: The continental air mass begins to weaken but the subtropical high air pressure does not completely form. Therefore, under the alternating influence of the northeast, southwest and sea and land winds, the general wind system weakens in northern Taiwan.

(3) Summer: Under the influence of the Pacific sub-tropical high air pressure, the southwest or southeast wind prevails (the southwest wind plays the major role) and when the large scale velocity weakens the sea-land wind becomes evident.

(4) Autumn: The variation of the wind direction is the opposite of that is spring and the north wind gradually takes the place of the south wind.

Table 2-5 shows the variety of wind velocity frequency in northern Taiwan (%) of 1980.

Table 2-5 Variety of wind velocity frequency in northern Taiwan (%), 1980

wind speed M/S	0-1.7	1.7-3.5	3.5-5.7	75.8
%	19.47	17.30	16.57	41.05

2-2-3 Atmospheric stability and dispersion ability in northern Taiwan

According to Table 2-6, the probability of D. E and F during the whole year is very high in northern Taiwan. During spring, autumn and winter in the Taoyuan region, the northeast and northeast-east winds play the most important role, with a probability of 45%.

In summer the west wind and the southwest wind prevail with a probability of 20%. According to the joint frequency functions there is no evident difference. Therefore we arrive at the following conlusions:

(1) In the Taoyuan region the dispersion of the three stability types D,E and F are frequent. Consequently serious pollution is not easily caused by the high stacks.

(2) In the Taoyuan region the frequency of the three types of stability A, B and C and a weak wind velocity is about 20%. Consequently there is a potential for serious pollution over short periods of time. This condition depends on the industrial development in the Taoyuan region. If the medium and small stacks are highly concentrated in the industrial zone, there will be serious pollution in the future.

(3) From late autumn to earily spring (October to March the following year), in the Taoyuan region, the northeast and northeast-east winds with a stable velocity and direction prevail. The most frequent class is D with a velocity of 6-7 m/s. It is also the most stable. It is easy for this condition to cause high wind fumigation from the high smoke stacks. That is to say, because the direction of the rising smoke is fixed, the change of ground contact points is small which then produces accumulated pollution over a long period of time.

Table 2-6 Stability and wind direction probability in northern Taiwan throughout the year 1978-1980, Taoyuan

wind direction	spring		summer		Autumn		winter	
	A,B,C	D,E,F	A,B,C	D,E,F	A,B,C	D,E,F	A,B,C	D,E,F
1	0.87	0.91	1.58	0.71	0.28	0.25	0.58	0.71
2	0.46	0.78	1.09	0.75	0.63	1.38	0.48	0.94
3	0.72	1.11	0.67	0.64	0.80	1.64	0.70	1.60
4	3.99	9.28	2.55	3.29	5.03	17.48	3.72	13.15
5	6.72*	20.81*	2.88	7.83	5.28*	24.21*	5.86*	22.25*
6	4.06	12.79	4.42	9.78*	4.88	14.65	4.05	14.91
7	0.87	2.26	1.67	2.73	0.94	1.60	0.78	2.27
8	1.39	3.90	4.29*	10.78*	1.53	3.81	1.35	4.19
9	0.85	2.49	2.11	5.25	0.90	2.04	0.61	2.06
10	0.72	1.55	1.14	2.60	0.63	0.91	0.53	1.80
11	0.85	1.77	1.55	2.35	0.67	1.24	0.70	2.21
12	1.30	1.89	2.64	3.20	0.52	1.40	0.73	2.04
13	1.27	2.21	3.40	3.46	0.62	0.93	0.62	1.41
14	2.80	2.80	5.30	3.10	1.02	1.14	1.86	2.15
15	2.85	2.14	3.11	1.08	1.48	0.77	1.80	1.47
16	2.12	1.47	2.99	1.06	0.92	0.42	1.50	0.97
TOTAL	31.84%	68.16%	41.39%	58.61%	26.13%	73.87%	25.87%	74.13%

Note: Spring----March, April and May
Summer---- June, July and August.
Autumn----September, October, and November.
Winter---- December, January and February,
* Prevailing wind directions

2-3 Comparison of diffusivity between northern and southern area of Taiwan

The probability of the atmospheric stability is usually considered as one of the best indices to indicate the potential of pollutant diffusivity. According to weather information in 1976, Lu, etal. (1977) compared that in every regions over Taiwan area as shown in Table 2-7.

Table 2-7 The probability of the atmospheric stability in every regions over Taiwan area (1976)

Region \ Stability		A		B		C		D		E		F	
Kingsan	NORTH	2	24	8	18	9	23	69	19	4	9	7	7
Taipei		5	4	19	10	20	20	23	17	9	9	24	40
Singchu		3	54	15	10	8	9	52	7	4	6	18	14
Wuchi		1	2	2	1	5	4	78	35	6	45	8	13
Chaii	SOUTH	10	4	28	8	21	17	18	18	6	11	17	42
Tainan		6	27	12	15	7	12	51	9	5	5	19	32
Kaohsiung		1	2	24	3	26	10	20	22	8	21	21	42
Yenliau		3	19	5	18	14	31	49	12	5	2	24	18
Hwalian		5	15	11	21	4	19	62	22	3	13	15	10
Hunchun		4	67	16	10	11	6	42	4	5	2	22	11

Note : Left side- P-G classification

Right side-stoner classification

In this table, the probability of unstable categories, B and C, of the southern area (such as Kaohsiung and Chaii) is higher than that of the northern area (such as Taipei and Singchu). We compare some places in southern Japan as shown in Table 2-8, and find that the unstable categories of northern Taiwan are higher than that of southern Japan.

Table 2-8 The comparison of probability of the atmospheric stability in southern, northern Taiwan and southern Japan (a), 1976

P-G stability / Region	A	B	C	D	E	F
Kaohsiung	1	24	26	20	8	21
Chaii	10	28	21	18	6	17
Taipei	5	19	20	23	9	24
Akasi	0.7	10.0	5.9	58.4	2.7	22.4
Takasago	2.2	12.0	4.4	55.1	2.7	23.8
Aioi	0.5	12.1	7.5	54.9	0.8	24.2
Akou	0.5	9.9	6.1	57.8	5.3	20.4
Himezi	1.3	12.7	4.6	54.3	1.8	25.4
Tazuno	2.1	10.8	5.0	5.8	5.3	18.8

We know that solar insolation and some other meteorology elements are quite different between northern and southern Taiwan, or between Japan and Taiwan. These are said to effect the diffusivity of pollutants. The following chapters will try to find some specific characteristics of diffusion in Taiwan.

CHAPTER 3 EXPERIMENTAL STUDIES OF DIFFUSION OF AIR POLLUTANTS FROM STACKS AT KAOHSIUNG AREA

3-1 The SF6 tracer experiment at the littoral industrialized area of Kaohsiung

3-1-1 Introduction

During these years a MESO Scale meteorology has been discussed relating to the characteristics of air pollution in Kaohsiung area, in the hope that it may be applicable to the optimum control planning of the environmental assimilating capacity in that area. However, the main pollution; sources in that area are apt to be effected by nature environment because of its special terrain and sea-breeze. Thus, it may impair its dispersion and removal ability in partial environment, above all, in the littoral industrialized region, and cause heavy pollution in the area. Therefore, it is necessary to tap the pollution characteristics on local scale. This chapter will discuss the data based on the SF6 air tracer experiment conducted at the fixed height 100 m and from the stack height 132 m of No.5 generator in littoral Talin thermo-electric plant at Kaohsiung, where this author presided over the work from September 8, 1981 to September 13, 1981.

The tracer gas is released from the source. It drifts with the wind to distant surveying points (sampling points). In case of a breeze, it may take two hours or more. Moreover, we must take into account the moving of air current and eddy and the influence of terrain. In a day there are only a few conditions which can cope with the condition of implementing dispersion experiment. In this experiment the time for releasing tracer is more than one hour and sampling time 15 minutes. The experimenting work is carried out at daytime only.

3-1-2 Theoretical Foundation

From the review study of atmospheric diffusion equations, it is concluded that there are many models which discuss miscellaneous analytical solutions, and the statistical atmospheric diffusion equations. The so called plume model and the puff model are the general dispersion formulas used by regulatory agencies in predicting air pollution concentrations. This assumption plume density and the shape of Gaussian horizontal or vertical dimensions is based upon field measurements and observations of emission from an isolated stack in gently rolling terrain. (b,c,d)

One of the most important variables, in determining whether a source emitting material from a stack is in compliance or not in compliance with air quality standards, is the maximum surface concentration of the pollutants that is likely to occur. Calculation of this concentration is generally based upon the Gaussian plume diffusion model and Briggs plume rise model, etc.. (14)

Dispersion phenomena can be shown by the following equation to develope the Gaussian plume diffusion model:

$$U \frac{\partial C}{\partial X} = \frac{\partial}{\partial z}(Kz \frac{\partial C}{\partial z}) + \frac{\partial}{\partial Y}(Ky \frac{\partial C}{\partial Y}) \qquad (3\text{-}1)$$

It is suitable for the foregoing equation to handle the continuous points source in constant condition X, Y, and Z in the formula are the rectangular coordinates respectively. X goes along the direction of wind velocity U, while Y goes horizontally and crosses with X axis. Z is the rectangular coordinate. In this equation, the wind direction was postulated not to change due to altitude but kept in a certain condition. At the low dissipating source, this postulation will not cause a great deviation. However, at the high dissipat-

ing source, the postulation is worth reviewing.

Wind velocity U usually changed due to the altitude. However, for the most part, the diffusion model should be used; the wind velocity was postulated to be constant and the mean wind velocity value in the diffused atmosphere was used. This postulation may have some problems. Especially, when the diffused range σ_z of vertical direction was calculated with the diffusion model from the distribution of ground concentration, the effect of the mean wind velocity was high.

C shows the concentration, Kz , Ky show the diffusion coefficient of the directions of Z and Y. Kz and Ky under the general conditions are affected by the atmosphere characteristics. Moreover, the roughness of ground and downwind distance from smoke source would cause great change. The variable diffusion model showed the different functions of the Kz and Ky only.

If Kz and Ky are the function of X, that is

$$Kz = Kz\ (X)\ ,\quad Ky = Ky\ (X)$$

and if $$\sigma_y^2 = \frac{2}{U}\int K_y^2\, dx\ ,\quad \sigma_y^2 = \frac{2}{U}\int K_z\, dx$$

and when the point source (o,o,h.) was affected by ground full reflection, that is

$$\left[K_z \frac{\partial C}{\partial z} \right]_{z=0} = 0$$

and the to meet continuous conditions

$$\int_{-\infty}^{\infty} \int_{0}^{\infty} UC\, dydz = Q$$

to solve (3-1) Equation, the following can be obtained:

$$C = \frac{Q}{2\pi U \sigma_y \sigma_z} \exp\left(-\frac{Y}{2\sigma_y^2}\right) \left\{\exp\left[-\frac{(z-He)^2}{2\sigma_z^2}\right] + \exp\left[-\frac{(z+He)^2}{2\sigma_z^2}\right]\right\} \quad (3-2)$$

this is called Normal Distribution or Gaussion plume diffusion model.

Because the Gaussian diffusion model has achieved considerable popularity among people attempting to describe the role of atmospheric dispersion, most engineers and scientists employing the model have used the classical dispersion rates originally designated by Pasquill and Gifford. Turner's workbook had provided additional impetus to use of this model, often by users not familiar with either the mathematics or the experimental data used to determine the dispersion rates.

In addition to these, BNL chart (1966), Fuguay chart (1964), TVA chart (1971), St. Louis chart (1969), SRI chart(1973), Bowne chart (1974), Colstrip chart (1975), MITI chart (1974), Yamamoto method (1974), Draxler method (1976), Sakagami method (1960), Yahatake method (1977), etc.. There are a number of methods for estimating spreads which have been surveyed by Okamoto in 1977. In the above methods, stability classifications such as Pasquill's class, Turner's class, Fuquay's 6 classes, gustiness class, rapse rate, SRI's class, MITI's class, Colstrip class, etc. had been erected. (e)

The method chosen to determine the plume rise is also one of the most important areas. Table 3-1 is a summary of power coefficients in various plume rise formulas.

Table 3-1. Power coefficeints in plume rise formulas:

(OKAMOTO)

	C	a	b
Lucas I	135.0	1/4	1
Lucas II	104.2+0.17 Hs	1/4	1
Csanady	9.5	1	3
Opt. Csanady	49.2 - 56.6	0.27	0.81
T.V.A.2/3 power law	39.9 - 61.3	2/3	1
Briggs(Neutral & Unstable)			
-Large Source-	$2.5\ Hs^{2/3}$	2/3	1
-Middle or Small Source-	$0.784\ Hs^{2/5}$	0.6	1
ASME(Neutral & Unstable)	5.7	1	1
CONCAWE(simplified)	5.53	1/2	3.4
Opt. CONCAWE	13.09	0.444	0.694
Moses & Carso, 1968*			
-All Stability-	5.35	1/2	1
-Individual Stability-	4.58 - 10.53	1/2	1
Priestley(simplified)	34.7**	1/4	1
Opt. Priestley	43.2	1/4	$36.1\ Qh^{-0.6}+0.75$
Holland*	0.04	1	1
Rauch	47.2	1/4	1
Whsley(C.C.R.L.)	66.4	1/4	1

* In case that momentum term is negligible in comparison with buoyant term.

** In case that Uc =4m/s , Xc=50m.

Symbols

Qh: heat emission rate (Kcal/s)
U : wind speed (m/s)
ΔH: plume rise (m)
Hs: stack height (m)

Over 20 years of comprehensive field surveillance and documentation of dispersion of power plant emissions for a varied range of unit sizes, stack heights, and meteorological conditions determined the Tennessee Valley Authority's interpretation of principal plume dispersion models. TVA's experience indicated that as unit sizes are increased and taller stacks are constructed, the plume dispersion type associated with maximun surface concentrations changed. Coning, Farming, Inversion Breakup, Looping and Trapping are five principal plume dispersion types. The coning type was considered the critical plume dispersion type because the frequency of recurrence of surface concentrations from this model was appreciably greater than other types.(15)

Over simple terrain and straight coastlines, the fate of aerosols, gases and photochemical pollutants is very hard to estimate indeed, and without extensive observations of these phenomena, we will never be sure of what aspects to model, and whether or not our models really have more than a passing similarity to reality. Yet if we wish to continue orderly economic development of the world's resources, we must gain a far greater insight into the behavior of the atmosphere in coastal regions where in a significant guantity of the world's population resides and its harmful effluents are released. (16)

3-1-3 The outline of tracer experiment

In this experiment, the focus is on tracing the whereabouts of the smoke emitted from Talin Power Plant. During experimentation, the stack of generator No. 5 has been chosen as the object to scatter tracer gas. The relevant data of this generator are as in Table 3-2.

Table 3-2. The data of Talin No.5 generator

Fuel consumption		110 Tons/hr	
Fuel component parts	C 83.28%	S	3.8%
	H 10.8%	Water	0.20%
	O_2 1.69%	N_2	0.21%
	ash 0.02%		
Stack height		132 m	
Stack top diameter		6.09 m	
Exhausting temp. in stack		420°K (147°C)	
Exhausting speed		18.48 m/s	
Total emission	369.85 M^3/s	(288°K)	
	or 539.0 M^3/s	(420°K)	

The outline of this experiment is summerized in the following two Tables, 3-3-a and 3-3-b.

Table 3-3-a The scheme of tracer experiment at Kaohsiung littoral area in 1981

ITEM	METHOD	INSTRUMENT
Tracer gas scattering	Use balance to weigh and determine the proper releasing volume	.SF6 (40Kg) bombe .pressure gage .temp. controller
Sampling network	Use air sampler 60 sets, 60 points at 1.25, 3, 5, 8, km from power plant (Refer to Fig. 3-1)	.sampler with time setting .sampling bag
Measurment of effective stack height	Use Briggs and other formulas to calculate	without observation this time, only check by photograph
Measurment of tracer gas	GC with electron capture detector and precut back-flush circuit	p-E Σ 3B type GC
Measurment of surface wind	Set up 6 meteorological Stations and use 2 fixed stations date (Refer to Fig 3-1)	simple wind direction and wind speed measuring machine with recorder
Measurment of the upper wind	Use pibal and observe its trace with theodrites	. tetroon . cowing balloon . pilot balloon
Measurment of the the vertical profile of temperature	every 50m vertical height with tetherd balloon and radio sonde.	.tetroon .radio sonde
Measurment of solar insolation	use solar insolator with recorder	.solar insolator
Measurment of mixing height	Use SODAR with recorder	.SODAR

Table 3-3-b The scheme of tracer experiment at Kaohsiung littoral area in 1981

RUN NO.	DATE IN SEPT.	Tracer release time	release rate 1/min.	release height stack* / 100m	Sampling 15 tim (min)	Wind direction / speed	Pasquill Stability (10^m H)	Tracer released
1	8	12:45 - 13:45	20.09	100 m	13:30 - 13:45	270° 2.7 m/s	B	SF_6 7.2kg
2	8	14:45 - 15:45	20.09	100 m	15:30 - 15:45	250° 2.7 m/s	B	SF_6 7.2kg
3	8	16:45 - 17:45	19.54	100 m	17:30 - 17:45	250° 1.6 m/s	C	SF_6 7.0kg
4	9	10:45 11:45	22.89	100 m	11:30 - 11:45	270° 4.0 m/s	B	SF 8.2kg
5	9	12:45 - 13:45	37.09	*	13:30 - 13:45	270° 4.0 m/s	B	SF_6 12.4kg
6	9	14:45 - 15:45	34.89	*	15:30 - 15:45	150° 2.0 m/s	B	SF_6 12.5kg
7	9	15:45 - 16:45	33.49	100 m	16:30 -	135° 2.0 m/s	B	SF_6 12.0kg
8	10	8:45 - 9:45	30.42	*	9:30 - 9:45	270° 1.0 m/s	A-B	SF_6 10.9kg
9	10	10:45 - 11:45	32.65	100 m	11:30 - 11:45	190° 3.0 m/s	A-B	SF_6 11.7kg
10	10	12:45 - 13:45	33.49	100 m	13:30 - 13:45	250° 2.5 m/s	A-B	SF_6 12.0kg
11	10	14:45 - 15:45	33.49	100 m	15:30 - 15:45	225° 3.5 m/s	B-C	SF_6
12	10	15:45 - 16:45	33.49	100 m	16:30 - 16:45	225° 4.0 m/s	C	SF_6 12.0kg
13	11	9:15 - 10:15	34.01	100 m	10:00 - 10:15	180° 2.0 m/s	A-B	SF_6 12.1kg
14	11	10:45 - 11:45	33.49	*	11:30 - 11:45	225° 4.0 m/s	B	SF_6 12.0kg
15	11	12:45 - 13:45	33.49	100 m	13:30 - 13:45	210° 3.5 m/s	B	SF_6 12.0kg

Table 3-3-b (continued)

Run No.	Date in Sept.	Tracer release time	release rate 1/min	release height stack* / 100 m	Sampling 15 time (min)	Wind direction / speed	Pasquill Stability (10^m H)	Tracer release
16	11	14:45 - 15:40	33.19	*	15:30 - 15:45	270° 2.5 m/s	C	SF_6 10.9kg
17	11	15:45 - 16:45	33.49	100 m	16:30 - 16:45	250° 2.6 m/s	C	SF_6
18	12	9:04 - 10:15	33.71	100 m	10:00 - 10:15	290° 2.5 m/s	A	SF_6 14.3kg
19	12	10:20 - 11:45	33.26	*	11:30 - 11:45	260° 4.8 m/s	A	SF_6 16.9kg
20	12	12:45 - 13:45	33.49	100 m	13:30 - 13:45	270° 4.6 m/s	B	SF_6 12.0kg
21	12	14:45 - 15:45	33.49	*	15:30 - 15:45	270° 4.6 m/s	B-C	SF_6 12.0kg
22	13	10:30 - 11:45	33.49	100 m	11:30 - 11:45	280° 5.5 m/s	A-B	SF_6 15.0kg
23	13	12:45 - 13:45	33.49	*	13:30 - 13:45	330° 3.6 m/s	B	SF6 15.0kg
24	13	14:45 - 15:45	33.49	*	15:30 - 15:45	330° 4.6 m/s	C-D	SF_6 12.9kg

There are many kinds of tracers to be used for dispersion experiments such as Hilst (1957) used smoke plumes; Barad and Shor (1954) used oil fogs; Hay and Pasquill (1957) used spores; Robinson, et al. (1959) used dyes such as uranine; Haines, et al. (1958) used antimony oxide which can be determined with high sensitivity by neutron activation analysis; and, Eggleton and Thompson (1961) and Leighton, et al. (1965) used inorganic fluorescent particles such as zinc-silicates, zinc sulphides and zinc-cadmium sulfite with small amounts of added activator elements. (17)

This experiment comprises two Approaches; one of which uses a 100 meter, Tack as a fixed scattering height, and the other is tack 132 meters high for scattering the smoke thereof. Testing networks are composed of downwind distance 1.25, 3, 5, and 8 km as in Fig. 3-1. Sampling machines 60 sets will be installed at adequate sampling points as in Fig. 3-1.

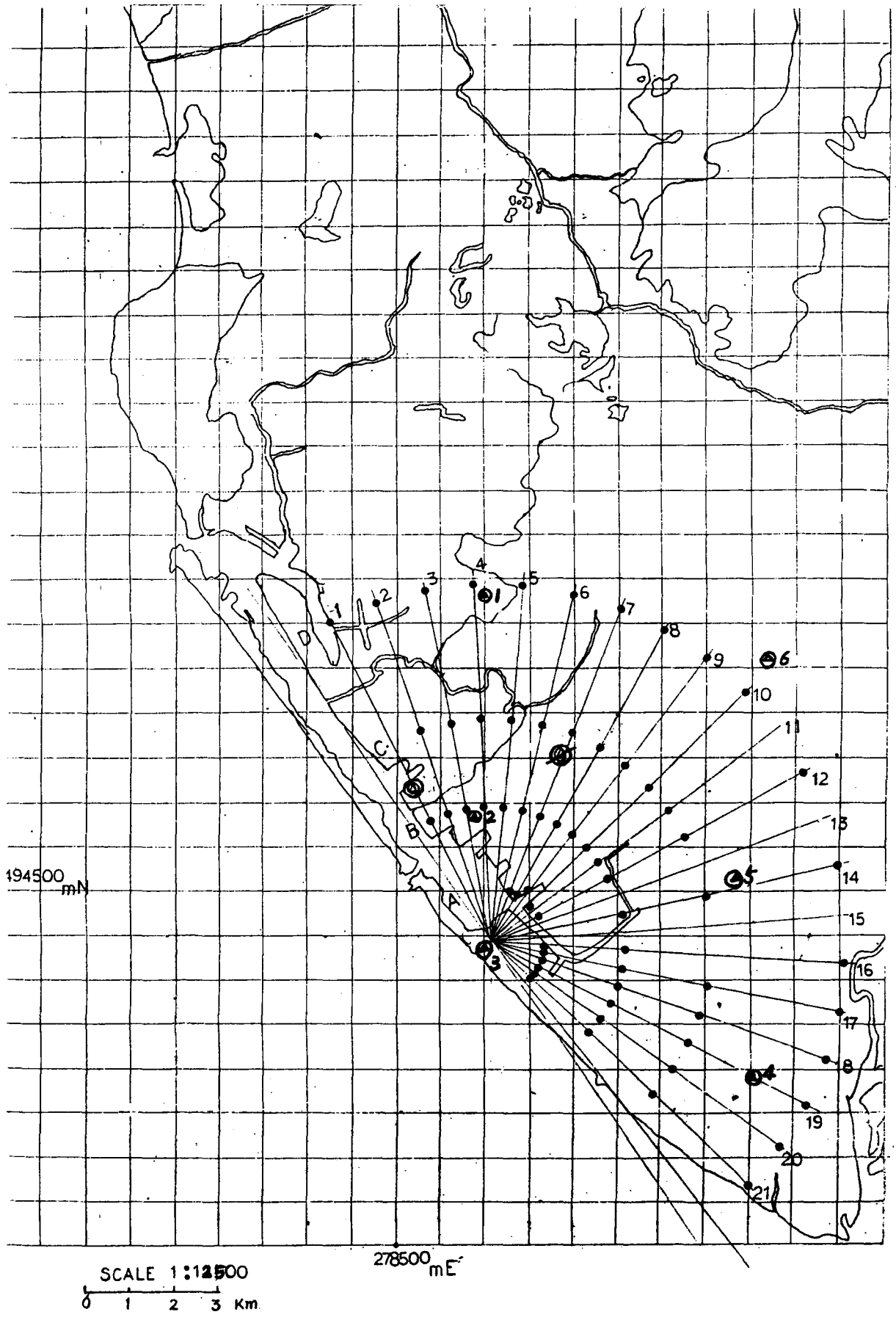

Fig. 3-1 Sampling network of tracer experiment

- gas sampling station
- meteorological observing station
- Harbor Meteorologica station
- Airport observing station

Leighton, et al. (1965) used ammoma and sulfur dioxide; Eggleton (1961) used radioactive Xenon-133; Collins, et al. (1965) and Turk, et al. (1968) used sulfur hexafluoride (SF6); Schulz (1957), Hester, et al. (1975) and Elias, et al. (1976) used various Freons; Cowan, et al. (1976) and Crawford, et al. (1978) used heavy methanes; and, the Air Resources Laboratory - NOAA (1978) used selected perfluorocarbons.

The implementation of sulfur hexafluoride (SF6) tracer gas technology provides quantitative information concerning air mass or pollutant transport and dispersion which cannot be readily obtained in any other manner.

Usually the implementation of dispersion is based on testing scale, expenditure and other factors to determine the kinds of tracer. However, they must be in conformity with the conditions as follows: (f,g)

1) The background concentration may be discerned conspicuously in atmosphere.

2) The substance is apt to be obtained and stored.

3) It is easy and convenient to acquire a quantitative analysis.

4) There will be no variation, deterioration, activation, and gas identification in atmosphere.

5) It is easy to control exhausting volume.

6) The implementing work is easy and not harmful to human beings, livestock, and plantlife.

During this experimentation, SF6 is chosen as the tracer. It is very simple to scatter liquidized SF6 in test. It is convenient to sample by automatic sampling device as well. Concurrently there are improved laboratory electron capture gas chromatograph methods for the direct determination of collected air samples containing as little as a few parts of SF6 in 10^{13} parts of air. (18)

3-2 The observation of meteorological condition of Kaohsiung Area

The objective of a tracer dispersion experiment is to understand the general rules relative to atmospheric pollution in a given area so as to acquire the effective basic data as to industrial construction and improved land usage thereof through experimental result.

Thus, the data acquired during experimentation, such as various meteorological factors and reference figures should be broadened to other adequate usages. Hence, it is advisable to choose the surface concentration distribution applicable to dispersion experiment and dispersion approach able to express an overall tendency. In such dispersion approaches the reference figures must be likely to be acquired and capable of being replaced at any time.

Especially, in recent years, most of the stack heights have been raised and the scope of pollution exhausted thereby enlarged. Thus, the meteorological reference figure in one locality cannot appraise the concentration distribution throughout the whole area.

During tracer experimentation, besides the sampling network set up at adequate points, it is advisable as well to establish a meteorological observing network for the dispersion ground at corresponding scope with weather chart for MESO scale meteorologic analysis so as to facilitate air-observing data to be coordinated with comprehensive appraisal.

I analyze the general climate, wind direction and velocity, temperature profile and atmospheric stability in the following sections. All of the data are obtained from the observation during the period of tracer experiment.

3-2-1 The analysis of general climate

The diffusion test began from September 7, 1981 and ended September 13, 1981. In the first day the main task was preparation, the SF6 was dissipated only one time. During the test period, the weather was fair for the most part except Septemer 7, 1981 which was a rainy day and not fit for test. The general climate before and after experiment is analysed as follows: (refer to APPENDIX A)

September 6, 1981 the barometric minimum 1008 mb moved eastward slowly at 21° latitude N. and 118° longitude E. North seas of the Pratas Islands. The barometric maximum 1021 mb moved east-south-eastward at 40° latitude N, and 112° longitude E., Mongolia, with the hour speed 15 Km. Under the effect of the variable air mass in the mainland, the weather in Taiwan was cold and it showered. Therefore, it was clouded and showered (the drizzling rain before noon or at noon) in the test area. September 7, 1981, the baromotric minimum 1008 mb moved eastward slowly at 21° latitude N. and 120° longitude E, in the Bashi Channel. The barometric maximum 1018 mb moved eastward slowly at 36° latitude N. and 123° longitude E, the south of the Yellow Sea. Under the influence of the barometeric minimum in the Bashi Channel, it showered in South Taiwan. In the test area, it was cloud and showered. As it rained cats and dogs before noon, sampling was difficult.

September 8, 1981, barometric minimum 1009 mb moved southwestward slowly at 19° latitude N. 117° longitude E. the South of the Pratas Islands. The barometric maximum 1013 mb moved eastward slowly with a speed 10 Km per hour at 29° latitude N. 124° longitude E in the East Sea. As the barometric minimum in the Pratas Islands went away, the weather was fair in South Taiwan. There were fair and cloudy days in the test area.

September 9, 1981, the barometric minimum 1009 mb moved westward slowly at 20° latitude N. and 115° longitude E., in the south of the Pratas Island. The barometric maximum 1023 mb moved eastward slowly at 20° Km per hour at 43 latitude N. 113° longitude E. in Mongolia. There was a fair and cloudy day in South Taiwan. There also was a fair and cloudy day in the test area. As the windsystem in the morning was not good, the test was started 10:00 a.m.. September 10, 1981, barometric maximum 1020 mb moved eastward slowly at 33 latitude 33° and 114° longitude E. in Honan Province. The barometric minimum 1012 mb moved with speed of 10 Km per hour. Northeastward at 28° latitude N. and 118° longitude E. in the Chekiang Province. The cold front moved from this center and extended to Kwangsi Province. There was a fair and cloudy day in South Taiwan. There was also a fair and cloudy day in the test area.

September 11, 1981, the barometric maximum 1016 mb moved eastward slowly at 310 latitude N. and 113° longitude E. in the Honan Province. The barometric minimum 1011 mb moved ENE slowly at 27° latitude N. and 118° longitude E. in Chekiang province. The cold front extended from this center southwest to Kwangsi Province. There was a fair and cloudy day in South Taiwan. There was also a fair and cloudy day in the test area.

September 12, 1981, the barometric maximum 1024 moved southwestward slowly at 41° latitude N. and 113° longitude E. in Mongolia. The barometric minimum 1010 mb stopped seemingly at 27° latitude N. and 116° longitude E. in Kiangsi Province. The cold front extended from this center westsouthward to Kwangsi Province. There was a cloudy, and fair day some times with the thunder storm in the mountain area in the test area.

September 13, 1981, the barometric maximum 1026 mb moved southeastward slowly at 41° latitude W. and 114° longitude E. in the Mongolia. The barometric minimum 1013 mb moved Northeastward slowly at 27° latitude N. and 125° longitude E.

in the sea of Ryukyu. The cold front extended from this center southwestward through the Taiwan north sea to Kwangsi Province. Under the effect of this cold front, there was a cloudy and thunder storm day in Taiwan area. It was also cloudy and rainy in the test area.

In short, before September 7, 1981, the study area, under the effect of the barometric minimum in Southwest Taiwan, the Southwest air-flow was very strong and brought about too much aqueous vapose which resulted in the rainy days. After September 7, 1981, as the barometric minimum went away from Taiwan and the Pacific barometric maximum was strong the weather became good.

3-2-2 The analysis of wind direction and velocity

In this experiment Hsiokang Airport observing station, Kaohsiung Harbor Meteorological Observing Station and Tungkang Meteorological Observing Station agreed to furnish relevant meteorological data at any time. There were six other stations set up during the tracer experiment period to conduct meteorological observation, as shown in Fig. 3-1, so as to cope with the analysis on the characteristics of experiment field.

Therefore the windsystem is analized run by run during this period and the wind profile of these six stations are shown in APPENDIX B.

On September 7, 1981, the air-flow in south was strong. The south wind prevailed in each station before noon but it changed by afternoon. However the south partial wind was strong. The mean windsystem in the air in the diffusion area during the tracer diffusion study time is described as follows: (refer to APPENDIX C)

RUN 1 : Before 11:00 AM the south partial wind prevailed and the wind changed into a west one at noon. This wind direction was kept at 330 meters high. From the ground to 330 meters high point, the west prevailed as a whole. However, in the space between 330 meters and 660 meters, the south partial wind prevailed. In the space between 660 meters and 1000 meters, wind direction changed into 2 streams of southeast.

RUN 2 : In the space between the power plant and 330 meters high level, the partial west wind prevailed. In the space between 330 meters and 660 meters high level, the partial wind prevailed. In the space between 660 meters and 1000 meters high level, the partial south east wind prevailed. The convergence

was formed at the north of the dissipating point of tracing agent.

RUN 3: In the space between power plant and 400 meters high level, the partial west wind prevailed. In the space between 300 meters and 660 meters high level, the partial southwest wind prevailed general. However, in the space between 660 meters and 1000 meters high level, the southeast wind prevailed.

RUN 4: The partial wind prevailed near the ground of the power plant but it was weak; in the space between the ground and 330 meter high level, the partial west wind prevailed. In the space between 330 meters and 660 meters high level, the windsystem was variable one which seeming formed a divergent area in the air of test area where the wind direction was variable. In the space between 660 meters and 1000 meter high level, the variable airflow of the partial southeast wind prevailed.

RUN 5: In the SPACE between power plant ground and 200 meter high level, the west wind prevailed; in the space between ground and 330 meter high level the partial wind prevailed in general. In the space between 330 meters and 660 meters high level, the partial south airflow prevailed. In the space between 660 meters and 1000 meters air level, the southeast airflow prevailed. The test area was the divergent area.

RUN 6: In the space between power plant and 400 meters high level, the partial south wind prevailed. In the space between diffusion ground and 330 meters high level, the partial west wind prevailed. The convergent band was formed in the air at 5 - 8 Km from dissipating point. In the space between 330 meters and 660 meters high level, the partial southeast wind prevailed. In the

space between 660 meters and 1000 meters high level, the partial southeast wind prevailed but the divergent area was formed in the air.

RUN 7: In the space between power plant ground and 200 meters high level, the partial south wind prevailed. In the space between divergent area ground and 330 meter high level, the partial southwest wind of airflow prevailed and it formed the convergent band in the mounds. In the space between 330 meters and 660 meters high level, the partial west wind prevailed and, at the same, the convergent band existed. In the space between 660 meters and 1000 meters high level, there was the variable convergent area with partial southeast wind.

RUN 8: The weak northeast wind prevailed on the power plant ground and it changed to a southeast wind at the 300 meters high level. In the SPACE between diffusion area and 300 meters high level, the northeast airflow prevailed. In the space between 330 meters and 660 meters high level, the southeast wind prevailed. In the space between 660 meters and 1000 meters high level, the southeast wind prevailed too.

RUN 9: In the space between power plant and 300 meters high level, the southwest wind prevailed. In the space between diffusion ground and 330 meters high level, the southwest wind prevailed and formed the convergent band at the mounds. In the space between 330 meters and 660 meters high level, the southeast wind prevailed and formed the convergent band north of the power plant. In the space between 660 meters and 1000 meters high level, the southeast wind prevailed generally.

RUN 10: In the space between power plant and 200 meter high level, the southwest wind prevailed. In the space between diffusion area and 330 meter high level, the southwest wind prevailed too. In the space between 330 meters and 600 meters high level, the southeast wind prevailed. In the space between 660 meters and 1000 meters high level, the southeast wind prevailed and formed the convergent area in the north power plant.

RUN 11: In the space between power plant and 900 meters high level, the southwest wind prevailed but it changed as the south wind from 1000 meters high level. In the space between diffusion ground and 330 meters high level, the southwest wind prevailed. In the space between 330 meters and 660 meters high level, the southwest wind prevailed generally. In the space between 660 meters and 1000 meters high level, the south wind prevailed.

RUN 12: In the space between power plant ground and 500 meters high level, the southwest wind prevailed but it changed to a south wind from 600 meter high level. In the space between 700 meters and 1000 meters high level, it changed as southwest wind. In the space between diffusion ground and 330 meters high level, the southwest wind prevailed. In the space between 330 meters and 660 meters, the southwest wind prevailed generally. In the space between 660 meters and 1000 meters high level, the southwest wind prevailed generally too.

RUN 13: In the space between power plant ground and 300 meters high level, the south wind prevailed and it changed as southwest wind to 330 meters high level. In the space between 330 meters and 660 meters, the divergent vortex

was formed. In the space between 660 meters and 1000 meters high level, the divergent area was formed.

RUN 15: In the space between power plant ground and 400 meters high level, the west wind prevailed. In the space between diffusion ground, and 330 meters high level, the west wind prevailed. In the space between 330 meters and 660 meter high level, the west wind prevailed too. In the space between 660 meters and 1000 meter, the complex divergent area was formed. The convergent area was formed in the southeast of the power plant.

RUN 16: In the space between power plant and 700 meters high level, the west wind prevailed. In the spaces between diffusion ground and 330 meters high level, the west wind prevailed. In the space between 330 meters and 660 meters high level, the west wind prevailed. In the space between 660 meters and 1000 meters high level, it changed as southwest one and then as northwest one.

RUN 17: In the space between power plant ground and 700 meters high level, the west wind prevailed. In the space between diffusion ground and 330 meters high level, the west wind prevailed. In the space between 330 meters and 660 meters, the southwest wind prevailed. In the space between 660 meters and 1000 meters high level, it changed as southwest one.

RUN 18: In the space between power plant ground and 300 meters high level, the west wind prevailed, and it changed as southwest wind from 400 meters high level. In the space between 500 meters and 1000 meters high level, the east wind prevailed. In the space between diffusion area and 330 meters high level, the partial southwest wind prevailed generally and formed in the

mounds as convergent band. In the space between 330 meters and 660 meters high level, the southeast wind prevailed and changed as west one. In the space between 660 meters and 1000 meters high level, the southwest wind prevailed and then changed as west one.

RUN 19: In the space between power plant ground and 400 meters high level, the southwest wind prevailed. In the space between 500 meters and 900 meters high level, the southwest wind prevailed and it changed as southwest wind from 1000 meters high level. In the space between diffusion ground and 330 meters high 330 meters and 660 meters high level, the southwest wind prevailed. In the space between 660 meters and 1000 meters, the southwest wind prevailed and then it changed as divergent area of southwest wind.

RUN 20: In the space between power plant ground and 400 meters high level, the west wind prevailed, and changed as southwest one from 500 meters high level. In the space between 600 meters and 700 meters the south wind prevailed. In the space between diffusion area and 330 meters high level, the southwest wind prevailed generally. In the space between 330 meters and 600 meters high level, the southwest wind prevailed generally. In the space between 660 meters and 1000 meters high level, the west wind prevailed and then changed as the southeast vortex.

RUN 21: In the space between power plant and 300 meters high level, the west wind prevailed and it changed as southwest one between 400 meters and 700 meters high level and as south wind between 800 meters between 800 meters and 1000 meters. In the space between diffusion ground and 330 meters high level, the west

wind prevailed. In the space between 330 meters and 660 meters high level, WNW wind prevailed and it changed as southwest wind between 600 meters and 1000 meters high level and formed the convergent area in the north of power plant.

RUN 22: In the space between power plant and 400 meters high level, the west wind prevailed. In the space between diffusion ground and 330 meters high level, the convergence of west wind and north wind prevailed. In the space between 330 meters and 660 meters high level, the divergence of the north wind, which changed as Northeast wind later, prevailed. In the space between the 660 meters and 1000 meters high level, the divergence of north wind, which changed as Northeast wind later, prevailed.

RUN 23: In the space between power plant and 900 meters high level, the west wind prevailed, and it changed as north wind at the level of 1000 meters. In the space between diffusion ground and 330 meters high level, the northwest wind prevailed, and it changed as complicated partial Northwest wind from 330 meters to 660 meters. In the space between 660 meters and 1000 meters high level, it changed as divergent partial north wind.

RUN 24: In the space between power plant and 1000 meters high level, the northwest wind prevailed. In the space between diffusion ground and 330 meters high level WNW wind prevailed. In the space between 330 meters and 660 meters high level, northwest wind prevailed. In the space between 660 meters and 1000 meters high level, the northwest wind prevailed.

In conclusion, the characteristics of wind field in the studied area are as follows:

(a) Before noon, in Kaohsiung urban area "hot island effect is obvious" in the situation of radiant zone and air current is rising at urban center.

(b) After noon, around 2-3 o'clock in the afternoon, there prevails sea breeze vigorously. Its blowing direction is WNW or WSW. Its thickness is less than 500 meters and most of the cycling current prevails in the direction of ESS.

(c) Due to the influence of sea breeze and cycling current, vertical wind cutting becomes larger to increase horizontal dispersing function.

3-2-3 The analysis of temperature profile

The characteristics of the atmosphere layer, especially the vertical distribution of the air temperature, has much to do with the atmosphere diffusion. This study period, the altitude of the tracer dissipated was as that of the stack of Talin Power Plant; 132 meter and 100 meters. Therefore, when we review the pollution concentration on the ground, in theory, for the weather in the diffusion field, the atmosphere characteristics from ground to about 500 meters high level should be analysed.

I hereby show the vertical distribution of ambient temperature observed with the tetherd balloon at the beach west of the power plant during the diffusion study period in APPENDIX D This shows the observation data of 2 occasions at Tunkang, 0000 Z, 1200 Z.

From APPENDIX D, we know that two diffusion studies, Run 2 and Run 3, 15:30, September 8, 1981, were made under meutralization of the atmosphere characteristics.

At 13:45, September 9, 1981, when the atmosphereic characteristic under 200 meters was neutral, the RUNS 4, 5 and 6 test were made. However, as the isothermal layer appeared between 250 meters and 350 meters high level, thanks to the invasion of sea wind, the atmospheric layer was more stable.

At 15:30, September 9, 1981, when Run 7 was being conducted, the atmospheric characteristics were neutral.

At 10:45, September 9, 1981, when Run 7 was going to finish, the isothermal layer formed between 300 meters and 350 meters altitude and the unstability appeared between

300 meters and 400 meters altitude. This phenomenon resulted from the invasion of sea wind reduced as the neutral condition, and the isothermal layer and unstability appeared in the air.

Refer to Fig. 3-2,

at 10:00, September 10, 1981, 30 minutes before Run 9 was made, the ground contacting layer below 50 meters was unstable. In the space between 50 meters and 150 meters, the neutral condition existed. In the space between 150 meters and 200 meters, under the effect of sea wind invasion, the counter layer formed. In the space between 200 meters and 400 meters, the neutral condition existed.

At 15:30, September 10, 1981, when the Run 11 was carried out, the neutral condition existed bellow 250 meters. As it became the isothermal layer below 250 meters, the isothermal layer atmsophere was more stable and the sea wind effect reduced gradually.

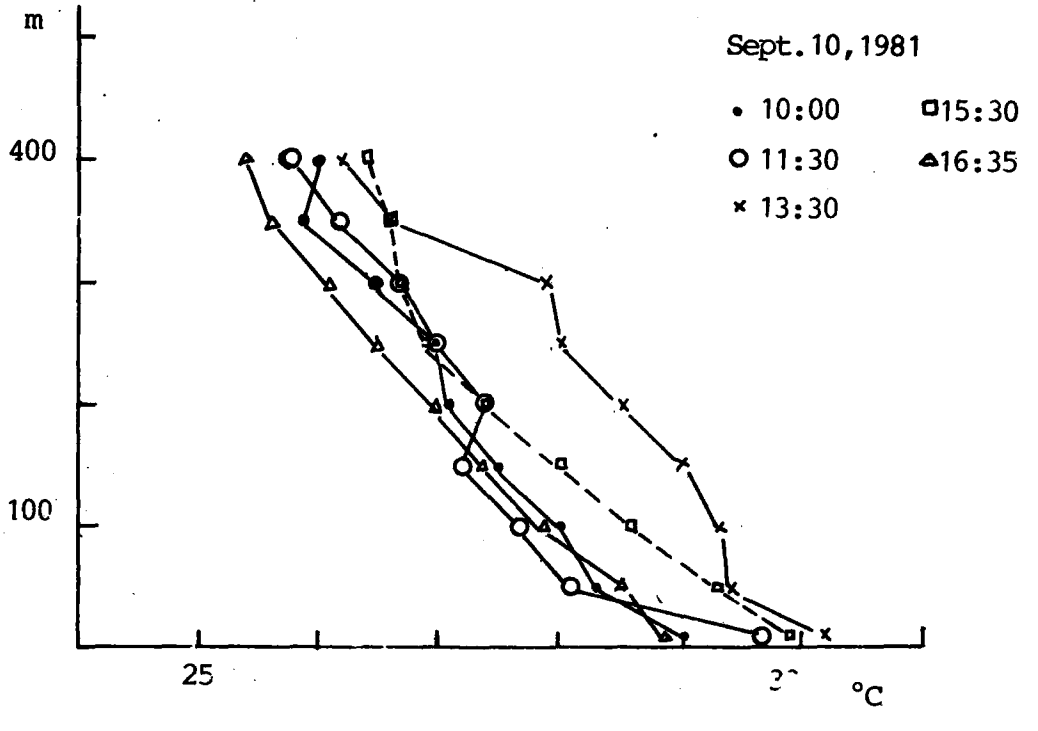

Fig. 3-2 Temperature profile on Sept. 10.

At 16:35, the isothermal layer altitude went up slowly to 350 meters to 400 meters altitude. The neutral condition existed below 350 meters when the Run 12 was carried out

At 10:00, September 11, 1981, due to the effect of solar radiation, the convection was strong in the contacting layer below 50 meters and the atmosphere was unstable. Thanks to the invasion of sea wind, in the layer of 100 meters to 200 meters altitude, the isothermal layer formed and the atmosphere was more stable. Over 200 meters it was, the neutral condition. At this time, the atmosphere characteristics could represent that when Run 14 was carried out. By 13:45, during the period, Run 15 and 16 were carried, the neutral condition went up to 350 meters altitude. Over 400 meters, it became the counter layer and atmosphere was more stable.
By 15:30, the atmosphere below 400 meters became the neutral condition, and the counter temperature was over it. By evening (1200 Z) the air test data of Tungkong showed that the unstable layer was formed over 500 meters which promised the invasion of cold front. Therefore, Run 17 might be affected by counter temperature layer.

At 9:45, September 12, 1981 due to the effect of solar radiation, the ground contacted below 50 meters was unstable. The neutral condition existed between 50 meters and 400 meters. By 10:20 the atmosphere under 400 meters was unstable and the counter temperature formed above 400 meters. By 13:30 15:30, two observations showed that all of the atmosphere was in a neutral condition.

Refer to Fig. 3-3 , at 10:30, September 13, 1981, due to the solar radiation, the ground contacting layer was unstable. The isothermal layer existed between 50 meter and 100 meters. The neutral condition existed between 100 meters and 400 meters. By 12:00, due to the strong insolation the ground contacting layer was unstable. The isothermal condition formed between 50 meters and 150 meters By 13: 30, due to the strong insolation, the convection altitude increased and the isothermal layer went up to 150 meters to 200 meters. The counter temperature formed between 250 meter and 300 meters. The air condition became unstable under the effect of sea wind, apparently.

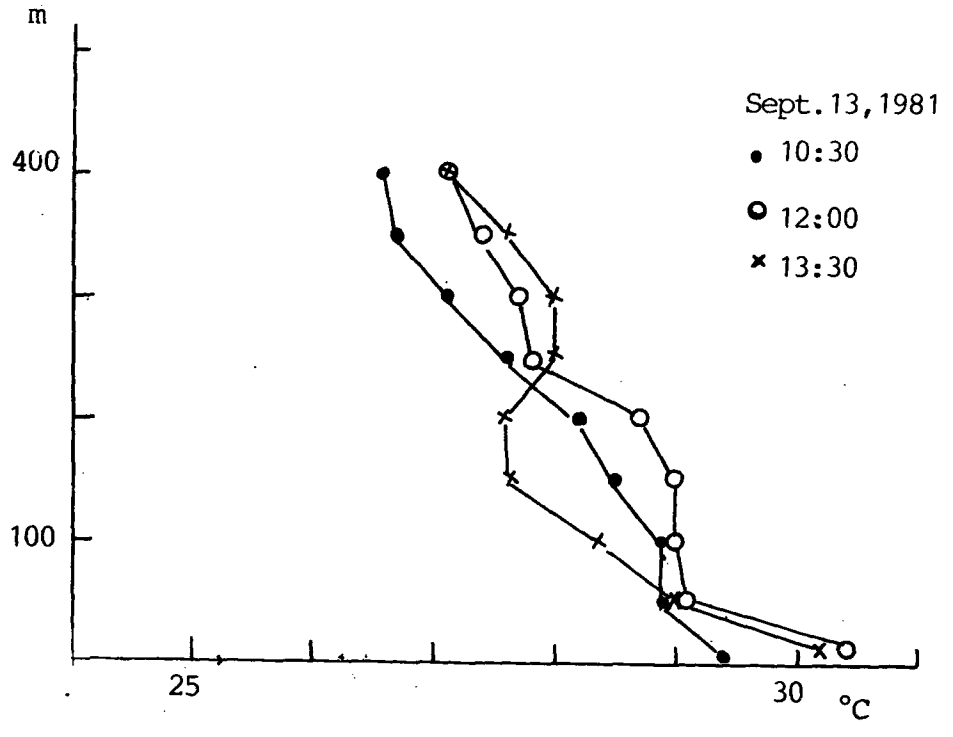

Fig. 3-3 Temperature profile on Sept. 13.

In conclusion, during the experiment period, the temperature profile was not obvious for the cause and disruption of inversion near the ground. But, it is obvious for the temperature near the surface to become warmer than the upper layer by insolation of strong sunshine, that is the real reason why sea and land breeze occur, and from previous chapter Table 2-1-a, from May to Sept. of every year, it is more obvious. From the diagrams shown in APPENDIX D, at about 600 meters height and in the afternoon, discontinuities of temperature can be found, these will be due to different masses of land breeze and sea breeze.

3-2-4 The analysis of atmospheric stability

There are many methods of atmospheric stability analysis. However, because of the limited data, the classification methods of Pasquill (1961) and Turner (1961) are used more universely. Table 3-4 shows the classification standard provided originally by Pasquill (1961). Table 3-5 shows the classification standard revised by Japanese scholar.

Table 3-4 The Pasquill stability classification

Surface wind speed (at 10 m) m/s	Day			Night	
	Strong	insolation moderate	slight	thinly overcast or 4/8 low cloud	3/8 Cloud
< 2	A	A-B	B	-	-
2 - 3	A-B	B	C	E	F
3 - 5	B	B-C	C	D	E
5 - 6	C	C-D	D	D	D
> 6	C	D	D	D	D

Table 3-5 The Pasquill stability classification revised by Japanese scholar

Surface wind speed (at 10 m) m/s	Insolation ($cal/cm^2/hr$)			overcast	Night	
	50	49 - 25	24	8 - 10	upper cloud (5-10) lower cloud (5-7)	thinly cloud 0 - 4
< 2	A	A-B	B	D	-	-
2 - 3	A-B	B	C	D	E	F
3 - 5	B	B-C	C	D	D	E
5 - 6	C	C-D	D	D	D	D
> 6	C	D	D	D	D	D

In this test time, the test was made in accordance with the Pasguill stable classification method revised by Japanese. The analysis of data from Kaohsiung harbor Observing Station, Hsiokang Airport and Talin Power Plant resulted in the stability shown on the Table 3-6. In the data of the ground weather observation, Kaohsiung Observation Station was used to test the insolation. Therefore, the classification of stability was affected greatly by wind-velocity. Moreover, as the two points of Talin Power Plant's wind test were at 10 meters and 64 meters, the stability of the two points were different. The stability at the 64 meters point was almost one grade different from that at the 10 meters point. (Table 3-7)

Table 3-6 The comparison of stability at different place

Date	Hr.	Kaohsiung Harbor Station	Hsiokang Airport Station	Talin at 10 m	Talin at 64 m
Sept. 8	9 h	A - B	A - B	A - B	-
"	10	B	A	A	-
"	11	A - B	A - B	A - B	C
"	12	B	A - B	A - B	C
"	13	C - D	B - C	B	C - D
"	14	C	B	A	C
"	15	B - C	B	B	C - D
"	16	C	C	C	C - D
Sept. 9	9 h	A - B	A - B	A - B	B
"	10	B	A - B	B	B
"	11	C	B	B	C
"	12	C	B	B	C
"	13	B	B	B	C
"	14	B - C	B	B - C	C - D
"	15	B	C	B	D
"	16	B	C	B	D
Sept. 10	9 h	A	A - B	A - B	B
"	10	A - B	A	A	B
"	11	A	A - B	A - B	B
"	12	A	B	A - B	C
"	13	A - B	B	A - B	C
"	14	B	B	A - B	C
"	15	B	B - C	B - C	C
"	16	C	C	C	C - D
"	17	C	C	C	D

(Continues)

Date	Hr.	Kaohsiung Harbor Station	Hsiokang Airport Station	Talin at 10 m	Talin at 64 m
Sept. 11	9 h	A - B	A - B	A - B	-
"	10	A	A	A - B	B
"	11	A	A - B	B	B
"	12	B	A - B	B	C
"	13	B	B	B	C
"	14	B - C	C - D	B - C	C
"	15	C	C	C	D
"	16	C	C	C	C
"	17	B	C	C	D
Sept. 12	9 h	A	A	A	A - B
"	10	A - B	A - B	A	B
"	11	B	A	A	C
"	12	B	A - B	A - B	C
"	13	B	B	B	C
"	14	B	B	B	C
"	15	B - C	B - C	B - C	C
"	16	-	C	C	C
Sept. 13	9 h	B	B	A - B	B - C
"	10	A	A - B	A	B
"	11	B	A	A - B	C
"	12	C	B	A - B	C
"	13	D	C	B	C
"	14	D	C - D	C - D	C
"	15	D	C - D	C - D	C - D

Table 3- 7 The comparison of stability frequency at different height of Talin Power Plant

		The stability frequency at 64 m height							sum
		A	A - B	B	B - C	C	C - D	D	
The stability frequency at 10 m height	A		1	3		2			6
	A - B			4	2	7			13
	B			2		8	2	4	16
	B - C					3	1		4
	C					2	2	3	7
	C - D					1	1		2
	D								0
Sum		0	1	9	2	23	6	7	48

CHAPTER 4 ANALYSIS OF AIR POLLUTION OF KAOHSIUNG AREA

4-1 Characteristic of Pollution Kaohsiung Area

Kaohsiung is located at the southwest of Taiwan. From the Kaoping river in the east, Lu Chu Hsiang in the north to the Taiwan Channel in the west and south, its area is 438 square kilometers. The Kaohsiung city is the essential part of that area, and the second largest city of Taiwan, the biggest harbour and industrial centre. As the setting of export processing zones and southern industrial parks, investment comes from everywhere, making the city prosperous. But the problems of sewage and air pollution occur, too. Since the second harbour of Kaohsiung opened, it became the 10th biggest harbour in the world. The littoral area became the corridor of transportation, vessels, trucks and trains brought smoke and waste gas which worsened the air pollution.

In the field of suspended particulates' pollution (e.g. dust, smoke, fume), Kaohsiung area wins the highest acclaim. The cement factories and steel factories are the largest producers. As to the pollution of poisonous gas, this area has all kinds of them, such as SO_2, NO_x, F^-, and disgusting odors mostly coming from the thermal generators, petroleum treatment factories, fertilizer factories, aluminium factories and petro-chemical factories.

Table 4-1 Shows the pollution percentage (%) of various industries regarding air pollution in the Kaohsiung area.[8]

Table 4-1 Emission and percentage of air pollution materials of the Kaohsiung area industries

Kaohsiung area % emitted in 1976 — Polluting materials / Sources	Suspended particulates		Sulphur Oxides		Nitrogen Oxides		HC		CO	
	quantity tons/year	%	quantity tons/year	%	quanity tons/year	%	quantity tons/year		quantity tons/year	%
Thermal power production	1.03×10^4	28.5	2.6×10^5	74.6	2.87×10^4	59	1.39×10^3	5.4	1.54×10^3	4.8
Petroleum treatment	2.26×10^3	6.3	4.29×10^4	12.2	6.46×10^3	13.3	2.18×10^4	85.5	6.53×10^3	16.3
Steel industry	1.68×10^3	4.6	1.51×10^4	4.3	1.64×10^3	3.3	2.24×10^3	0.9	6.57×10^3	16.4
Chemical industry	1.06×10^3	2.9	2.58×10^4	7.3	3.1×10^3	6.25	1.38×10^2	0.5	1.91×10^2	0.4
Cement industry	1.67×10^4	46.3	3.55×10^2	0.1	5.62×10^3	11.5	0	0	2.27×10^4	57
Porcelain industry	8.89×10^2	2.5	2.66×10^4	0.7	6.47×10^1	1.3	3.99×10^2	1.5	1.56×10^3	4
Wood Industry	2.45×10^3	6.8	1.02×10^4	0.3	1.43×10^3	2.9	2.7×10^2	1	2.73×10^2	0.7
Others	7.65×10^2	2.1	7.5×10^3	2.1	1.08×10^3	3.2	1.27×10^3	5	1.15×10^2	0.3
Total	3.6×10^4	100	3.5×10^5	100	4.85×10^4	100	2.55×10^4	100	4×10^4	100

Up to the end of 1974, the population of Kaohsiung city was 972,828. And that of Kaohsiung county was 922,522. The population density of Kaohsiung city was 325.69 per square kilometer. The population increase rate of the city was 33.40% and the county's was 23.70%. The area of the city is 114 Km^2 with most of it developed and flat. And the county has an area of 2832.5175 Km^2 with 51.42% flat area, and the rest being hills and mountains. The unlisted area is about 62.59%. Because the factories are mostly gathered in concentrated area, pollution occurs easily.

According to the data for rainfall from the Kaohsiung weather station between 1970 and 1975, we know that except in 1971, the rainfall around the area was between 2000 to 2600 mm/year. This abundant rainfall is concentrated in June, July and August (except in 1970). Within the 3 months, the rainfall amounted to about 60-80% of the yearly amount. Aside from summer, there was little rain, especially from Jan. to Mar.. The average rainfall from Jan. to Mar. was less than 10 mm. According to the records of 1974, the wind at 8:00 AM was mostly north northeastern, east northeastern, northern, north northwestern and northeastern. That of 8:00 PM were mostly north northwestern, northern, north northeast. In general, the wind cam from north northeast, north northwest and north. There is very seldom a calm period. At 8:00 AM, the ratio of calm was about 1.657%. At noon, the ratio was zero. And at 8:00 PM it was about 3.57%. The wind speed in the morning and night was from 1 to 4 m/sec. And at noon was 3-4 m/sec.

Some brief points on the characteristics of the Kaohsiung area are:

(1) The factories are adjacent to the city. The popllution situation is complex with the concentrated population, industries, transportation and commercial affairs.

(2) The sulfur oxides and suspended particulates mostly come from the factories. The nitrogen oxides, hydrocarbon compounds, and CO mostly come from the traffic vehicles on a gradual basis.

(3) The big power plants emit the major part of the pollutants. But the smaller sources emit the high concentration because such sources are near the ground.

(4) The emission rate of pollutants remains stationary throughout the year. It is different from Japan and America for their heating equipment and severe climates cause high pollution in winter.

(5) With the petroleum treatment factory in the North Tawu Ind. park and the cement, wood, and porcelain factories under the northern wind, the city was in danger all the time. The Cheng Chen Ind. park in the city caused the high density pollution daily under the cycle of the wind. The power plants, littoral industrial park, Linyuan and Tafa park in the South caused little threat to the city. But there was harm to the interior-land area due to the sea winds which blew in approximately half of the time.

(6) This area has about 14% of the country's vehicles. As that figure rises rapidly, the pollution spreads everywhere in the area. The tendency of thermal photo chemical pollution such as oxidants and other active chemical species will be more serious in this sunny area.

(7) Disgusting smells were the most frequent source of complaint made by the inhabitants.

4-2 Determination of dispersion coefficients σ_y, σ_z and comparision with the Pasquill-Gifford's chart

4-2-1 General Aspects

With the dispersion experiment referred to in CHAP. 3, we understand the characteristics of the disperion field around the Talin power plant, especially the continuous variety of the upper wind field. Its variety directly effects the dispersion ability and the ground level concentration of the pollutants.

The upper wind field indicates that during the experiment period, except for a few times, the prevailing wind blew island, and the air current in the mixing layer was processing high convection, especially during the 6, 7, 8 and 14 runs, in which the rising air current was strong.

The stability of the upper atmosphere was always more stable in one grade than that near the ground surface. This can be shown from the observed data. Especially under the influence of the surface roughness and temperature profile in the coastal region, it is evident for the sea breeze fron to form and resist the pollutants from dispersing. In 24 runs using tracer, there were 16 runs in which the value of diffusion standard deviation in lateral direction Sigma-Y was calculated. However, using the meteorological data of 64 meters height in Talin power plant, the stability was analysed by cross reference to Pasquill and Gifford's classification, there were only 2 classes C-D and unstable B found, because the experiement was only carried in daytime. (refer to Table 3-6)

The determination of effective stack height and Sigma values shall be discussed in the next section in more detail.

4-2-2 The determination of effective stack height and dispersion coefficient Sigma Z

In this study, as there is no actual observation of plume rise, the determination way of H_e and sigma is stated as follows:

The tracer experiment resulted in the Tables and Figures of tracer concentration distribution (refer to Appendixes E and F), then we can read X_{max}, the maximum ground level cencentration contact distance. If this value is formulated in the following formula:

$$a_z X_{max}^{bz} = \sqrt{\frac{bz}{by + bz}} \cdot H_e \qquad (4\text{-}1)$$

a_z, b_z can be otained. However, if the SF6 releasing altitude is the constant one 100 M, it must be amended (refer to the followings) and revalue H_e. As the individual numbers of the data are not many, I will not classify the various tability B, C, or D, but see them as the mother group. Moreover, if the upper air σ_z will not change as the altitude Z changes (a_z, b_z will not change as the H_e changes). (h)

I. If Internal Boundary layer does not exist:

(1) The calculation of σ_z and H_e

If H_e = Run of 100 m, then

$$H_e = 100 + \frac{\alpha}{u} \qquad (4\text{-}2)$$

α should be calculated by the function of released heat but I hereby decide it as a constant value.

Table 4-1 show the relation between wind velocity and X max.

The Table shows that Xmax has to do with wind velocity.

From (4-1), (4-2) we know:

$$\epsilon = \left[X_{max} - \left\{ \frac{H_e}{a_z} \sqrt{\frac{b_z}{b_y + b_z}} \right\}^{\frac{1}{b_z}} \right]^2 \qquad (4\text{-}3)$$

If $0 < \alpha < 400$, hereby indicates a parameter, in addition as a value of minimum, a_z , b_z can be calculated.

Fig. 4-2 on the basis of the value of ϵ , indicates the relations among the parameters.

In runs of $H_p = 132m$, H_e is calculated with the experience formula.

From Fig.4-2 we know the smaller the α , the smaller the ϵ is.

The reasonable value is as follows:

$$a_z = 0.463, \quad b_z = 0.751, \quad \alpha = 320$$

However, assumed by = 0.9. From the foregoing result, if IBL does not exit, $\sigma_z = 0.463\ X^{0.751}$ can be gotten. The Table 4-3 (a) indicates that with the foregoing value of parameters, the X_{max} is calculated when

Data

Run No.	$X_{max(m)}$	U(m/s)
2	2591	2.7
3	2864	1.6
13	2180	2.0
22	1227	5.5
1	2045	2.7
7	2045	2.0
9	1227	3.0
10	2045	2.5
11	2045	3.5
12	1500	4.0
18	2454	2.5
4	5180	1.2
mean	2284	2.68

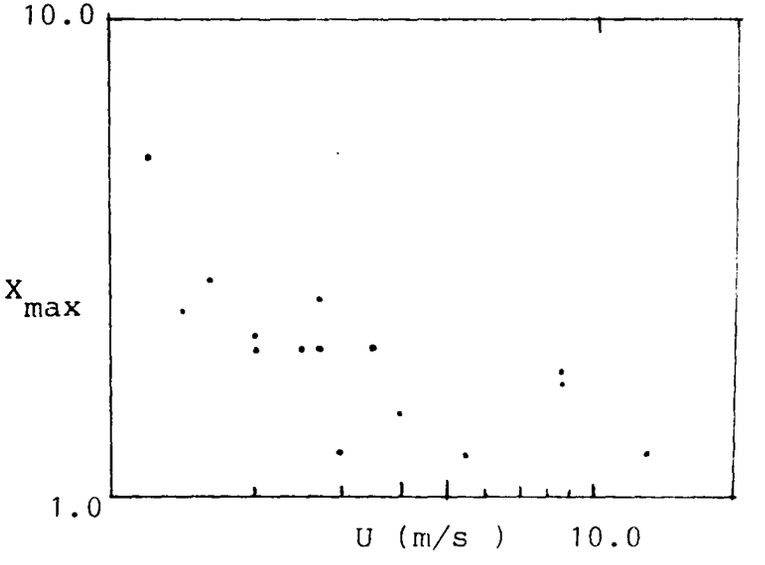

Fig. 4-1 When the trace is released in H_o = 100m, the relations between wind velocity and X_{max}.

Table 4-2 The determination of the distance of maximum ground concentration.

Run No.	Stability	H_0 or H_e (m)	Surface wind (m/s)	X_{max} (m)
1	C	100(219)	2.7	2045
2	B	100(219)	2.7	2591
3	B	100(300)	1.6	2864
4	C	100(367)	1.2	5180
5	C	362	4.0	1364*
6	C	582	2.0	--
7	C	100(260)	2.0	2045
8	B	1132	1.0	3136*
9	C	100(207)	3.0	1227
10	C	100(228)	2.5	2045
11	C	100(191)	3.5	2045
12	C	100(180)	4.0	1500
13	B	100(260)	2.0	2180
14	B	382	4.0	3820
15	C	100	3.5	--
16	C	492	2.5	5045
17	C	100	2.6	--
18	C	100(228)	2.5	2454
19	B	322	4.8	1636
20	C	100	4.6	--
21	C	322	4.6	3000
22	A	100(158)	5.5	1227
23	C	382	3.6	6818
24	C	332	4.6	5454

Note: ( ) indicates $H_e = 100 + \frac{320}{u}$

As *value does not belong to observed one in the stable air-flow, it is excluded.

Table 4-3-(a) indicates the Xmax value when the internal boundary layer does not exist.

Parameter condition	$a_z = 0.4775$ $b_z = 0.7502$ $b_y = 0.9$ (assumed)	
H_e (m)	235	370
X_{max}(km)	2.380	4.363

Table 4-3-(b) indicates that with the foregoing formula, the X_{max} is calculated when H_e= 235 m and 370 m.

H_e(m)	370			235		
P-G Stability	B	C	D	B	C	D
X_{max}(Km) by Formula(4-1)	2.34	6.27	25.39	1.545	3.79	12.35

Note: *This figure is calculated with 12 datum.

$$* \epsilon = \left[X_{max} - \left\{ \frac{100 + \frac{\alpha}{u}}{a_z} \sqrt{\frac{b_z}{b_y + b_z}} \right\} b_z^{\frac{1}{2}} \right]^2$$

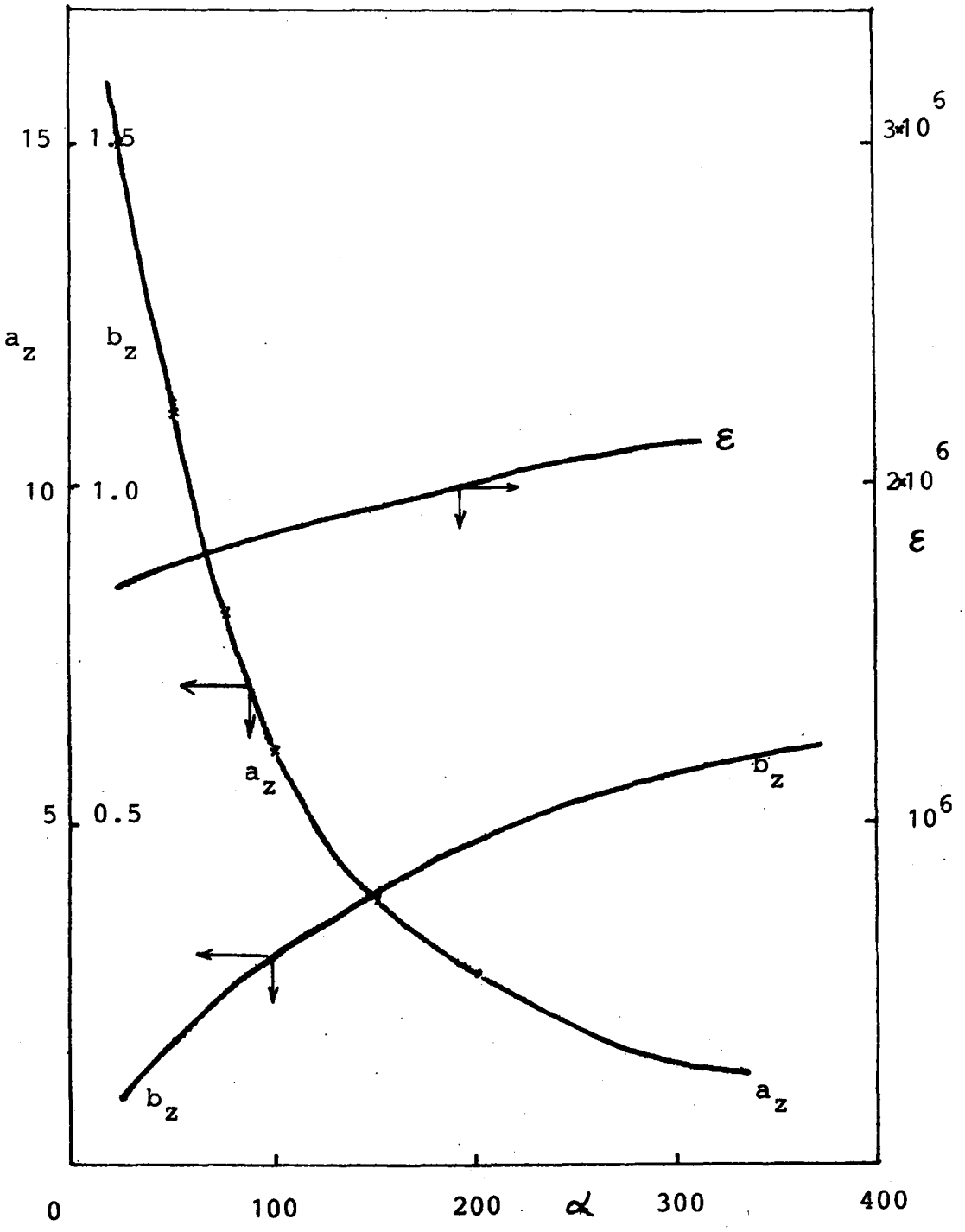

Fig. 4-2 ϵ value indicates the relations between a_z , b_z.

II. If it is the condition that internal boundary layer exists:

If we consider that the vertical concentration in IBL is the homogeneous condition (i.e. $0 < Z < h$ of IBL and concentration is homogeneous). The dispersion condition can be indicated with the following formula and Table:

$$C(x,0,z,) = \frac{Q}{\sqrt{2\pi}\ \sigma_y\ u\ h} \int_{-\infty}^{P_o} \frac{1}{\sqrt{2\pi}} \exp\left\{-\frac{P^2}{2}\right\} dp \qquad (4\text{-}4)$$

where,

$$P_o = \frac{h - H_e}{\sigma_z} \qquad (4\text{-}5)$$

$$h = d\sqrt{x} \qquad (4\text{-}6)$$

$$\left.\begin{aligned} \sigma z &= a_z\ X^{b_z} \\ \sigma y &= a_y\ X^{b_y} \end{aligned}\right\} \qquad (4\text{-}7)$$

H_e indicates the altitude of IBL, and the rest symbols as the same as before. The schematic diagram is as follows, (i)

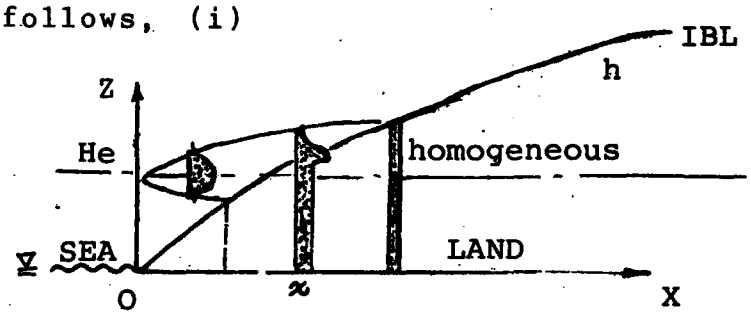

The max. cencentration of down wind ground can be calculated with the following formula:

If $\frac{dc}{dx} = 0$, and only if the x = x max,

$$\frac{dc}{dx} = 0 = \frac{Q}{\sqrt{2\pi}u}\left\{-\frac{(b_y + 0.5)}{y\ hx}\int_{-\infty}^{P_o}\frac{1}{\sqrt{2\pi}}\exp\left\{-\frac{P^2}{2}\right\}dp\right.$$

$$\left. + \frac{1}{\sqrt{2\pi}}\exp\left\{-\frac{P_o^2}{2}\right\}\cdot\frac{1}{\sigma_{yh}}\cdot\frac{\partial p}{\partial x}\right.$$

(4-8)

$$\frac{\partial p}{\partial x} = \frac{(0.5-b_z)}{\sigma_z\ X} + \frac{H_e\cdot b_z}{\sigma_z\cdot X}$$

$$\therefore\ \frac{by + 0.5}{\sigma_z\ hx}\int_{-\infty}^{P_o}\frac{1}{\sqrt{2\pi}}\exp\left\{-\frac{P^2}{2}\right\}dp$$

$$= \frac{(0.5 - b_z)h + b_zH_e}{\sqrt{2\pi}\ \sigma_y\ h\ \sigma_z\ x}\cdot\exp\left\{-\frac{P_o^2}{2}\right\}$$

$$\text{i.e}\int_{-\infty}^{P_o}\frac{1}{\sqrt{2\pi}}\exp\left\{-\frac{P^2}{2}\right\}dp$$

$$= \frac{(0.5 - b_z)\ h\ + b_z\cdot H_e}{\sigma z\ (b_y + 0.5)\sqrt{2\pi}}\cdot\exp\left\{-\frac{P_o^2}{2}\right\}$$

(4-9)

If we want to satisfy this formula, x = Xmax.

If we put He, α and the dispersion parameters into (4-5), (4-6) and (4-9), we can calculate the Xmax.

Table 4-4 indicates the X max that is calculated when H_e = 235m and 370m, α = 5.0 and 6.0 and the atmospheric stability is B, C, and D.

value is generally calculated with the data obtained from experiment. This time it was calculated on assuming of α = 4,6,8 respectively in order to realize the different α value; the relation with H_e and Xmax in the different IBL altitude, as Fig. 4-3, Fig. 4-3 indicates the mean Xmax value of IBL boundary and H_e= 132 m, H_e = 100 m.

Table 4-4-(a) Parameters and X_{max}

H = 370 m, $h = \alpha\sqrt{x}$ (α = 5.0, 6.0), The Xmax value						
P-G Stability	B		C		D	
a_z	0.057		0.1		0.40	
b_z	1.094		0.9		0.63	
b_y	0.865		0.9		0.89	
H_e	370		370		370	
α (assumed)	5.0	6.0	5.0	6.0	5.0	6.0
X_{max} (Km) from Form.(4-9)	2.33	1.88	3.75	3.05	5.87	4.54

Table 4-4-(b) Parameters and X_{max}

H_e = 235m, $h = \alpha\sqrt{X}$ (α = 5.0, 6.0), The Xmax value						
P-G Stability	B		C		D	
a_z	0.057		0.1		0.40	
b_z	1.094		0.9		0.63	
b_y	0.865		0.9		0.89	
H_e	235		235		235	
α (assumed)	5.0	6.0	5.0	6.0	5.0	6.0
X_{max} (Km) from Form.(4-9)	1.13	1.07	1.50	1.18	2.44	1.75

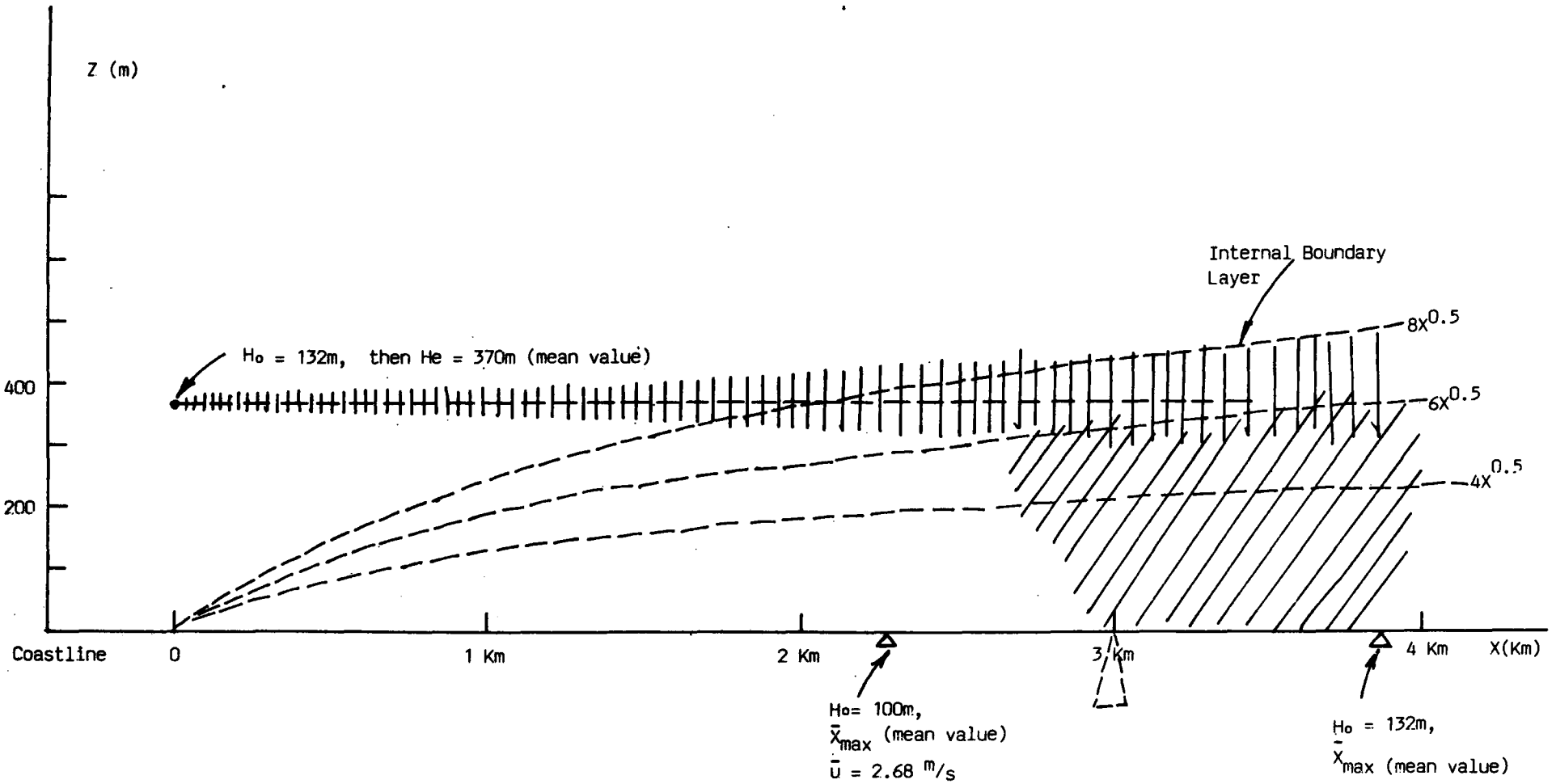

Fig.4-3 The schematic procedures of relations among supposed I.B.L. altitude, He and Xmax.

Table 4-4 is the diffusion formula that theorized IBL and calculates Xmax. This value indicates the limit value at the nearest smoke source only because it is impossible that the pollutants are mixed entirely in the vertical direction of IBL. However, Table 4-4 Assumes that it is mixed entirely. Therefore, Xmax value has the certain scope: it should be between the value from Table 4-3 and the one from Table 4-4. Fig.4-3 indicates the Xmax scope determined by a_z , b_z , b_y calculated by Table 4-3 and Table 4-4 on the basis of P-G stability classification and P-G chart. Xmax is apparently propotional to the H_e. Fig. 4-4 indicates $h = 6\sqrt{x}$. From this we know that the more the atmosphere is unstable, the more narrow the scope of it is.

Fig. 4-5, plots the relations between Xmax and He observed, The difference between the stabilities is not remarkable. The full line in the Fig. indicates the Xmax scope when stability C (refer to Fig. 4-4). From this Fig. we know som observed value is distributed in class C for the most part.

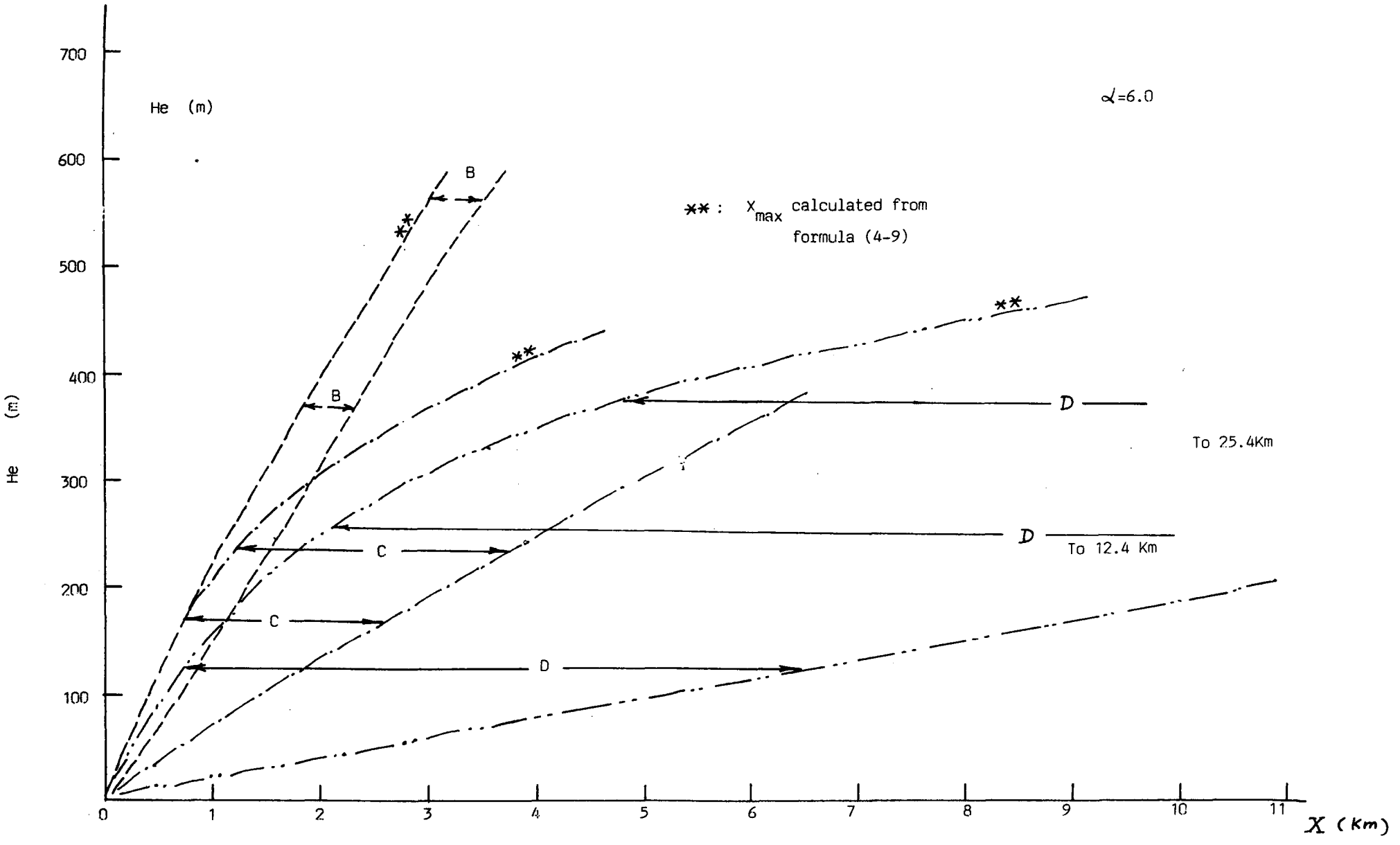

Fig. 4-4. The X_{max} possible scope of B,C, and D P-G stability class

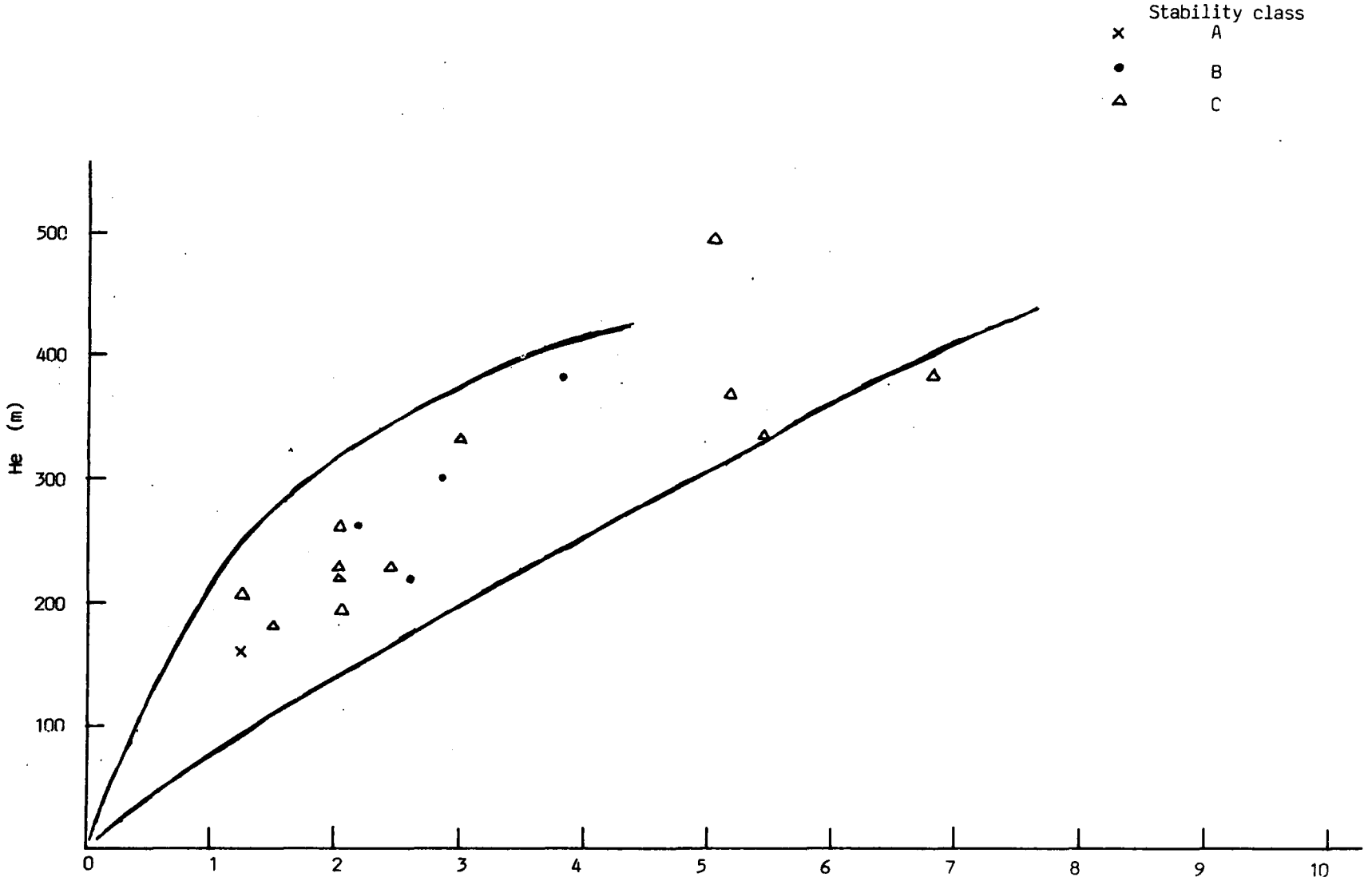

Note : Stability when Ho = 100m, to amend He with $He = 100 + \frac{320}{u}$ (m)

Fig. 4-5 The relations between Xmax and He

III. Conclusion

As Table 4-3 (a) shows, in the condition when the internal boundary layer is not formed, the comparison between the σ_z distribution of stability c in a_z = 0.478, b_z= 0.750 and P-G Chart calculated from the concentration value tested by tracer is as follows:

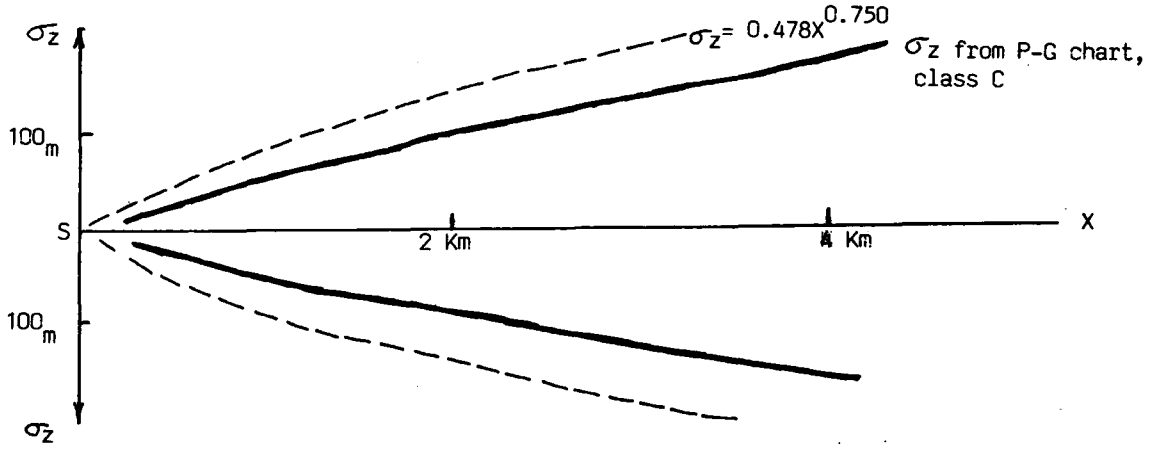

From this diagram, we know the σ_z value calculated from observed value diffused quickly near the smoke source and then went parallelly to σ_z in P-G Chart. This difference can be explained as follows:

(a) It indicates the characteristic of diffusion field in the tropical climate area.

(b) In the case of the outside of IBL, P-G Chart can be applied. However, if the IBL exists, the fumigation is reflected by parameters. Because, in the study period, the wind from sea to land prevailed and this area is near the sea, it is reasonable there is the effect caused by IBL near sea. Table 4-4 indicates the postulation that $h = 6\sqrt{x}$. From Table 4-5, we know that the Xmax value from observed value is distributed in

the scope of P-G stability C class for the most part. Estimating from this, we know the function of fumigation caused the max. cencentration ground contact point to go near smoke source. The IBL scope is not over 10 Km and IBL formation gives the quite complicated effect on diffusion. Therefore, there are many things to be studied because it does not attain the stage that it can be combined with dispersion model for practical use.

Therefore, if we estimate the effect caused by the smoke source difusion in some down wind point, we may use the diffusion parameter value observed and analysed directly. In case of the area or weather condition which cannot be tested and analysed, it should be amended on the basis of P-G Chart. Due to the strong insolation in Kaohsiung area, if we consider the diffusion above 200 - 300 m in the air, the result studied and analysed may be considered as the one which is more unstable than that of stability C and should be amended. The next Chapter will compare the difference of the diffusion characteristics between North Taiwan and Japan area.

4-2-3 The determination of dispersion coefficient Sigma Y and another method to determine Sigma Z.

The form of the gaussian plume diffusion equation recommended for use by Turner and others for a continuous elevated point source is:

$$C(x, y, z; H_e) = \frac{Q}{2\pi\sigma_y \sigma_z U} \exp\left[-\frac{1}{2}\left(\frac{y}{\sigma_y}\right)^2\right] \left\{\exp\left[-\frac{1}{2}\left(\frac{Z - H_e}{\sigma_z}\right)^2\right] + \exp\left[-\frac{1}{2}\left(\frac{Z + H_e}{\sigma_z}\right)^2\right]\right\} \quad (4\text{-}10)$$

The maximum surface concentration will occur along the centerline of the plume. This concentration may be obtained by setting y and z equal to zero in Eq. (4-10).

.The result is

$$\frac{xU}{Q} = \frac{1}{\pi \sigma_y \sigma_z} \exp\left[-\frac{1}{2}\left(\frac{H_e}{\sigma_z}\right)^2\right] \quad (4\text{-}11)$$

where Q : emission rate of pollution source

U : speed of wind

H_e : the effective stack height

X : the downwind distance from the source

σ_y, σ_z : the standard deviation in the crosswind and vertical direction of the plume concentration distribution.

The surface concentration is obtained from Eq. (4-10), also we may rewrite it as suppose Z = 0, that is

$$C\ (x,y,0;\ He) = Ca\ \exp\ (\ -\frac{y^2}{2\ \sigma_y{}^2}\ ) \qquad (4\text{-}12)$$

where

$$Ca = \frac{Q}{\pi\ \sigma_y\ \sigma_z\ U}\ \exp\ (-\ \frac{He^2}{2\ \ \sigma_z{}^2}\ ) \qquad (4\text{-}13)$$

Ca is called Axial Concentration or Centerline Concentration, is the function of downwind distance.

The accumulated value of Y direction C_{cic} can be determined by following

$$C_{cic} = \int_{-\infty}^{\infty} C\ (x,y,o)dy = \sqrt{2\pi}\ \ \sigma_y\ \ Ca \qquad (4\text{-}14)$$

putting Eq. (4-14) into Eq. (4-13), then we get

$$\frac{C_{cic}}{Q}\ \ \frac{U\ H_e}{2} = t\ \phi(t) \qquad (4\text{-}15)$$

where,

$$t = \frac{He}{\sigma_z}$$

$$\phi(t) = \frac{1}{2\pi} \cdot\ \exp\ (\ -\frac{t^2}{2}) \qquad (4\text{-}16)$$

We may know the distributing situation of surface

concentration. As dispersion formula assumes its concentration as regular distriubtion, these unkown figures should take adequate digital value in testing the distribution of surface concentration to apply t/z as regular distribution.[19]

From the survey of surface concentration distribution, in the direction of y applicable to regular distribution in y=0, it is easier to obtain the centerline concentration Ca and standard diviation σ_y. Furthermore, although it may presume the value of x from Eq, (4-1) as to whether the vertical direction is applicable to regular distribution, there seems to be a problem before understanding the atmospheric surrounding layer situation. It will be more suitable to obtain distributing pattern out of testing value.

Consequently, in setting up sampling network, it should be considered likely to appreaise the centerline concentration at y=0 and the maximum interval of σ_y value. According to the characteristics of regular distribution, at least there are three points of highly reliable testing value at regular distributing curve; thus, the Ca and σ_y value may be acquired from the relative concentration and interval distance at the three points.[20]

Usually, σ_y value and one tenth concentration v ry with atmospheric stability, wind downward distance. Therefore, from tracer scattering time it may predict predict dispersion volume and decide the interval between testing stations, i.e. the interval of sampling points.[21]

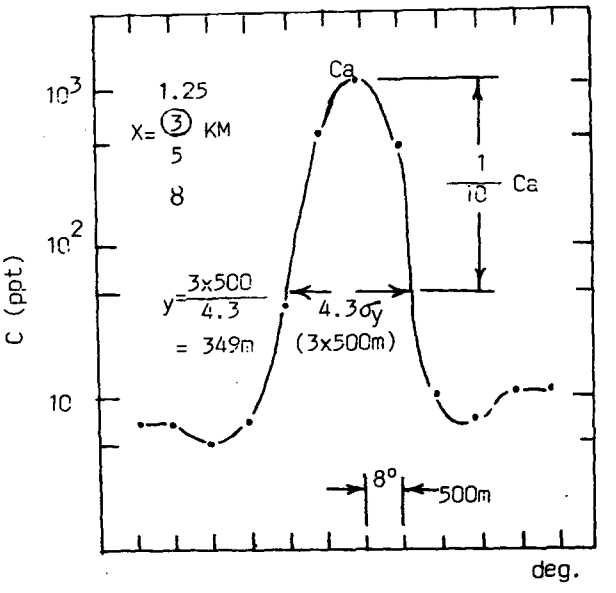

An example showing how to determine σ_y

The upper diagram shows an example as how to determine σ_y value in this study, in this section we also try to use Eq. (4-16) to calculate σ_z as a comparison with Section 4-2-2, Table 4-5 shows the results.

In Table 4-6, two Sigma-Y values at 3 and 5 Km are near to the σ_y of class B either by P-G CHART or Briggs' Equation, however σ_y at 8 Km is quite different. In the case of class C-D, the gained σ_y value is different from those of P-G or Briggs' value. (refer to Fig. 4-6 and Fig. 4-7)

In other words, when a large air mass is unstable and the downwind distance from the source is small, the gained dispersion width, Sigma-Y value, and the value calculated from the P-G CHART or Briggs' formula is roughly equal. But when it is stable, the difference is large, and moves in the unstable side one grade.

Table 4-5. Calculated σ_y and σ_z value

RUN NO.	downwind distance(Km)	Stability	σ_y	σ_z**
2	3	C-D	350	35
10	3	C-D	523	33
11	3	C-D	311	35
8*	3	B	410	-
9	3	B	383	36
18	3	B	514	26
4	5	C-D	422	38
5*	5	C-D	647	237
10	5	C-D	610	40
11	5	C-D	647	41
12	5	C-D	573	31
19*	5	C-D	735	161
21*	5	C-D	832	195
38*	5	B	951	-
9	5	B	685	38
13	5	B	501	35
14*	5	B	547	156
10	8	C-D	1051	36
11	8	C-D	933	38
12	8	C-D	633	30
19*	8	C-D	970	169
22	8	C-D	1190	34
8*	8	B	1394	-

* tracer released from stack (132 m Height)

** this σ_z value calculated only for the comparison with which got from section 4-2-2 as reference use

Table 4-6. Compare the σ_y value among P-G CHART value, Briggs' Eq. value and observed value

downwind distance (Km)	A	A-B	B	C	C-D	D
1.25	260	-	190	128	105	85
	-	327	255	163	137	112
	-	-	-	-	-	-
3.00	550	-	425	285	230	188
	-	647	445	324	273	222
	-	-	(436)	-	(394)	-
5.00	870	-	670	450	370	300
	-	924	635	462	390	318
	-	-	(671)	-	638	-
8.00	1300	-	970	690	560	455
	-	1249	859	625	527	429
	-	-	(1394)	-	(960)	-

NOTE: UP - Pasquill-Gifford
MIDDLE- Briggs
DOWN-Mean value of this experiement

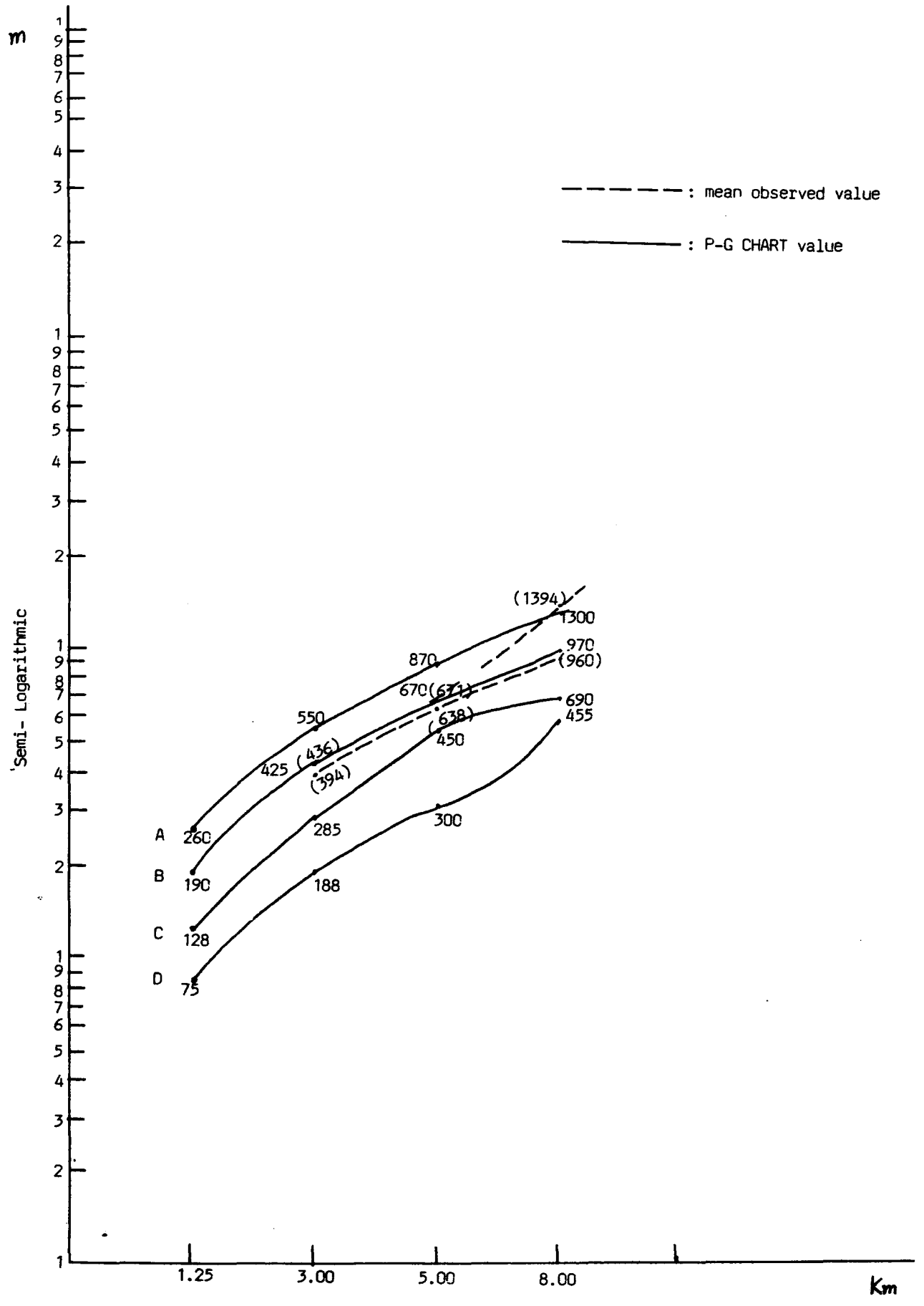

Fig. 4-6 The comparison between observed σ_y and P-G CHART value

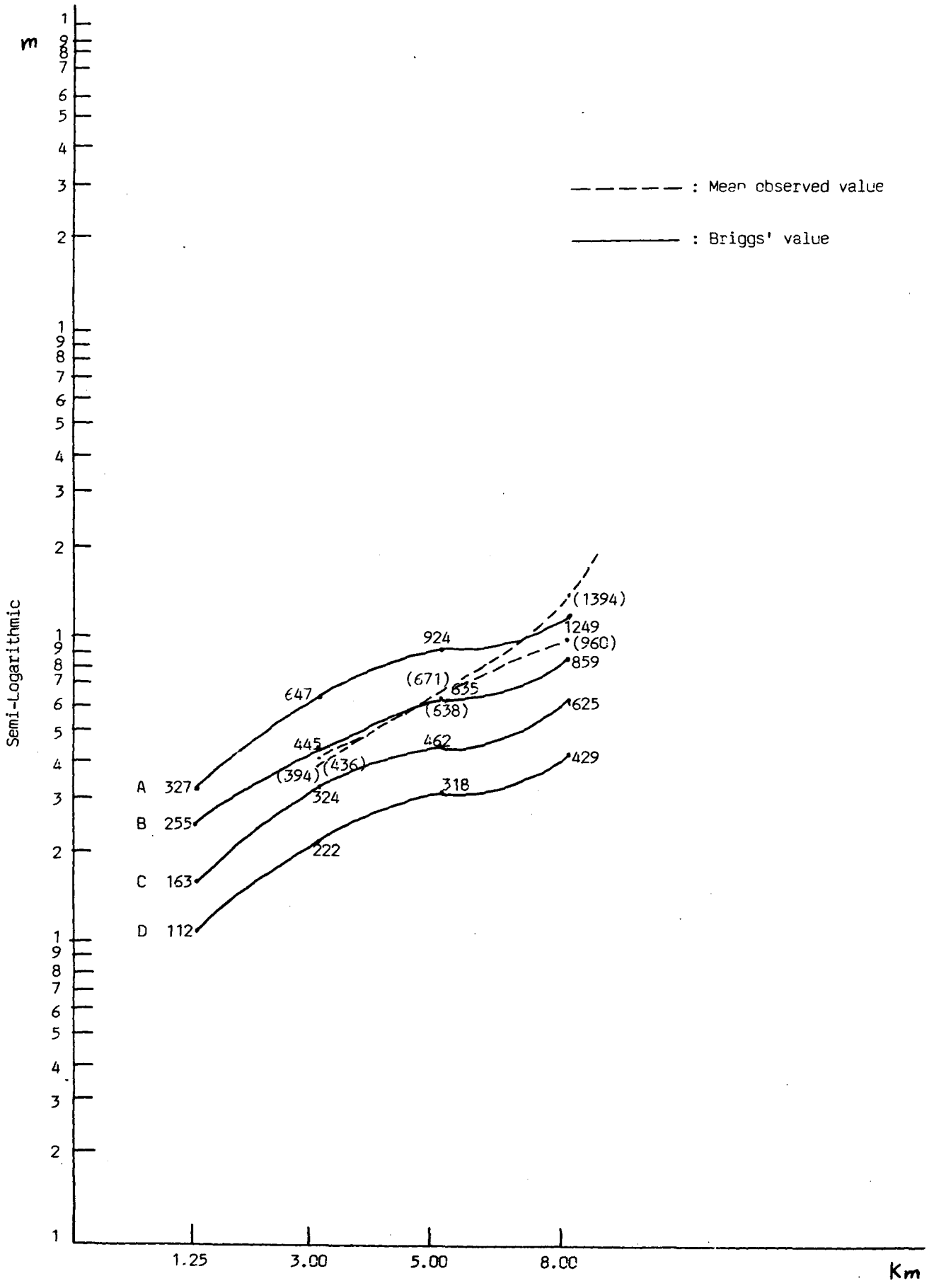

Fig. 4-7. The comparison between observed σ_y and Briggs' value.

Moreover, when we use the value Sigma-Y to show as the linear function of the downwind distance X, i.e. Sigma-Y = bx as shown in Fig.4-8, the b value of the proportional coefficient is 0.11 for the near distances (below 5 Km), regardless of whether the P-G stability class is B or C-D. If it is over 8 Km, it moves one grade in the unstable direction, and it is prone to increase.

This phenomenon is similiar to the dispersion of smoke when the high flowing smoke goes into the interior boundary layer, which the author wants to discuss in more detail in the next section.

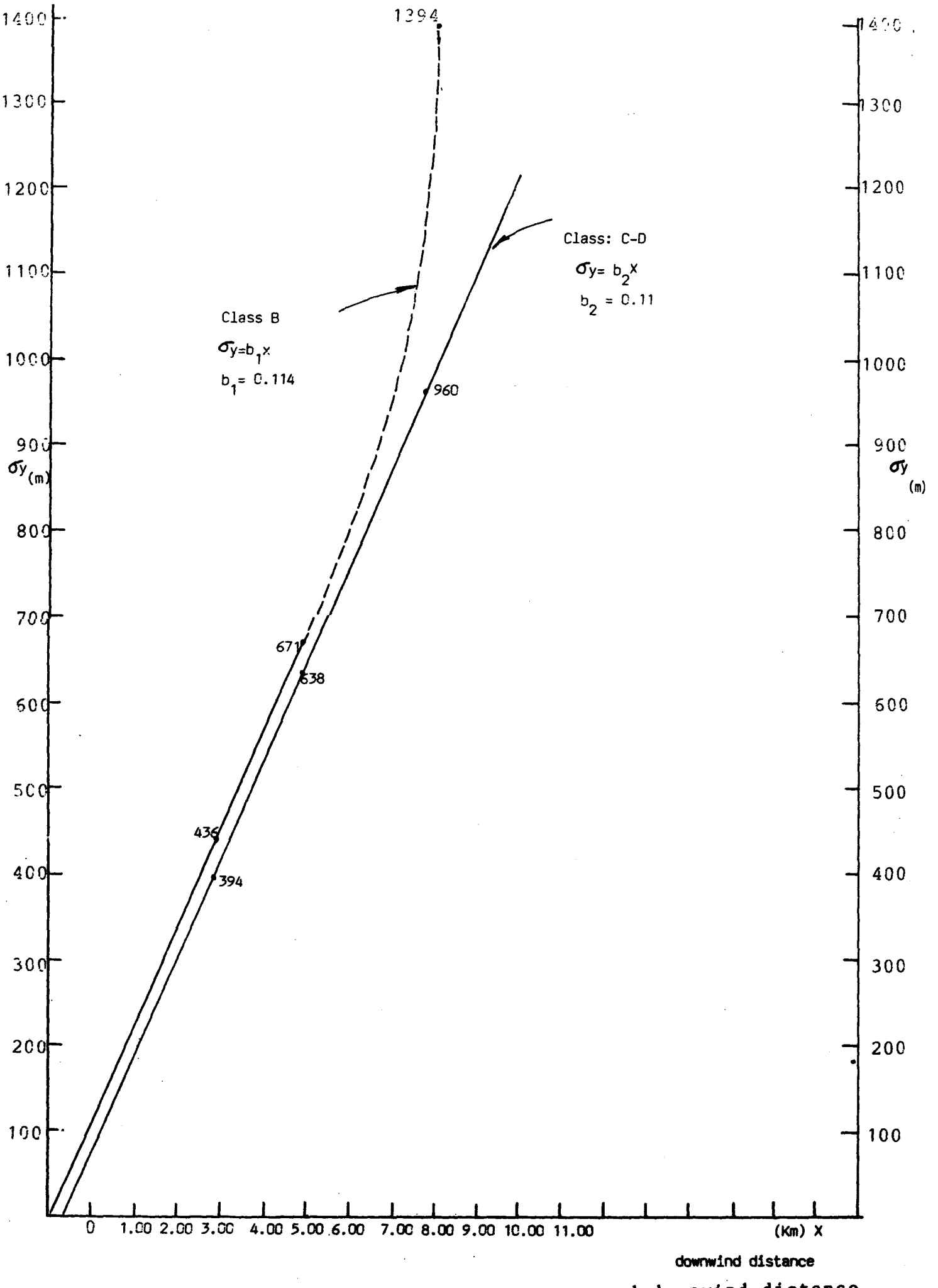

Fig. 4-8 The relation between σ_y and downwind distance

4-3 Fumigation phenomena of Kaohsiung littoral area

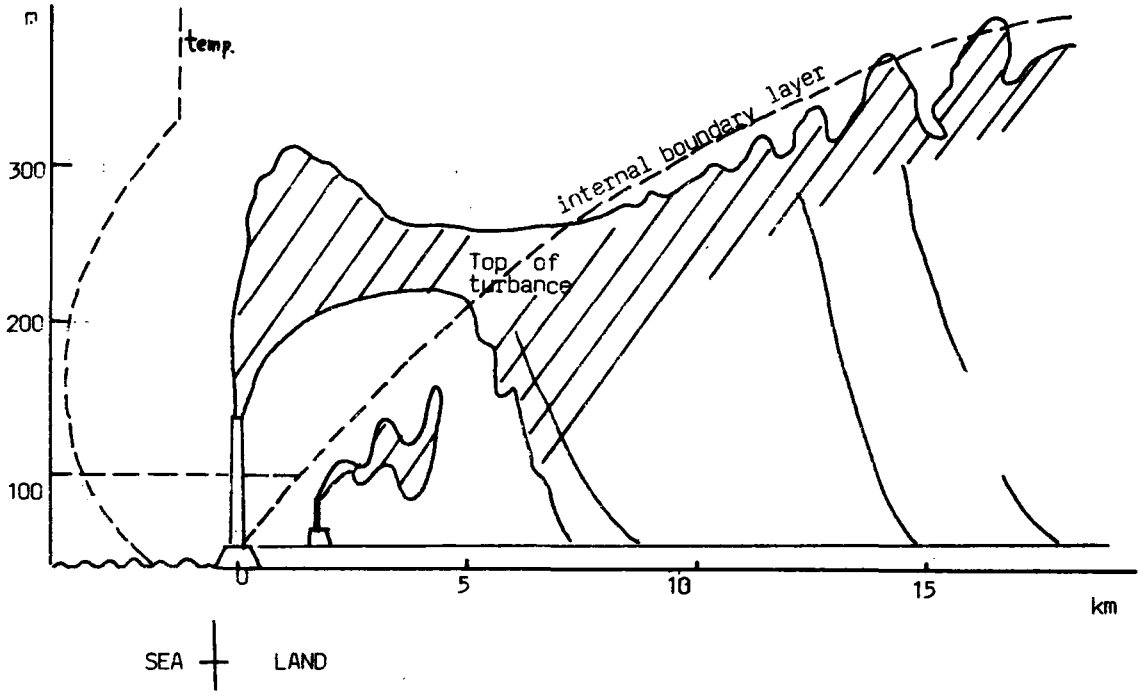

As the upper figure shows, the region near the seashore is subject to the sea wind. In the direction of the inland, the internal boundary layer is formed and the smoke flowing in the internal boundary layer easily disperses. When the smoke flowing beside the boundary layer goes near the boundary layer, its dispersion range is small. After it goes into the boundary layer, its dispersion range increases. As the internal boundary layer is generally influenced by solar radiation and convection, high concentration by funigation is likely to appear.(j,k) (22,23)

From the result of previous section, we see that the σ_y and σ_z values are larger with downwind distance, and it is likely to increase drastically from about 5 Km.

Talin power plant is located at the outside of the internal boundary layer. When the atmosphere is unstable

in the near distance, the dispersion parameter Sigma-Y can be estimated by the P-G or Briggs' formula. However, if it is in the far distance, because the atmosphere is stable, the dispersion parameter Sigma-Y is higher than the calculated value of the two methods. Furthermore, to analyse it from the point of view of the weather in the Kaohsuing region, the smoke flowing from the Talin power plant which is prone to affect the urban district should be in the SSE-SSW wind cirection.

The frequency of the wind direction is 2% in winter, 8% in spring, 14.4% in summer and 4.1% in autumn (refer to Table 2-2). Due to the greater frequency in summer, the smoke flowing from the Talin power plant will effect the urban district during the summer.

On the other hand, when we review the ground contact point and the concentration of the smoke at ground level at the Talin power plant (refer to Table 4-7), we find that when the effective stack height is at 300-400 m, its ground contact point is 8000-10000 m away. When the effective stack height is over 400-m, the ground contact point moves to 10-15 Km away. When the height is 1000m or more, the ground contact point moves to over 30Km away.

In this experiment, the plume rise was not observed, but estimated by Brigg's formula and others as shown in Table 4-7 and Table 4-8. The maximum concentration of ground level is below 0.03 ppm.

Using the Texas Climatological Model (TCM) as abstracted in APPENDIX G, the author Tries to find the long-term mean concentration of tracer as shown in APPENDIX H, the results are very similiar with that shown in APPENDIX F which are obtained from the experiment.

Table 4-7 Calculated effective stack height by Briggs' Equation and C_{max}, X_{max}

RUN NO.	wind speed (m/s)		stability class	H_e (m)	C_{max}			X_{max} (m)
	U	$\bar{U}$			S=3.5%	S =3.32%	S = 2.0%	
5	7.6	5.8	C	362	0.0263	0.0250	0.0150	9475
6	3.8	2.9	D	582	0.0204	0.0193	0.0116	16303
8	1.7	1.3	B	1132	0.0120	0.0114	0.0068	34871
14	6.8	5.4	B	382	0.0264	0.0251	0.0151	10076
16.	4.8	3.7	D	492	0.0226	0.0214	0.0129	13455
19	9.1	7.0	C	322	0.0278	0.0264	0.0159	8288
21	8.7	6.7	C	332	0.0274	0.0259	0.0156	8583
23	6.8	5.2	C	382	0.0264	0.0251	0.0151	10076
24	8.7	6.7	C	332	0.0274	0.0259	0.0156	8583

Note:(1) Wind speed: $U_T = U_{10}(\frac{132}{10})^n$, n = 0.25 (assumed)
(at the top of stack)

(2) $\Delta H = 0.25 Q_H^{\frac{1}{3}} H_O^{\frac{2}{3}} U_T^{-1}$ $Q_H = \rho . Q . Cp . \Delta T$

(3) Concentration : $Xmax = (\frac{H_e}{Cz})^{2T/2-n}$, Cz = 0.12, n = 0.25

(4) max. concen. of ground level: $Cmax = 0.234\, Q_s/UH_e^2$

Table 4-8. Ratio of calculated to observed plume rise in neutral conditions

Formula	Reference (all data)	Reference (select)
Holland	0.44±37%	0.47±26%
Moses & Carson	0.54±34%	0.48±19%
Priestley	1.44±26%	1.41±18%
Lucas, et, al.	1.36±21%	1.24±22%
" Stumke	0.79±27%	0.72±24%
Briggs (1970)	1.12±17%	1.13±6%
Lucas	1.18±20%	1.16±14%

* G.A. Briggs (1970). p22, Table 2.

** G.A. Briggs, plume Rise, AEC Critical Review Series, JIP-25075, (November, 1969).

From the above conclusion, we find that when the high flowing smoke penetrates in the internal boundary layer, special phenomenon caused by this will appear. That is, when the internal boundary layer is formed, turbulence intensity between the upper layer and under layer is very different, therefore in the area downwind from the pollution source over 5 Km, the fumigation is formed.

CHAPTER 5 ANALYSIS OF AIR POLLUTION OF TAIPEI AREA

5-1 Characteristic of Pollution of Taipei Area

In Taiwan, the two most populated centers, Taipei and Kaohsiung area, are generally regarded as the sites of the more serious air pollution problems. Characteristic of pollution differ sharply between the two locations as shown in Table 1-2 .

In Taipei, automobiles are responsible for over 90 percent of the total pollution tonnage, with carbon monoxide and hydrocarbons dominating. Because of climatic conditions in Taipei, sulfur dioxide levels tended to peak in mornings and evenings, reportedly exceeding 0.05 ppm in 1982 in annual average. This means, though, that the overall levels were within the 0.14 ppm maximum 24-hour concentration and the 0.03 ppm annual arithmetic mean allowed by R.O.C. ambient air quality standards (general environment). In 1970, the annual average hourly concentration in Taipei City was estimated to be 0.044 ppm, and the levels remained high until about 1973 when a slow decent began, and could meet NAQS. Level of carbon monoxide (CO) in Taipei are high, averaging about 10 ppm for any 24-hour period and reaching a high of about 40 ppm on Chung Shan North Road, a major "Hot spot".

Between 1970 and 1978, concentrations of sulfur dioxide dropped drastically in the city of Taipei, but levels in Taipei County remained high. Elsewhere, levels alternately rose and fell, appearing more influenced by meteorological condetions than long-term factors.

5-2 The SF 6 Tracer Experiement at Littoral Industrialized Area of Taipei

5-2-1 The outline of tracer experiment

In order to compare the difference between the diffusibility of pollution ingredient in northern part of Taiwan and in southern part of Taiwan as affected by weather, geographic and other factors, the scheme of tracer experiment at Ta Lin Firepower Plant, Kaohsiung and the one at Lin Kou Firepower Plant in 1981 and Jan. 25, to 27, 1983 respectively were carried out. The data of Linkou No. 1 Generator representing the exhausting source of SF6 is shown in Table 5-1 below:

Table 5-1 The data of Linkou No. 1 generator

Stack Height	70 m
Stack top diameter	3.2 m
Exhausting temperature in stack	130°C
Exhausting speed	8.2 m/s
SO_2 emission	299 gr/s

The overlay of experiment is shown as Table 5-2:

Table 5-2 The scheme of tracer experiment at Taipei littoral area in 1983

Run No.	Date & Time	Wind Dire. & Speed	Pasquill stability	Mixing height (M)	Run No.	Date & Time	Wing Dire. & speed	Pasquill Stability	Mixing height (M)
1	Jan. 25 1100	40° 70m/s	D	1000	11	1500	45 8.0	D	670
2	1200	40 7.0	D	1030	12	1600		C	
3	1300	40 7.0	D	1030	13	Jan. 27 1030	70 3.0	C	1020
4	1400	40 7.0	D	1030	14	1130	45 4.0	C	1030
5	1500	40 7.7	D	1100	15	1230	30 4.0	C	1080
6	1600	40 7.0	D		16	1330	30 3.5	C	1030
7	Jan. 26 1100	45 7.7	D	600	17	1430	30 3.5	C	1030
8	1200	45 8.0	D	600	18	1530	30 3.5	C	1070
9	1300	45 8.0	D	630					
10	1400	45 9.0	D	630					

Release rate of tracer : 7.2 kg/hr

Release height : 70 m (inside the stack)

Sampling time : 15 min.

A sampling network is shown in Fig. 5-1, and the Linkou Power Plant is made as the originated point. 46 sampling stations are installed from the point toward the south-west in distances of 3,4,5, 8 and 12 km respectively. In addition to the above, there 9 pollution ingredient and meteorological observation stations installed.(1) Figure 5-2 shows the terain at Littoral area of Northern part of Taipei.

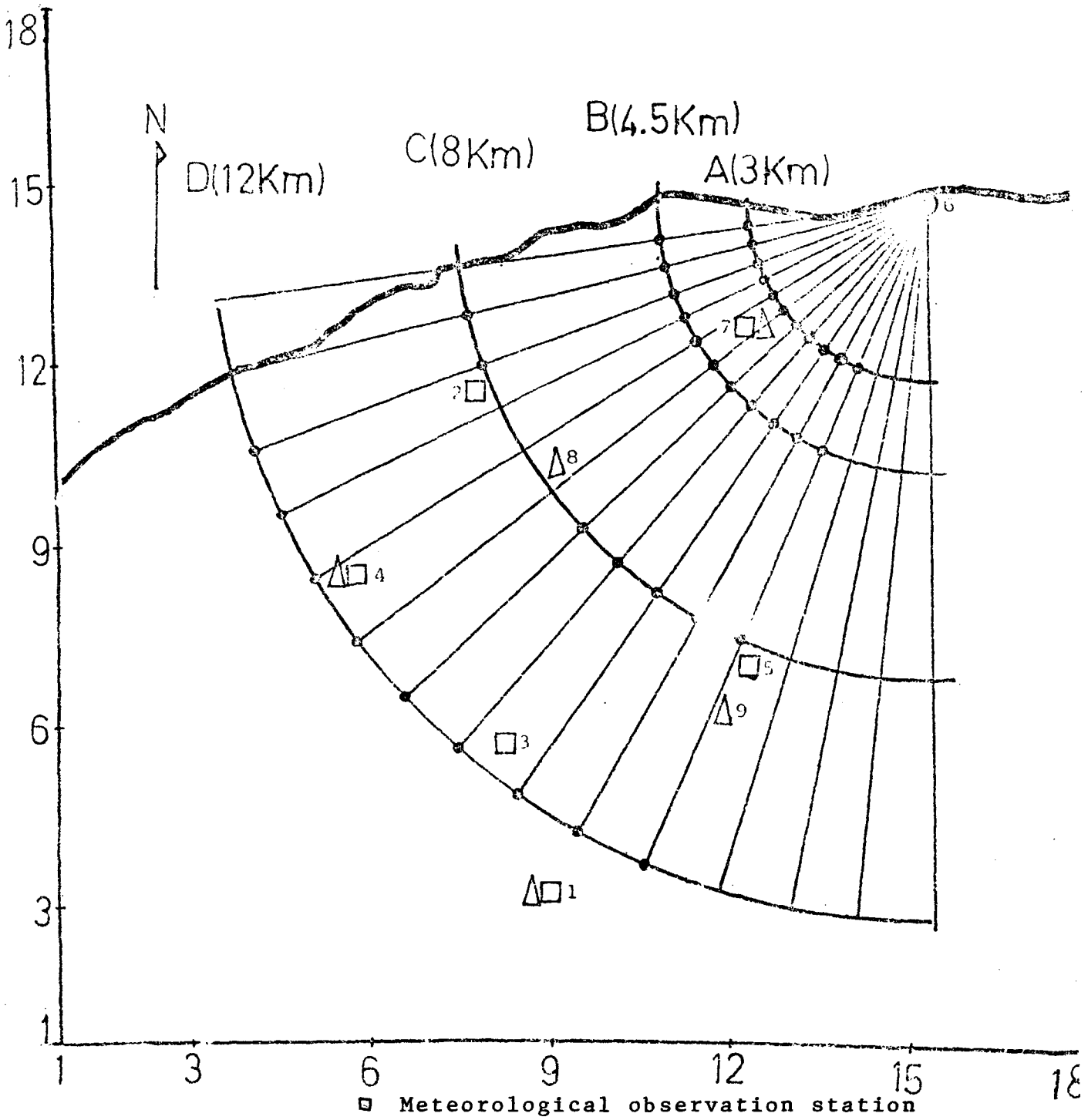

□ Meteorological observation station

△ SO_2 observation station

• SF6 survey station

1. WU CHUAN Primary School
2. SHALUN Primary School
3. CHEN KANG Primary "
4. TAYUAN Industrial Area
5. LUCHU Primary School
6. LINKOU Power Plant
7. HAIHU Primary School
8. CHIANG KAI-SHEK Air Port
9. TA HUA Transform er House

Fig. 5-1 The Layout of meteorological O.S. and Sampling Net Work

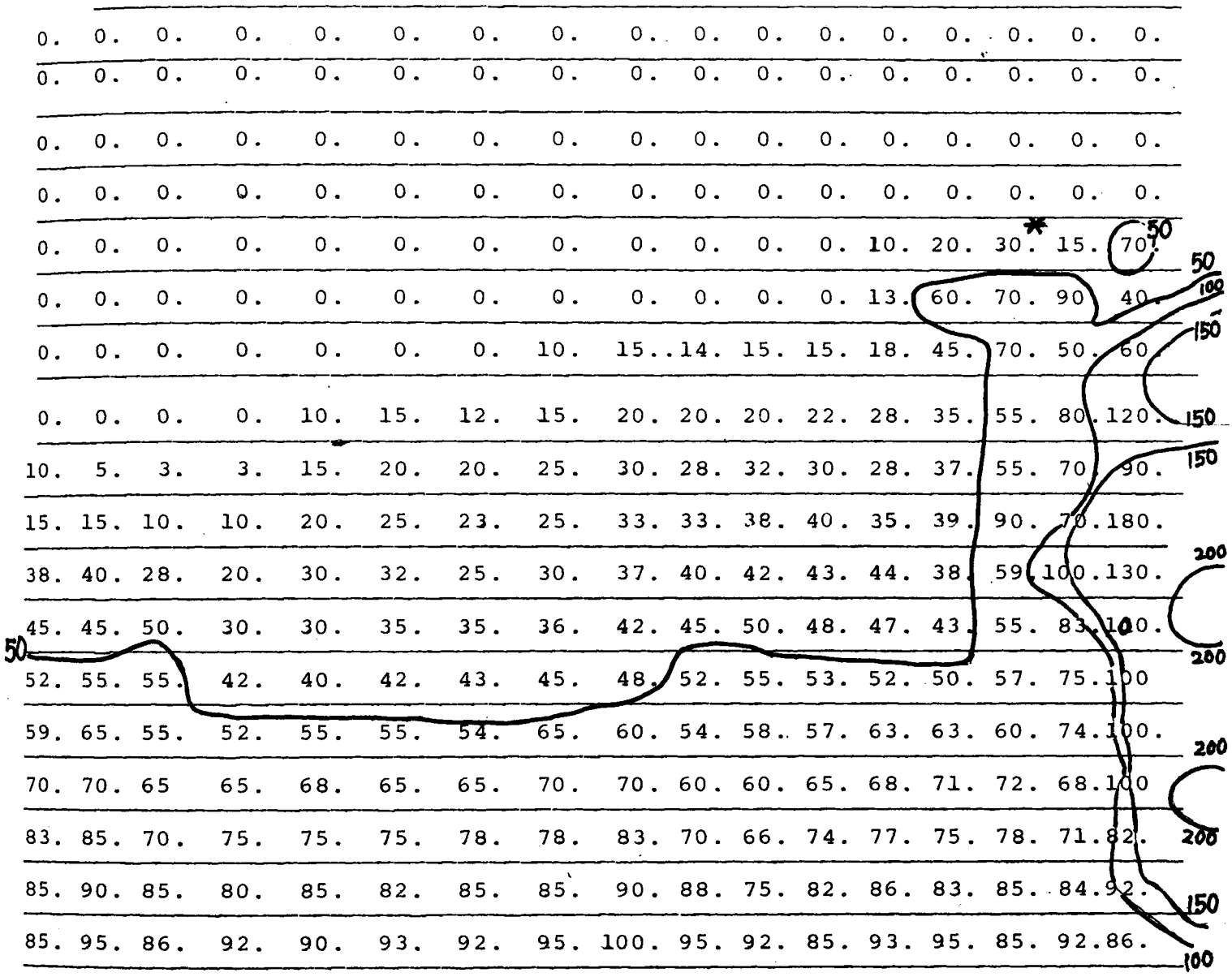

Unit : m

* LIN KOU Power Plant

Fig. 5-2 Diagram of the Terain at Littoral Area of Northern Part of Taipei

5-2-2 The observation of Meteorological Condition of Taipei Area

In Winter, the weather condition in Taipei Area, espesially the wind field, is completely dominated by synoptic current, which is obtained by the analysis of diagram of ground surface weather. The following is the status of weather in these five days. (refer to Fig. 5-3)

Jan. 24, High barometric pressure of 1033 mmb located at 33 of north latitude and 121° of east longitude, at littoral area of Kiangsu Province, slowly moving toward the east. Another high pressure of 1042 mmb, located at 41° of north latitude, 111° of east longitude at the center of south Mongolia, nealy staying. As affected by the changeable air mass from mainland, the weather of various places in Taiwan turns out from being cloudy to being clear and the temperature turns out be high again. In central and southern part of Taiwan, dense fog is partly existed. It is a rainy weather in experiment area. Wind direction is toward the northeast and wind speed is 7 m/s.

Jan. 25, High pressure 1034 mmb at 29° north latitude, 120° east longitude at Chekiang Province, slowly moving toward east. Another high pressure 1039 mmb at 39° north latitude 109° east longitude at center of southern part of Mongolia, nearly staying. As affected by the weak northeast monsoon, except being cloudy and partly rainy at east part, it turns out from being cloudy to being clear at other areas. During daytime, temperature turns out to be high again. The weather is cloudy after raining at experiment area. Wind direction is northeast. Average wind speed is 6 m/s.

Jan. 26, High pressure 1032 mmb at 30° north latitude, 122° east longitude, at Chekiang Province, slowly

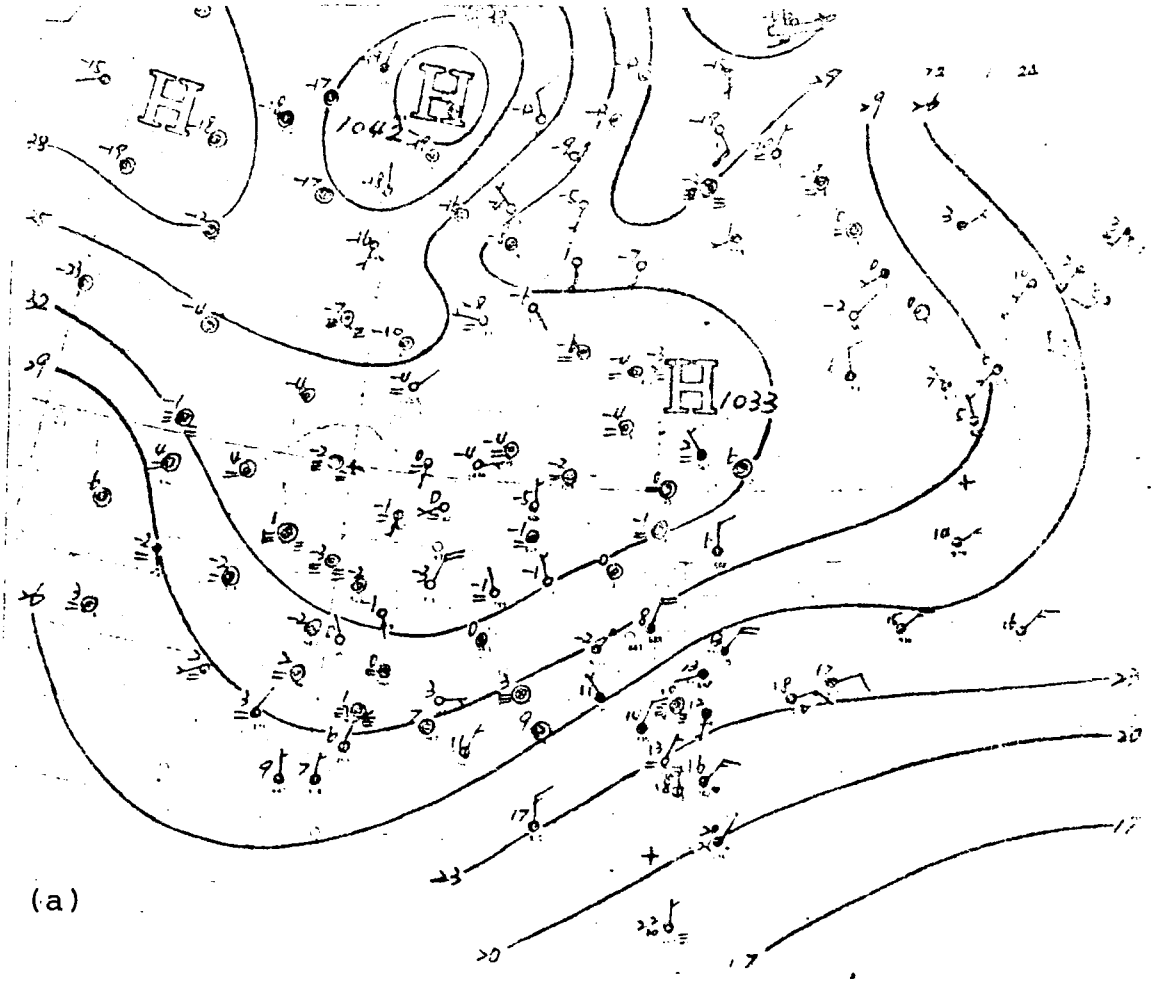

Fig. 5-3 Ground surface weather of Jan. 24-Jan. 28 (a-e)

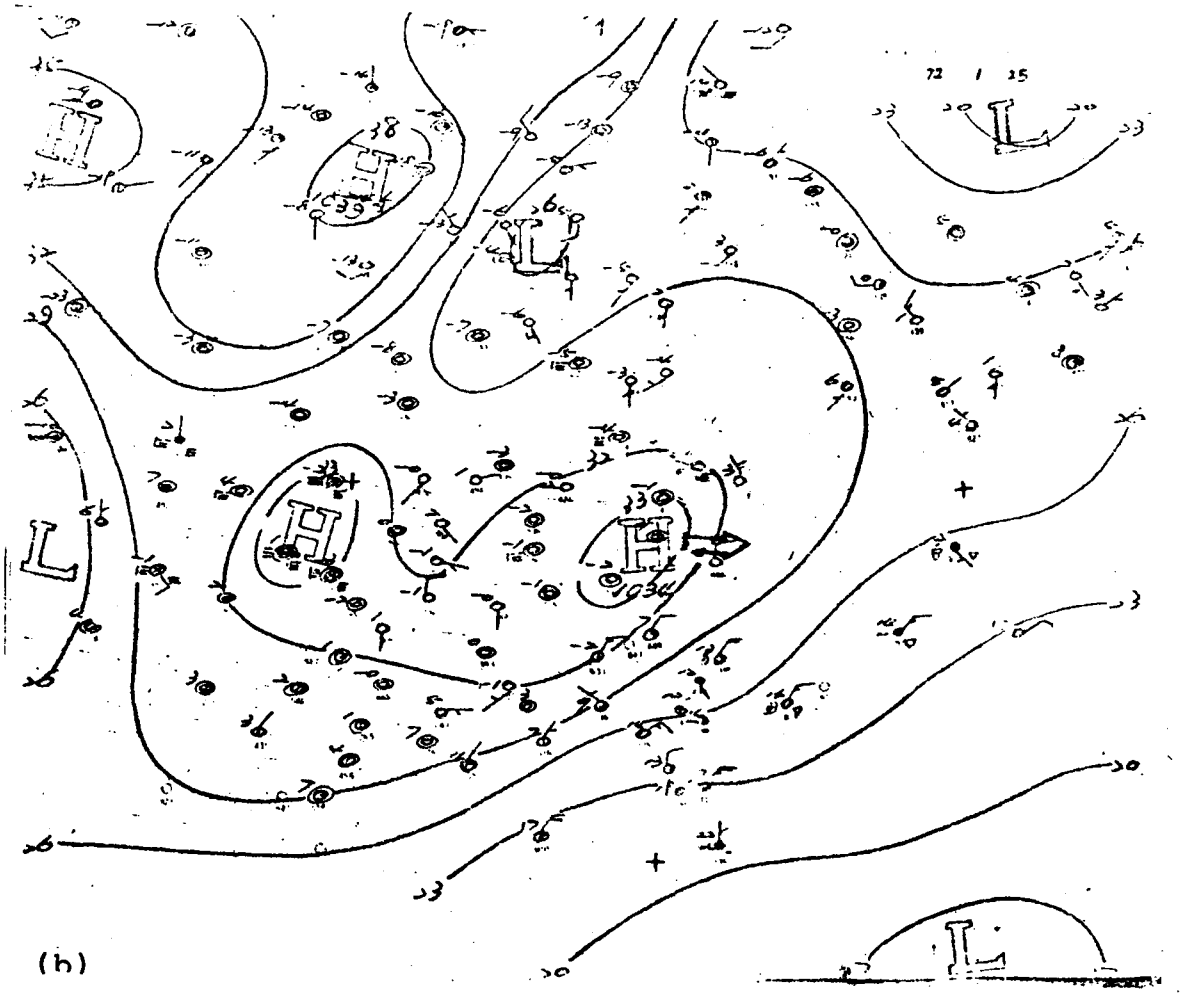

Fig. 5-3 (continued)

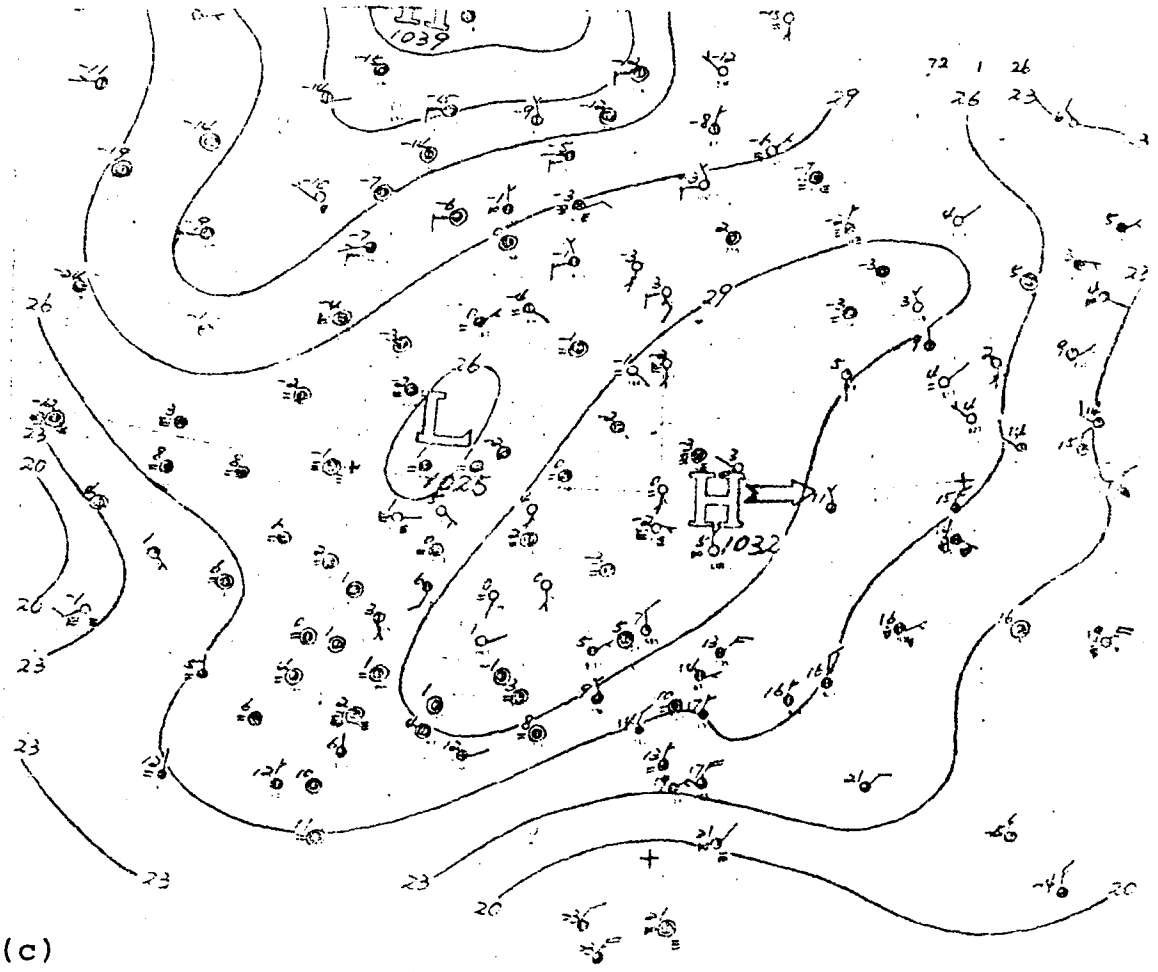

(c)

Fig. 5-3 (continued)

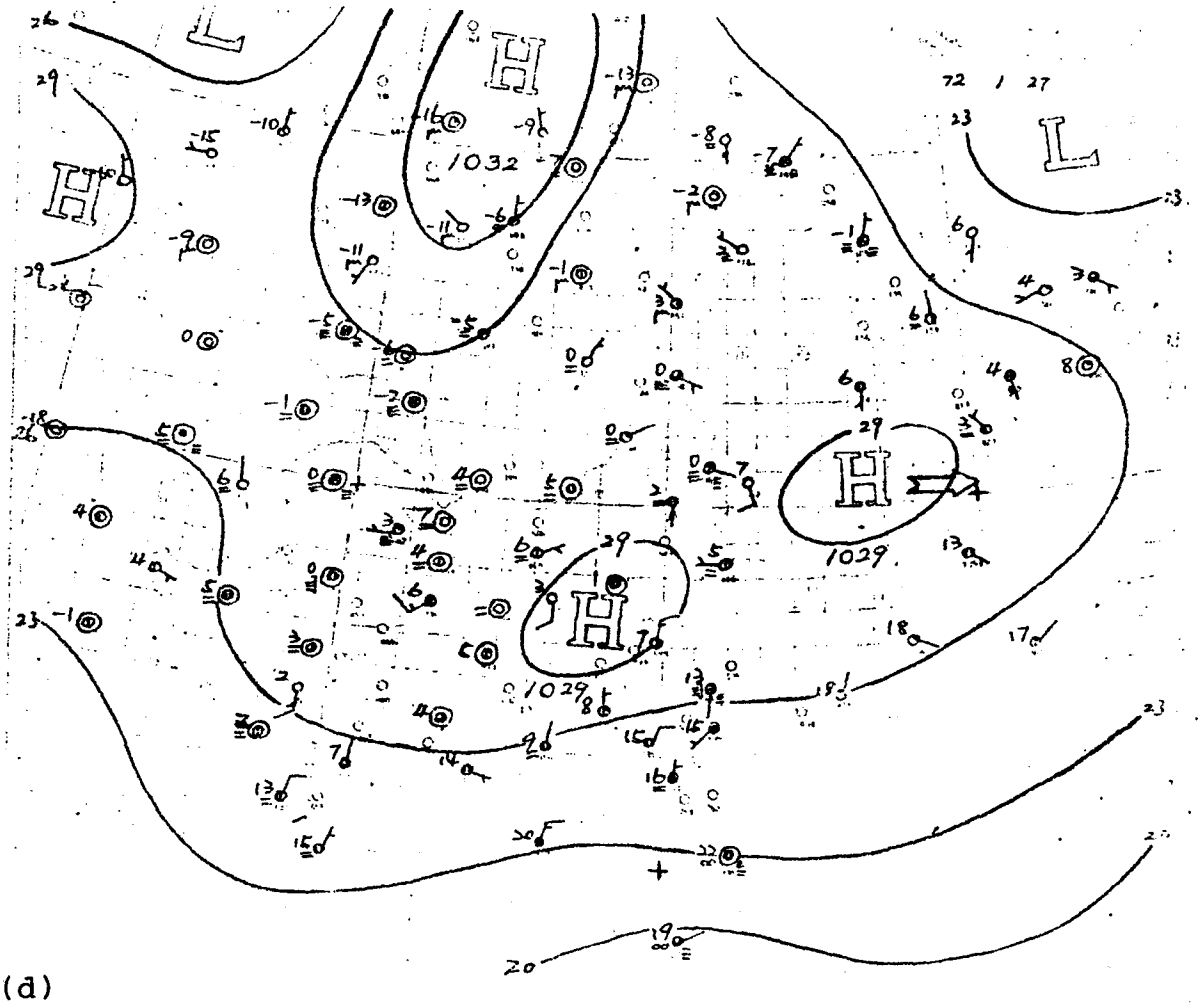

(d)

Fig. 5-3 (continued)

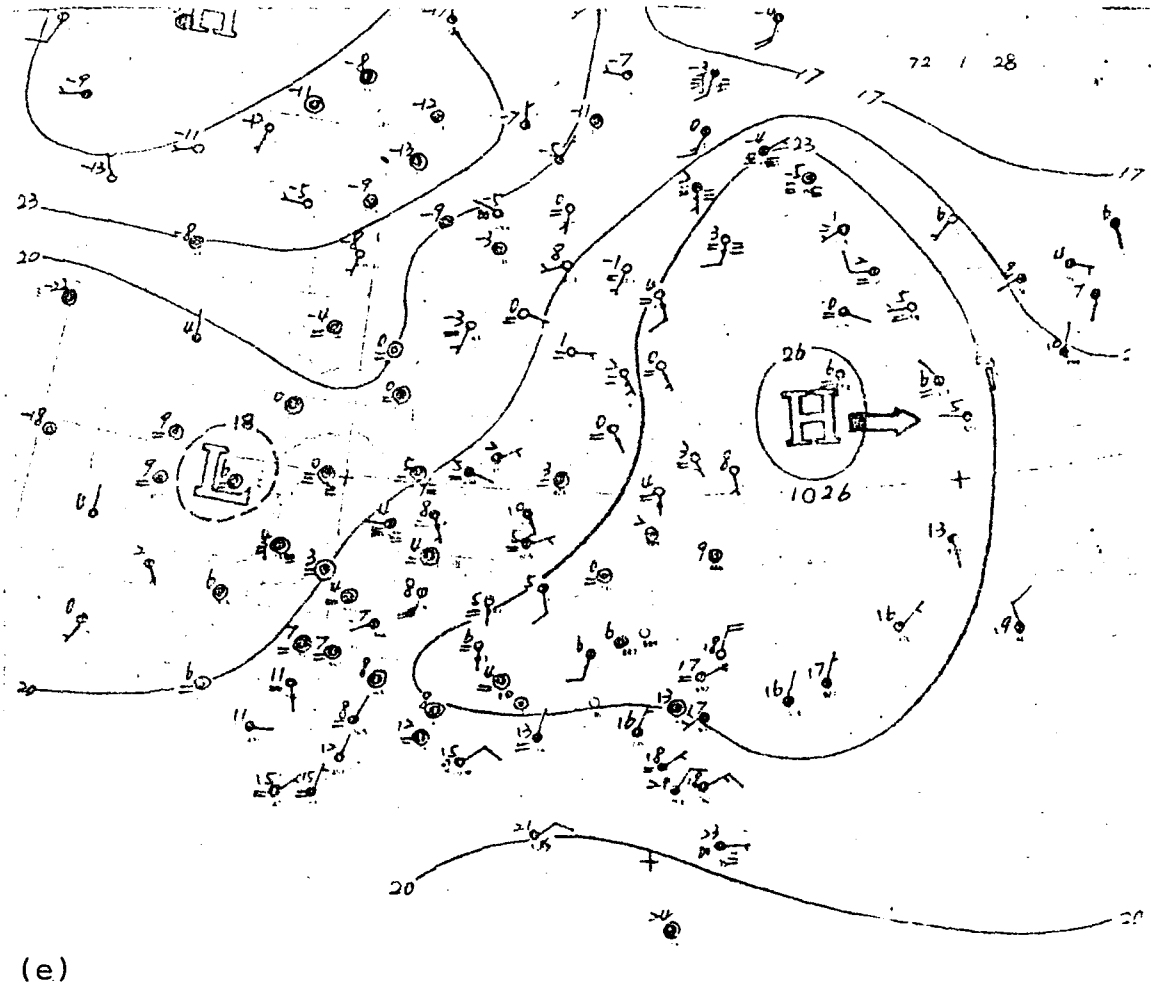

(e)

Fig.5-3 (continued)

moving toward east. Another high pressure 1039 mmb. at 44° north latitude, 110° east longitude, at the center of Southern part of Mongolia, nearly staying. As affected by the changeable air mass from the mainland it turns out from being cloudy to being clear in various places. Temperature comes high again. For next day as affected by the weak northeast monsoon, there is party light rain in northeast and east areas. It turns out from being cloudy to being clear in experiment area. Wind direction is northeast. Average wind speed is 7 m/s.

Jan. 27, High pressure 1029 mmb. at 31° north latitude, 126° longitude, moves toward the east at East Sea, speed of 10 km. Another high pressure 1035 mmb at north latitude 43°, east longitude 114°, at the center of east part of Mongolia, nearly staying. In Taiwan area, it is still affected by the changeable air mass from the mainland this day. Except there is party light rain in northeast and east part, it turns out from being cloudy to being clear in the rest areas. The weather turns from being cloudy to being clear. Wind direction is east, northeast. Average speed is 4 m/s.

Jan. 28, High pressure 1026 mmb. at 32° north latitude, 125° east longitude, moves slowly toward east at the north part of East Sea. Another high pressure 1040 mmb at north latitude 48° east longitude 98° , at the northwest part of Mongolia, nearly staying. In Taiwan area, as affected by the changeable air mass from the mainland, there is more cloudy at east part and partly light rain. There is partly shower at south area, and cloudy turning out to be clear for the rest areas. It turns out to be cloudy to clear. Wind direction is declined to east and speed is slightly weak.

From the analyzing synoptic current, it is found

that the wind blows toward northeast and the weather is exactly what we have often seen in winter the class D stability. It is quite consistent with the determination of sampling network.

Table 5-3 Shows:

The possibility of occurance of atmospheric statibility and wind direction in Taipei area for the year of 1980.

Table 5-3 The Probability of Atmospheric Stability and Wind Direction in Taipei Area for the year of 1980

Wind Direction	Spring		Summer		Autumn		Winter	
	A,B,C,	D,E,F	A,B,C,	D,E,F	A,B,C	D,E,F	A,B,C	D,E,F
1	2.73	5.10	3.03	2.42	2.21	2.02	1.38	4.40
2	1.67	4.74	1.50	1.05	1.69	4.19	1.24	9.75
3	0.96	22.00*	0.47	1.37	1.41	16.54	9.57	21.00*
4	0.71	19.97*	0.05	1.23	0.47	28.58*	0.48	27.68*
5	0.44	7.25	0.42	3.67	0.66	19.75*	0.81	13.00
6	0.25	2.59	0.82	3.68	0.24	4.43	0.43	2.73
7	0.39	2.11	1.13	2.44	0.38	1.78	0.38	1.25
8	1.00	3.50	2.54	7.27	1.17	3.39	0.38	2.06
9	1.39	4.13	2.73	8.18	1.03	3.11	0.57	1.58
10	0.34	1.08	1.59	5.77	0.18	0.85	0	0.67
11	0.34	1.63	1.59	6.99	0.19	0.80	0.15	0.44
12	0.69	1.97	3.10	13.80*	0.24	0.28	0.15	0.63
13	1.43	2.83	3.73	7.12*	0.62	0.34	0.15	0.79
14	0.82	1.11	3.36	1.23	0.66	0.28	0.77	0.43
15	0.96	1.78	4.22	0.96	2.08	0.19	0.58	1.11
16	1.93	1.59	2.18	0.51	0.90	0.28	0.57	0.86
Total	15.98%	81.02%	32.46%	67.54%	14.13%	85.85%	8.35%	91.65%

Note : Spring covers March, April, and May;
Summer June, July and August;
Autumn September, October and November;
Winter December, January and February;
* Indicates Wind Direction at most.

Fig. 5-4 Indicates the distribution of wind speed and wind direction in perpendicular wind field as observed by that 6 stations. Black point means so data available. On 25th, wind blow strongly toward northeast at high level of various observation stations. On 26th, the wind blows toward northeast at the bottom level of various stations, but it turns out to incline to the east up from the level of 45 km. It indicates another air is getting close from high system.

Fig. 5-5 Indicates the horizontal wind field within these three days at a height 225 m of Taipei and Taoyuan area. It is tound that the variation of wind direction is considerable slim. Wind blows northeast, it turns out to NNE as from the afternoon of the third day. It turns out to ENE from 1600 PM and the wind speed becomes weak.

It is otherwise analyzed that the wind speed at high level wind field is less powerful than that at bottom level (high level goes 450 meters up) As from 26th, the wind is getting inclined to east. High pressurized circulating current is getting strong. The steam from south is getting increased.

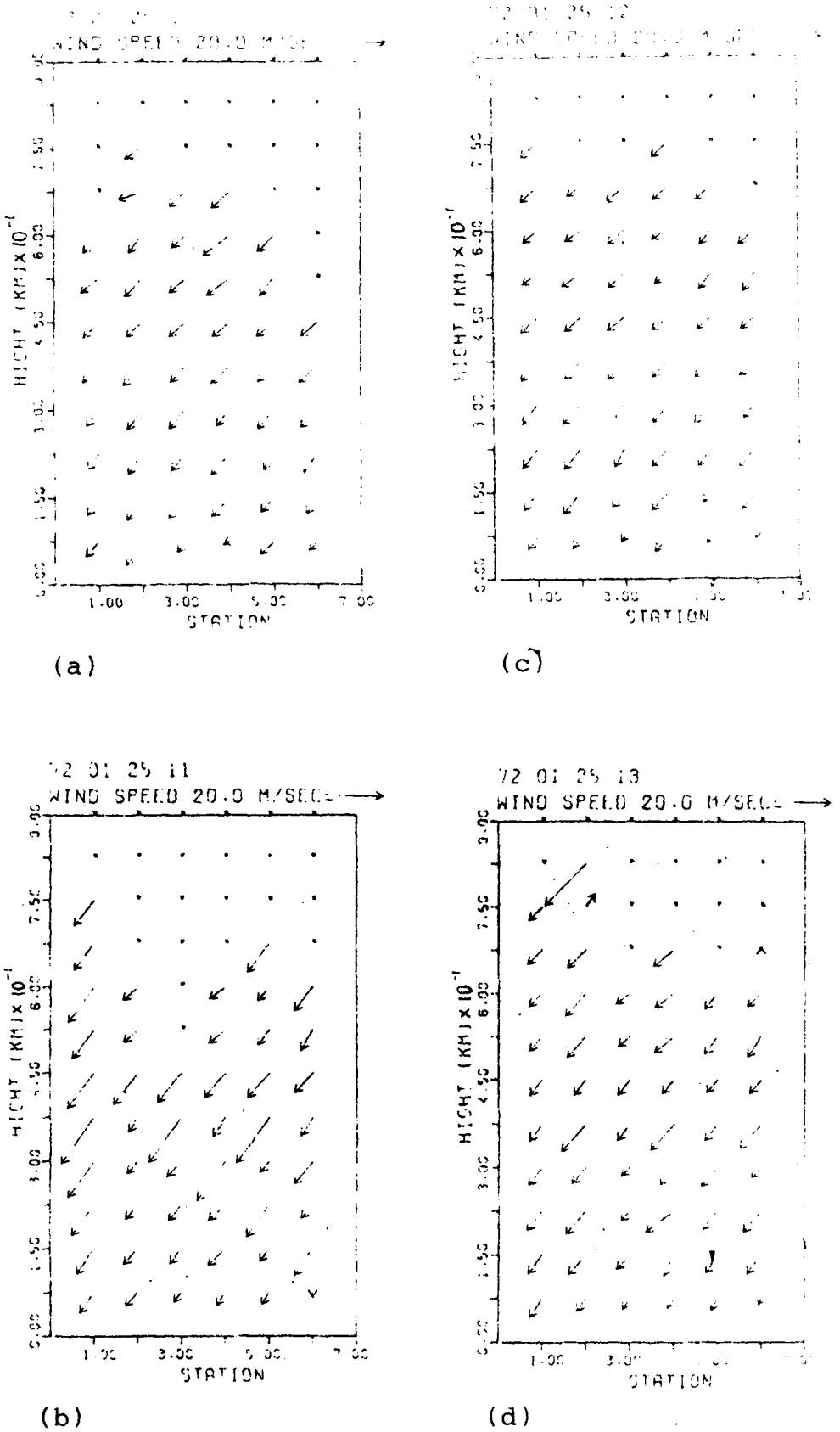

Fig. 5-4 The Distribution of Perpendicular Wind Field at Various Stations during Experiment Period (a-h)

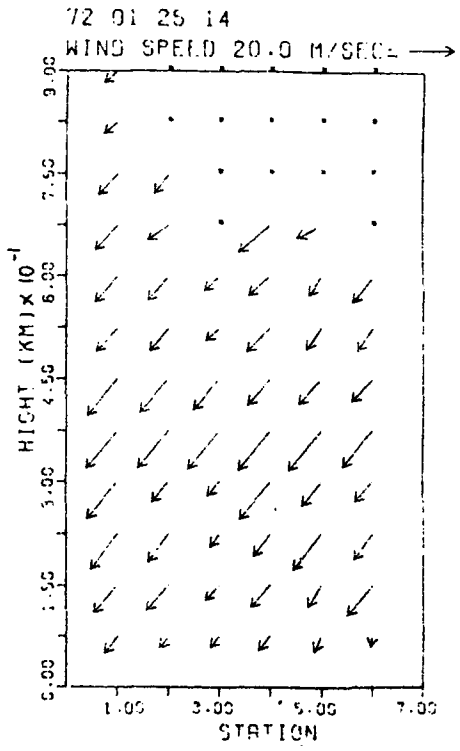

(e)

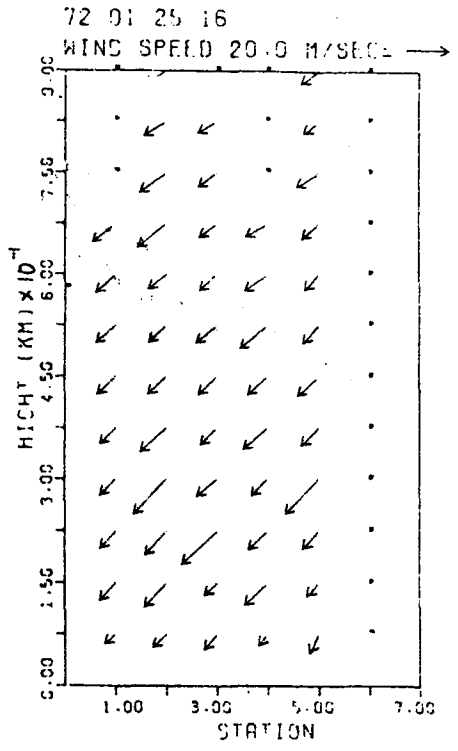

(g)

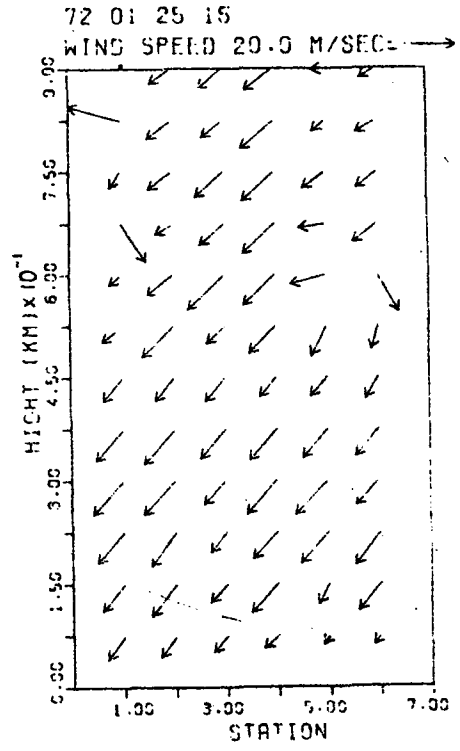

(f)

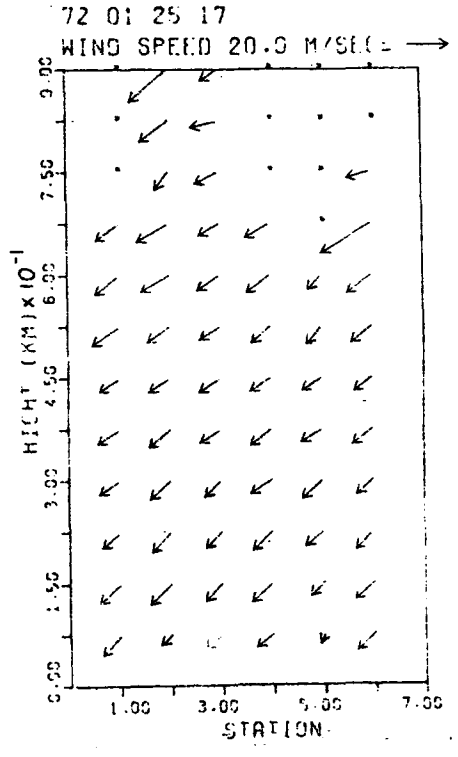

(h)

Fig. 5-4 (continued)

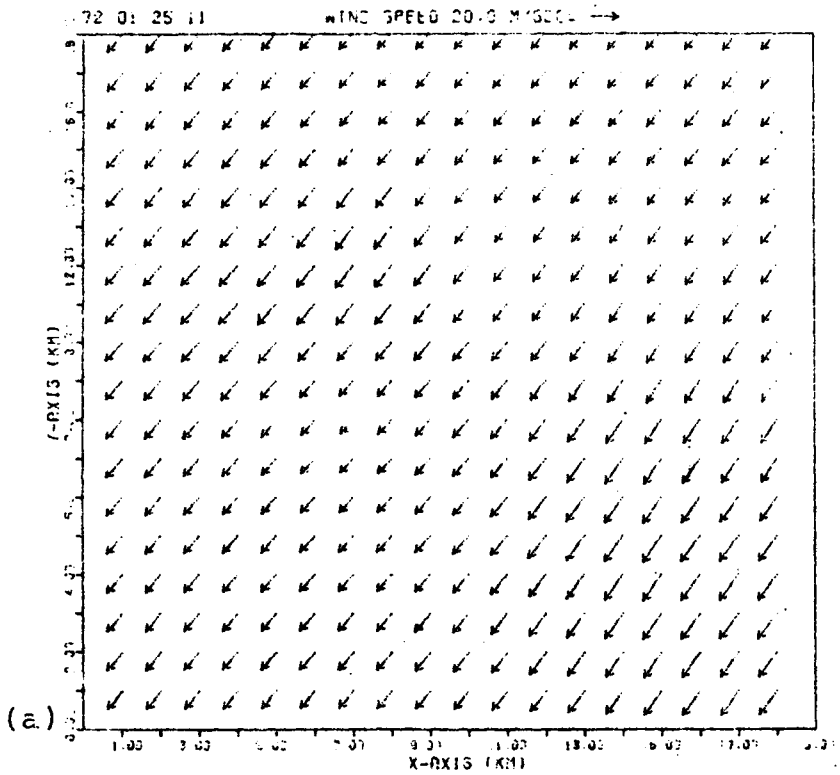

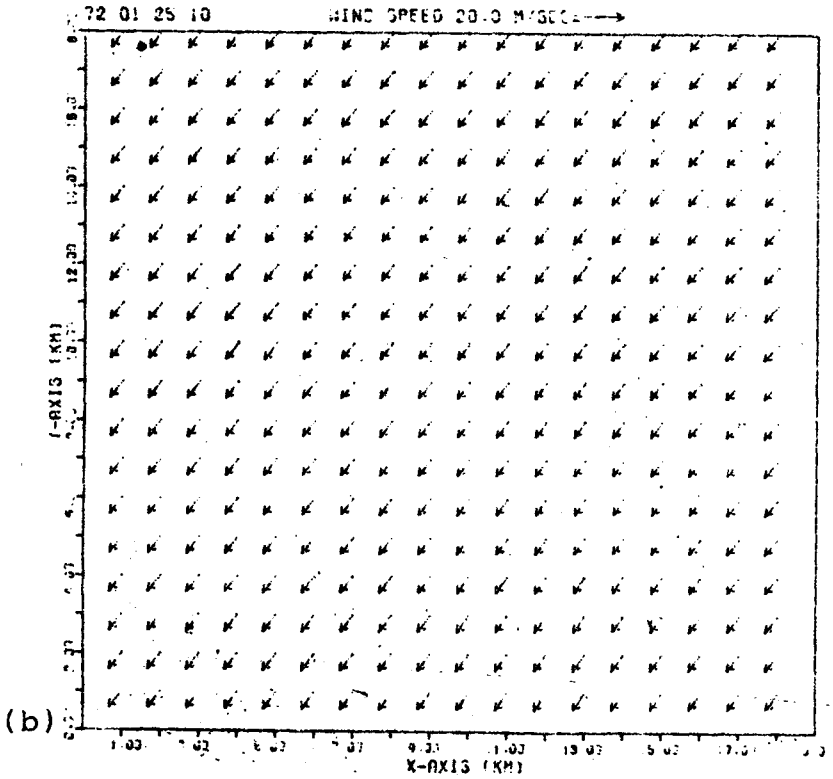

Fig. 5-5 Horizontal Wind Field at all areas during Experiment Period (Height 2.25m) (a-d)

(c)

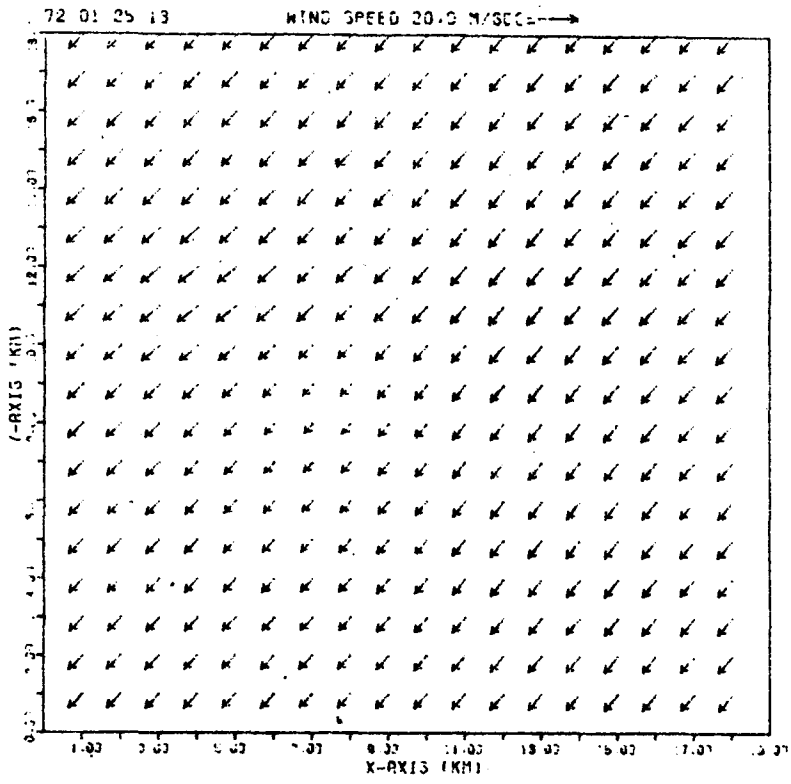

(d)

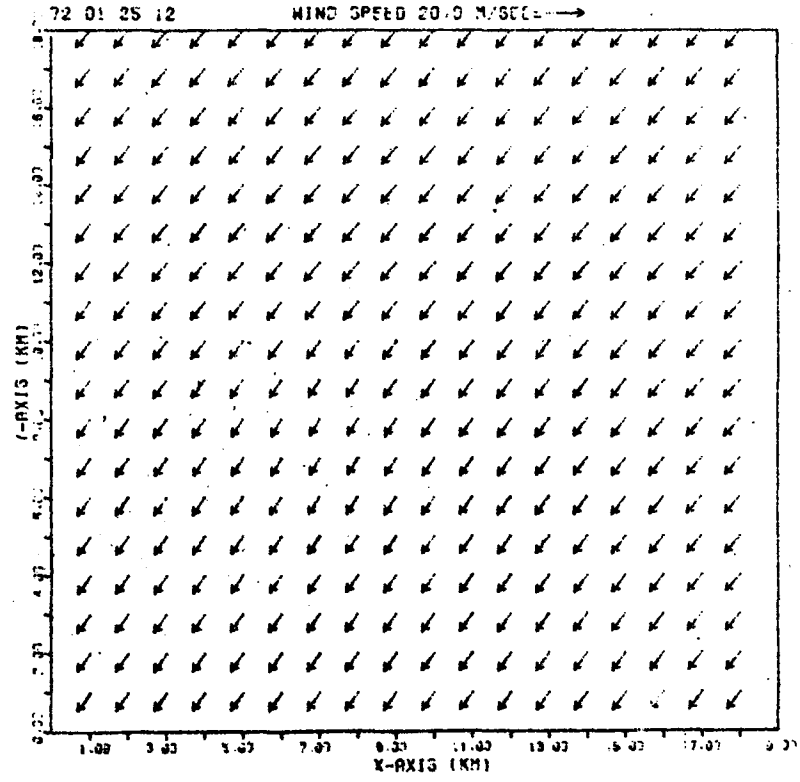

Fig. 5-5 (continued)

5-3 Determination of dispersion coeff. Sigma Y, Sigma Z and comparison with the P-G chart

5-3-1 General aspects

Gauss Plume Model is assumed that a steady state of distribution is carried out from long-time diffusion and conveyance of pollutants without consideration of the effect of terrain and local current. Owing to the irregular terrain in Taipei and Taoyuan area, the employment of Gauss Plume Model may cause a great discrepancy. However, if the consideration of effect made by ground surface roughness and the height of plume, probablly, the phenomenon of diffusion in ground surface may be consistent with the actual enviroment. Major purpose of this experiment is to find the distribution curve of σ_y , σ_z.

5-3-2 The determination of effective stack height and dispersion coefficients sigma Y and sigma Z.

The result of sampling in these three days is shown in the attached list. From the list, we are aware of that the wind direction is steady, mostly toward north-east, mainly the synoptic prevailing wind. The effective-ness of terrain and local circulating current is not obvious. High concentration is mostly concentrated in the line of 7,8,9, but there is still discrepancy in the range of concentration. On the other hand, from the result of the list, we find that most of the experiments are successfully obtained three sampling points in the data of concentration. We may find the coefficients sigma Y and Z as according to the method in paragraph 4-2-3. As indicated in Table 5-4 to 5-7, (based on the meteological data of Chiang Kai-shek Airport), the coefficients sigma Y and Z in each experiment are not increased in related with the increase of down wind distance, but, the average of sigma Y and Z within these three

Table 5-4 σ_y, σ_z value (Arc A)

Time		RUN NO.	Stability	σ_y (m)	σ_z (m)
1/25	1100	1	D	260	56
	1200	2	D	202	60
	1300	3	D	209	45
	1400	4	D	324	48
	1500	5	D	209	45
	1600	6	D	-	-
1/26	1100	7	D	-	-
	1200	8	D	202	60
	1300	9	D	144	55
	1400	10	D	216	53
	1500	11	D	195	68
	1600	12	D	187	65
1/27	1030	133	D	245	57
	1130	14	D	216	87
	1230	15	D	505	206
	1330	16	D	238	54
	1430	17	D	144	52
	1530	18	D	216	52
		Average Value		219	66
		Briggs City Area		324	305
		Briggs Rural Area		211	77
		EPA		174	60

Table 5-5 σ_y, σ_z value (Arc B)

TIME		RUN NO.	Stability	σ_y(m)	σ_z(m)
1/25	1100	1	D	219	53
	1200	2	D	295	66
	1300	3	D	208	59
	1400	4	D	317	112
	1500	5	D	208	62
	1600	6	D	-	-
1/26	1100	7	D	295	86
	1200	8	D	306	72
	1300	9	D	328	69
	1400	10	D	-	-
	1500	11	D	328	100
	1600	12	D	481	75
1/27	1030	13	D	219	49
	1130	14	D	219	108
	1230	15	D	426	77
	1330	16	D	328	77
	1430	17	D	-	-
	1530	18	D	-	-
		Average Value		303	76
		Briggs City Area		431	412
		Briggs Rural Area		300	97
		EPA		249	74

Table 5-6 σ_y, σ_z value (Arc C)

TIME		RUN NO.	Stability	σ_y(m)	σ_z(m)
1/25	1100	1	D	344	62
	1200	2	D	-	-
	1300	3	D	364	70
	1400	4	D	-	-
	1500	5	D	809	93
	1600	6	D	607	50
1/26	1100	7	D	526	146
	1200	8	D	607	78
	1300	9	D	567	229
	1400	10	D	405	68
	1500	11	D	769	73
	1600	12	D	607	69
1/27	1030	13	D	607	86
	1130	14	D	506	63
	1230	15	D	590	74
	1330	16	D	583	113
	1430	17	D	541	66
	1530	18	D	647	102
Average Value				572	90
Briggs City Area				624	609
Briggs Rural Area				478	133
EPA				417	102

Table 5-7 σ_y, σ_z value (Arc D)

TIME	RUN NO.	Stability	σ_y(m)	σ_z(m)
1/25 1100	1	D	-	-
1200	2	D	-	-
1300	3	D	1144	103
1400	4	D	1144	113
1500	5	D	1144	56
1600	6	D	-	-
1/26 1100	7	D	1087	89
1200	8	D	-	-
1300	9	D	1001	82
1400	10	D	372	61
1500	11	D	-	-
1600	12	D	858	60
1/27 1030	13	D	-	-
1130	14	D	858	84
1230	15	D	1430	164
1330	16	D	1058	227
1430	17	D	1058	96
1530	18	D	1230	230
Average Value			1010	114
Briggs City Area			800	785
Briggs Rural Area			649	166
EPA			598	128

days may incline to increase is related to the increase of the down wind distance.

Let $\sigma_y = ax^b$,

$\sigma_z = cx^d$

a, b, c, d can be obtained through the minimized square method based on the four average data. It is shown as follows:

a = 0.031 b = 1.10

c = 3.1 d = 0.38

The comparison between the average figure of σ_y and σ_z and the data of Ta-lin Power Plant and the distribution curve of Brigg's rural and city area is shown as follows: As indicated in Fig. 5-6, it is found that σ_y in Taipei and Taoyuan area at a short distance of the stack (shorter than 4.5 km) is quite similiar with the figure of Braggs' (rural) distribution curve As to long distance, it is larger than that of Braggs' in city and suburb area. σ_y distribution curves are all larger than that in Taipei and Taoyuan area regardless of the distance on account of its ground surface roughness and its C-D stability. Owing to the momentum and buoyancy of plume, it normally goes up to a certain height, then disperses in the influence of wind. Therefore, the effective stack height is usually the total of actual height and plume height. The formula is shown as follows:

$$H_e = h_s' + h$$

h : plume height

Applying to the Air Quality Model, the effective stack height would attect the ground surface concentration

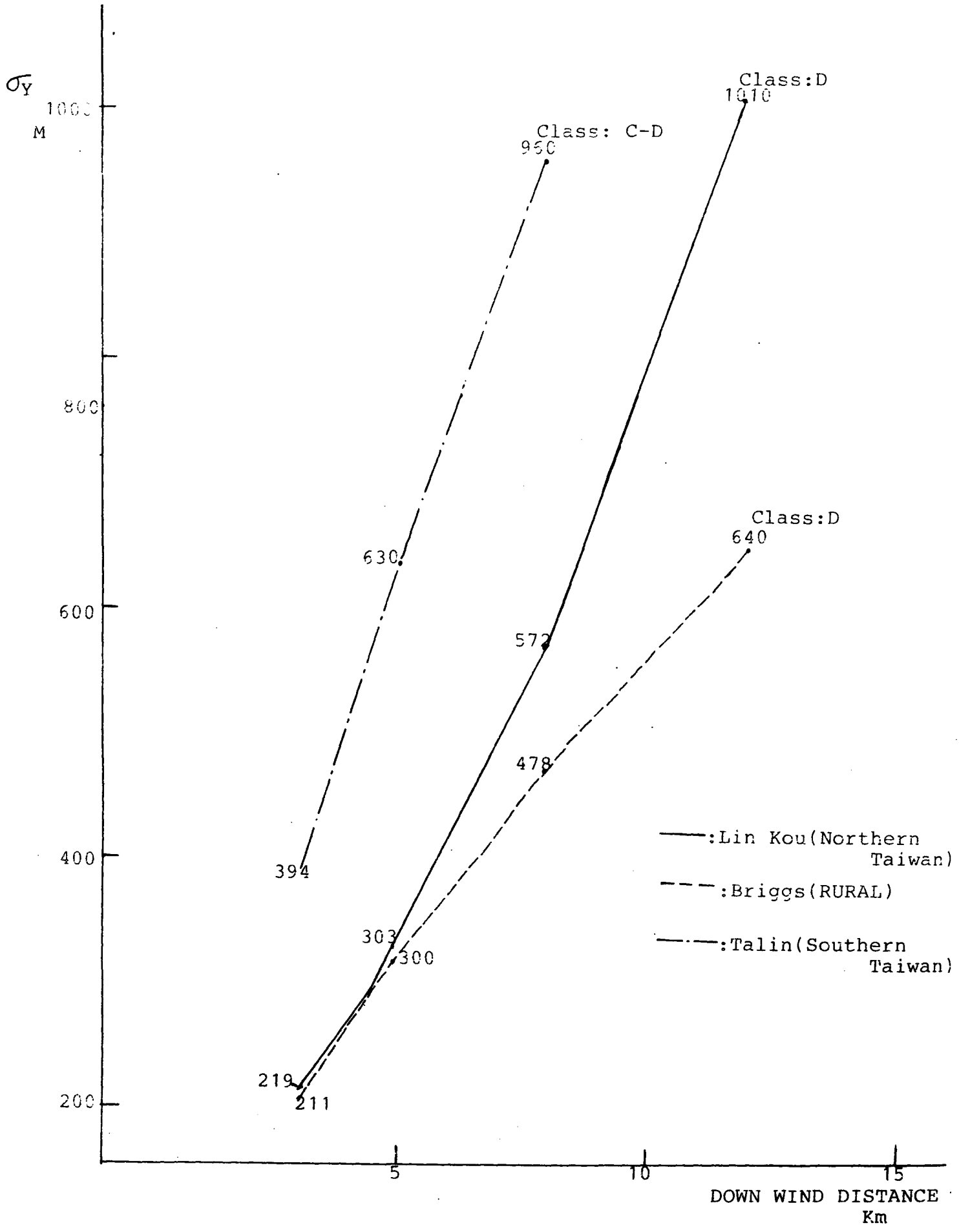

Fig. 5-6 The relation between downwind distance and sigma y

greatly. Especially, the maximum surface concentration is in proportion to the square figure of H_e . Therefore, for better understanding, and experiment of two times a day is carried out under the condition of shutting EP for five minutes so that such experiment for plume rise measurment may smoothly be carried out. The figure as attained (H and X relationship) is shown as on attached Table 5-8.

The function between plume height and X as based on Briggs (1969) 2/3 Power Law which is shown as below:

$\Delta H = CF\ 1/3\ U^{-1}\ X\ 2/3 \quad X < 10\ h_s$ (formula 1)

F = Buoyancy flux (m^4 / sec^3)

U = Average wind speed (m/sec)

$F = gv_s D^2 \left(\frac{Ts-Ta}{Ts}\right)$

g : Gravity acceleration

Vs : Emission speed (m/s)

D : Diameter of Stack (m)

Ts : Temperature of exhausting air (^oK)

Ta : Temperature at ground surface (^oK)

Find out the figure of C, to average the figure is 0.81, then find the correlation coefficient of calculating figure and actual figure.
Find the figure of C by using the formula of Moore (1974) as:

$$\Delta H = CF\ 1/4\ U^{-1}\ X^{3/4} \quad \text{(formula 2)}$$

The average C is 1.01. Then, find out the correlation coefficient of calculating figure and actual figure, such as shown in Table 5-9.. From the comparison of the both, we know that formula 1 is more accurate.

Table 5-8 (Seq. 1-5) The effective stack height from the observation of plume rise for five times

Sequence	Time	He(m)	X(m)	C	Sequence	Time	He(m)	X(m)	C
1	250942	79	0	1.18	3	26045	85	0	1.37
		99	44	0.93			107	64	1.00
		106	87	0.88			112	125	0.89
		114	129	0.85			118	182	0.82
		121	169	0.84			123	236	0.79
		128	208	0.83			128	287	0.76
		134	245	0.75			132	335	0.67
		139	317	0.69			134	424	0.60
		143	390				135	517	0.55
		140	462				136	605	
							134	689	
Sequence	Time	He(m)	X(m)	C	Sequence	Time	He(m)	X(m)	C
2	251618	75	0	1.10	4	261600	85	0	1.53
		101	54	0.86			110	61	1.13
		108	106	0.77			116	119	0.97
		114	156	0.74			121	173	0.91
		120	203	0.72			127	225	0.87
		126	248	0.72			132	274	0.85
		132	292	0.63			137	320	0.73
		134	373	0.57			138	407	0.66
		137	457	0.53			140	497	
		139	537				134	582	
		134	614						

Table 5-8 (continued)

Sequence	Time	He(m)	X(m)	C
5	271625	90	0	1.35
		119	42	0.99
		125	82	0.86
		132	121	0.81
		140	159	0.77
		147	196	0.74
		153	232	0.66
		158	302	0.61
		163	372	0.57
		167	441	0.53
		172	507	0.48
		136	572	0.42
		180	635	
		177	697	

Table 5-9 Calculate the correlation coefficient between calculating value and actual value

sequence No. of experiment	Briggs	Moore
1	0.989	0.987
2	0.974	0.969
3	0.960	0.954
4	0.975	0.970
5	0.987	0.983

5-4 The analysis of ground surface concentration of SO_2

The dispersion concentration of SO_2 on ground surface is attained by the data of meteorology at the vicinity of input airport during the period of experiment and the data of two another stacks not for dispersing SF6 through the TEM Model, which is shown on Fig. 5-7 and 5-8. We find from the result that concentration dispersion goes along the main axis. i.e. from northeast to southwest. The max ground level concentration is approximately 0.227 ppm, and the maximum concentration of ground level is happened approximately 6 km from the emission source, but it is about a distance of 3.5 km as based on the meteorological data of Linkou Power Plant.

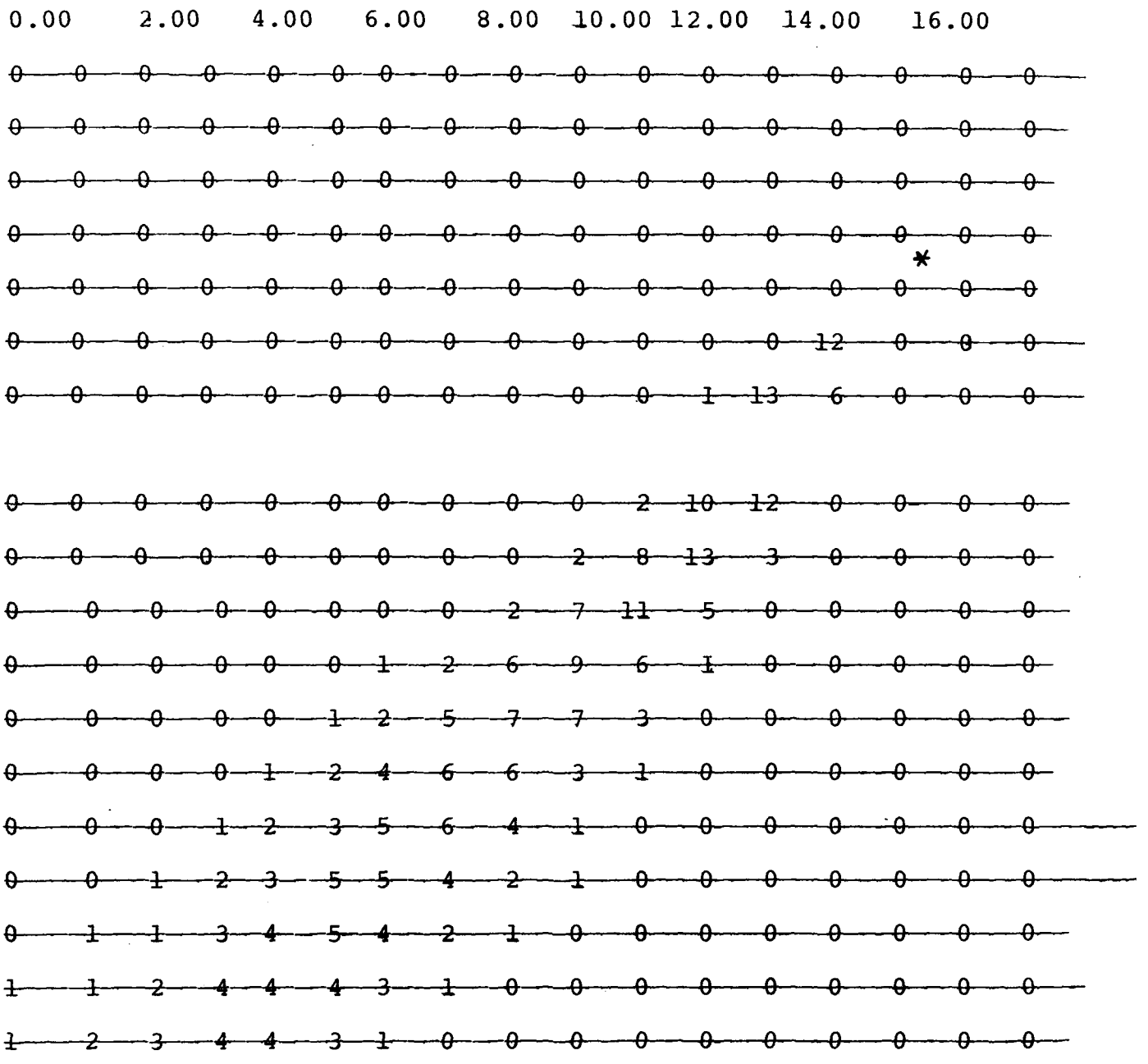

UNIT : $\times 10^{-2}$ PPM

* Location of LIN Kou Power Plant

Fig. 5-7 The Ground Surface Concentration of SO_2 on Jan. 25

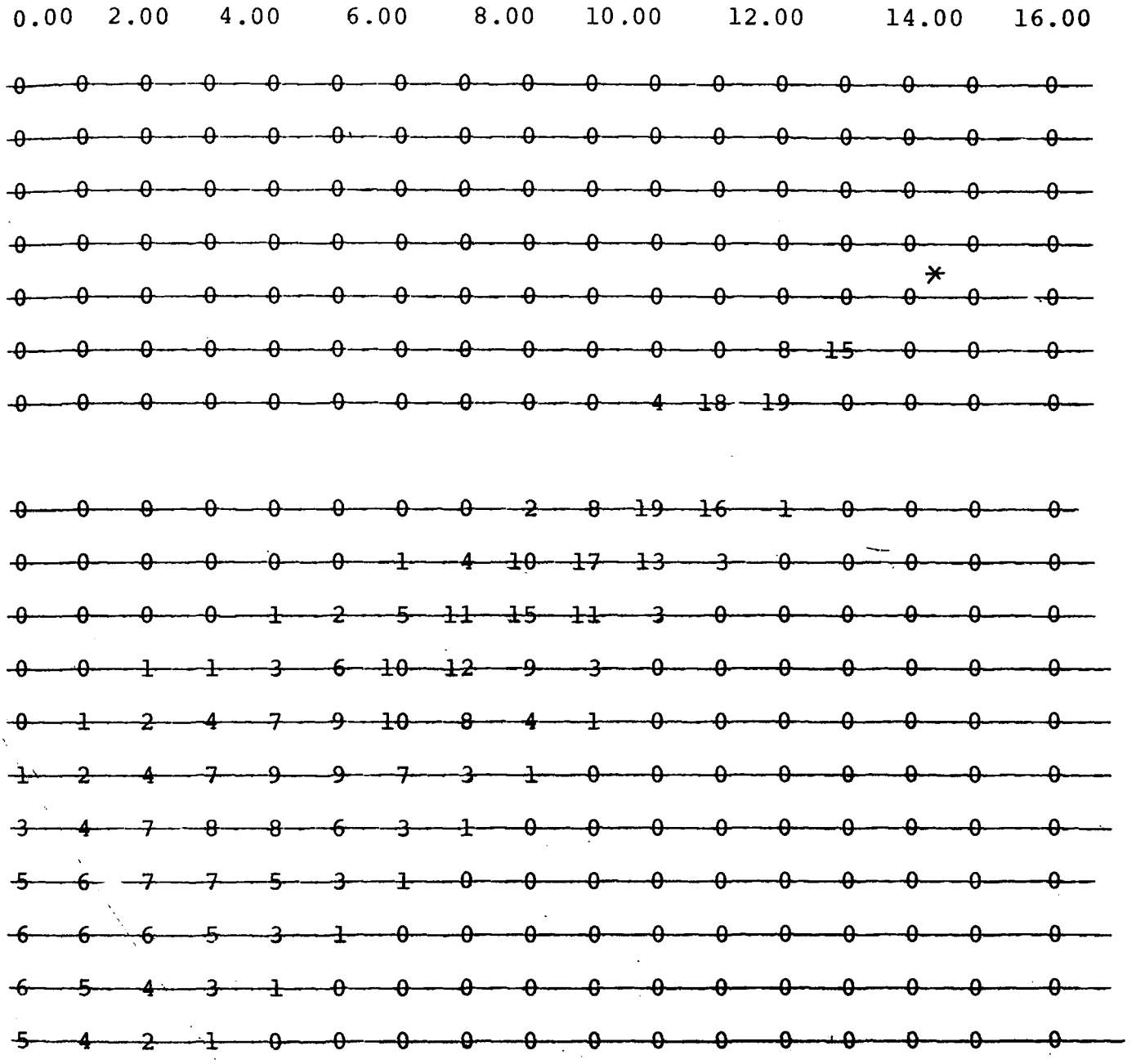

UNIT : $\times 10^{-2}$ PPM

* Location of LIN KOU Power Plant

Fig. 5-8 Ground Surface Concentration of SO_2 on Jan. 27

5-5 Conclusion

It is easy to obtain the stability of Class D, as the experiment is carried out in the winter (based on the data of Chiang Kai-shak Airport). The meteorological joint frequency as shown in Table 5-3 of Chiang Kai-shak Airport indicates that it appears stability Class D,E,F in winter is approximately 91.65%. Due to few times of experiments carried out in experiment period, it won't represent much sense for Class C or other stabilities.

As σ_y and σ_z of Class D stabilities adapting a dispersion curve and plume height in this experiment is made, it is quite meaningful as on the period of winter and to power plant stack. From this point of view , this experiment is successful. From this experiment, we are aware that σ_y is similiar with that of Brigg's suburb in short distance in Taipei Area, and is inclined to increase in long distance. σ_z is inclined to small, it is even smaller than that in plain areas on account of the terrain and wind direction or any other manmade errors.

The flow characteristics of regions of complex terrain (such as in northern Taiwan area) differ significantly from plain terrain (such as in southern Taiwan area) was found. It may be as a funtion of topographic details and meteorological conditions, but there is a need for more measurement and theoretical studies which can be made and completed site-specific types of flow phenomena in future.

PART II

DEVELOPMENT OF AIR POLLUTION CONTROL STRATEGIES FOR MAINTAINING ASSIMILATING CAPACITY IN TAIWAN , R.O.C.

CHAPTER 6 CONTROL STRATEGIES OF AIR POLLUTION IN TAIWAN

6-1 The analysis of the future strategy for air pollution of the leading countries of the world

An international perspective for air pollution constraints on increased energy use by industry, national decisions regarding acceptable tradeoffs among energy, environmental, and economic costs-these factors, will determine the extent to which compatible policies for energy development and environmental quality can be pursued in industrial countries.(24)

Conceptually, the preventative measures of pollution include "how to restrain" and "how to control". The sources of air pollutions are always combustional equipment, various producing procedures and all kinds of vechiciles. The restraint work of these pollution emitters were (A) to reduce the total emissions, (B) put all the stacks together or increase the height of stacks so as to dilute them, (C) supervise the dispersion procedures of the pollution materials. For (A), we could (a) improve or replace the fuel or change the producing procedure (b) fix the particulates and poisonous materials' treating equipment. As for (C), we may reach the goal by a monitoring system and management, transmission system. (m)

Stack height requirements are a common and effective method of minimizing local ambient concentration of SO_2, though no reduction in total atmospheric emission is achieved. A related strategy, known as intermittent control, involves using a low sulfur fuel during periods of adverse meteorology, and a higher sulfur fuel during conditions conductive to good dispersion. From a technical

perspective stack height requirements are relatively easy and inexpensive to implement. (n)

Intermittent control systems are more difficult to implement since the capability must exist to store and switch between fuels of different sulfur contents, and to monitor and forecast local ambient air quality and/or meteorological conditions.

The need for close interaction between energy and environmental policy makers and analysts is paramount if conflicts are to be minimized and compatible policies developed.

Japan is so-called "the leading country for anti-pollution strategies in the world".

Reviewing the basic control policy of Japan, there was first the "Basic Law for Environmental pollution Act" in Aug. 1967 then they modified column 10 of that Act to be the "Air Pollution Control Act" of Dec. 1968. The goals which the Act pursued was (1) from a point of view of prevention, to assign control areas (2) severe control on the newly established factories in the highly polluted areas and set a strict standard for new coal oriented equipment, (3) setting the emission standard of sulfur oxides (4) to limit the emission of vehicles (5) to enforce the management of emergency situations. (o,p)

The 28 poison materials listed on the Act. were those which spread into large areas and influence the health of people, such as sulfur oxides, particulates and vehicles' emission. Regarding the sulfur oxides, we must match the "Low sulfur content policy" to reach the environmental standard of 1969. The combined energy research

council of Japan has the following results. They though that the following items should be taken to go with the "Low sulfur content policy":

(1) import oil with low sulfur content,
(2) consider replacing the energy, such as L.N.G., low sulfur coal, etc.
(3) develop the skills of flue gas desulfurization to get rid of sulfur from heavy oil.

But no matter how the skills of (3) are improved, it is not easy to reduce the absolute quantity of the polluted materials which have been disposed into the air. So the best action is to make a proper location of main sources and procure the control of total emission during emergency situation. To settle the highly polluted areas problems, it must be settled from a long term point of view. It might concern regional land use, urban planning, transportation planning, re-establishment of city and the use of high stacks and compound chimneys. If we could find out the relation between the pollution resources and the pollution situation, we could obtain the best plan of action. Prediction of pollution emergency situations is also important.

In brief, the control strategy for air pollution of Japan was worked out according to the following three procedures. And the final goal is to control the total pollutants emission. (q,r)

(1) Uniform control of emission sources --- the predication of pollution level, whether by quantitative or by qualitative, was not accurate enough.
(2) Block control of emission sources --- even if a prediction of pollution level is accurate, an objective function of optional control is undefinite.

(3) Individual control of emission sources --- with the established data bases, a prediction of pollution level is accurate and an objective function is definite.

Japan began her control of sulfur oxides by K value from Dec. 1968. After that, she modified the K value several times: second modification in Jan. 1972, fifth in Jan. 1973, sixth in Apr. 1974, seventh in Dec. 1975 and eigth in Sept. 1976. The allowed wasting (venting) volume of each productive equipment unit is $q = K \times 10^{-3} \times He^2$

q : allowed venting volume of sulphide oxide (m^3/hr)
K : area coef. (3.0 -- 17.5 with 16 grades)
He: effective height of stack (m)

As for the newly established factories, the particular K values were set to 1.17 to 2.34 with 3 grades.

Japan used the "Total emission control" from June 1974. And the control was fulfilled in 11 areas from Nov. 1976. The government assigned another 8 areas to take control in Dec. 1975 and another five areas in 1976.

It is still difficult to reach the ambient standard only by setting the allowed emission in massive factory areas. To solve this, the government assigned these areas to be the "total emission control" areas. The local governments settled the emission planning of each place, then districted the larger factories to be the control projects of "total emission control" and the small ones controlled by the use of fuels only.

6-2 The settlement of stack dispersion coefficient $\tilde{K}$

To manage effectly the "Air pollution control act of ROC", we assigned the control area so as to make the quality of air reach the national standard. It is impossible to reach the goal just by control of the concentration of the emission from stacks. Therefore, we must limit the venting emission (i.e., mass in unit time). The stack dispersion coef. is a coef. which expresses the relation between the stack's height and the emission of specified materials. The author conducted this study in 1977.

The Settlement of Stack Dispersion Coef.:
(factors)

(1) The national ambient quality standard of specified pollutants
(2) The weather factors which effect the dispersion, transport and dilution of the pollutant concentrations in the control areas.
(3) The number of stacks, their height, location and their emission in the control area.
(4) The air quality at present time.
(5) The industrial tendency of the area.
(6) The possibility of technology and policy to reduce the emission so as to reach the coef.

Definition of stack dispersion coef. ($\tilde{K}$) is from eq. (6.1),

$$Q = \tilde{K} H_e^2 \qquad (6.1)$$

Q : emission rate of stack's pollutants, g/sec.
H_e: stack effective height, m.
$\tilde{K}$: stack dispersion coef.

For a stack (point source), the dispersion value of the neighboring area (10 Km form its downwind side) can be represented by Gaussian Model.[25] The maximum concentration

of the ground level can be found out by eq. (6.2),

$$C_{max} = KQH_e^{-2} \tag{6.2}$$

$$\text{where } K = \frac{1}{\pi \bar{u} \hat{\sigma}_y^* \hat{\sigma}_z^*} \exp\left[-\tfrac{1}{2} \hat{\sigma}_z^{*-2}\right] \tag{6.3}$$

$$\hat{\sigma}_y^* = (\sigma_y \mid c = C_{max})/H_e \tag{6.4}$$

$$\hat{\sigma}_z^* = (\sigma_z \mid c = C_{max})/H_e \tag{6.5}$$

(6.2) expresses that the maximum concentration is directly proporational to the emission Q and inverse proportional to the square of stack effective heigh in the downwind area.[26]

K is different from K. The constant K is relative to the wind direction and speed of the stack effective height and the stability condition.[27] If we set "C" to be the air quality standard and "B" to be the environmental background concentration, then the pollution control would be asked the C_{max} in the following relation:

$$C_{max} + B \leq C \tag{6.6}$$

$$\text{i.e.} \quad C - B \geq KQH_e^{-2} \tag{6.7}$$

From eq. (6.7), (6.1) and, (6.3) we can see that the stack dispersion coef. $\tilde{K} = \frac{1}{K}(C-B)$. or

$$\tilde{K} = \pi \bar{u} \hat{\sigma}_y^* \hat{\sigma}_z^* \exp[\tfrac{1}{2} \hat{\sigma}_z^{*-2}] (C-B) \tag{6.8}$$

In eq. (6.8), for background concentration "B" of a specific stack, we should give further explanation.[28] In the control area, if there is only a single source exist, the "B" can be treated as the influence from anyother unknown sources inside or outside the area. But, if there

are other sources, the "B" means the influence from other stacks in the area. Therefore, qualitatively speaking, the background "B" value would be bigger as the regional pollution get more serious and various.

If I said $K_{\phi,\ell,m}$ is the set of ambient diffusion constants,

where ϕ = 1-16, as the 16 directions of wind
ℓ = 1- 6, as wind speed, for 6 grades
m = 1- 6, as stability class, for 6 grades

Then, we understand the above K is one case of $K_{\phi,\ell,m}$, rewrite and difine the total average K with a new concept as

$$K^* = \sum_{\phi}\sum_{\ell}\sum_{m} K_{\phi,\ell,m}\, f(\phi,\ell,m) \qquad (6.9)$$

where K^* : the total average K
K : the ambient diffusion constant in one case
$K_{\phi,\ell,m}$: the set of ambient diffusion constants
$f(\phi,\ell,m)$: the combined frequency function,

So $f(\phi,\ell,m)$ could be treated as the possibility of any case of wind direction, wind speed and stability occured in a period.[29] For instance, in Kaohsiung area, 1979, the K values were calculated by using the observation data of wind and stability, and shown in Table 6-1 with different stack height. Using these data and air quality model called TCM, calculation of average annual pollution concentration of Kaohsiung area could be compared with the observed ground concentration of SO_x from the foregoing study of Kaohsiung littoral areas (refer to Fig. 6-1). The areas which were damaged by SO_x are Cheng Chen area, littoral ind. area, Kushen area and the pertroleum treatment factory. The monitoring station in Taiwan Machinery Manufacturing Corp. obtained the average SO_x value of 0.15 PPM in 1976.

Table 6-1 The season and annual values of the ambient diffusion parameter of Kaohsiung area.

season / K (sec/m) / H(m)	Spring	Summer	Autumn	Winter	Annual
10	0.08851	0.08139	0.08627	0.07936	0.08388
20	0.06847	0.6255	0.06644	0.06059	0.06451
30	0.05769	0.05242	0.05559	0.04987	0.05389
40	0.04802	0.04344	0.04593	0.04115	0.04463
50	0.04534	0.04075	0.04297	0.03857	0.04191
60	0.04125	0.03634	0.03801	0.03428	0.03747
70	0.04005	0.03534	0.03688	0.03322	0.03637
80	0.03636	0.03211	0.03325	0.03031	0.03301
90	0.03557	0.03141	0.03250	0.02957	0.03226
100	0.03400	0.02997	0.03087	0.02845	0.03082
110	0.03288	0.02908	0.02983	0.02774	0.02988
120	0.03163	0.02792	0.92849	0.02663	0.02867
130	0.03054	0.02718	0.02789	0.02589	0.02788
140	0.02998	0.02659	0.02734	0.02540	0.02733
150	0.02897	0.0263	0.02714	0.02517	0.02707
160	0.02886	0.02557	0.02628	0.02440	0.02628
170	0.02855	0.02532	0.02599	0.02420	0.02602
180	0.02828	0.02514	0.02580	0,02407	0.02583
190	0.02688	0.02409	0.02470	0.02337	0.02476
200	0.02687	0.02411	0.02471	0.02341	0.02478

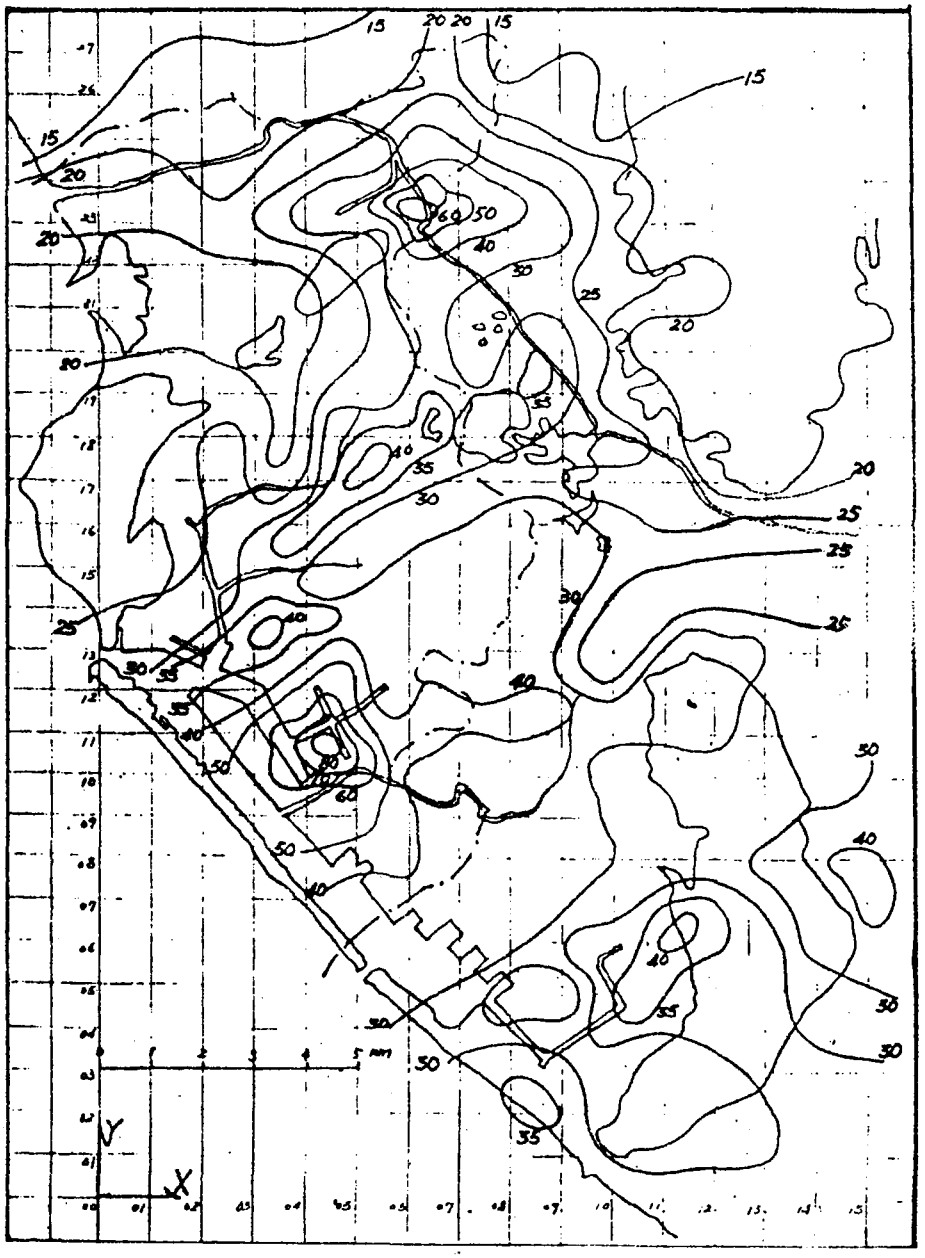

Fig. 6-1 The isopleth of annual average sulfation ($mgSO_3$/ $100cm^2$ PbO_2/30 days) from Apr. 1976 to Mar. 1977.

In figure 6-1 and figure 6-2, we can find that the concentrations of the mentioned area was over the national standard (0.075 PPM).

As a result, we shall find the calculated average annual value (using TCM model) was high corresponding to the observation value which we concerned. [30,31]

The following issue will try to establish air quality control regions in Kaohsiung area, and from the reasonable assumption, the stack dispersion coef. ($\tilde{K}$) of different height of stacks can be obtained for control use.

We devide the Kaohsiung area into 3 parts:(Fig.6-3)

(1) B_1 section: slightly polluted area.
(2) B_2 section: seriously polluted area. (medium)
(3) B_3 section: the most seriously polluted area.

If we set B_1, B_2, B_3 to be the background concentration of B_1, B_2, B_3 area. Plan I to plan III are established as follows:

(A) Plan I,

Let $B_1 = 0.6C$, $B_2 = B_3 = 0.9C$,

then from Eq. (6-8)

get $\tilde{K}_1 = 0.4$ C/K , $\tilde{K}_2 = 0.1$ C/K

(B) Plan II,

Let $B_1 = 0.1C$, $B_2 = B_3 = 0.2C$,

then from Eq. (6-8)

get $\tilde{K}_1 = 0.9$ C/K, $\tilde{K}_2 = 0.8$ C/K

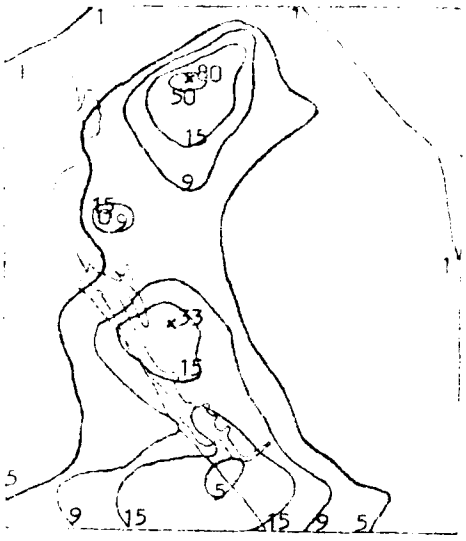

Fig.6-2 Annual average SO_X Conc.(10^{-2} PPM) simulated by TCM model in littoral area of Southern Taiwan

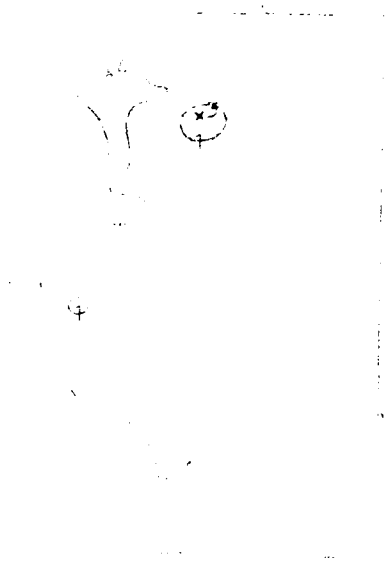

Fig. 6-4 Annual average SO_X Conc. (10^{-2} PPM), result of control by plan I.

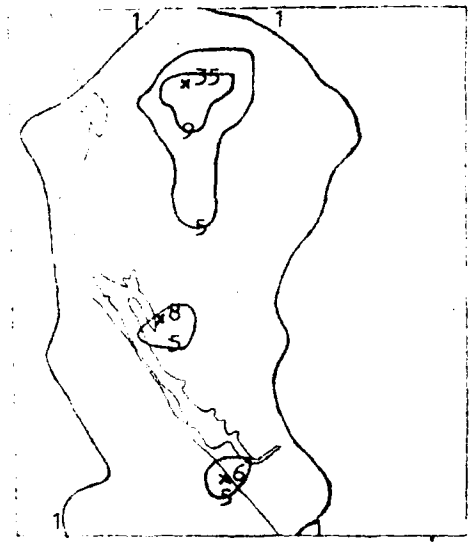

Fig. 6-5 Annual average SO_X Conc.(10^{-2} PPM), result of control by plan II.

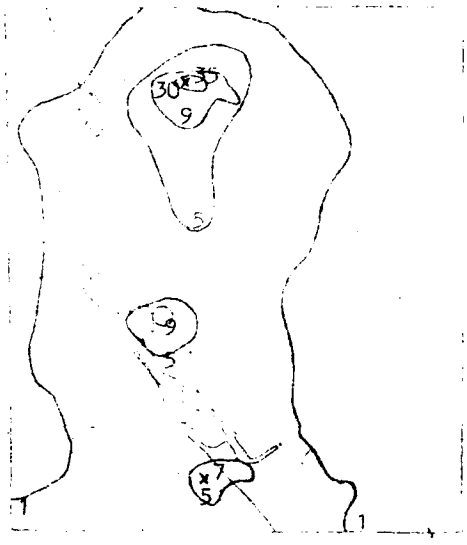

Fig. 6-6 Annual average SO_X Conc.(10^{-2} PPM), result of control by plan III.

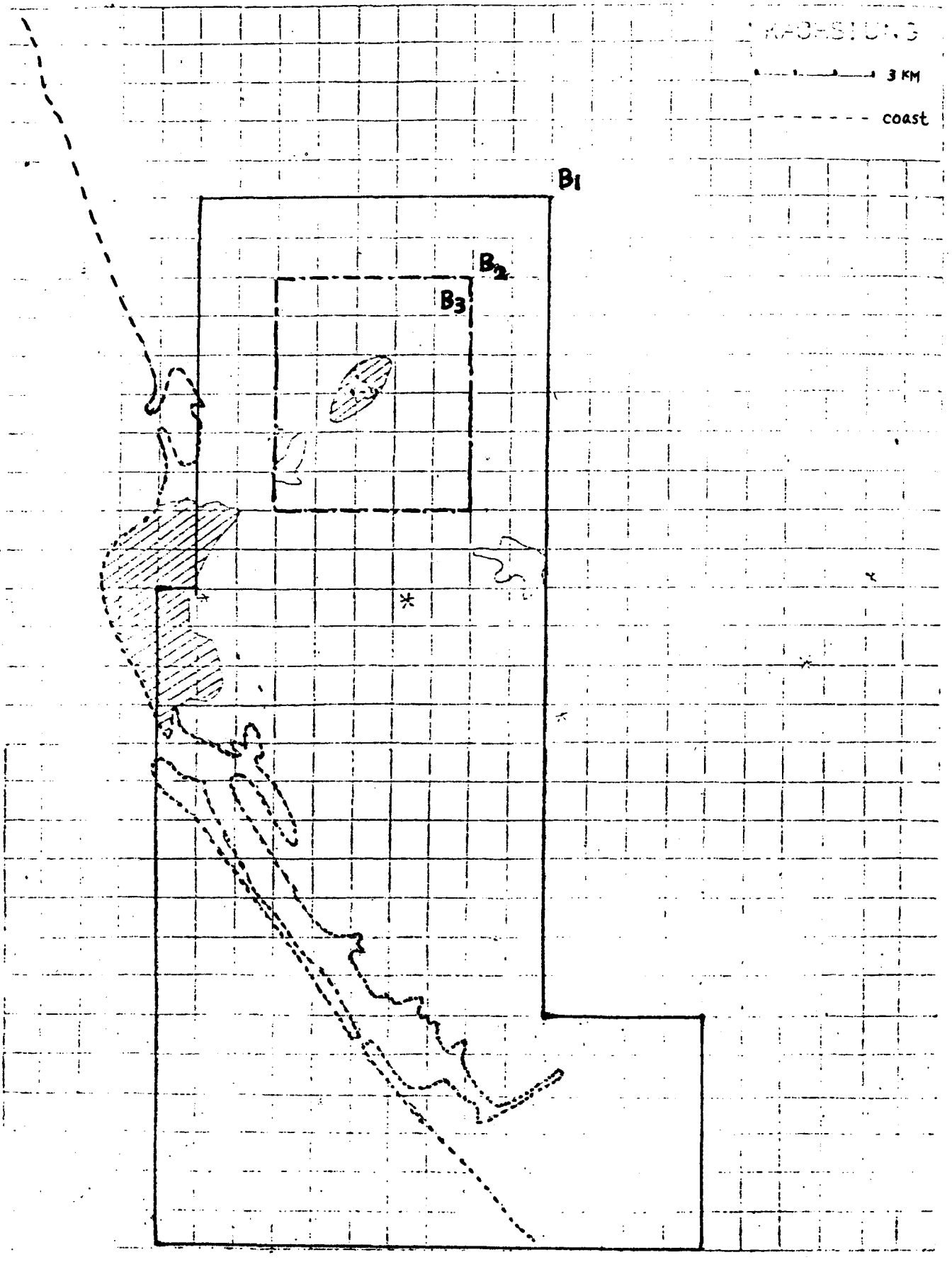

Figure 6-3 The control sector of air pollution in Kaohsiung area.
B_2 sector in the bold area,
dotted area is the B_3 sector, the rest is B_1 sector.

(C) Plan III,

Let $B_1 = 0.05\ C$, $B_2 = 0.08C$, $B_3 = 0.2C$,

then from Eq. (6-8)

get $\tilde{K}_1 = 0.95\ C/K$, $K_2 = 0.92\ C/K$, $K_3 = 0.8\ C/K$

here C is the annual quality standard of SO_x.

If we set the quality standard to be the national standard 0.05 PPM. Then B_1, B_2, B_3 can be determined as shown in Table 6-2, we can control the SO_x emission of the area under different stack dispersion coef. by the simulation of air quality model.

(A) Plan I, as showed in figure 6-4, will control the emission. This means to reduce the emission by a large amount. The reduced amount even reaches 86.2% average. Therefore, the ground concentration level will be of low value. Even the petroleum refinery is just about 0.01 PPM. It is less than the 0.05 PPM of national ambient quality standard.

(B) Figure 6-5 is the result from Plan II. Most parts of the area met the national standard. Only the 3 to 5 Km area from the Petroleum factory was over the allowed value. The average emission of stacks were reduced by 66.2%. According to stack height under 50m, were reduced 66%, height from 50 to 100m reduced 64%, height over 100m reduced 88%. If the sulfur in the heavy oil can be reduced from 4% to 1.2 - 1.5%, the area can be under the standard of Plan II. But, since the height of petroleum refinery's stacks are about 30 m, the pollution is serious. We can improve the pollution as soon as we increase the height of the stacks.

(C) Plan III separated the Kaohsiung area into 2 parts, with not very good control result as shown in Figure 6-6.

Table 6-2 SO_x emission rate (Q) and Stack Dispersion Coef.($\tilde{K}$) of Kaohsiung area.

B / h(m)	0.9C		0.6C		0.2C		0.1C		0.08C		0.05C	
	$\tilde{K}(10^{-3})$	Q	$\tilde{K}(10^{-3})$	Q	$\tilde{K}(10^{-3})$	Q	$\tilde{K}(10^{-3})$	Q	$\tilde{K}(10^{-3})$	Q	$\tilde{K}(10^{-3})$	Q
10	.2805	0.0281	1.1219	0.1122	2.2440	0.2244	2.5243	0.2524	2.5803	0.2580	2.6645	0.2664
20	.3664	0.1466	1.4655	0.5862	2.9312	1.1723	3.2972	1.3189	3.3706	1.3483	3.4805	1.3922
30	.4388	0.3950	1.7553	1.5798	3.5111	3.1600	3.9500	3.5550	4.0372	3.6335	4.1689	3.7520
40	.5302	0.8481	2.1223	3.3952	4.2405	6.7848	4.7705	7.6329	4.8765	7.8025	5.0356	8.0569
50	.5647	1.4118	2.2588	5.6470	4.5176	11.2939	5.0823	12.7057	5.1952	12.9881	5.3646	13.4116
60	.6321	2.2759	2.5288	9.1034	5.0574	18.2067	5.6896	20.4826	5.8160	20.9378	6.0057	21.6206
70	.6513	3.1913	2.6052	12.7653	5.2103	25.5306	5.8616	28.7219	5.9919	29.3602	6.1873	30.3176
80	.7175	4.5920	2.8700	18.3676	5.7399	36.7358	6.4574	41.3277	6.6009	42.2461	6.8162	43.6237
90	.7342	5.9466	2.9366	23.7864	5.9102	47.5730	6.6073	53.5196	6.7541	54.7087	6.9744	56.4927
100	.7683	7.6825	3.0730	30.7299	6.1460	61.4598	6.9142	69.1423	7.0679	70.6787	7.2983	72.9834
110	.7921	9.5848	3.1685	38.3392	6.3370	76.6786	7.1292	86.2634	7.2876	88.1802	7.5252	91.0556
120	.8258	11.8914	3.3032	47.5656	6.6063	95.1314	7.4321	107.0228	7.5973	109.4009	7.8450	112.9683
130	.8490	14.3476	3.3959	57.3904	6.7917	114.7810	7.6407	129.1286	7.8105	131.9979	8.0652	136.3022
140	.8628	16.9113	3.4513	67.6451	6.9026	135.2904	7.7654	152.2017	7.9379	155.5840	8.1968	160.6573
150	.8711	19.5987	3.4842	78.3941	6.9684	156.7896	7.8395	176.3883	8.0137	180.3080	8.2750	186.1876
160	.8973	22.9699	3.5890	91.8784	7.1781	183.7592	8.0659	206.7291	8.2548	211.3231	8.5240	218.2141
170	.9063	26.1906	3.6250	104.7626	7.2500	209.5248	8.1562	235.7154	8.3374	240.9535	8.9094	248.8107
180	.9130	29.5815	3.6521	118.3259	7.3041	236.6520	8.2171	266.2335	8.3997	272.1498	8.6736	281.0242
190	.9523	34.3768	3.8091	137.5085	7.6181	275.0144	8.5704	309.3912	8.7608	316.2665	9.0465	326.5796
200	.9516	38.0643	3.8063	152.2539	7.6129	304.5160	8.5645	342.5805	8.7548	350.1934	9.0403	361.6127

6-3 The selection of total emission control coef.(K)

In this section, we shall discuss another concept to select the control coefficient.

6-3-1 Theory of Computer Simulation

The purpose of setting or calculating the polluted concentration of ground level is to understand the relation between total emission intensity and concentration level.[32] We may obtain optimum strategy to satisfy the air quality standard only after we are aware of the above relation. It is easy to settle the emission standard according the monitoring station observation value directly. We call it a simple rollback model, moreover, we have the modifed rollback model as follows

(1) Simple Rollback model [33]

If the concentration of an area about some long half-life pollutants is equal to a background value plus some other value which is in propotion to the emission, then we can show with the following equation:

$$C(r) = B + K^*(r)E \qquad (6.10)$$

C(r) is the concentration in spot r, r is the spot located at (x,y,z), B is the background concentration, $K^*(r)$ is the proportional factor.

E is emission intensity of pollutants.

The background concentration is the concentration which does not change by emission.

Applying Eq.(2.10), we may obtain the permitted emission intensity E_a as following.

$$E_a = (C-B)/k^*$$

where C is the national air quality standard, K^* is a parameter of weather, emission condition and location, and will change with place, then E_a will be determined by K^*. So we should choose the Cmax for K^*. Then

Putting $K^* = (C_{max} - B)/E$ into Eq.(6.11), we have

$$E_a = (C-B)E/(C_{max}-B) \qquad (6.12)$$

We'd like to modify Eq. (6.12) for use in the next few years with the following equation:

$$E_a = (C-B)E/G(C_{max} - B)$$

where G means the growth rate of emission after several years.

Therefore, the reduction percentage of emission R is,

$$R\% = 100 \left\{1 - \frac{E_a}{E}\right\}_{(\%)}$$

$$= 100 \left\{1 - \frac{(C-B)}{G(C_{max}-B)}\right\}(\%)$$

$$= 100 \cdot \frac{GC_{max}-C + B(1-G)}{G(C_{max} - B)} (\%)$$

$$= 100 \cdot \frac{GC_{max}- C + B(1-G)}{GC_{max}-B+B(1-G)} (\%) \qquad (6.13)$$

Since B(1-G) is very small as compared with other terms in general. We may omit it. Rewriting Eq. (6.13) as

$$R\% = 100 \frac{GC_{max}-C}{GC_{max}-B} (\%) \qquad (6.14)$$

It is called simple rollback model. The reduction percentage can be gained by putting Cmax, B, C and G into the equation.

(2) Modified Rollback Model[34]

If the long half-life pollutants have emission E(r,t), then the concentration C(r,t) could be shown as

$$C(r,t) = \int_0^t dt' \int dr' F(r,r';t,t') E(r',t') + \int dr' [C(r',t') F(r,r';t,t')]t' \qquad (6.15)$$

where F(r,r';t,t') is the function of atmospheric dispersion,

r is somewhere space location (x,y,z)

t is time,

suffix(1) means a position and emitted time of source.

F(r,r';t,t') is decided by wind direction, wind speed, stability and other boundry condition such as land appearance and height of mixing layers. E(r,t) should include all the emission sources, such as large factories, domestic houses, small factories, vehicles and aircrafts.

To control the environmental quality, the standard should reach the average $\bar{C}(r)$. The value of Eq.(6.15) could be replaced by B if the time period is quite long. B has nothing to do with the control of emission sources.

Suppose the average of C(r,t) of time interval $T = t_2 - t_1$ is called $\bar{C}(r)$.

$$C(r) = \frac{1}{T} \int_{t_1}^{t_2} dt \int_{o}^{t} dt' \; F(r,r';t,t') \cdot E(r',t') + B \qquad (6.16)$$

Eq. (6.16) form can be simplified as (6.17) if we set the manner unchanged in time T.

$$\bar{C}(r) = \int dr' \; F(r,r') E(r') + B \qquad (6.17)$$

Eq.(6.17) is analogous with eq. (6.10), which was modified from Eq.(6.10). The concentration in a few years $C_f(r)$ is

$$C_f(r) = \int dr' \; F(r,r') \; [1-R(r')] \; E(r') G(r') + B \qquad (6.18)$$

R(r') is the reduction rate of emission.

As setting the emission standard, the environmental quality standard concentration C should be large than $C_f(r)$.

$$C_f(r) \leq C, \quad r = (x,y,0) \qquad (6.19)$$

From Eq.(6.18), Eq.(6.19) we can find the allowed emission $E_q(r)$ as

$$E_a(r) = [1-R(r)]E(r)G(r) \qquad (6.20)$$

If there are several sources, then Eq.(6.20) becomes

$$E_a(r) = \sum_i [1-R_i(r)]E_i(r)G_i(r) \qquad (6.21)$$

The 99.3% for emission inventory of Kaohsiung area are occupied by those from point sources.

$$E(r,t) = \sum_i E_{pi}(t)\,\delta(r-r_i) = \sum_i \bar{E}_{pi}\delta(r-r_i) \qquad (6.22)$$

E_{pi} is the point source. $\delta(r_i)$ is Delta function.

$\bar{E}_{pi}$ is the emission amount in stable condition.
To set Eq.(6.22) into Eq. (6.18), Eq.(6.20) we have

$$C_f(r) = \int dr'\ F(r,r')\ [1-R(r')] \sum_i \bar{E}_{pi}\,\delta(r'_i)G(r')+B$$

$$= \sum_i F(r,r_i)\ [1-R(r_i)]\ \bar{E}_{pi}G(r_i) +B \qquad (6.23)$$

$$Ea = \sum_i [1-R(r_i)]\ \bar{E}_{pi}G(r_i)$$

$$E_{ai} = [1-R(r_i)]\ \bar{E}_{pi}G(r_i) \qquad (6.24)$$

Transfering Eq.(2.23), and Eq.(2.24) into vertical coordinates, the ground concentration can be found by Eq.(6.25) and Eq.(6.26)

$$C_f(x,y,o) = \sum_i F(x,y,o;\ x_i,\ y_i,\ H_e)\cdot(1-R_i)E_{pi}G_{pi}+B \qquad (6.25)$$

$$E_{ai} = (1-R_i)E_{pi}G_{pi} \qquad (6.26)$$

He is the effective height of source.

Convert the spreading equ. into the Gaussian[35] equ.

$$F(x,y,o;\ x_i,\ y_i,\ H_e) = \frac{1}{\pi\,\sigma_y\,\sigma_z\,u}\ \exp\ [-\frac{R^2}{2\,\sigma_y^2}]\exp[-\frac{He^2}{2\sigma_z^2}] \qquad (6.27)$$

if $H_e + \sigma_z \leq L$

$$F(x,y,o;\ x_i,\ y_i,\ H_e) = -\frac{1}{\pi \sigma_y \sigma_z U} \exp\left[-\frac{R^2}{2\sigma_y^2}\right]$$

$$\sum_{N=-\infty}^{\infty} \exp\left[-\frac{(H_e+2NL)^2}{2\sigma_z^2}\right]$$

(6.28)

if $L < H_e + \sigma_z < 1.6L$

$$F(x,y,o;\ x_i,\ y_i,\ H_e) = \frac{1}{\sqrt{2\pi}\sigma_y} \frac{1}{LN} \exp\left[-\frac{R^2}{2\sigma_y^2}\right]$$

(6.29)

if $H_e + \sigma_z > 1.6L$

$$\sigma_y = aS^b,\ \sigma_z = cS^d,\ U = U_o\left(\frac{H_e}{Z_o}\right)^P \qquad (6.30)$$

where

$$R = (y_i - y)\sin\theta - (x_i - x)\cos\theta$$

$$S = (y_i - y)\cos\theta + (x_i - x)\sin\theta$$

θ is the angle between wind and N-direction.

L is mixing layer height.

U is the wind speed.(m)

S is the distance from source to polluted area.

R is the lateral distance of wind.

σ_y is the diffusion standard deviation in lateral direction.

σ_z is the diffusion standard deviation in vertical direction.

a,b,c and d are constants of diffusion standard deviation [36]

From the Gaussian equ. we have

$$S_{max} = \left(\frac{2d}{b+d}\,\frac{H_e^2}{c^2}\right)^{\frac{1}{2d}} \qquad (6.31)$$

Therefore, we can expres the max. concentration as

$$\frac{C_{max}U}{E_{pi}} = \exp\left[\frac{-(b+d)c^2}{4d}\right] / \pi \left(\frac{2d}{b+d}\,\frac{H_e^2}{C^2}\right)^{\frac{b+d}{2d}} \qquad (6.32)$$

from Eq.(6.31) and Eq.(6.32) we know that $C_{max} \propto 1/H_e^{\frac{b+d}{d}}$

and $C_{max} \propto H_e^{\cdot\frac{1}{d}}$ and then if $E_{ai}=K_iH_e^{\frac{b+d}{d}}$ (6.33)

If consider that the max. concentration due to single source will happen in downwind direction and use constant K, the next Eq. are gained from Eq.(6.32)

$$C_{max}U = K_i\exp\left[\frac{-(b+d)c^2}{4d}\right]/\pi \left[\frac{2d}{(b+d)c^2}\right]^{\frac{b+d}{2d}} \qquad (6.34)$$

As K_i is fixed, no matter how decrease E_{ai} or increase H_e, the C_{max} of Eq.(6.34) remain unchanged under Eq.(6.33). But if S_{max} changes with $H_e^{1/d}$, the position where max. concentration will happen, is the function of H_e. But for multi-source region, we consider where C_{max} happened

is not only the function of H_e, but also the concentration of sources. Put Eq.(6.33) into Eq.(6.23) and Eq.(6.24), then

$$C_f(r) = \sum_i F(r,r_i) K_i H_e^{\frac{b+d}{d}} + B \qquad (6.35)$$

$$1 - R(r_i) = \frac{K_i H_e^{\frac{b+d}{d}}}{E_{pi} G(r_i)}$$

$$R_i = \frac{E_{pi} G_i - K_i H_e}{E_{pi} G_i} \qquad (6.36)$$

By converting K_i and H_e, we can find $C_f(r)$ value with computer, by using reasonably assumed K_i, H_e and Eq. (6.19), finally we can find out the reduction percentage R_i. (37)

6-3-2 Collecting the Necessary Data for Computer Simulation

1. Setting Monitoring Stations and Samplong Networks

There are 184 P_bO_2 stations in Kaohsiung 276 km^2 area. (Fig. 6.7) They are located in the high density of 1 in km^2, Average 1.5 in 1 km^2 area.

We sampled 9 times from the 11.5 months testing (from Apr. 1976 to Mar. 1977). One of them was months long and the other was 1.5 months. Figure 6.8 shows the most polluted situation of Jan. Feb., 1977, Fig.6.1 shouws the annual average situation of 1976 to 1977.

The P_bO_2 method (Ref. B. S. 1747-Part 4 (1963), ASTM D 2010 (1962) tested the SO_x quantity which passed through a cylinder and reacted with PbO_2, and did not represent the SO_x amount of air.

So it should find the relation to convert sulfation degree per months into SO_2 concentration in ppm.

The correlation experiment was conducted within a 50 days period by operating one automatic SO_2 analyzer together with 21 lead peroxide candles circle around the air inlet of the analyzer. One candle was taken to be analyzed about every 2 or 3 days. The hourly average SO_2 conc. displayed by automatic SO_2 analyzer was summed in the same time period for each candle analyzed. These results are shown on Table 6-3. It is obvious that the analyzer was located in a highly polluted area. The data treatment of finding the correlation relationship follows the assumption that we can consider the data listed on column 3 of Table 6-3 as the sulfation degree of a 30 days period and the data listed on column 4 as total SO_2 hourly conc. summing over this 30 days. [38,39]

Table 6-3 Comparison of PbO_2 and test of electric conductivity

No.	Days	SO_3 mg		SO_2 ppm		$\frac{SO_2 \text{ ppm}}{SO_3 \text{ mg/Day}}$	Wind speed m/sec	Temperature °C	Moisture %
		Total	Ave. daily	Total	Ave. daily				
1	3.5	8.012	2.289	0.1554	0.0444	0.0194	1.04	25.7	78.25
2	5.5	13.72	2.494	0.245	0.0446	0.0179	0.919	26.03	77.00
3	7.5	22.89	3.052	0.333	0.0445	0.0146	0.962	26.39	76.88
4	9.5	33.60	3.537	0.479	0.0504	0.0142	0.886	26.49	76.50
5	11.5	42.09	3.660	0.580	0.0504	0.0138	0.859	25.92	75.83
6	15.5	33.56	2.165	0.937	0.0604	0.0279	0.831	25.86	74.13
7	17.5	48.42	2.767	1.122	0.0641	0.0232	0.836	26.06	74.50
8	19.5	62.19	3.189	1.279	0.0656	0.0206	0.819	26.21	74.85
9	21.5	47.58	2.213	1.441	0.0670	0.0303	0.825	26.29	74.77
10	23.5	62.86	2.675	1.673	0.0712	0.0266	0.830	26.40	74.58
11	25.5	84.28	3.305	1.848	0.0725	0.0219	0.841	26.53	74.58
12	27.5	84.48	3.072	1.904	0.0692	0.0225	0.878	26.71	74.54
13	31.5	60.95	1.935	2.105	0.0668	0.0345	0.897	27.00	74.47
14	33.5	62.86	1.877	2.204	0.0658	0.0351	0.884	27.11	74.41
15	35.5	93.97	2.647	2.231	0.0654	0.0247	0.938	27.18	74.25
16	39.5	78.01	1.975	2.590	0.0656	0.0332	0.914	27.18	75.15
17	41.5	114.54	2.760	2.690	0.0648	0.0235	0.890	27.17	75.81
18	43.5	106.58	2.450	2.790	0.0641	0.0262	0.882	27.26	76.07
19	45.5	85.59	1.881	2.902	0.0638	0.0339	0.873	27.28	76.33
20	47.5	81.99	1.726	3.023	0.0636	0.0368	0.863	27.28	76.42
21	49.5	87.91	1.776	3.170	0.0640	0.0382	0.853	27.26	76.64

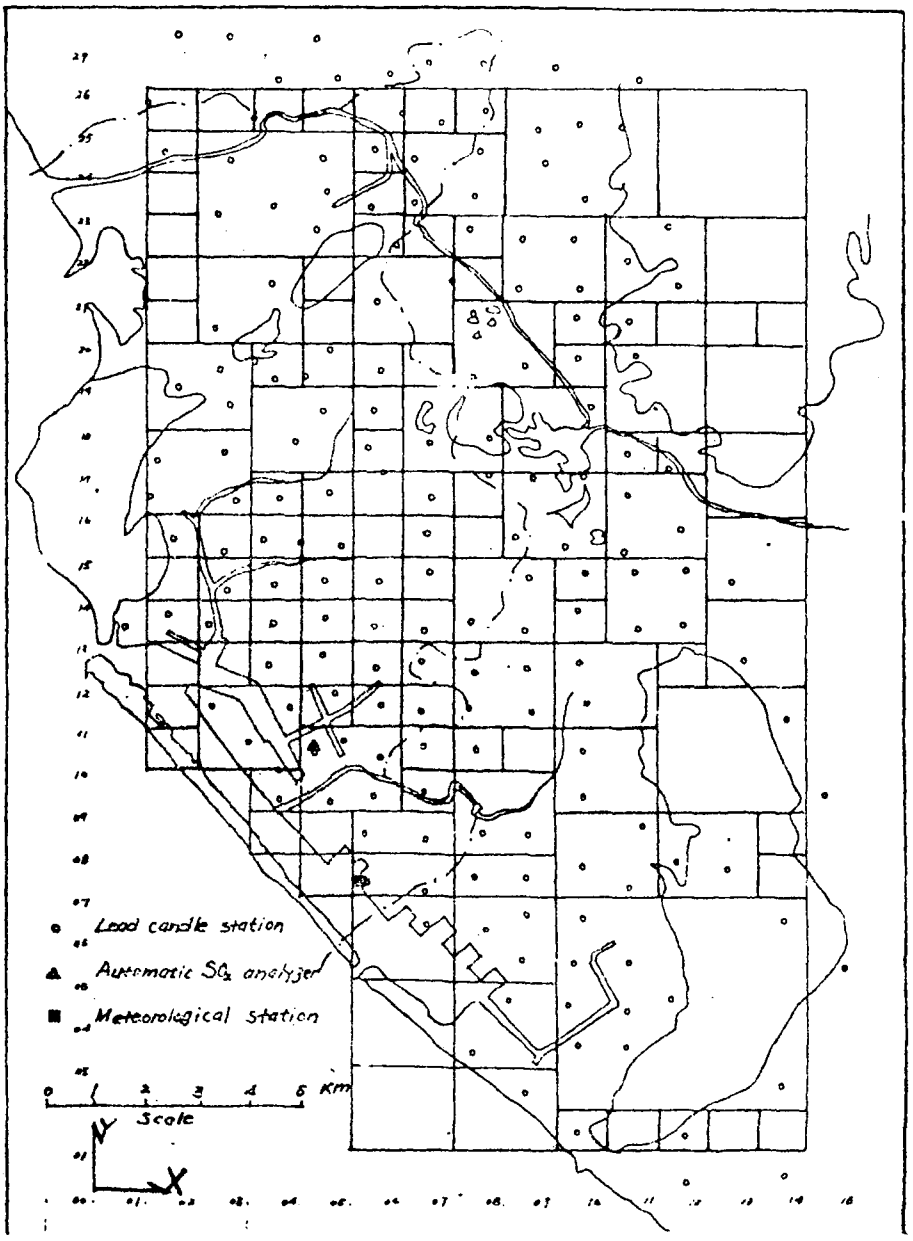

Fig. 6-7 The distribution map of monitoring network and the area source grids on Kao-Hsiung City.

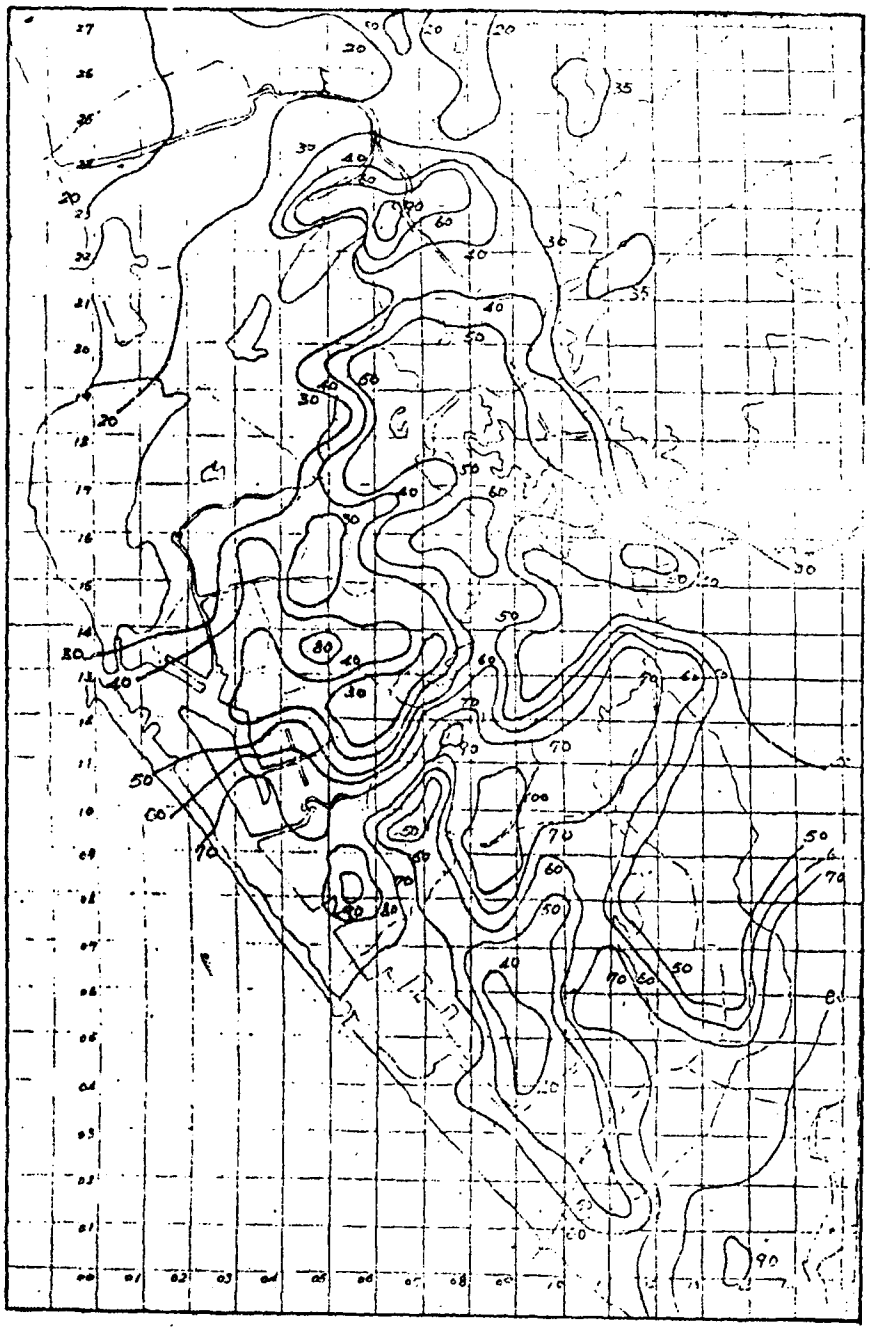

Fig. 6-8 The isopleth of monthly average sulfation degree (mg SO_3/100 cm^2 PbO_2/30 days) of Jan. Feb. 1977.

2. Emission Inventory

0.357 million tons sulfur dioxide was emitted from this area in 1976. About 99.3% come from the 252 point sources (SO_2 emission greater than 50 Tons per year). 74% of total amount released by the power plants. The largest sources (68%) having six stacks greater than 70m in height was located in grid (07,04) of Figure 6-7. This largest source plays the major role of pollution in winter days when the prevail winds blowing toward inland and the frontal of air mass passing freguently. During the other seasons, serious pollution are caused by smaller and dense distributed sources. Little amount of total emission was contributed by commercial, traffic and other combustion sources. In spite of this, the whole area is divided into 135 area sources. Each area source has square area with minimum 1 km in side length. The SO_2 was considered uniformly emitted from each area sorces. Figure 6-7 shows these grids with broad black line.

3. Meteorological Data

We classified the meteorological data of one station by the Turner (1961) method from Apr. 1976 to Mar. 1977. The percentage of stability is shown in Table 6-4.

Under 8 observations each day, we have the distribution diagram Fig. 6-9. Most of them were from north, northwest, northeast. And most of them are in medium D class of stability. Wind speed was between 1.8-3.5m/sec. and modified speed was 3.33m/sec. We put the weather conditions and D class stability and speed 3.33m/sec for computing the ground concentration of

Table 6-4 Stability of each grade in Kaohsiung area (Apr. 1976 to Mar. 1977)

Stability	A	B	C	D	E	F
PERCENT (%)	0.59	9.39	12.67	43.77	10.58	22.93

Table 6-5 Distributing percent of wind grade in Kaohsiung area

Wind speed (m/sec)	0 - 1.7	1.8 - 3.5	3.6 - 5.7	5.8	Average
Percent (%)	24.82	36.71	25.1	13.37	3.33

pollution. After doing that for 16 directions, we found the average value. Table 6-5 shows the distributing percentage of wind grade.

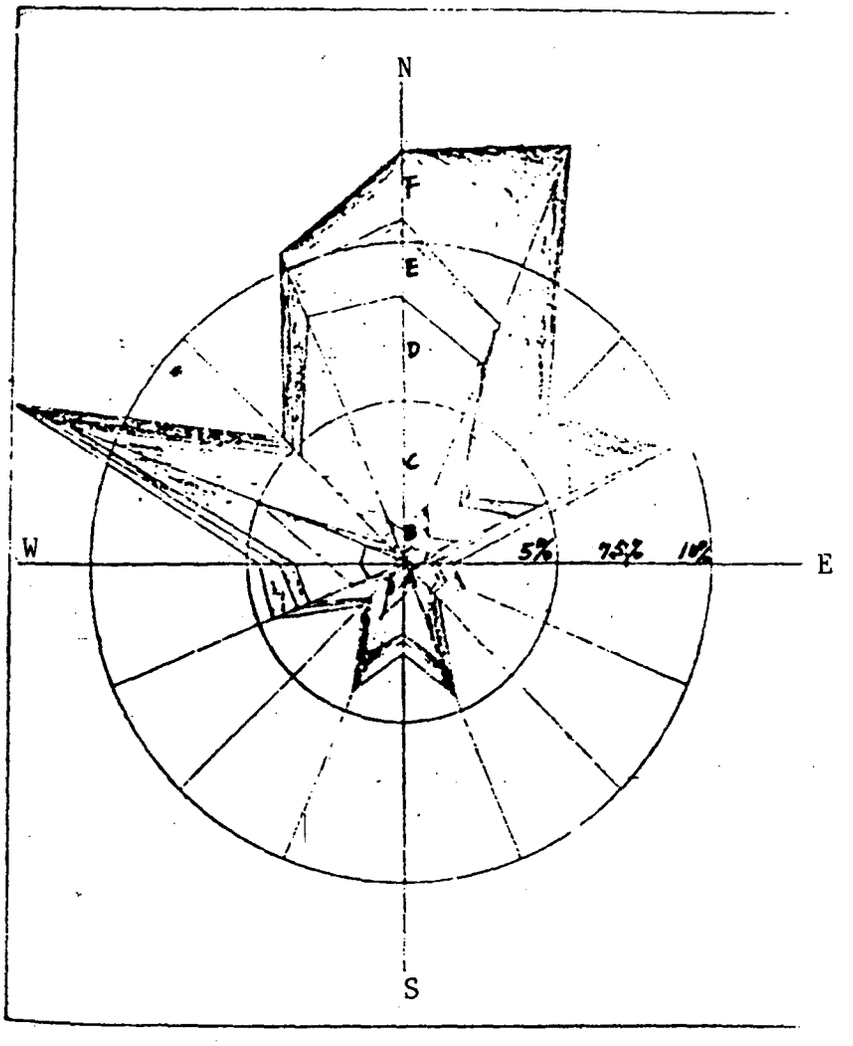

Fig. 6-9 Wind rose and stability class on Kaohsiung from Apr. 1976 to Mar. 1977.

The height of the mixing layer is another important item. Because we didn't have the actual value, we set the height of layer to be 500 m. The farthest boundary of the Kaohsiung area is about 50 km away, the standard deviation in vertical direction of diffusion is less than the height. So the height we set does not quite influence the calculation of ground concentration.[40]

In the next section the author will try to claculate the annual average concentration of SO_2 in this littoral area. The application of computer simulation model after strict examination is thought the best implementation to determine the total emission control coefficient.

6-3-3 Computer Simulation and Examination

Gaussian steady state diffusion model is used here. The algorithm of calculating the ground SO_2 conc. contributed by point sources and area sources is similiar that used by RAM.[41] When trying to get the annual average conc., two kinds of algorithm have been tested:

(1) Seperate wind directions into sixteen parts. Calculate the hourly SO_2 conc. distribution of each wind direction using average emission rate of each source, annual average wind velocity and mixing height and diffusion rate of D stability class. The results of each wind direction were multiplied by the annual probability of that wind direction. Then, summing over the results of the sixteen wind direction the anuual average conc. is obtained.

(2) Each wind direction is divided into six stability classes further 96 sets of the distribution of SO_2 conc. are calculated using annual average emission rate of each source, annual average wind velocity, mixing height and diffusion rate of that stability class. The annual average conc. is obtained by summing over the 96 sets data after each data weighted by annual joint probability.

Diffusion rate in ruban areas recommended by N.E. Bowne[36] and Plume rise by Briggs[26] are used here. Wind velocity is corrected fro different stack heights. The half life of SO_2 is assumed to be 30 minutes. (s,t)

Simulating results, by IBM 370 computer, are shown on Figure 6-10 and Figure 6-11. Both have similar shape when compared with Figure 6-1. But higher value in high conc. area and lower value in low conc. area can be found in both calculated results. Algorithm 2 gives higher maximum value and wider high conc area since stability F classes play a significant role in this case. The major power plant which emits 68% of total SO_2 emission from this area doesn't give the most serious pollution of this area as can be seen from any one of those three isopleths map. The maximum value in the southern area is lower than the other two maximum in middle and northern area. (u,v)

Figure 6-12 and Figure 6-13 give the regression lines of measured versus calculated annual average SO_2 conc. For algorithm 1 $Y = 0.430\ X + 0.011$ with $r = 0.78$, for algorithm 2 $Y = 0.374\ X + 0.011$ with $r = 0.73$. It seems that algroithm 1 gives the results more like the measured value. It is possible that a more elaborate model may catch more uncertainty in the input data and finds no advantage. This conc., 0.011 ppm, can be taken as the ground conc. of this area. It is brought by wind from the emission sources of adjacent area. (w,x,y)

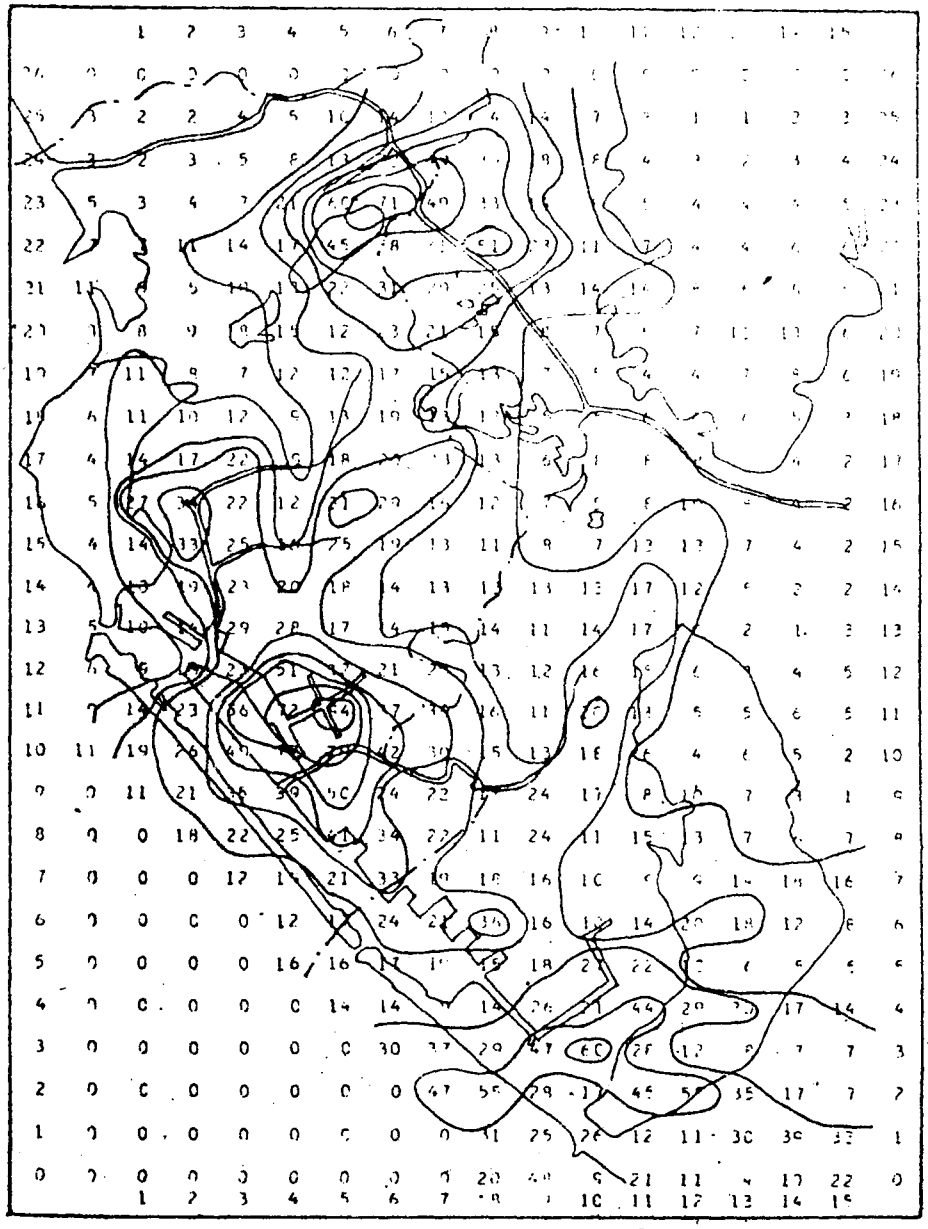

Fig. 6-10 Annual average SO_2 conc. (10^{-3} ppm) simulated by algorithm 1 : 16 wind direction, 3.3 m/sec wind speed, D stability class and 500 meter mixing height.

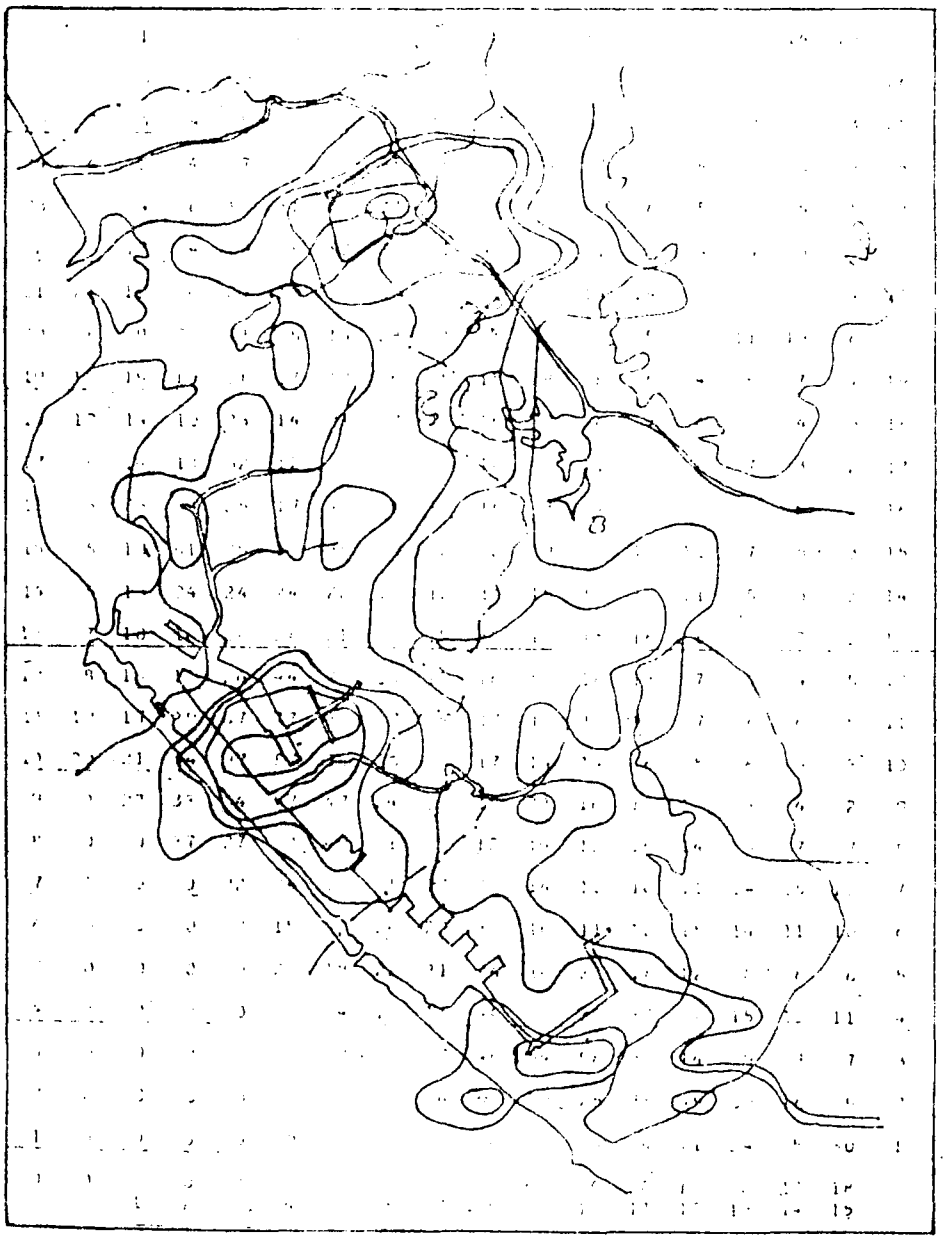

Fig. 6-11 Annual average SO_2 conc. (10^{-3} ppm) simulated by algorithm 2 : 16 wind directions, 6 stability class each, i.e. 96 sets meteorological conditions in total.

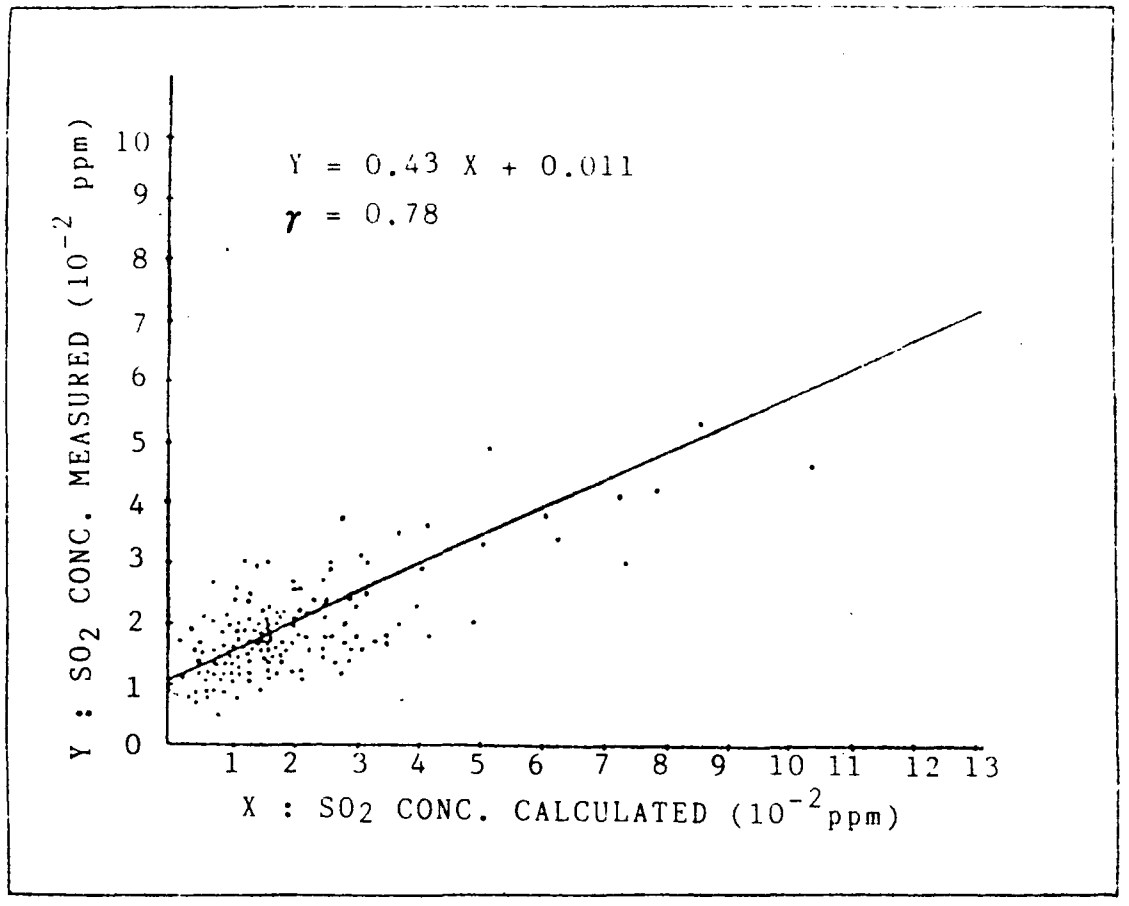

Fig. 6-12 Regression line of annual average SO_2 conc. measured by lead candle network versus calculated by algorithm 1.

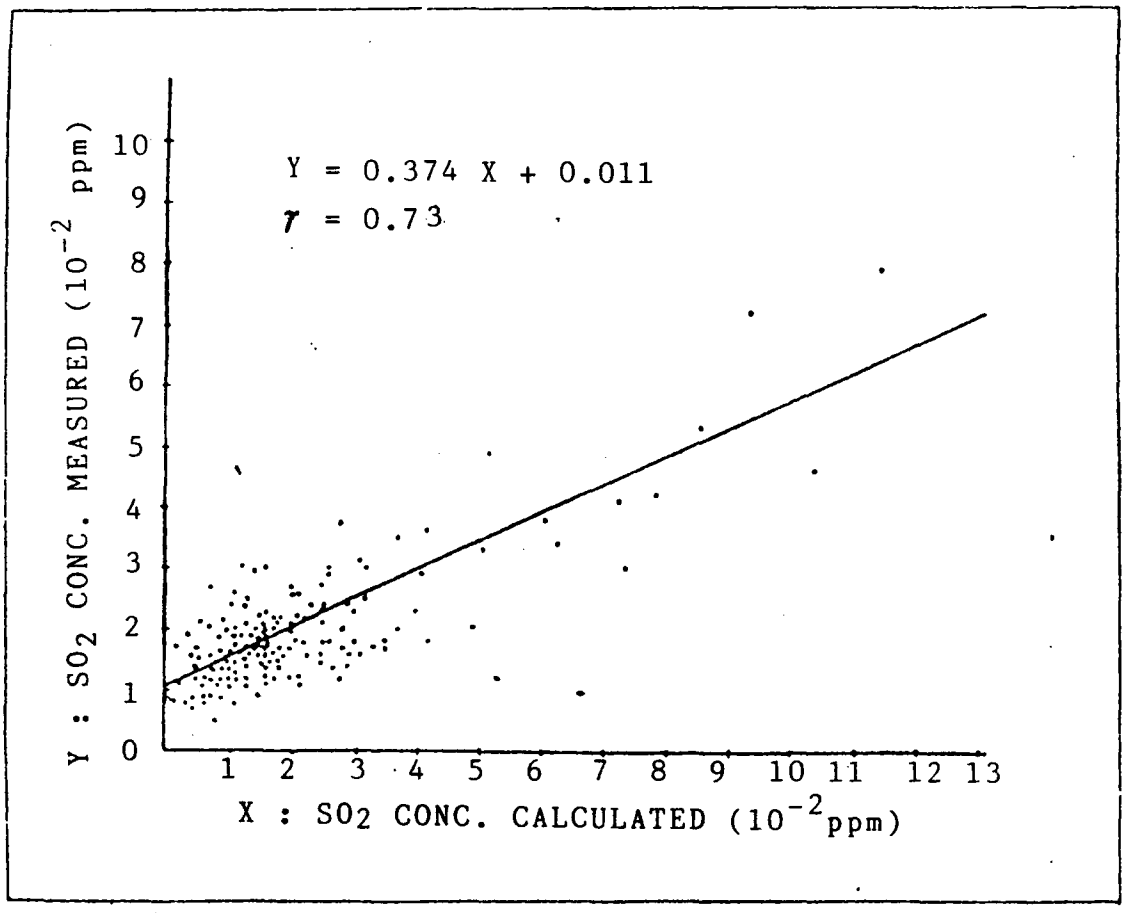

Fig. 6-13 Regression line of annual average SO_2 conc. measured by lead candle network versus calculated by algorithm 2.

6-3-4 The Determination of Total Emission Control Coef.(K)

As the author has discussed in CHAP.4, the σ_y and σ_z curves determined by Pasquill and Gifford were derived from measurements taken in open, level to gently rolling terrain of continent, and may not be the best estimate of dispersion coefficients for littoral urban areas like Kaohsiung or areas with rough terrain like Linkou in the Taiwan island.

For the purpose of obtaining the general methodology for the furture to determine the total emission control coef. around the island, the Kaohsiung area is undertaken as a pilot study region. A number of uncertain parameters such as σ (Sigma) must be studied firts. These standard deviation functions may be approximated by a power law curve as follows:

$$\sigma_z = a_z x^{bz}$$

$$\sigma_y = a_y x^{by} \qquad (6.37)$$

where: a_z, b_z, a_y and b_y are functions of downwind distance x and atmospheric stability, as the author has discussed with the data of tracer experiment before. Table 6-6 and Table 6-7 are a summary of power law exponents and coefficents.

Table 6-6 Power law exponents and coef. for σ_y

P-G Atmospheric Stability Class		Downwind Distance, meters $X < 10,000$		Downwind Distance meters $X \geq 10,000$	
		a_y	b_y	a_y	b_y
Busse and Zimmerman (e)	A=1	.495	.873	.606	.851
	B=2	.310	.897	.523	.840
	C=3	.197	.908	.285	.867
	DD=4	.122	.916	.193	.865
	DN=5	.122	.916	.193	.865
	E=6	.0934	.912	.141	.868
	F=7	.0625	.911	.0800	.884
The author, 1977	A	2.719	.722	.081	1.027
	B	1.408	.750	1.164	.767
	C	1.277	.732	.776	.772
	D	1.257	.692	.683	.830
	E	1.091	.668	.516	.787
	F	.782	.671	.217	.769
The author, 1982	*	1.0	.865		
	B **	1.0	.90		
	C *	1.0	.90		
	**	1.0	.90		
	*	1.0	.89		
	D **	1.0	.90		

* : Internal Boundary Layer exist

** : Internal Boundary Layer doesn't exist

Table 6-7 Power law exponents and coef. for σ_z

(a) B & Z[e]

P-G Atmospheric Stability Class	Downwind Distance, meters $100 < x \leq 500$		Downwind Distance meters $500 < x \leq 5000$		Downwind Distance meters $5000 < x$	
	a_z	b_z	a_z	b_z	a_z	b_z
A = 1	.0383	1.281	.0002539	2.089	.0002539	2.089
B = 2	.1393	.9467	.04936	1.114	.04936	1.114
C = 3	.1120	.9100	.1014	.926	.1154	.9109
DD = 4	.0856	.8650	.2591	.6869	.7368	.5642
DN = 5	.0818	.8155	.2527	.6341	1.297	.4421
E = 6	.1094	.7657	.2452	.6358	.9204	.4805
F = 7	.05645	.8050	.1930	.6072	1.505	.3662

(b) The author, 1977

P-G Atmospheric Stability Class	Downwind Distance, meters $100 < x < 500$		Downwind Distance, meters $500 < x < 10000$		Downwind Distance meters $10000 < x$	
	a_z	b_z	a_z	b_z	a_z	b_z
A	0.0362	1.4517	0.0233	1.5229	0.0233	1.5229
B	0.1056	1.1386	0.0407	1.2922	0.407	1.2922
C	0.0956	1.0829	0.0634	1.1490	0.0634	1.1490
D	0.3278	0.8153	0.1792	0.9124	22.381	1.1383
E	1.0285	0.5675	0.7044	0.6285	10.2981	0.3372
F	2.1380	0.4081	1.4656	0.4689	6.875	0.3010

(c) The author, 1982

P-G Atmospheric Stability class	Downwind Distance, meters, x <10,000	
	a^z	b^z
B *	0.57	1.094
**	.463	.751
C *	.10	.90
**	.463	.751
D *	.40	.63
**	.463	.751

*: IBL exist **: IBL does not exist

In Eq.(6.30), we use a,b,c, and d as a_y, b_y, a_z, and b_z in CHAP.4 and here. From Table 6-6 and Table 6-7, we can see a, b, c, d change with stability and distance. So it is the same as (b+d)/d (refer to Table 6-8). We find the the average (b+d)/d is about 1.9. So Q=(k) x $0.0008\ H_e^{1.9}$ (6.38) can be obtained, where, Q is the emission rate (g/sec), H_e: stack effective height (m), (K): constant. In calculation, we first set (K)=1 to find the emission value. Then we put the emission and weather information in to find the polluting concentration of each place.

The places are set at the edge of each right rectangular area with an area of 1 Km^2. There are 398 places. After finding out the concentration of each place, we divided the concentration by 0.05 ppm, and get the result as shown in Table 6-9.

Table 6-8 The $\frac{b+d}{d}$ value in 10 km of grades of stability

Stability	A	B	C	D	E	F
< 1 km.	1.5008	1.6540	1.6767	1.8229	2.1003	2.3739
> 1 km.	1.4743	1.5803	1.6367	1.7587	2.0804	2.4289

Table 6-9 (K) value of Kaohsiung area

Area \ Factory Pattern	Established	Newly established
Nantz	(1) 3	(1) 3
Taser	(1) 6	(1) 6
Chengchen, Tsoyin, Tsnwoo	(1) 9	(1) 7
Hsiaokan, Koshan	(1) 16	(1) 10
Other areas	(2) 2	(2) 2

(1) $Q = (K) \times 0.0007936 H_e^{1.9}$

(2) $Q = (K) \times 0.0007936 H_e^{2.37}$

Q : Allowed emission g/sec

H_e: Effective height of chimney, from Brigg's equ.

H_e: 0.48F1/3 (3.5X) 2/3

$X = 14F^{5/8}$ if $F \leqslant 55$

$X = 34F^{2/5}$ if $F > 55$

$F = 1.9 \times 10^{-4} \times V (Ts-20)$

V = Emission volume

Ts = Emission temperature

If the Q value is larger than that of (2) then use the Q value of (2)

As Table 6-9 obtained from simulation, the number in brackets indicates the equ. That should be used. We use(1) as gathering sources. Use(2) for independent source. Figure 6-14 shows the relation between permitted emission rate and stack effective height.

From the figure, we can see the importance of improved emission method by changing stack heights over 40 m.

In Table 6-9, as (K) and raising stacks height over 40 m. we know that Ta-Lin thermal power plant must reduce its 40% emission of SO , i.e. 96 thousand tons per year. Southern thermal power plant's emission should be reduced by 16 thousand tons/year (52%). That of petroleum refinery was 6 thousand tons/year (14%). Total of the others was 24 thousand tons/year.

Under the restraint of Table 6-9 (K) value, there are 3 methods to improve the situation:

(1) Increase the stack height.
(2) Use low sulphur content fuel.
(3) Use desurfurization equipment.

For (1), if stack's height is increased to 40 m, there is no effect to (K). But with a height over 40 m, (K) should be reset.

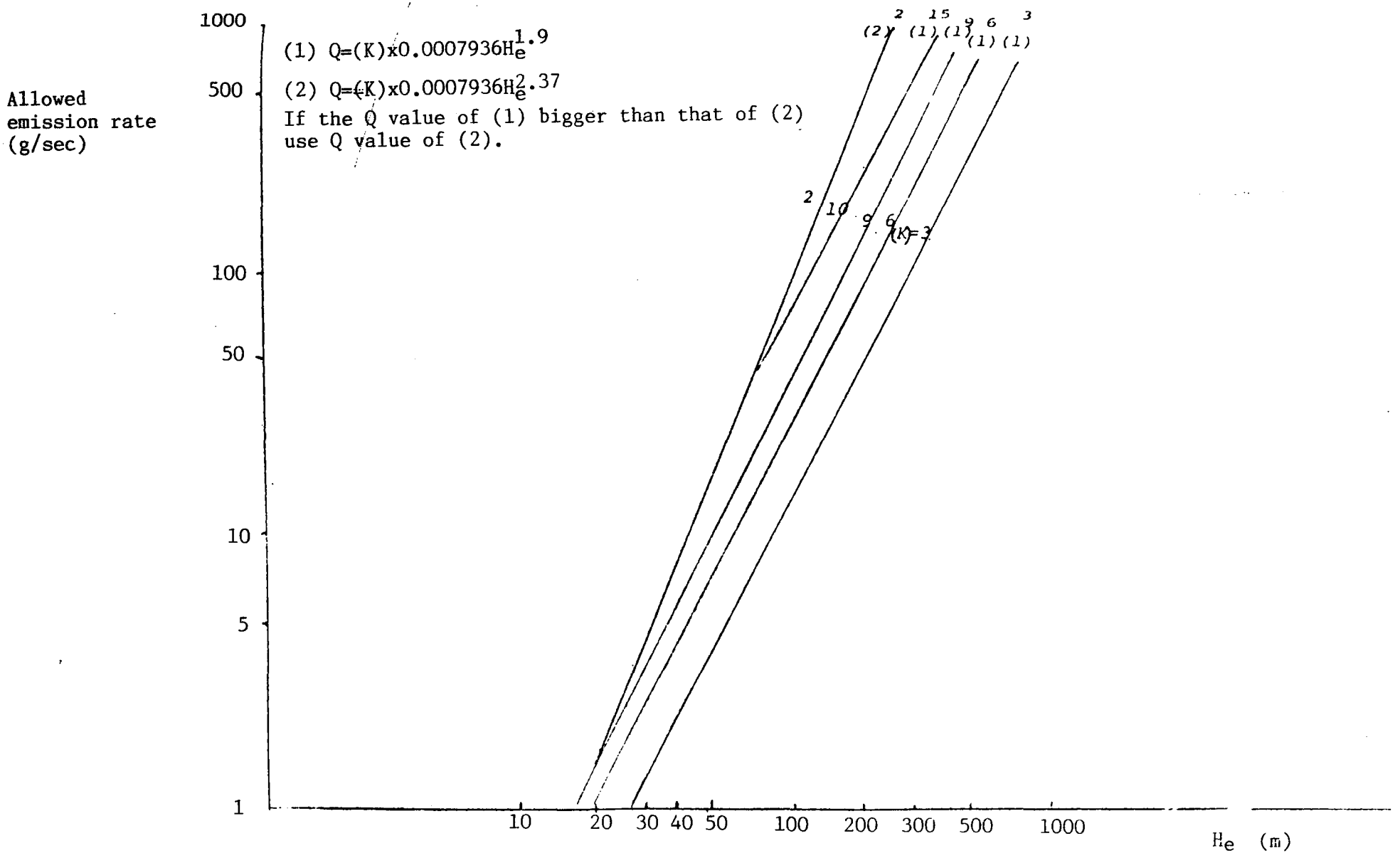

Fig. 6-14. H_e: effective height of stack

Relation between emission rate and stack effective height.

6-3-5 Conclusion

(1) The simulation models give fairly good correlation with the results of lead candle network. This work reveals that if a lead candle network can be correlated well with the results of automatic SO_2 analyzer and a simulation model can be modified by the results of lead candle network such that both network and model can be used as effective information of strategy de esion making of air pollution control.

(2) Simple rollback model's application
Our country restrained the average annual value of SO_2 to be under 0.05 ppm. Daily average value is 0.1 ppm. And the hourly is 0.3 ppm. Thus we could use the simple rollback model to find out the reduction percentage. From PbO_2 and conductivity method, we can see the SO_2 concentration is 0.05 ppm for 50 mg SO_3/30 days/100 cm^2 PbO_2. In Fig. 6-1. we find the high concentration areas are located in (2, 16), (5, 11), (6, 23), (10, 3) and (14, 1) with 28, 86, 58, 65 and 41 ppm, respectively. Its background concentration B is 5 mg SO_3 or 0.0025 ppm. SO_2. Despite the growth factor, the reduction ratio should lie as follows:

(2,16) It is lower than the environmental quality standard R=0%

(5,11) :R_2= 47%

(6,23) :R_3= 25%

(10,3) :R_4= 35%

(14,1) :R_5= 0% (The average value of the year is lower than the environmental quality standard, but the value of Jan. & Feb. should not take into).

(3) Modified rollback model's application

The concentration distribution in figure 6-15 is analogous with the value of figure 6-1.

For low concentration part; figur 6-15 is lower than Fig. 6-1. Possibly for (1) the error assumption for half-life (assume 30 min. in this article) (2) despite the area sources (0.7% of the area) (3) despite of background concentration. So, we must give further study for a better answer.

Figure 6-16 was obtained from equ. (6-38) with (K)=1. To find a reduction emission, we can find out the downwind distance from Eq. (6-31) first, then make a circle in figure 6-16 with the above distance as the radius. The smallest (K) in the circel will be taken as the value to set into Eq. (6-36) for reduction percentage Figure 6-18 was obtained from equ. (6-38) as (K) = 1 and height of stack under 40 m. Figure 6-17 is the (K) distribution of Figure 6-16. From Figure 6-17, 6-19, we can see that the ground concentration standard can be reached by increasing the height to increase the dispersion ability. Figure 6-20 showed the change of (K) value of 4 different places under different heights. From this, one can see the relation between Q and (K). (K) decreased and Q decreased, also Q increased as H increased. Their relation still should be researched to find the best situation. The cost of increasing height and the reduction cost shall be studied carefully. If we consider the background concentration, growth factor etc. we shall obtain a more rational (K) value to limit the environmental air quality of life.

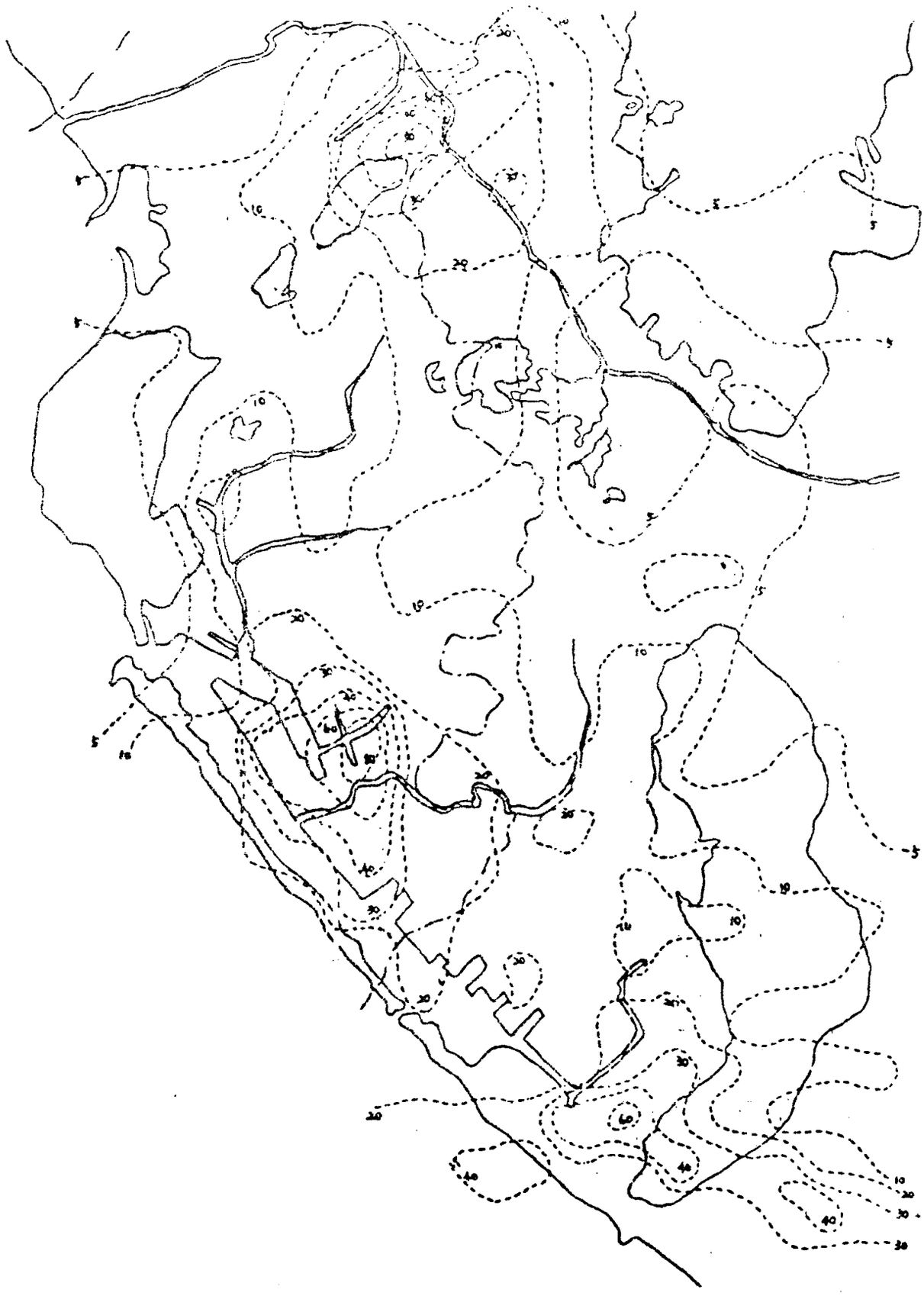

Fig. 6-15 Simulation result of annual SO_2 concentration (10^{-3}ppm)

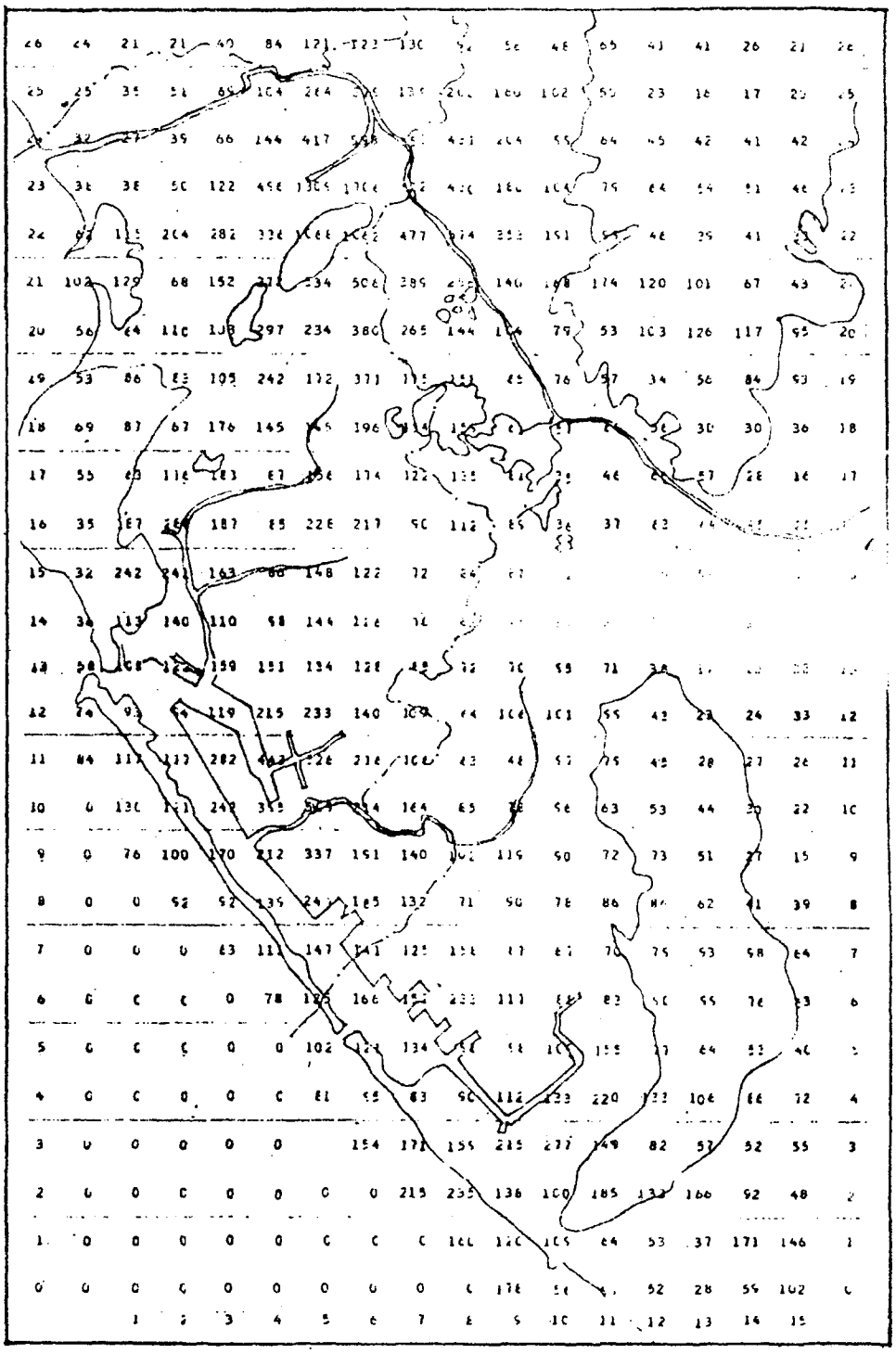

Fig. 6-16 The ambient diffusion constant (K) = 1, simulation result of annual SO_2 concentration (10^{-5} ppm)

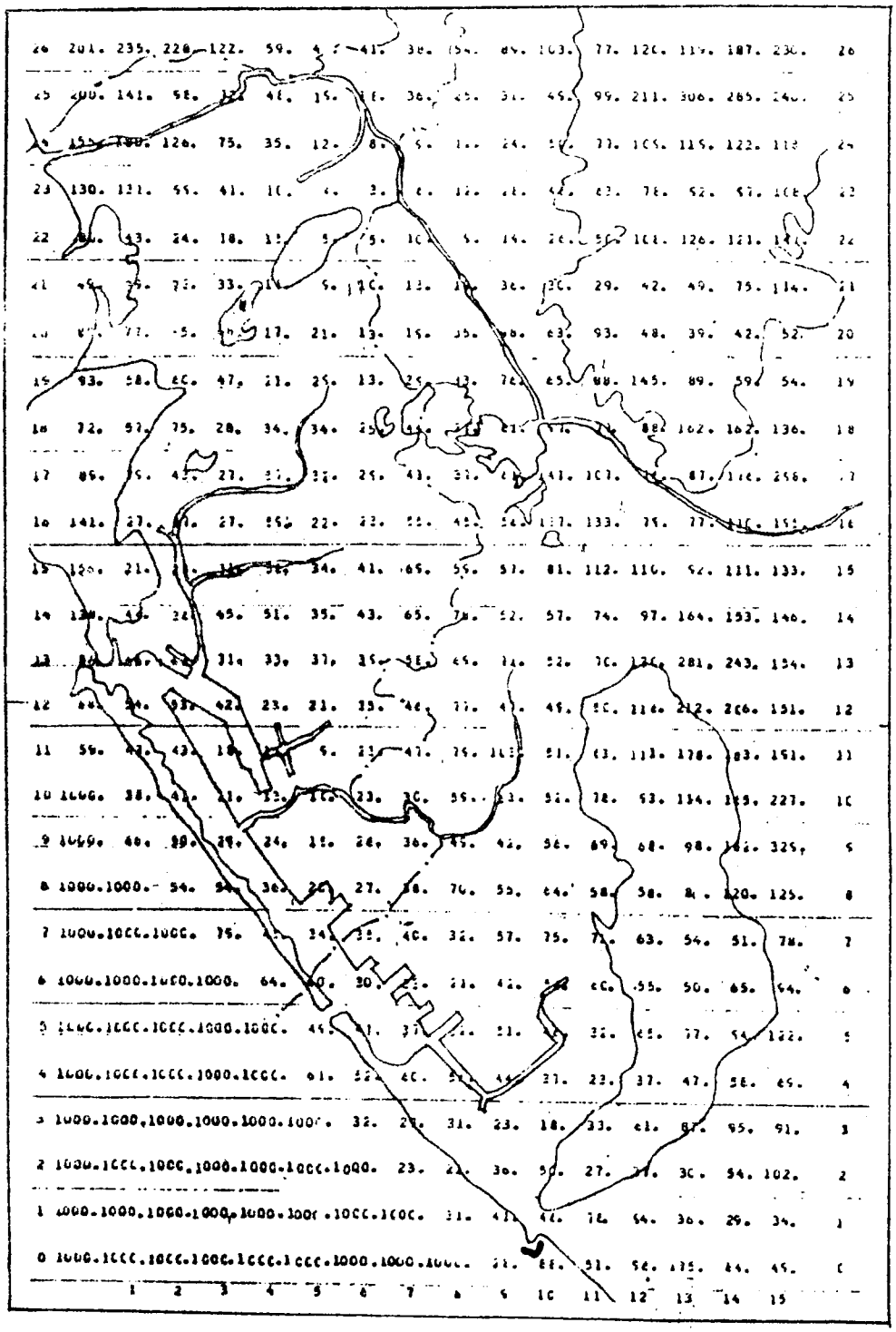

Fig. 6-17 Allowed (K) distribution, divide each concentration shown in Fig. 6-16 with 0.05, stack height not changed, can meet CNS too.

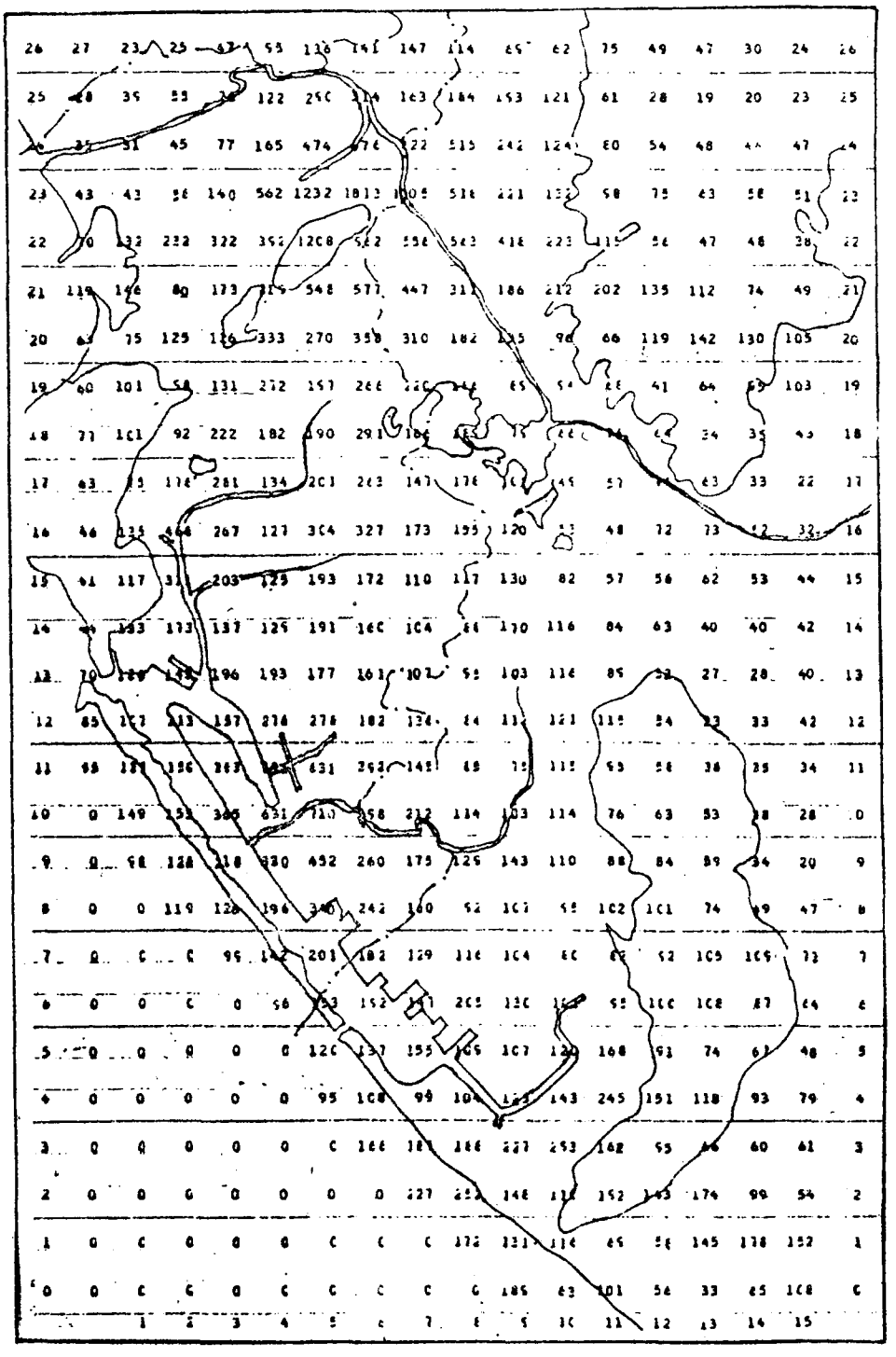

Fig. 6-18 (K)=1, stack height not less than 40 m, annual SO2 concentration (10^{-5}ppm)

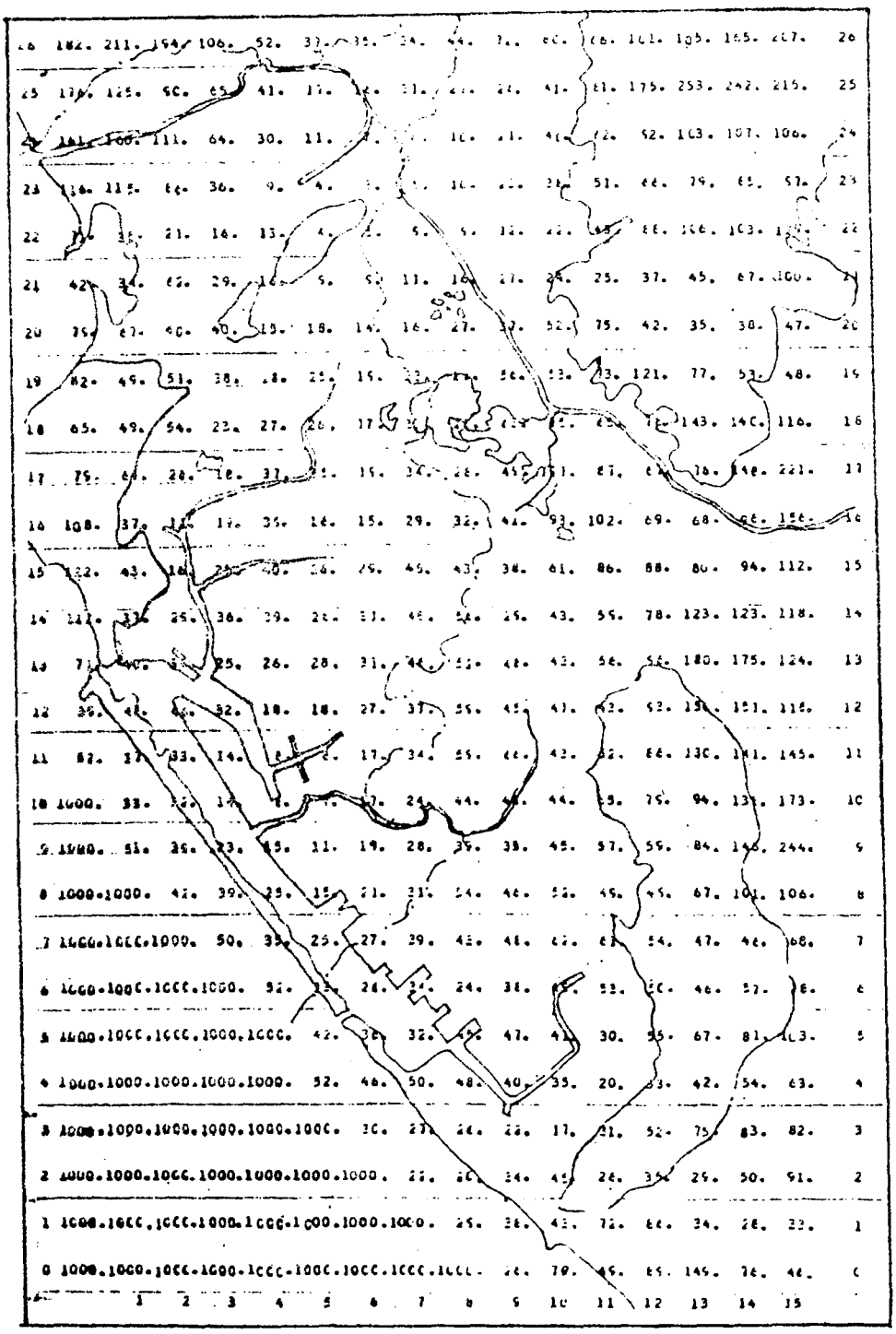

Fig. 6-19 (K) = 1, stack height not less than 40 m, allowed (K) distribution

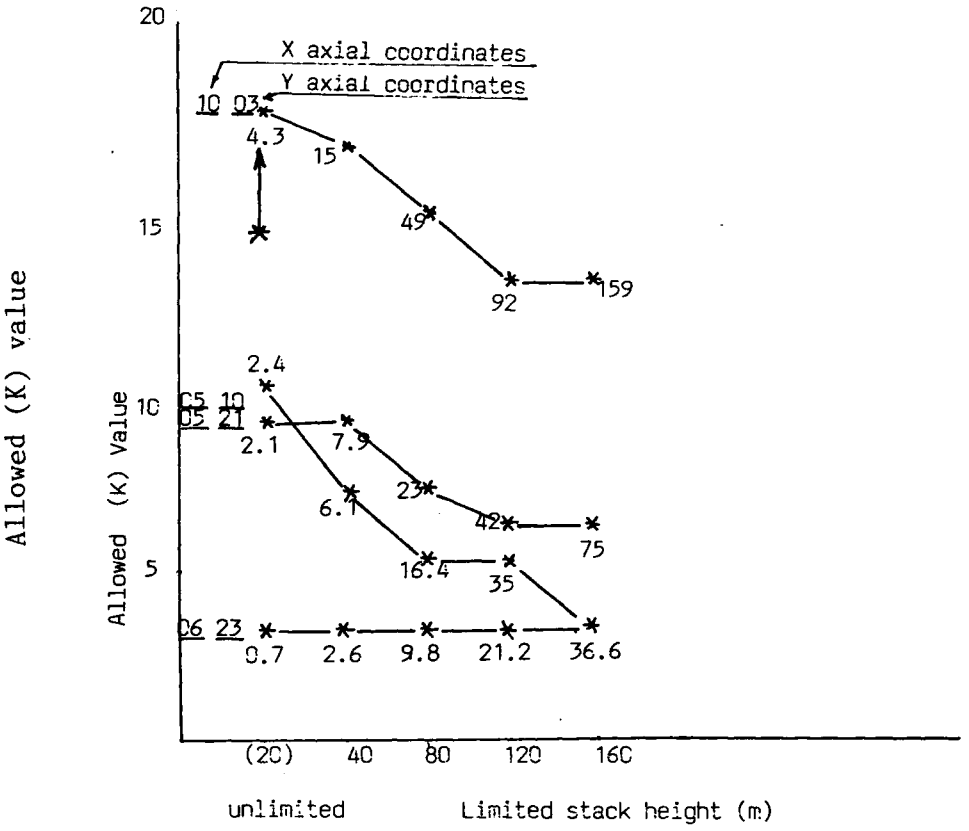

NOTE: * value means emitted volume (g/sec)
for example 4.3 this number indicates at
20m stack height, (K) = 18, emitted volume = 4.3 g/sec.

Fig. 6-20 The change of allowed (K) value of 4 different places under different stack height

6-4. SYMBOLS USED IN CHAP. 6

Q : emission rate of stack's pollutants (g/sec.)

H_e: stack effective height (m)

$\tilde{K}$: stack dispersion coefficient (-)

C_{max}: the maximum concentration of the ground level

K : the ambient diffusion constant (-)

K^* : the total average K

U : the average wind speed at stack's height (m/sec.)

σ_y : the diffusion standard deviation in lateral direction

σz : the diffusion standard deviation in vertical direction

σ_y^* : $\sigma y/H_e$ at C_{max}

σ_z^* : $\sigma z/H_e$ at C_{max}

C : national air quality standard

B : environmental background concentration

ϕ : 1-16, as the 16 directions of wind

l : 1-6, as wind speed, for 6 grades

m : 1-6, as stability class, for 6 grades

$K_{\phi,l,m}$: the ambient diffusion constant set

$f(\phi,l,m)$: the combined frequency function

B_1, B_2, B_3: background concentration of region 1, 2 and 3

$\tilde{K}_1$, $\tilde{K}_2$, $\tilde{K}_3$: stack dispersion coefficient of region 1, 2 and 3

$C(r)$: the concentration at spot r

r : the spot located at (x, y, z)

$K^*(r)$: the proportional factor at sport r

E : the emission amount of pollutants

E_a : permitted emission amount of pollutants

K^* : a parameter of weather, emission condition and location

G : the growth rate of emission after several years

$R\%$: the reduction percentage of emission

t : time

$C(r,t)$: the concentration at r, t

$F(r,r';\ t,t')$: the function of atmospheric dispersion

$E(r,t)$: the emission volume at r,t

$\bar{C}(r)$:C(r,t) time average from t1 to t2

$C_f(r)$: the concentration after a few years

E_p : the emission amount from a point source P

(K) : the total emission control coef.

i : constant 1-n

(r_i): Delta function

$\bar{E}_{pi}$: the emission amount in stable condition

θ : the angle between wind and N-direction

L : mixing layer height

U : wind speed

S : distance from source to polluted area

R : the lateral distance of wind

a,b,c,d : constant of diffusion standard deviation

CHAPTER 7 CONCLUSION FOR THE STRATEGY OF AIR POLLUTION CONTROL

The control strategies for air pollution may be summarized in the following categories:

(1) Density control (exhausting criterion)
(2) Uniform reducing approach for exhausting volume
(3) Distributing approach of varied tolerable exhausting volume
(4) Approach based on linear programing
(5) Controlling model of K value
(6) Density controlling model for the largest key base
(7) Control on Aggregate volume
(8) Controlling model for fuel replacement and distribution
(9) Approach of taxing imposed on pollution

According to these measures applied in advanced countries, in terms of developing tendency, the above-mentioned approaches, or gradual adoption step by step, or several programs combined thereby, may assist one another. The controlling target cannot be reached until environmental technology is overcome and administrative function is achieved. The approaches involved in this study comprise(5), (7) & (8).

7-1 Formulation of Total Emission Controlling System

Assume that the current exhausting volume of pollution substance totals "a" tons per day and "A" tons per year, and the environmental tolerable volume "b" tons per day and "B" tons per year, in case of $a > b$ or $A > B$, each unqualified exhausting source should be reduced to reasonable exhausting volume according to the following concept. Thus, it can render the air quality within the controlled area capable to cope with national standard.

(1) To distribute the responsibility of reduction on various enterprises and workshops in proportion of their production capacity or fuel consumption volume;

(2) To replace the raw material for production with substance of low pollution and to seek change in manufacturing process and outputs;

(3) To apply fuel of low pollution. For instance, use those with low sulfur and less heavy oil to reduce the exhausting total volume of sulfur dioxide;

(4) To encourage enterprises toward the installation of developed excellent equipment of low public harm and to foster public harm controlling technique positively;

(5) To utilize the integration of developed atmospheric computerized data, mathematical and physical technology for the calculation of reducing pollution volume so as to reach the continued control right away.

As its theoretical concept has beeen offered at section 6-2 and section 6-3 of Chapter 6, it is summarized herein.

Based on the conclusion in Chapter 6, in order to reach the target at 1st stage as to the tolerable SO_2 exhausting volume (268,000 tons/year), the reduction ratio should be 27% basedown the assumed exhausting volume in 1976 of 357,000 tons/year. However, since the target year is 1981, it is predicted that at that time the exhausting volume of oxide sulfur will be 405,000 tons/year; thus, the reduction volume should be 137,000 tons/year, i.e., reducing ratio 34%. Table 7-1 represents the necessary reduction of tolerable exhausting volume in key exhausting sources at the 1st stage target.

Table 7-1 Necessary Reducing Volume of Sulfur Oxides from Key Exhausting Sources

Predicted Total Exhausting Volume in 1981	405,000 tons/year
Reduction of Talin Thermo-electricity plant	96,000 tons/year (23.7%)
Reduction of South Taiwan Thermo-electricty Plant	11,000 tons/year (2.7%)
Reduction of Chinese Petroleum Corporation	6,000 tons/year (1.5%)
Reduction of K Value Limit	24,000 tons/year (5.9%)
Total Reduction	137,000 tons/year (33.8%)
Tolerable Exhausting Volume	268,000 tons/year (66.2%)

In Table 7-1 it is indicated respectively relating to the estimation on 229 main chimneys in Kaohsiung area. The executive process of its control measures is as in Fig. 7-1.

Fig. 7-1 Percentage of Exhausting Reduction and Number of Chimneys in Kaohsiung Area

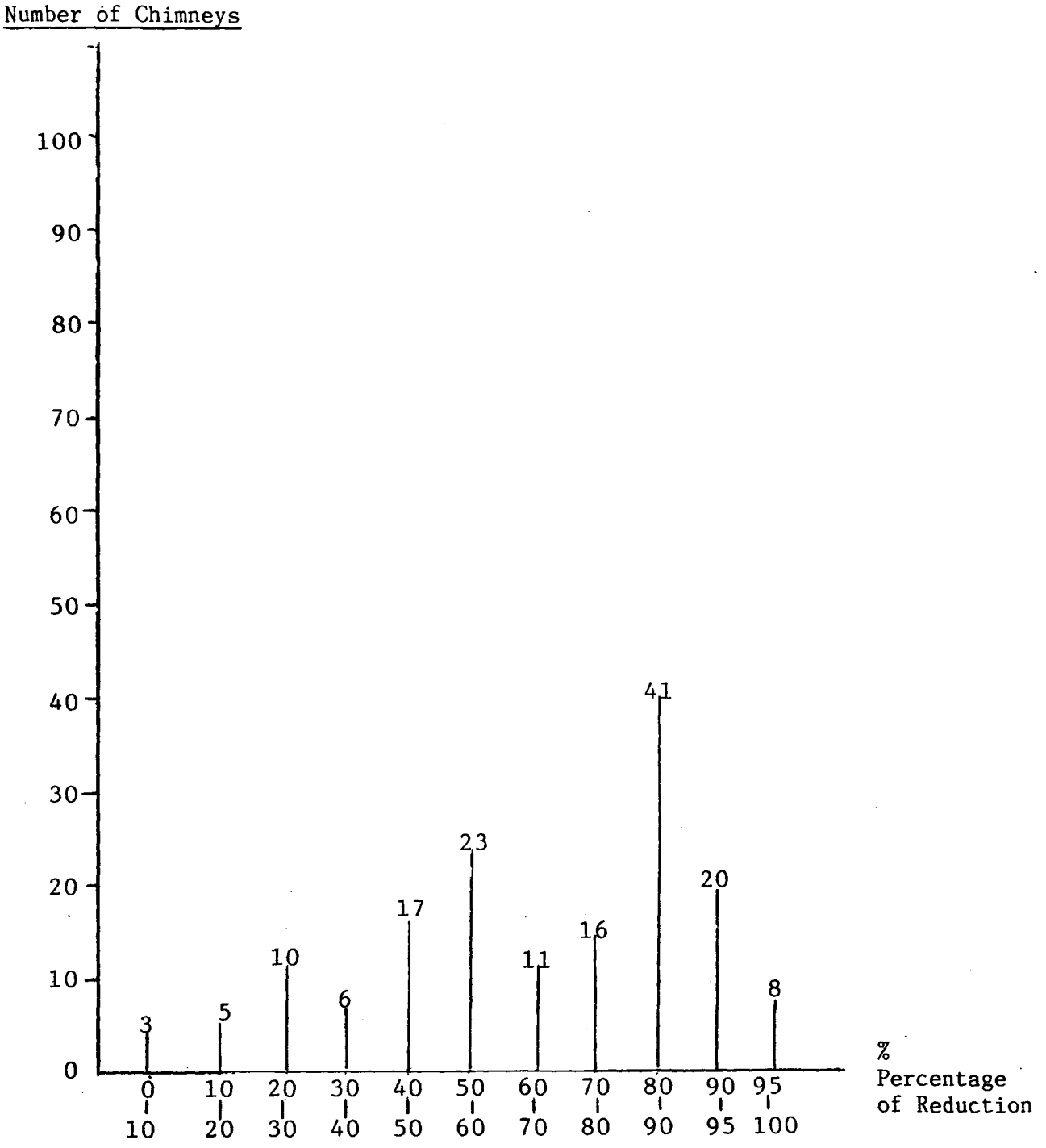

7-2 Technical System of Total Emission Control

In general, the air pollution control measures adopted by advanced countries based on the kinds of exhausting sources may be divided into two categories as follows:

The first one is the measure for fixed exhausting sources. It comprises 1) To replace fuel (or raw material); 2) to improve burning method (or manufacturing, disposing and storing method); 3) to install or improve controlling equipment; 4) to shrink enterprise and production scale; 5) to alter enterprise operating approach so as to reduce exhausting volume, such as (a) raising the effective height of chimney, (b) changing the position of exhausting source, (c) installing control buffer zone to facilitate dispersion. On the other hand, it may establish regional pollution supervision and environmental management of order transmission according to systematic engineering principle as indicated in Fig. 7-2.

The second one is the measure for removal of exhausting sources. It comprises 1) to improve combustion engine and its accessory device; 2) to adopt combustion engine of new type; 3) to guide the usage of small cars with low public harm; 4) to reduce the polluting coefficient caused by vehicles through traffic signals, hourly speed limit, three dimentional intersection and the desire to controltransport. On the other hand, it may be accompanied by (a) changing the rush hour of vehicles in urban area, such as the different office time regulated. (b) changing current routes of vehicles, such as the freeway constructed circling the city, (c) raising the loading ratio of vehicles so as to improve transport situation, or in accordance with guiding public transit system, (above all, tramcar), physical restraint, such as strengthening traffic rules, economic restraint, such as taxation on public harm, changing the way of life, changing urban structure, and restraining traffic volume. The technical system suggested in this study as shown in Fig.7-3.

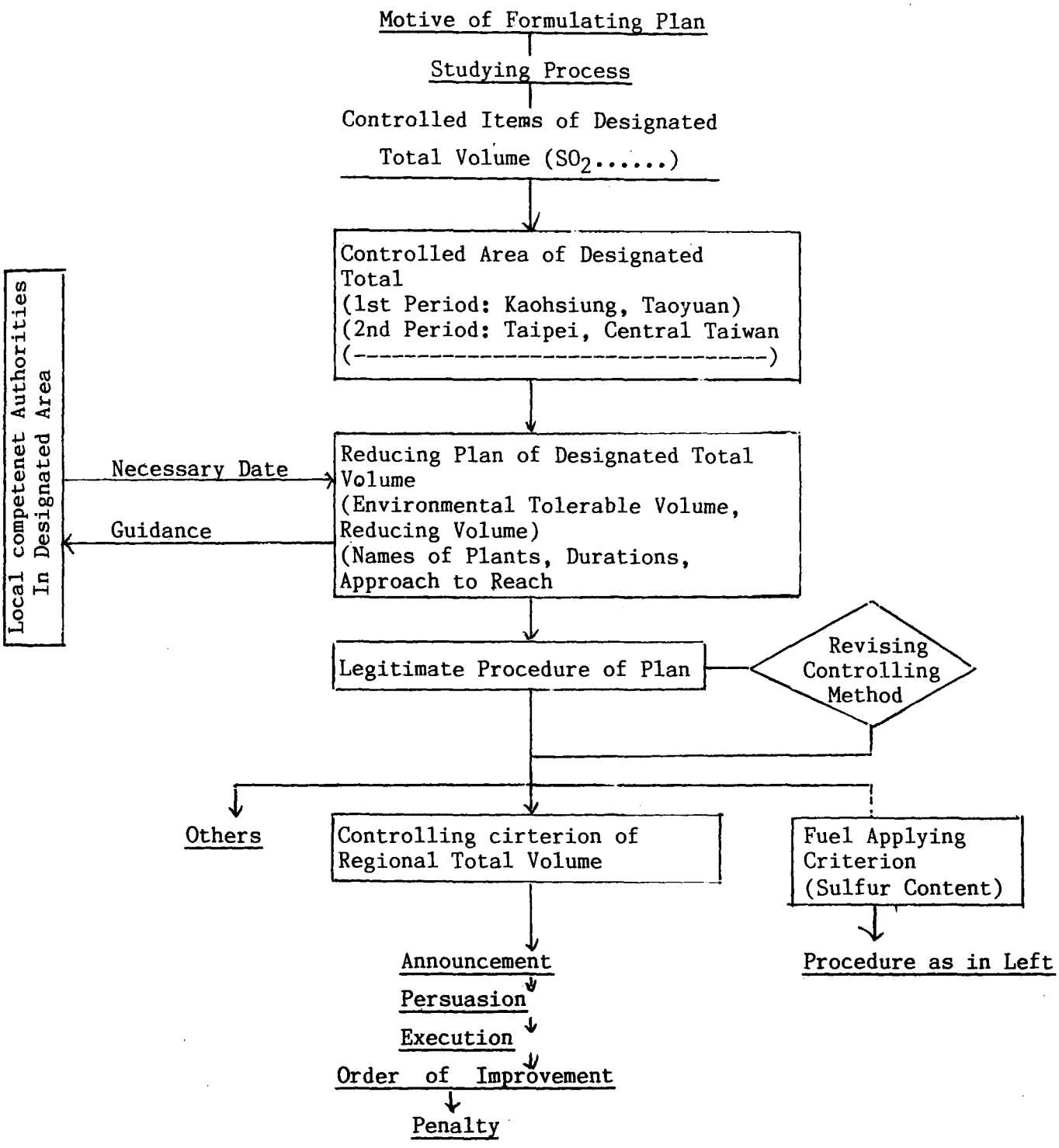

Fig. 7-2 Executive Procedures of Total Emission Controlling Measures

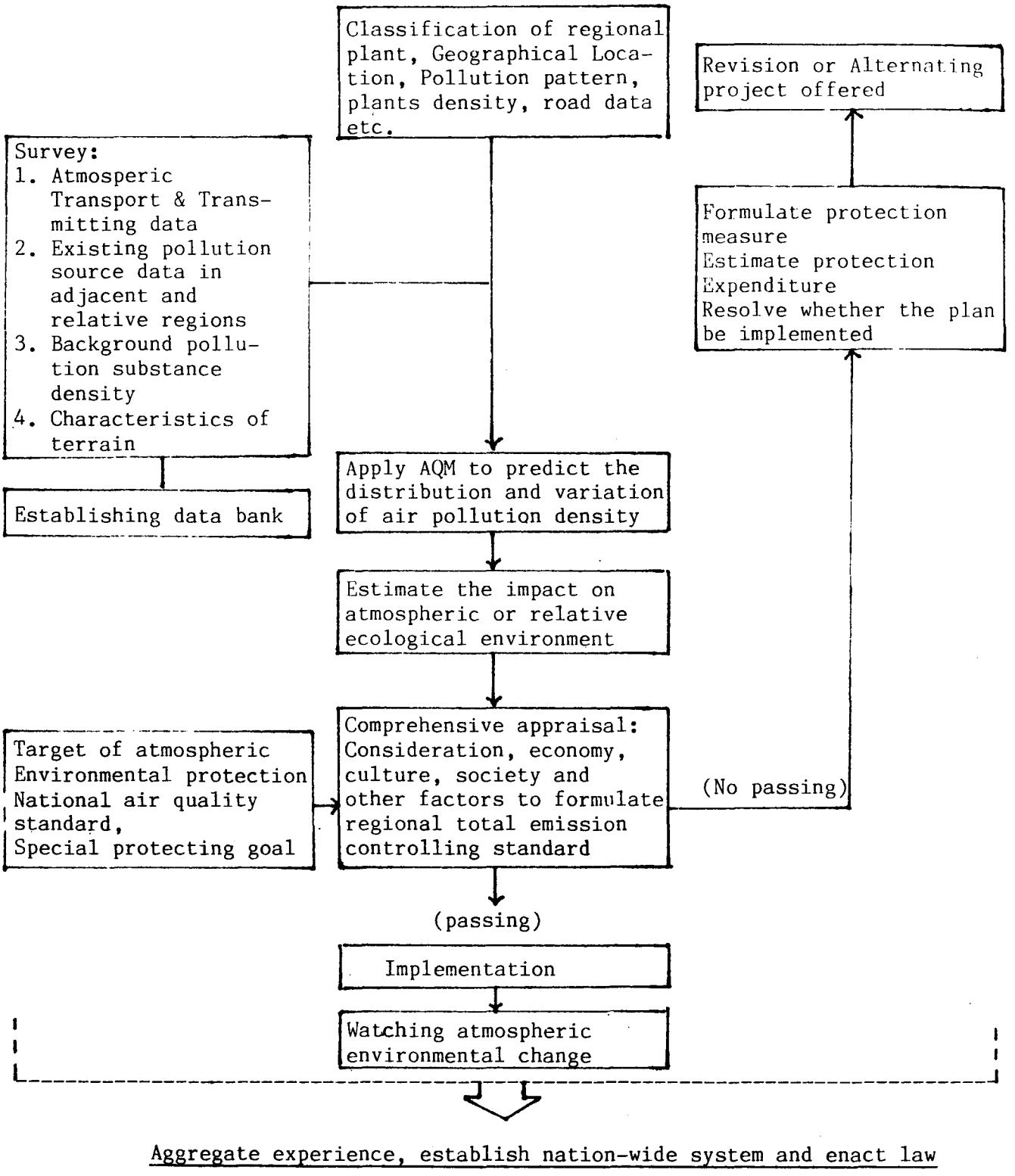

Fig. 7-3 Technical system of total emission control

ACKNOWLEDGEMENTS

The author wish to thank the personnel of the following research projects directed by him during these years:

* " Pilot Project of Environmental Pollution Control in Southern Taiwan", sponsored by Department of Health, R.O.C., from 1975 to 1977.

* " Study of Stack Dispersion Coefficient", sponsored by Department of Health, R.O.C., from 1979 to 1982.

* " Tracer Experiment at TaLin power plant" sponsored by Taiwan Power Company, from 1980 to 1981.

* " Tracer Experiment at LinKou power plant" sponsored by Taiwan Power Company, from 1982 to 1983.

Especially appreciation is expressed to professor S.C.Lu and Mr. K.H.Huang for their assistances to finish this study. In problems of diffusion in different regions, the assistance of the numerous other proffessionals , Professor M. Hiraoka, Professor T. Yamamoto & Dr. Y. Ikeda in Kyoto University and others who have generously supplied technical documents and recommendations for use and supplement in these chapters is also appreciated.

REFERENCES

Publication since 1970 by Chin-Yuan Chuang

1. "Environmental pollution and its control measures", Urban Planning Manual, Taipei Municipal Planning Committee, 1971.

2. "Air pollution and control measures in Taipei city", Engineering, Ministry of Economic Affair (MOEA), Vol. 44, No. 8-9, Aug. - Sept. 1971.

3. "Research on the disposal of solid waste in Taipei city", Engineering, MOEA, Vol. 44, No. 8-9, Aug. - Sept. 1971.

4. "Design for the exhausted gas system of metallurgical furnace", Energy Quarterly, MOEA, Vol. 2, No. 3, July 1972.

5. "Research on air pollution in Taipei city (in English)", Energy Quarterly, Energy Policy Committee, MOEA, Vol. 3, No. 1, Jan. 1973.

6. "Outline of industrial waste disposal", Lecture in China Management Research Center, 1973.

7. "Relationship between living environment and pollution problem in Taiwan (in English)", Sino-American Seminar on Environmental Pollution - Estuaries and Coastal Waters, Jan. 1974.

8. "Study of the possibility of a closed cycle system of organic waste disposal (in English)", Energy Quarterly, MOEA, Vol. 4, No. 1, Jan. 1974.

9. "Marine disposal of refuse", Proceeding of Sino-American Seminar on Environmental Pollution-Estuaries and Coastal Waters, Jan. 1974.

10. "Air pollution control in Taiwan (in English)", Sino-American Technical Cooperation Association (SATCA) Review, Vol. 19, No. 1, Mar. 1974.

11. "Environmental pollution and its control measures in Taiwan area", Environmental Science Research Center (ESRC), Tung Hai University, ESRC Review Series, No. 9, Oct. 1974.

12. "Air pollution", ESRC, Review Serieo, No. 10, Oct. 1974.

13. "Research on establishment for emission standard of exhausted gas from vehicular and maximum allowable content of sulfur in fuel in Taipei city", Energy Quarterly, MOEA, Vol. 5, No. 1, Jan. 1975.

14. "Study on establishment of air pollutant emission standard in Taiwan", Ad Hoc Collection of Modern Engineering and Technology Seminar (METS), Session of Environmental Protection, July 1976.

15. "Environmental protection", Engineering, Journal by Chinese Engineering Society, Vol. 49, No. 11, Nov. 1976.

16. "Characteristics of air pollution in Taiwan area (in English)", Environmental Protection, Journal by Environmental Protection Society (EPS), 1st edition, Jan. 1977.

17. "Study on the air pollution in Kaohsiung area", Environmental Protection, Journal by EPS, 1st edition, Jan. 1977.

18. "Interaction of man and environment in Taiwan", Environmental Protection, Journal by EPS, 1st edition, Jan. 1977.

19. "The characteristics of air pollution in Taiwan area, R.O.C. (in English)", Proceeding of the 4th International Clean Air Congress, Tokyo, Japan, PP. 539-545, May 1977.

20. "Evaluation of pollution control effect between electric and fossil fuel vehiculars", Transportation Planning Quarterly, Vol. 6, No. 3, July 1, 1977.

21. "Assessment on the effect of oil spilt at Keelung harbor by defection of hydrocarbon pollution in sea products", Research Report, National Science Council, June 1978.

22. "Prospective of the solid waste disposal in Taiwan", Proceeding of METS, Vol. 5, PP. 605-606, 1978.

23. "Outline of disposal of solid waste in Taiwan, R.O.C.", Proceeding of Regional Seminar on Solid Waste Management, CDG-AIT, Sept. 1978.

24. "Experimental study on treatment of electric plating waste water by Hy-Jet (in English)", Proceeding of the Colloquium on Aquatic Environment in Pacific Region at Academic sinica, Taipei, Aug. 21-23 1978.

25. "New conception of environmental health", Health Education Journal by National Taiwan Normal University, No. 42, Dec. 1978.

26. "Environmental pollution and its impact on health caused by industrialization in Taiwan, R.O.C. (in English)", Minutes of the 14th Council Meeting of Taiwan Medical Association, No. 9-12, PP. 237-243, 1979.

27. "Coming problem of environmental pollution of toxic substances" Taiwan Medical Journal, Vol. 22, No. 5, May 1979.

28. "A preliminary study on the diffusion model applied to air pollution control", Atmospheric Science, Journal by Meterological Society, Vol. 6, No. 1, May 1979.

29. "Comparison on environmental administrative system and ordinances between R.O.C. and Singapore", Committee of Research and Development, Executive Yuan, June 1979.

30. "Research on investment rate and operational cost for pollution control in industries of Taiwan, Ditto, Sept. 1979.

31. "Briefing for environmental protection in Taiwan area and review on environmental control from energy saving viewpoint", Proceeding of METS, July 1980.

32. "Assimilation of wind observation data and its application to environmental impact analysis (in English)", Proceeding of the 5th International Clean Air Congress, Vol. 1, PP. 460-465, Oct. 1980.

33. "Preliminary results of numerical study of planetary boundary layer development over a coastal urban area (in English)", Ditto, Vol. 1, PP. 466-474, Oct. 1980.

34. "Research on environmental indices in Taiwan area" Publication by Bureau of Environmental Protection, Dec. 1981.

35. "Prospective of the marine pollution in Taiwan, R.O.C.", Assimilative Capacity of the Oceans for Man's Wastes, Scope/ICSU Academia Sinica, Taipei, R.O.C., PP. 289-296, April 26-30 1982.

36. "Policies for maintaining ambient assimilating capacity (in English)", Proceeding of the 6th International Clean Air Congress, Vol. 3, PP. 535-541, May 1983.

37. "The SF_6 tracer experiment at littoral industrialized areas (in English)", Ditto, Poster, PP. 5-6, May 1983.

38. "Air pollution in the Republic of China (Taiwan) (in English)", Journal of the Air Pollution Control Association, USA, Vol. 33, No. 8, PP. 768-770, Aug. 1983.

REFERENCES IN ENGLISH

(1) Chuang C.Y. : "Research on Air Pollution In Taipei City" Journal of Energy Quarterly. Energy Policy Committee, MOEA, R.O.C. No.3, Vol. III, 1972. No.1, Vol. IV, 1973.

(2) D.G. Scarpelli, R.L. Woolridge : "a review of programs to control environmental hazards in the Republic of China", 1981.

(3) Chuang C.Y. : "Air Pollution Control in Taiwan, SATCA Review, Vol.19, No.1, March 1974.

(4) Chuang C.Y. : "Air Pollution and Control Measures in Taipei City" Engineering Journal, Vol. 44, No.8-9 Aug. -Sept. 1971.

(5) Chuang C.Y. and Cheng F.T. : "Research on Establishment for Emission Standard of Exhaust Gas from Vehicular and Maximum Allowable Sulfur Content in Taipei City" Journal of Energy Quarterly, NOEA, R.O.C., Vol.V, No.1. Jan. 1973.

(6) E.S. Rubin : "Air pollution constraints on increased coal use by industry" JOPACA, Vol.31, No.4, PP.349-360, April 1981.

(7) Chuang C.Y. : "A Study on the Cost Analysis of Environmental Pollution Control", NHA Published, 108P, 1978.

(8) NHA : Interim Report on Pilot Project of Environmental Pollution Control In Taiwan, R.O.C., 1976.

(9) Taipei Municipal Dept. of Environmental Sanitation : Statistic Data of Air Pollution Survey, 1970-1976.

(10) Taiwan Institute of Environmental Sanitation: Statistic Data of Air Pollution Survey, 1968-1976.

(11) LTIL : "Final Report of National air Monitoring Network Site Selection and Network Specifications", 1980 (unpublished)

(12) S.C. Lu,et al. : "The effect of land and sea breeze on air pollution at Kaohsiung area", National Science Council Monthly, Vol. 7, No.7, PP. 741-752, 1979.

(13) S.C. Lu, et al. : "A study of the atmospheric stability and dispersion potentiality over Taiwan area", National Science Council Monthly, Vol. 8, No.9, PP. 855-863, 1980.

(14) D.B. Turner : "A diffusion model for an urban area", Journal of Applied Meteorology, Vol. 3, PP. 83-91, 1964.

(15) S.B. Carpenter, Thomas L. Montgomery, : "Principal plume dispersion models; TVA power plants", ibid., Vol. 21, No.8, 1971.

(16) American Meteorological Society : "Lectures on air pollution and environmental impact analyses", 29 Sept. -3 Oct. 1975, PP. 296, 1975.

(17) J.L. Deuble : "Atmospheric Tracer gas technology, techniques and applications", Technical Bulletin of Environmental Sciences, 79-5, 1982.

(18) B.K. Lamb : "Atmospheric tracer techniques and gas transport in the primary aluminum industry", Journal of the Air Pollution Control Association, Vol.30, No.5, PP. 558-566, 1980.

(19) R.N. Dietz and E.A. Cote : "Tracing atmospheric pollutants by gas chromatographic determination of sulfur hexafluoride", Environmental Science & Technology, Vol.7, No.4, PP. 338-342, 1973.

(20) H.B. Singh, et al. : " Distribution, sources and sinks of atmospheric halogenated compounds", Journal of the Air Pollution Control Association, Vol. 27, No.4, PP. 332-336, 1977.

(21) P.A. Sackinger, et al. : "Uncertainties associated with the estimation of mass balances and Gaussian parameters

from atmospheric tracer studies", Journal of the Air Pollution Control Association, Vol. 32, No.7, PP. 720-724. 1982.

(22) B.R. Kerman : "A similarity model of shoreline fumigation", Atmospheric Environment, Vol. 16, No.3, PP. 467-477, 1982.

(23) P.K. Mista and S. Onlock : "Modelling continuous fumigation of nanticoke generating station plume", Atmospheric Environment, Vol. 16, No.3, PP.479-489, 1982.

(24) E.S. Rubin : "Air pollution constraints on increased coal use by industry, an international perspective", Journal of the Air Pollution Control Association, Vol. 31, No.4, PP. 349-360, 1981.

(25) Gifford F.A. : "Atmospheric dispersion models for environmental pollution applications", Lectures on Air Pollution and Environmental Impact Analyses, Chap.2, A.M.S., 35-58, 1972.

(26) Briggs, G.A. : "Plume rise predictions", Lectures on Air Pollution and Environmental Impact Analyses, Chap.3, A.M.S., 59-111, 1975.

(27) Csnady, G.T. : "Turbulent Diffusion in the Environment" D. Reidel Publishing Company, 248 PP, 1973.

(28) Businger, J.A. : "Turbulent transfer in the atmospheric surface layer", Workshop on Micrometeorology, Chap.2, A.M.S., 67-100, 1972.

(29) Golder, D. : "Relating among stability parameters in the surface layer", Boundary Layer Meteor, 3, 47-58, 1972.

(30) Pasquill, F.: Atmospheric diffusion (2nd Ed.), 429pp, John Willey and Sons, 1974.

(31) Turner, D.B. : "Workbook of atmospheric dispersion estimates", U.S A. Public Health Service Publication No. 999-AP-26, 1970.

(32) Robert, J. Bibbero, Irving; G. Young,: "Systematic approach to air pollution control", Honeywell Inc., 1974.

(33) Noel de Nevers, J. Roger Morris,: "Rollback Modeling, Basic and modified", Journal of the air pollution control association, Vol. 25, No.9, 1975.

(34) T.Y. Chang and B. Weinstock, : "Generalized Rollback modeling for Urban air pollution control", ibid. Vol.25, No.10, 1975.

(35) Joan Herenko Novak and D.B. Turner : "An efficient Gassianplume multiple-source, air quality algorism: J. Air Poll. Control Assoc. 26:570, 1976.

(36) N.E. Bowne: "Diffusion rate:, JAPC, Vol.24, No.9, 1974.

(37) "User's guide for the climatological dispersion model" EPA, 1973.

(38) N.A. Huey: "The lead dioxide estimation of sulfur dioxide pollution" J. Air Poll. Control. Assoc. 18: 610, 1968.

(39) F.W. Thomas and C.M. Davidson: "Monitoring sulfur dioxide with lead peroxide cylinders" ibid., 11:24, 1961.

(40) Turner, D.B. : "Relationships between 24-hour mean air quality measurements and meteorological factor in Nashville, Tennessee", ibid., 11:483, 1961.

(41) S.F. Liang, C.V. Sternling and T.R. Galloway : "Evaluation of Effectiveness of the lead peroxide method for atmospheric mornitoring of sulfur dioxide" ibid., 23: 605, 1973.

REFERENCES IN JAPANESE

a. 氣象廳：氣象データ資料集，1976

b. 平岡正勝（M. Hiraoka），古市徹（T. Furuichi ），北田敏廣（T. Kitada ）：大氣擴散式の概觀,An Outline of Atmospheric Diffusion Equations, 空氣清淨第15卷第6號，PP 2-10, 1977

c. 西田薰：汚染物質の大氣擴散，環境技術，VOL. 6 No.7, PP509-806, 1977

d. 池田有光：都市域における大氣汚染濃度予測に關する研究，京都大學學位論文, 1973

e. 岡本真一：都市大氣汚染の數式モデルに關する研究，早稻田大學學位論文，1977

f. 櫻庭信一，森口實，佐藤純次："小名浜"大氣擴散實驗の概要，產業公害，VOL.3, No.5, PP11-24, 1966

g. 氣象研究所應用氣象研究部：臨海工業地域の大氣汚染を對象とした大氣擴散調查，The Tracer Study of Atmospheric Dispersion at 9 Littoral Industrialized Areas of Japan and the Plume Rise Measurement, 氣象廳技術報告第72號，PP1-66, 1970

h. 蒲生稔，横山長之：いぶし現象の擴散モデル，大氣汚染學會大會誌No.532, 1982

i. 溝尻純枝，伊藤昭三：フユーミゲーション狀態下での大氣擴散のモデル化，大氣汚染學會誌 VOL.17 NO.3, PP228-235, 1982

j. 岡本真一，塩澤清茂：擴散實驗データに基づく水平方向擴散幅 σ_y についての

解析，天氣，27.2., PP29-34, 1980

k. 岡本真一，村上俊一，塩澤清茂：擴散實驗データに基づく水平方向擴散幅の推定方法について，天氣 27.2., PP35-38, 1980

l. 日本氣象協會：大氣汚染氣象予報指針，P265, 1976

m. 平岡正勝(M. Hiraoka)，池田有光(Y. Ikeda)：大氣汚染の對策技術とコントロール，化學工學，VOL.35 No.1, PP29-36, 1971

n. 三菱總合研究所：環境質變化及びその生活環境への影響の予測と評價手法の檢討，1977

o. 高松武一郎，内藤正明：大氣汚染の計算機制御，計測と制御，VOL.8, No.12, PP33-38, 1969

p. 高松武一郎，内藤正明，Liang-Tseng Fan ：環境システム工學，日刊工業新聞社，P250, 1977

q. 井上市郎：大氣汚染物質の總量規制導入の經緯とその基本構想産業公害，VOL.10, No.3, PP1-5, 1974

r. 森口實：SO_x總量規制の算定方法について，大氣汚染研究，VOL.9, No.5, PP1-19, 1975

s. 産業公害防止協會：産業公害總合事前調査におけるSO_x, NO_xに係る環境濃度予測手法マニュアル，P290, 1982

t. 公害資源研究所：大氣汚染質の擴散に關する研究，研究所報告第15號，P408，1979

u. 北林興二，横山長之：工業都市域の大氣汚染シミュレーション，產業公害，VOL.10，No.8，PP28-37，1974

v. 横山長之：大氣境界層と汚染物質の擴散，產業公害，VOL.17，No.2，PP55-22，

w. 庄司光（H. Shoji），山本剛夫（T. Yamamoto ），石川義紀（ Y. Ishikawa）亂流境界層内の擴散に關する考察—オイラー相關とラグランシュ相關の關係について— ON THE RELATION BETWEEN EULERIAN CORRELATION AND LAGRANGEAN CORRELATION，土木學會論文報告集第173號，PP35-45，1970

x. 菊池幸雄：大氣汚染氣象に關する環境アセスメント手法の開發に關する研究，官公廳公害專門資料，VOL.13，No.6，PP55-76，1978

y. 設樂正雄，大瀧厚：大氣汚染防止への多變量解析の應用，產業公害，VOL.7，No.11，PP22-31，1971

APPENDIX A ---- I

APPENDIX A Surface weather map (Sept. 5 - Sept. 15)

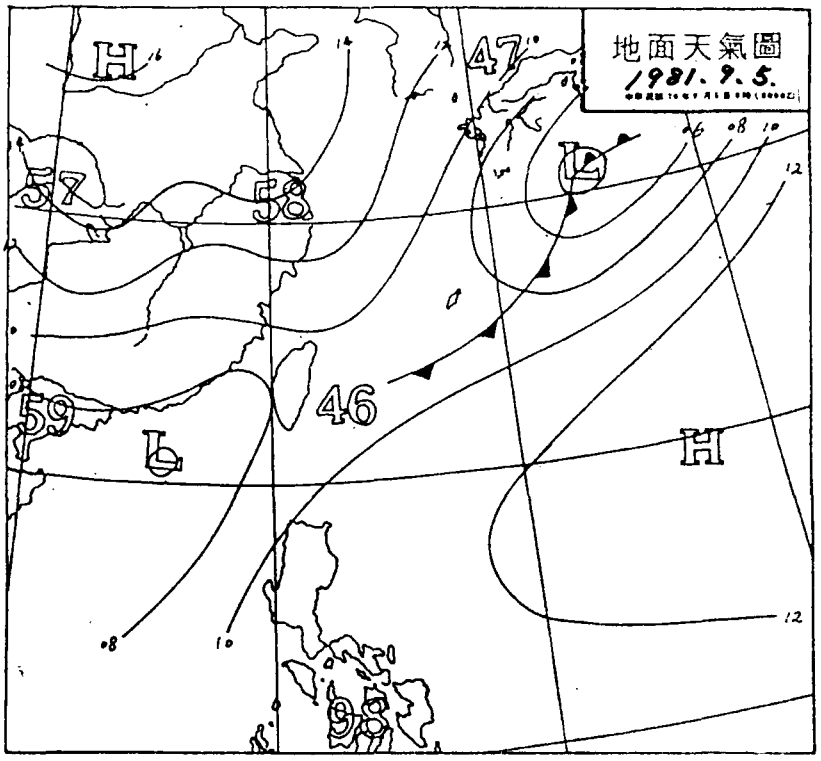

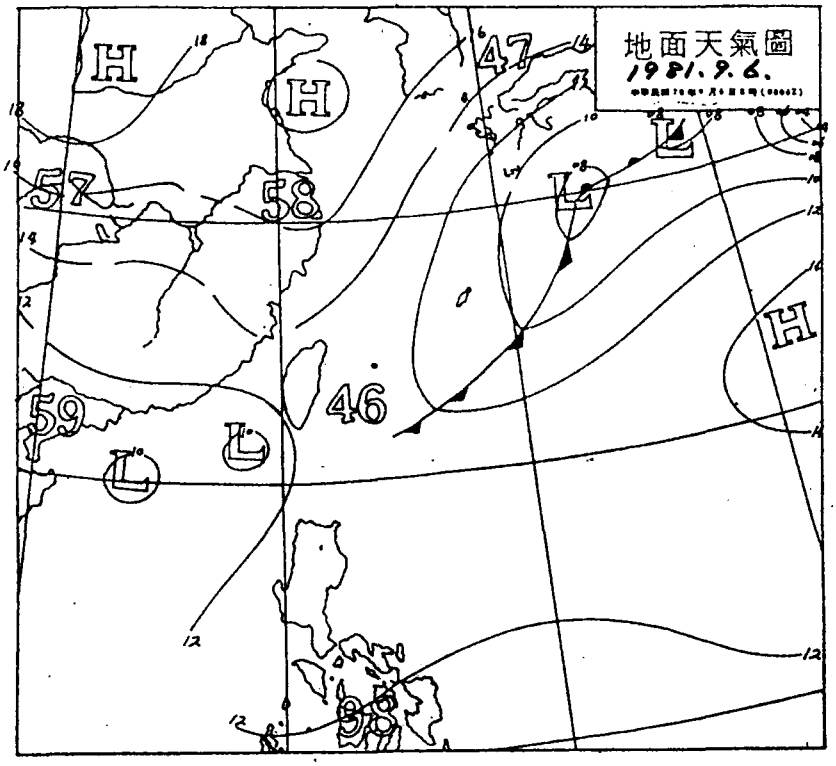

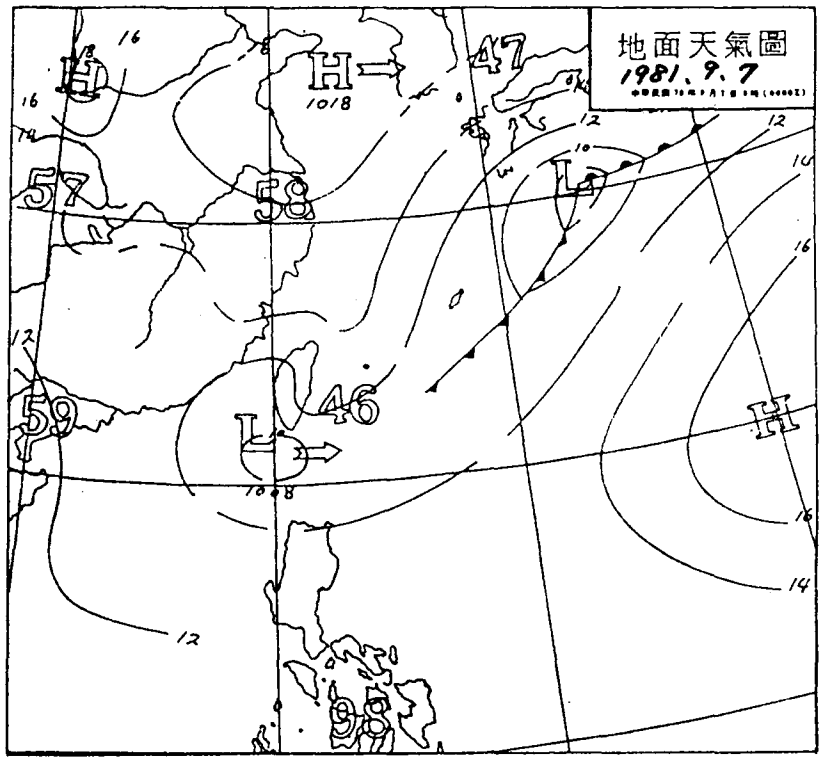
地面天氣圖
1981、9、7
H
1018
47
57
58
L
46
59
H
L
1008
98

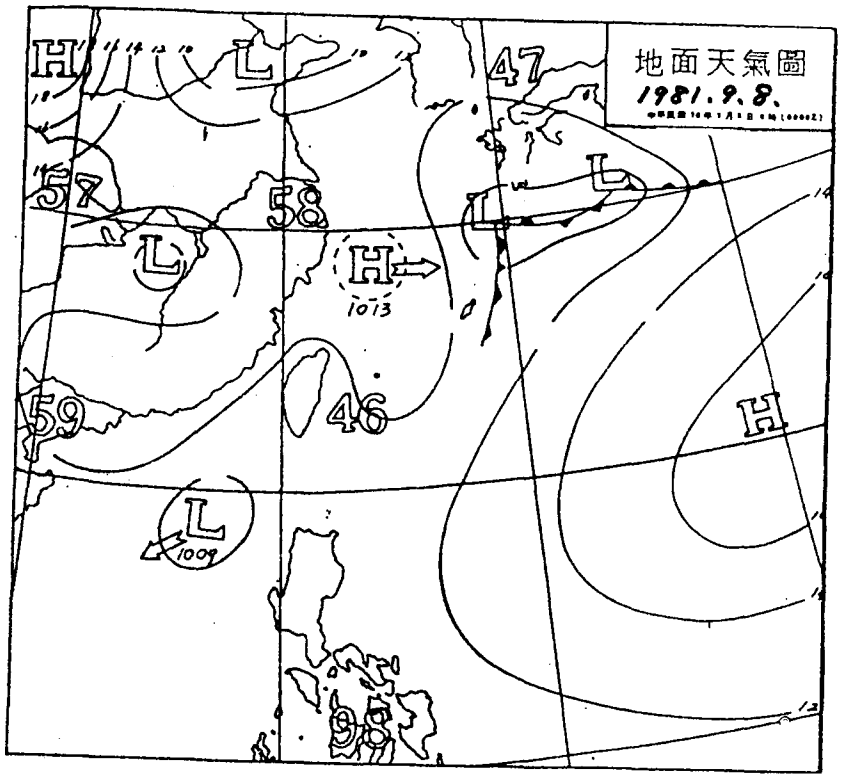
地面天氣圖
1981、9、8、
H
L
47
57
58
L
L
H
1013
59
46
H
L
1009
98

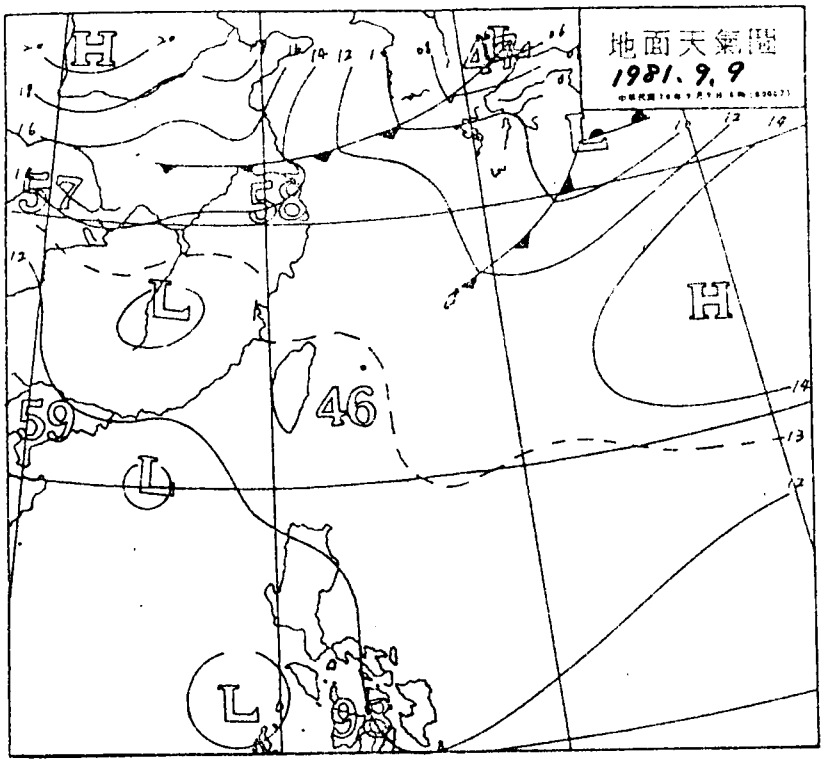
地面天氣圖
1981、9、9
H
L
57
58
46
59
98

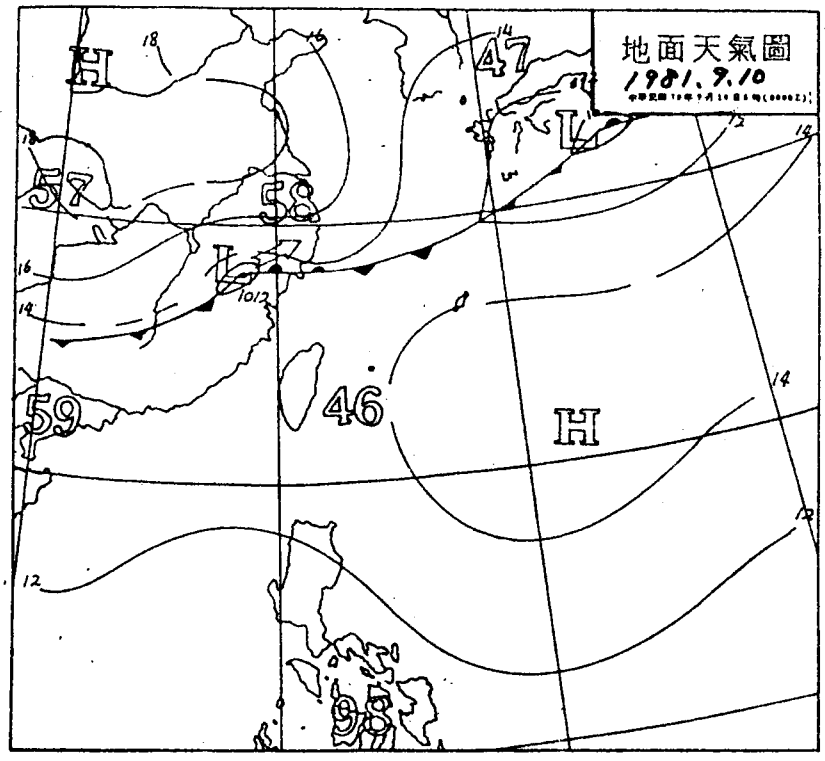
地面天氣圖
1981、9、10
H
L
47
57
58
46
59
98

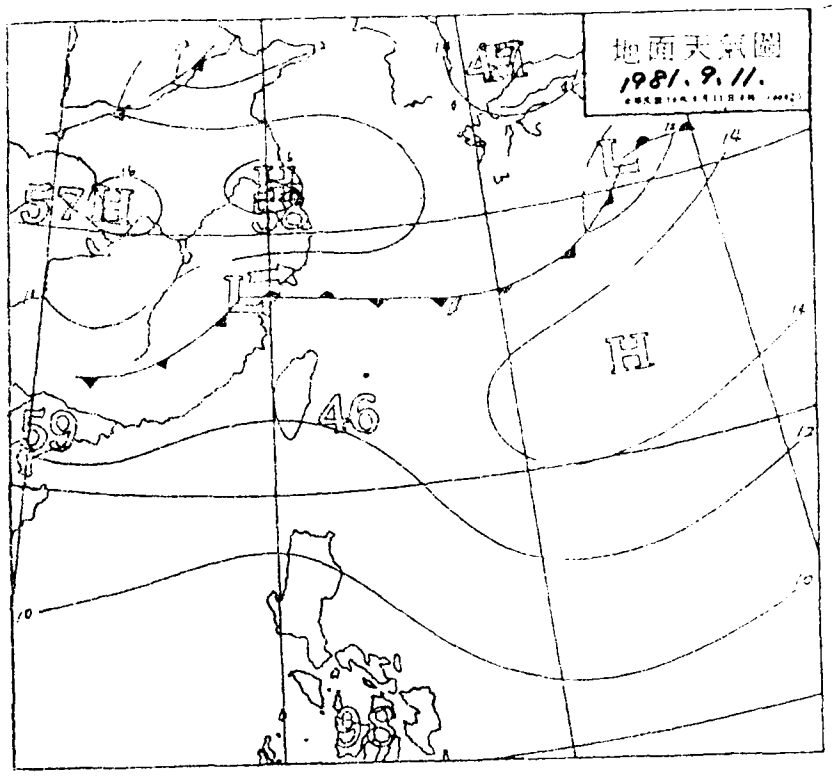
地面天氣圖
1981.9.11.
H
L
57
58
59
46
38

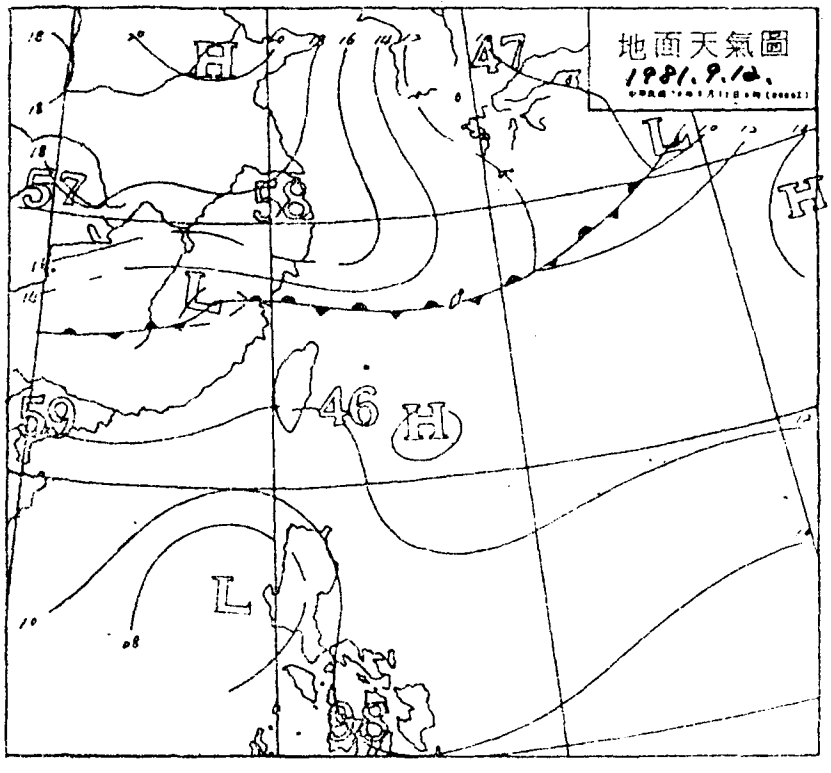
地面天氣圖
1981.9.12.
H
L
47
57
58
59
46
38

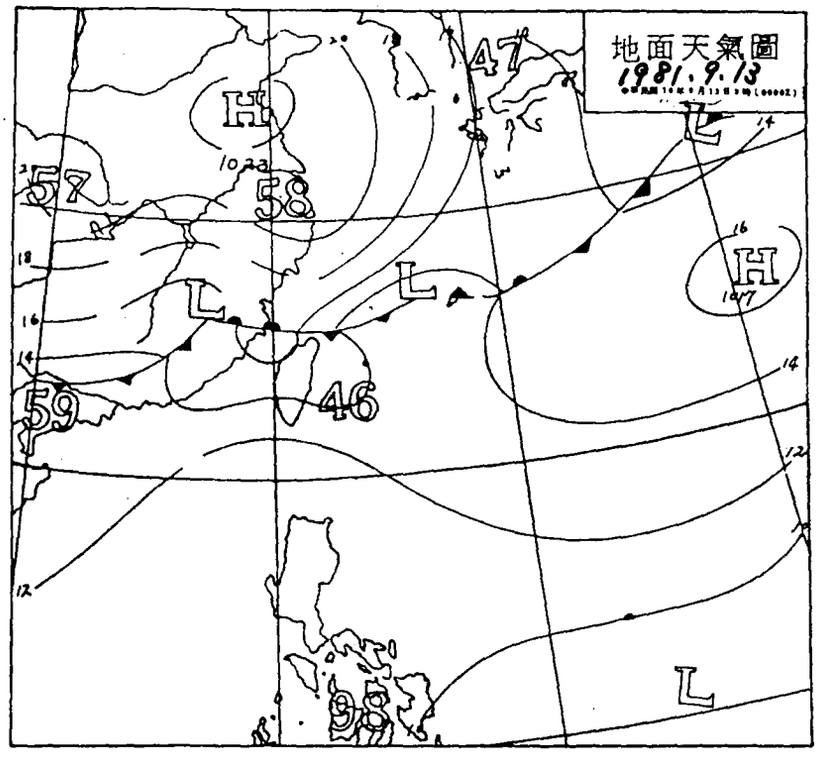
地面天氣圖
1981.9.13
H
L
47
57
58
59
46
98

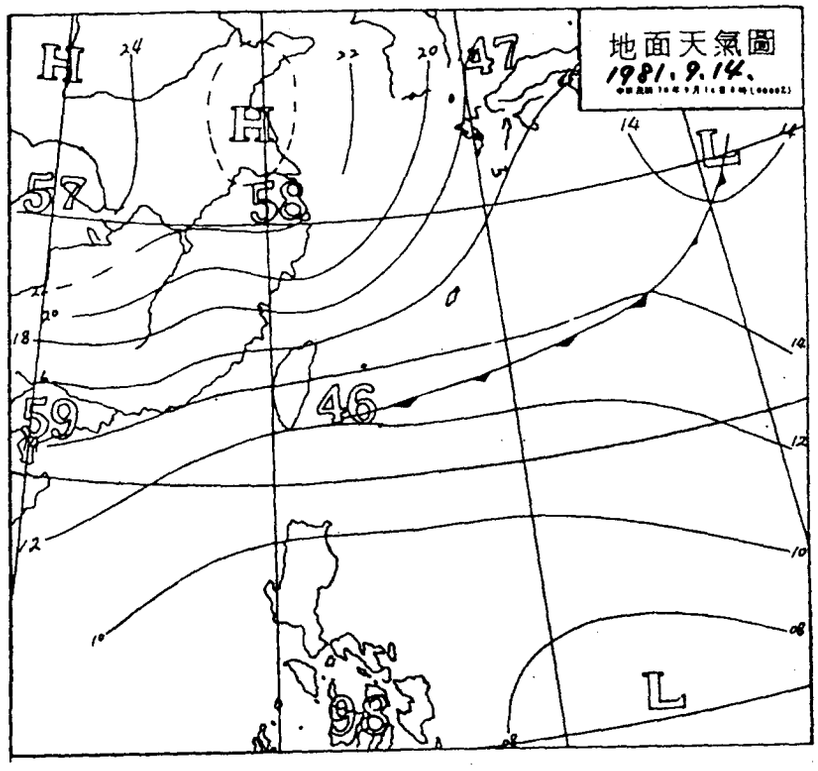
地面天氣圖
1981.9.14.
H
L
47
57
58
59
46
98

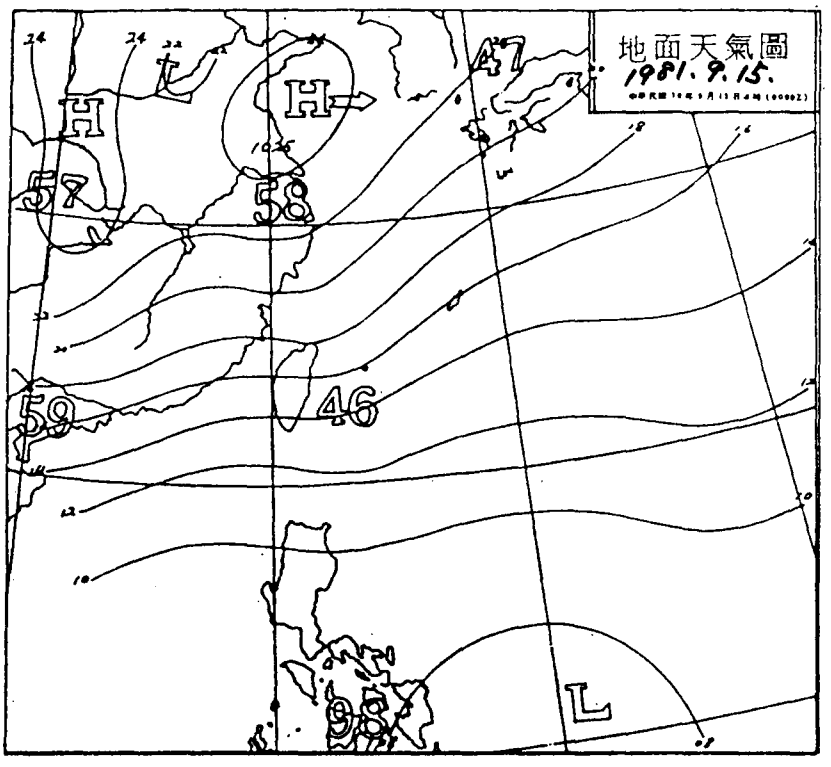
地面天氣圖
1981. 9. 15.
H
H
L
L
57
58
59
46
98

APPENDIX B The wind profile (Run 1 - Run 24)

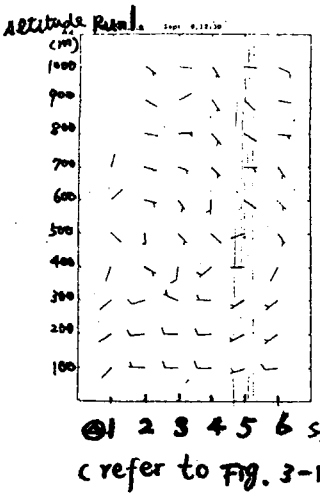

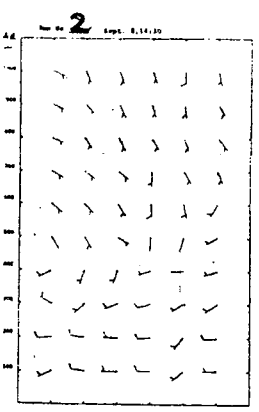

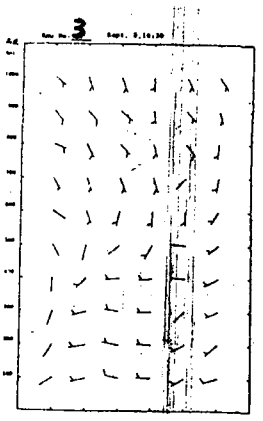

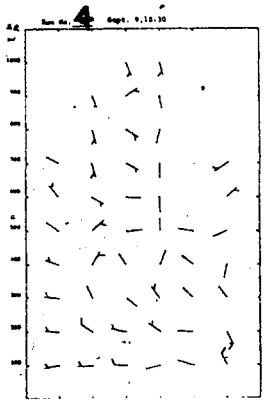

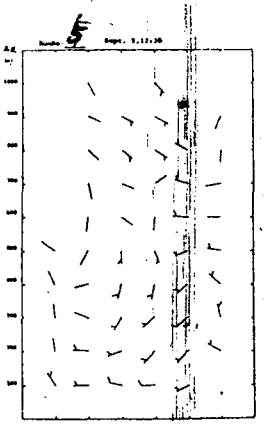

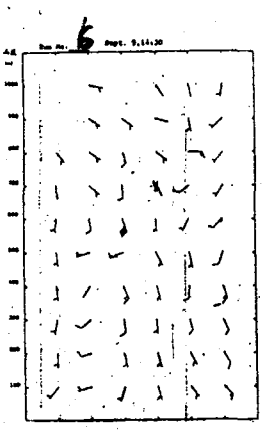

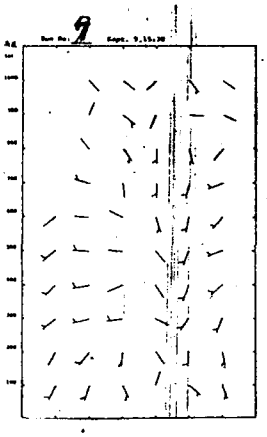

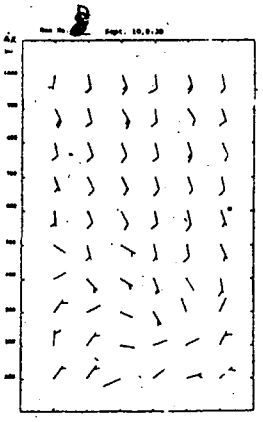

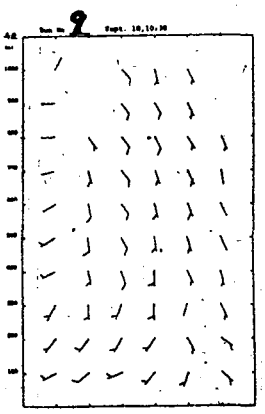

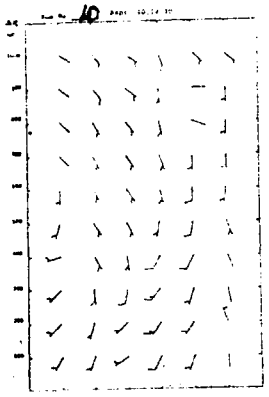

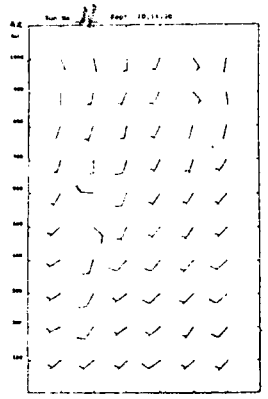

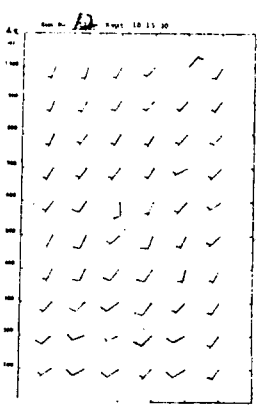

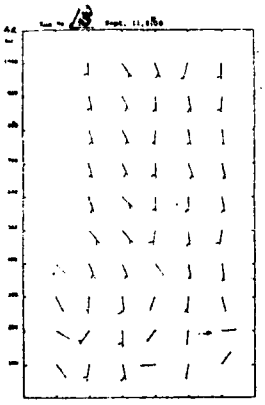

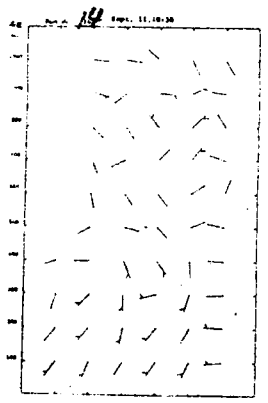

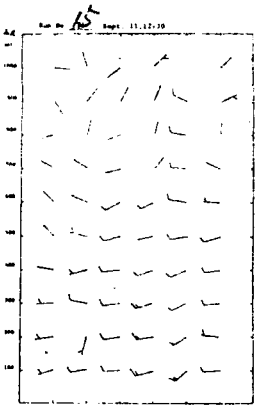

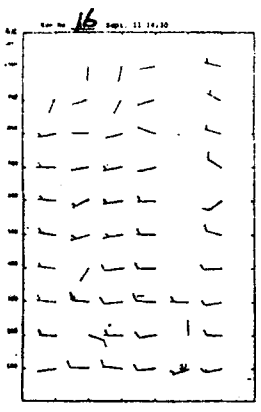

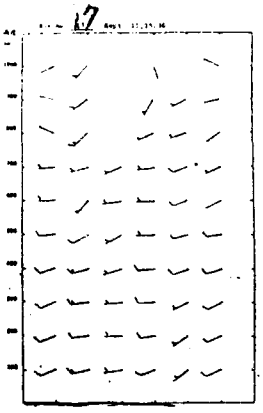

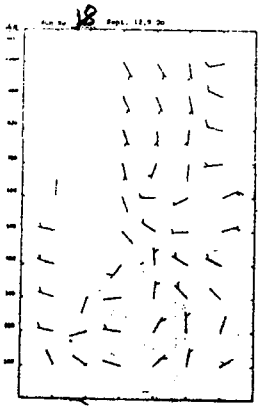

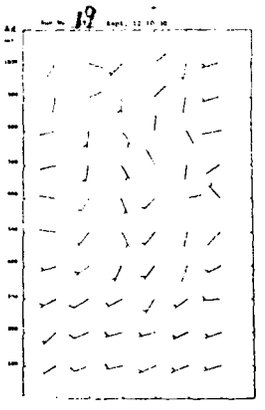
19

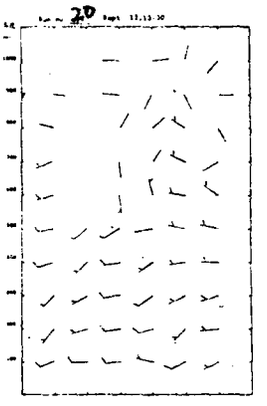
20

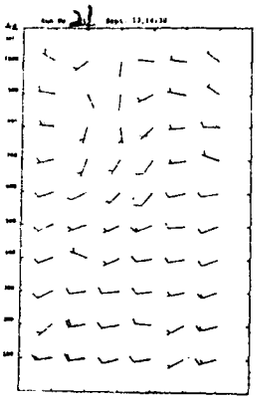
21

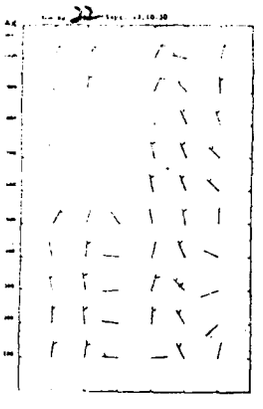
22

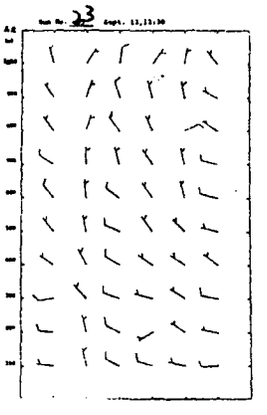
23

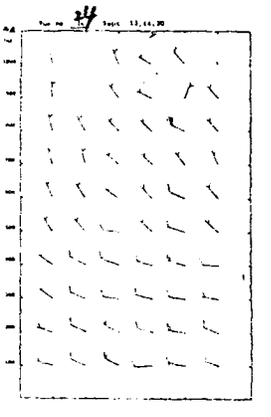
24

APPENDIX C - 1 The wind field of Kaohsiung area
(Run 1 - Run 24 , 0 - 330m)

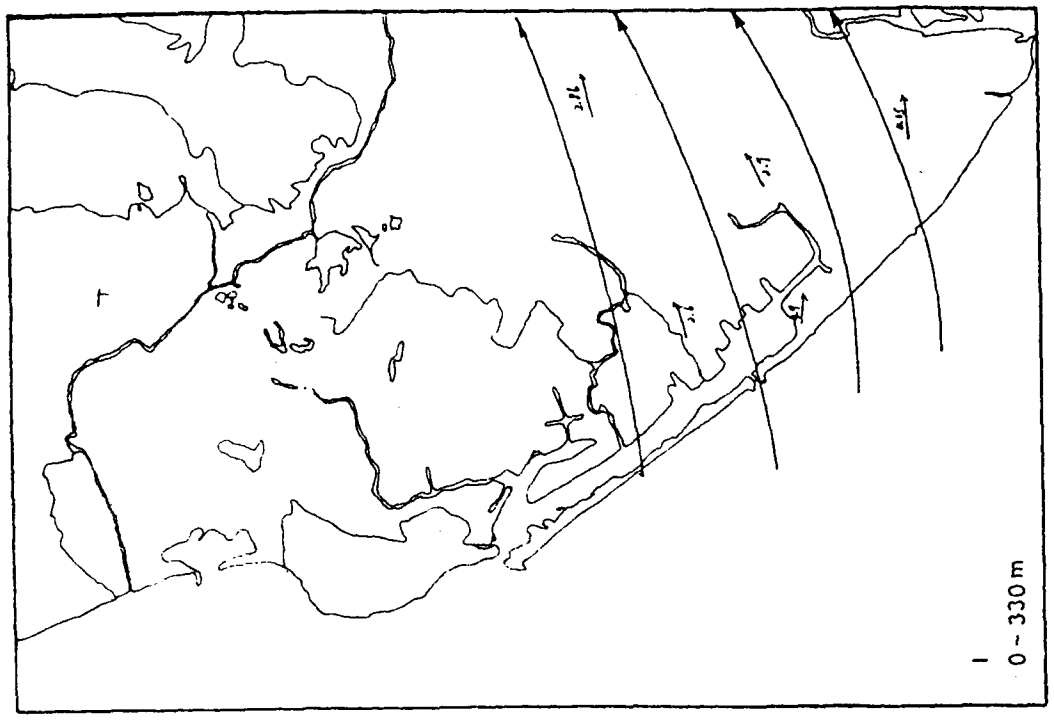

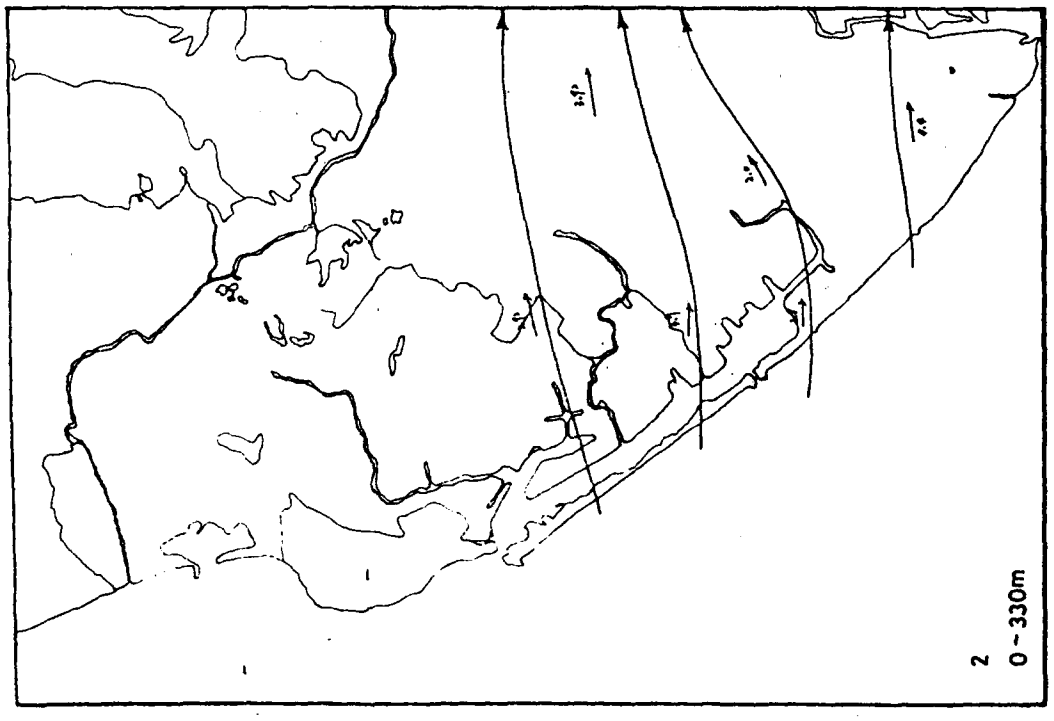

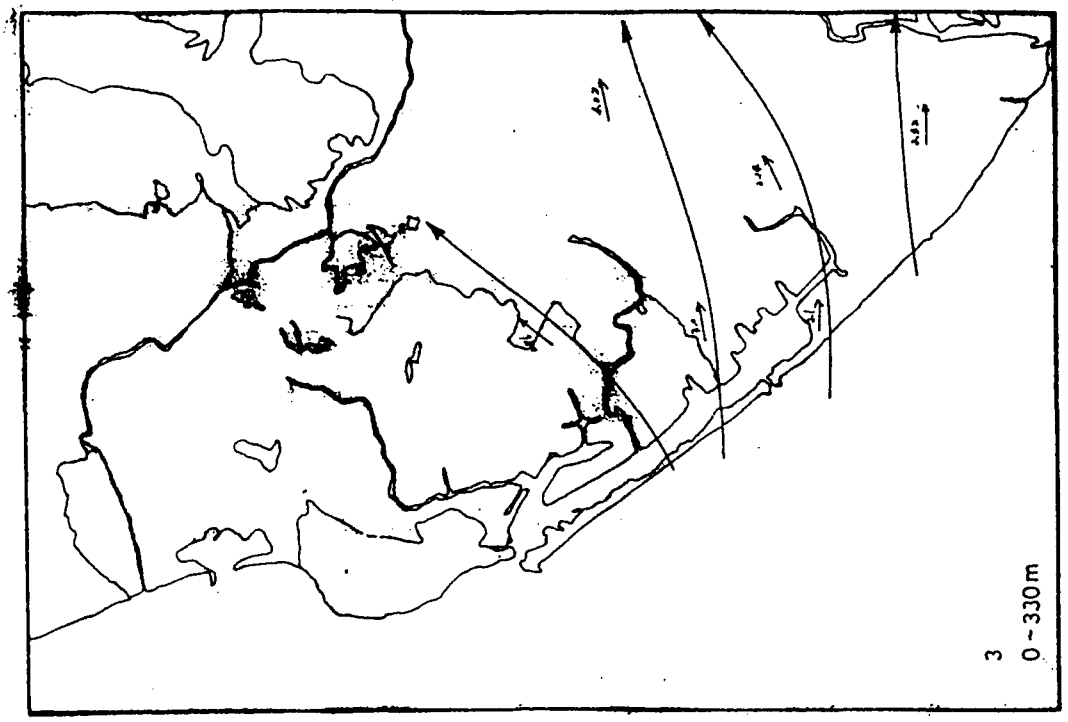
3
0-330m

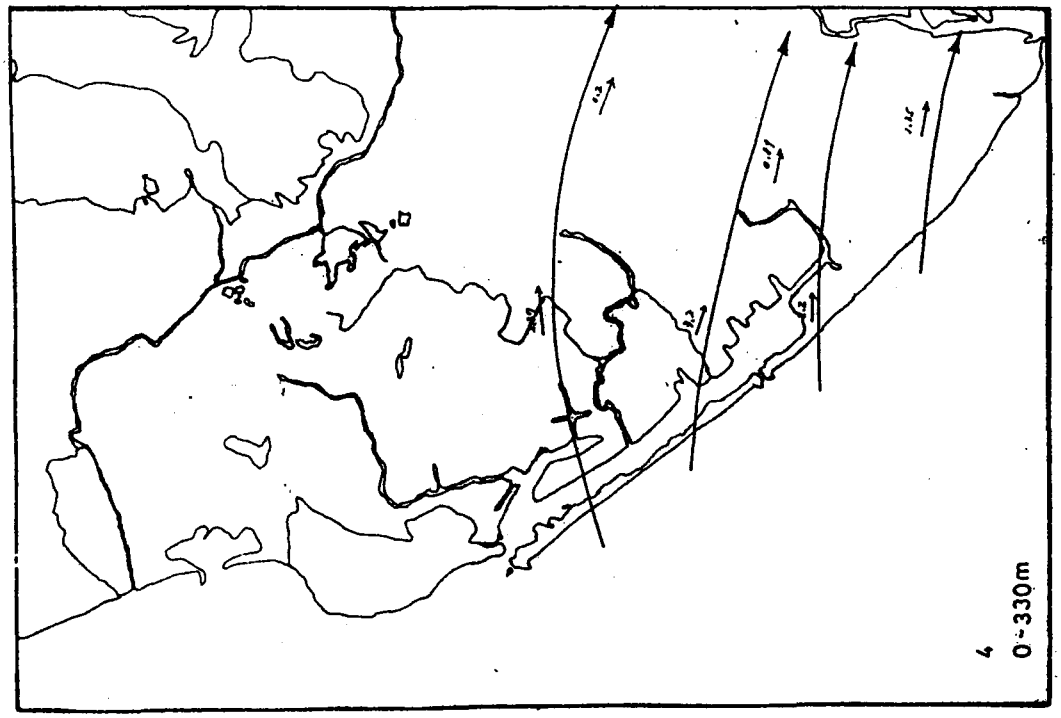
4
0-330m

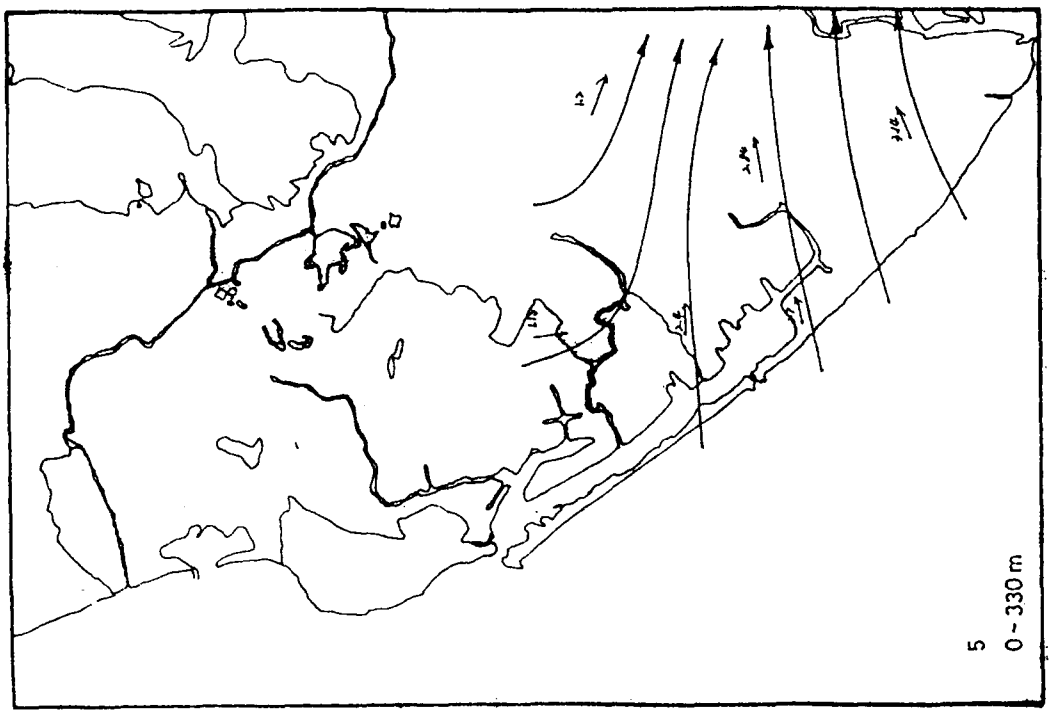
5
0 - 330 m

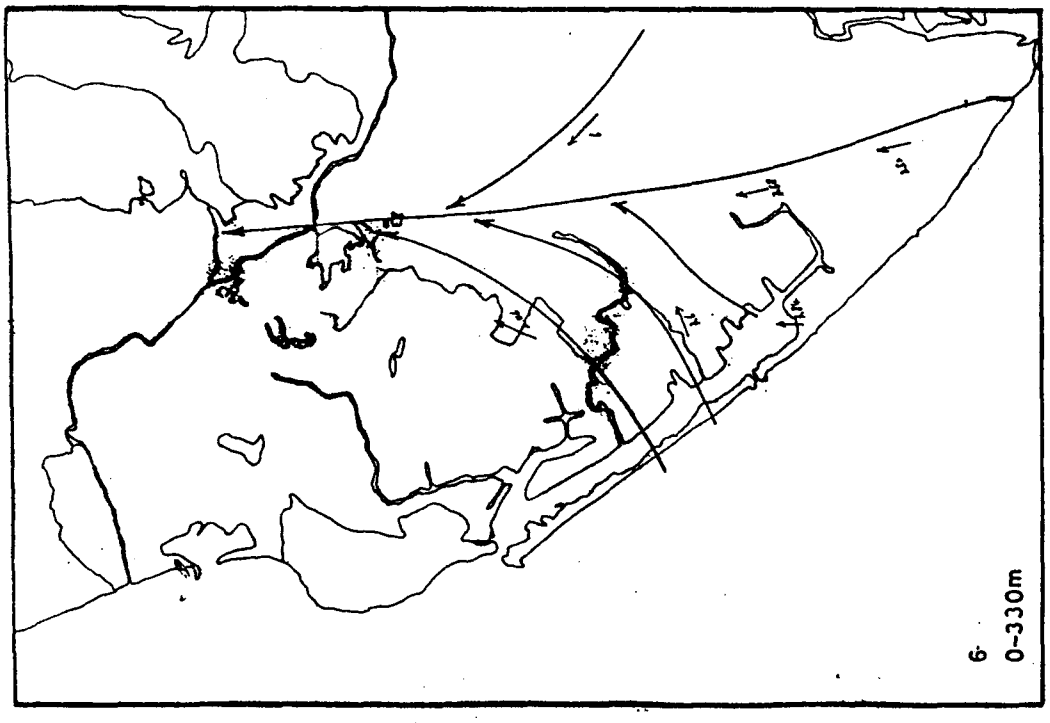
6
0-330m

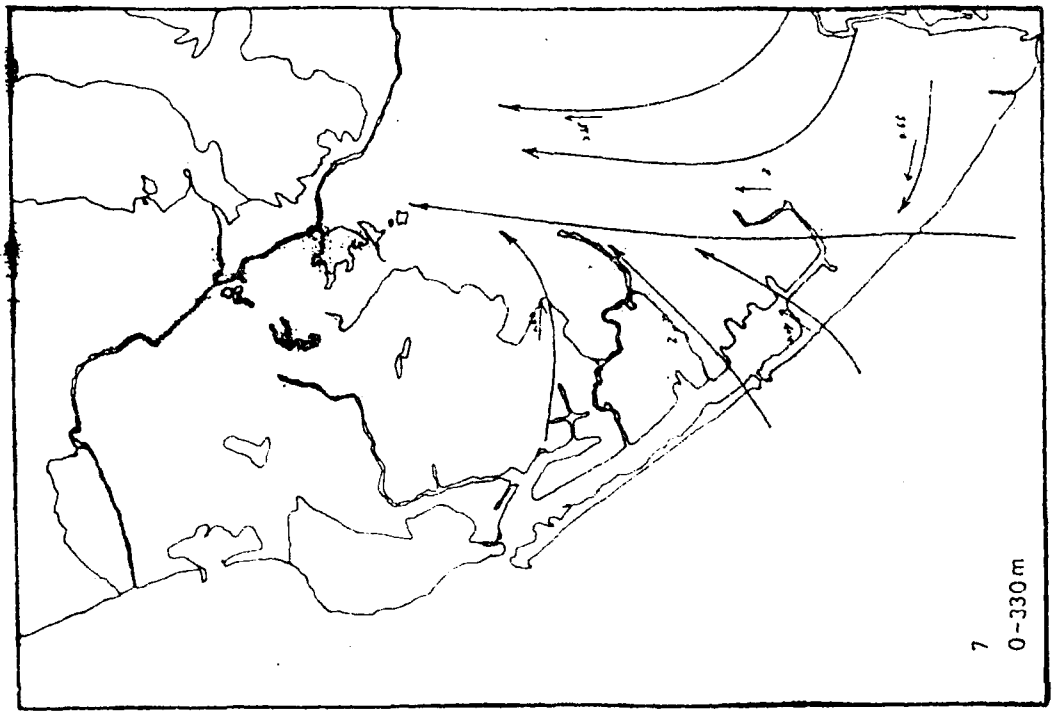
7
0-330 m


8
0-330m

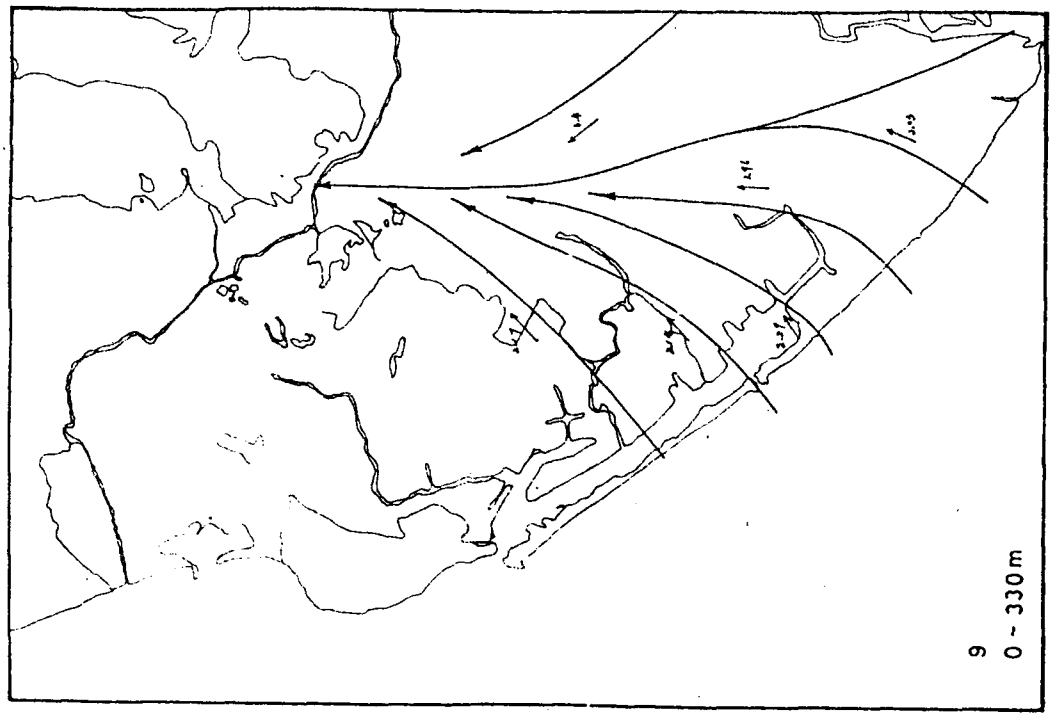
9
0 - 330m

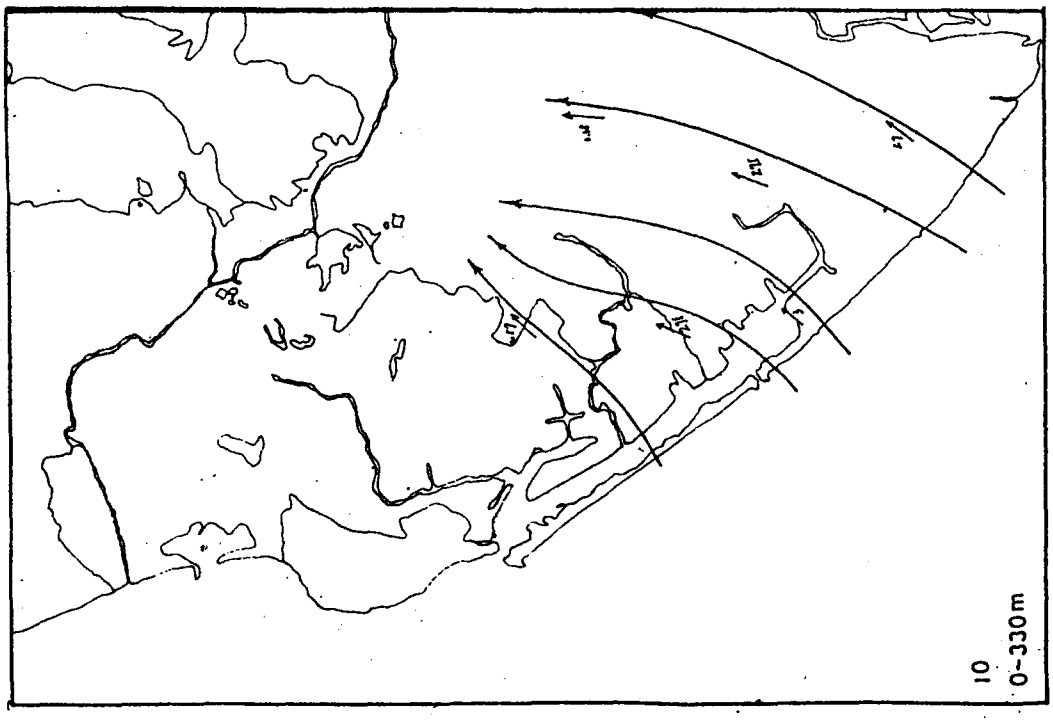
10
0-330m

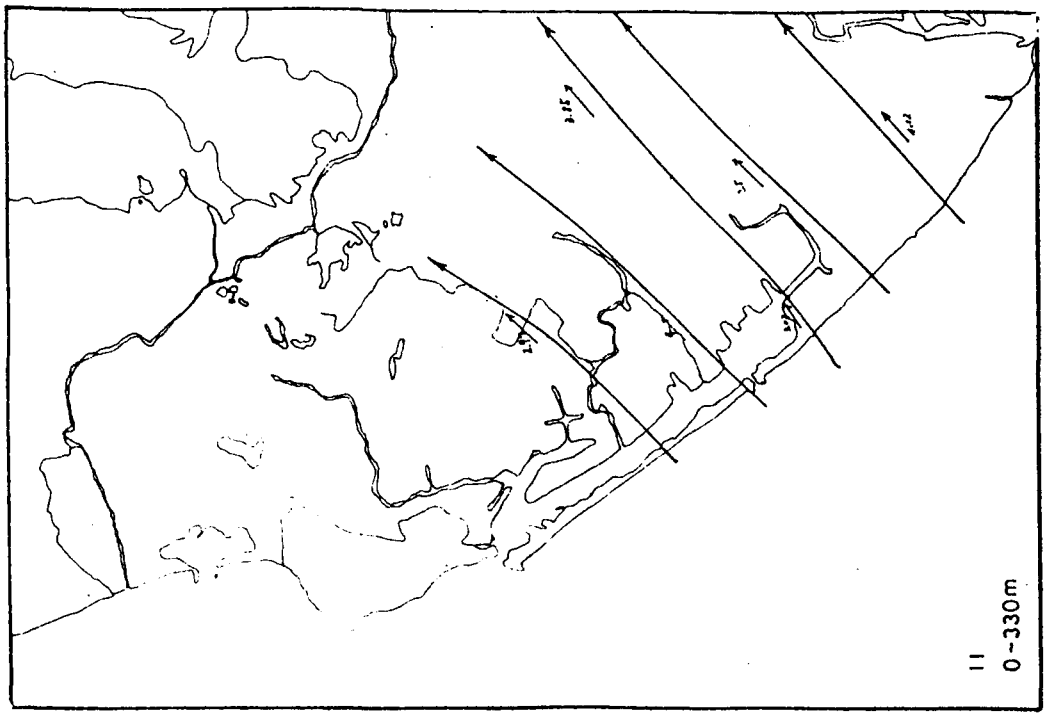
11
0-330m

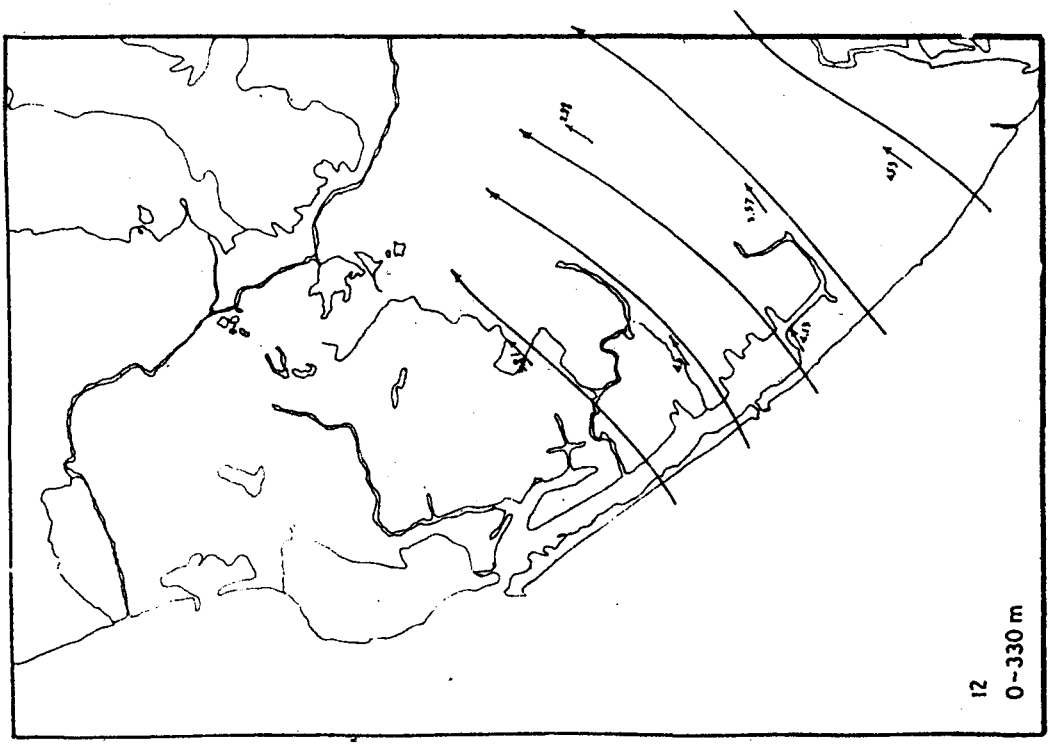
12
0-330 m

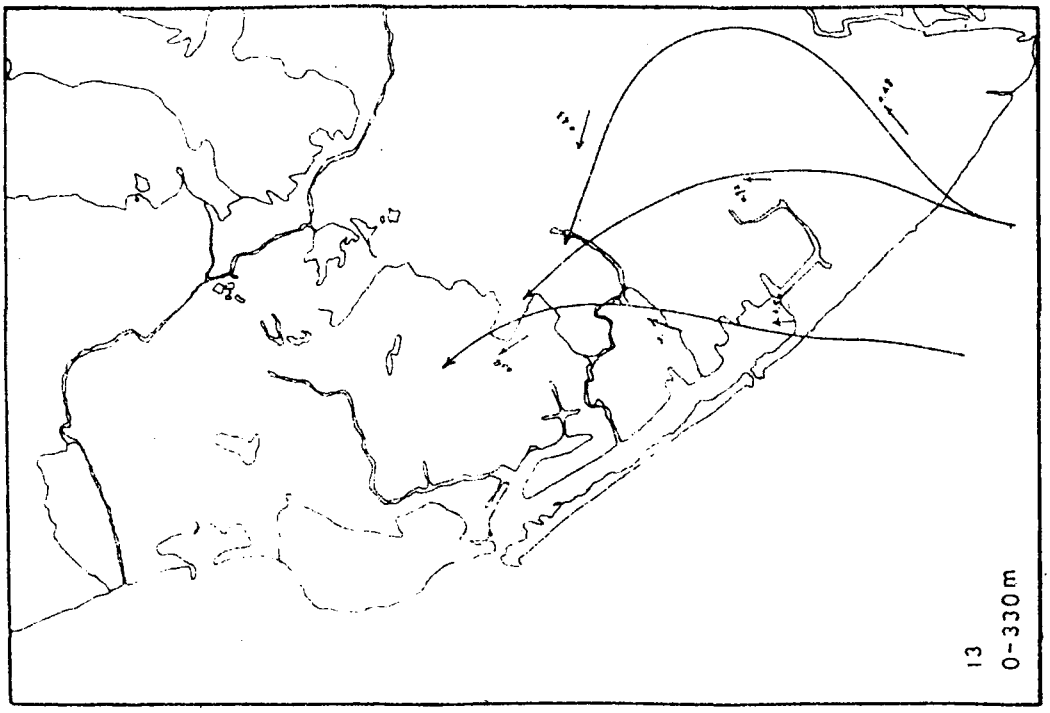
13
0-330m

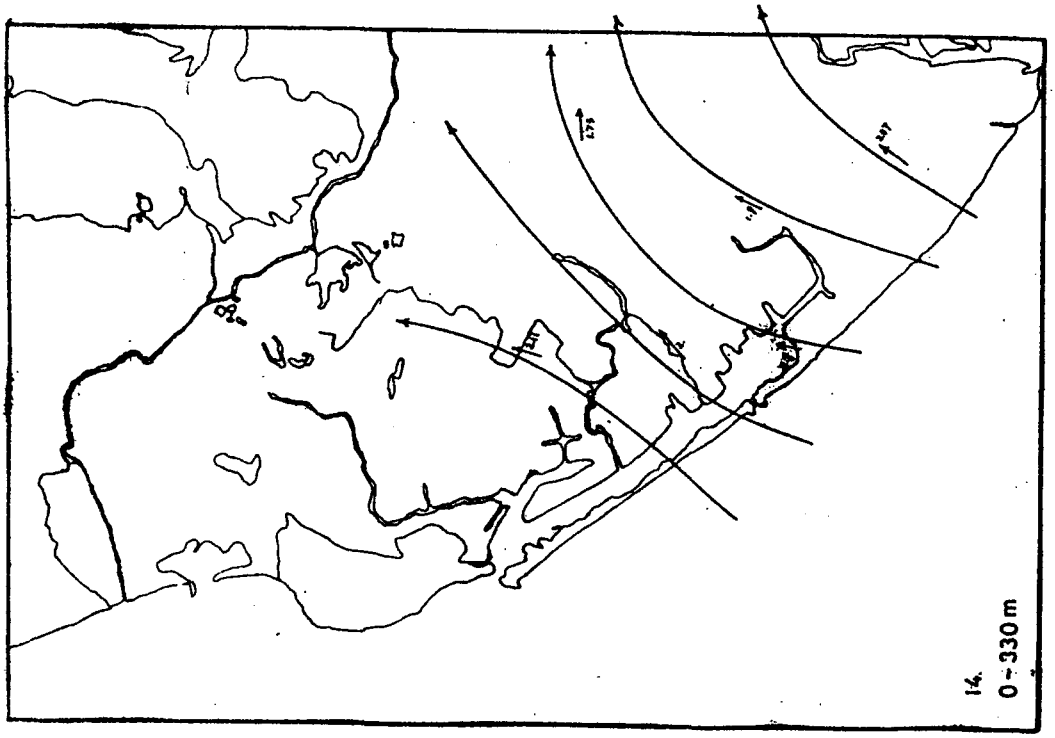
14.
0-330m

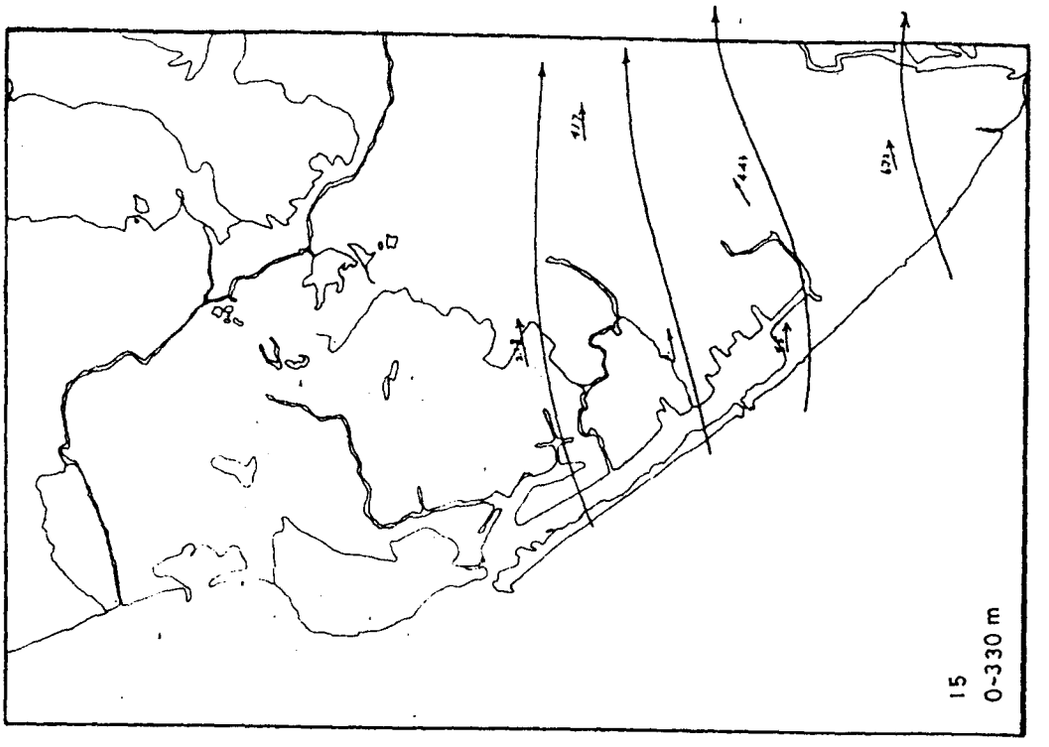
15
0-330 m

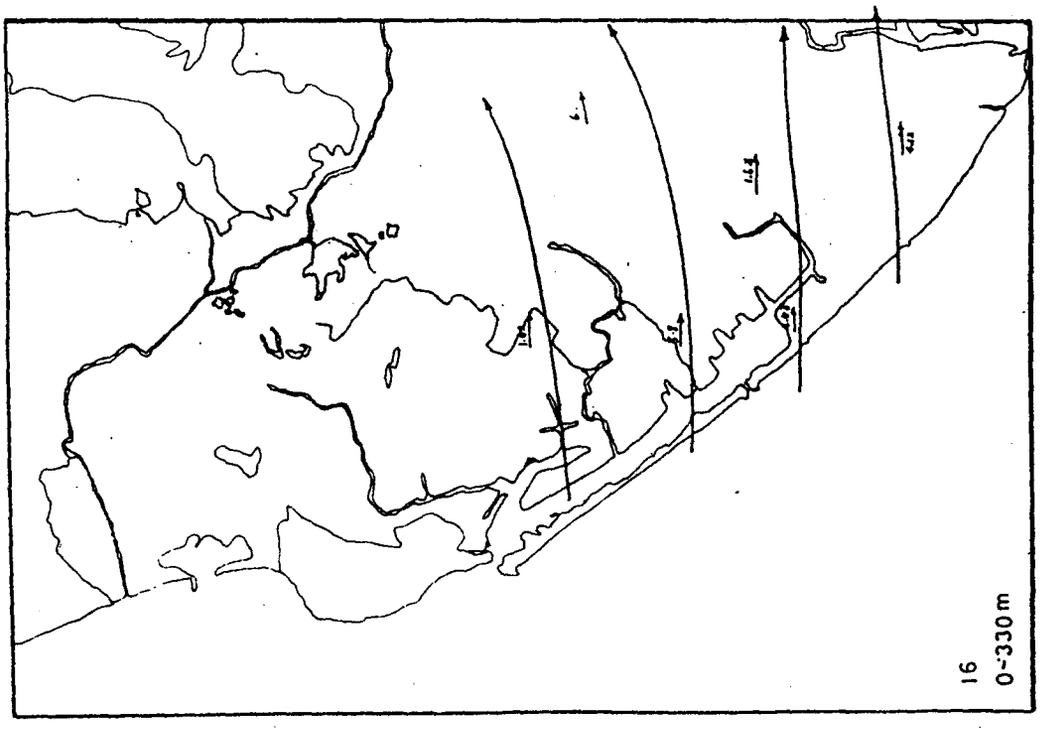
16
0-330 m

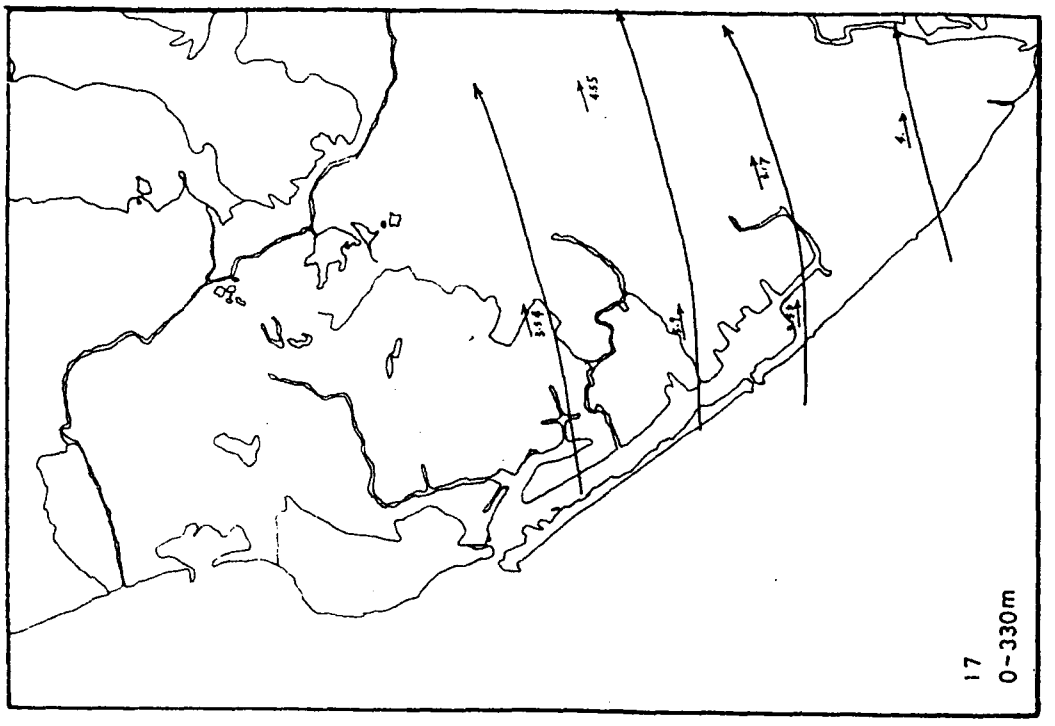
17
0-330m

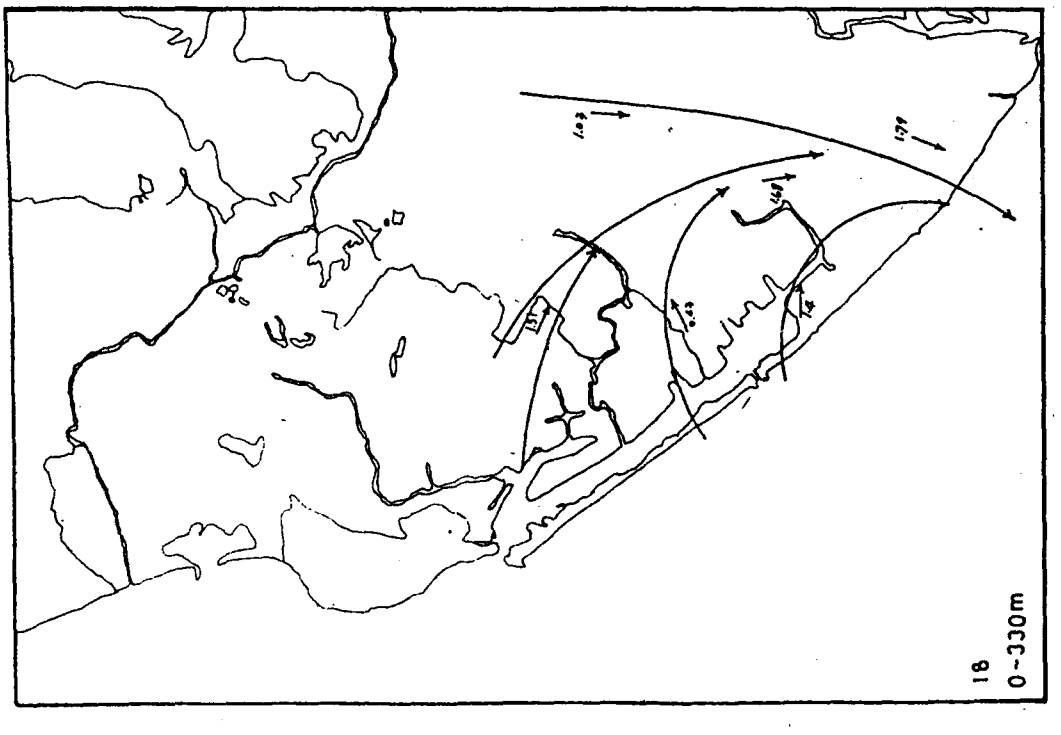
18
0-330m

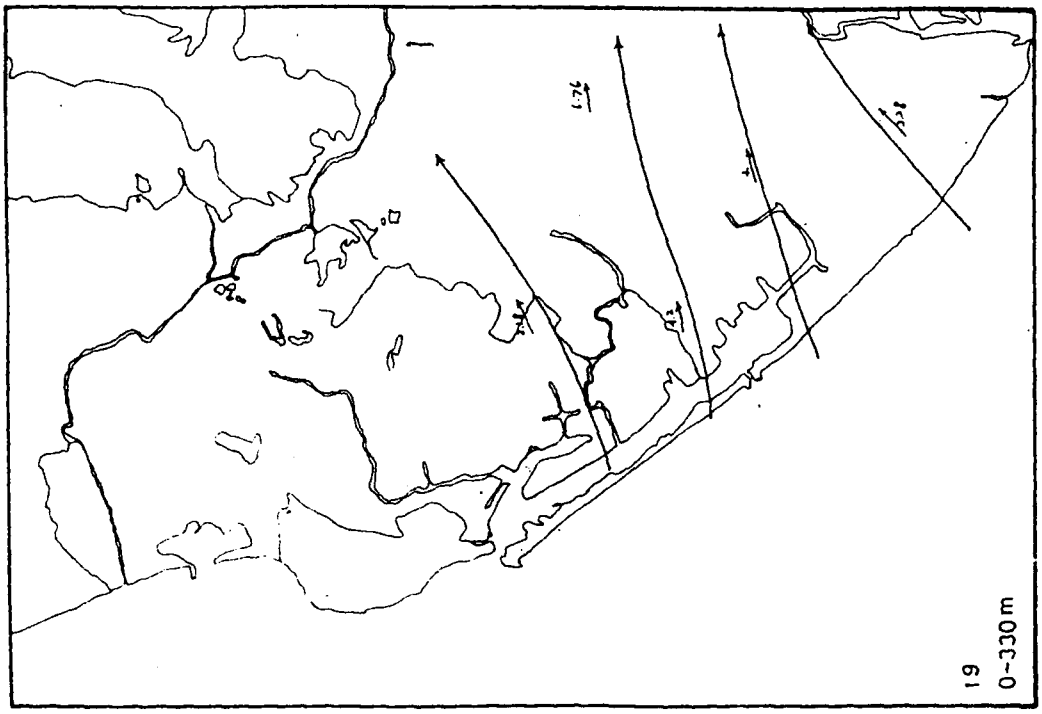
19
0-330m

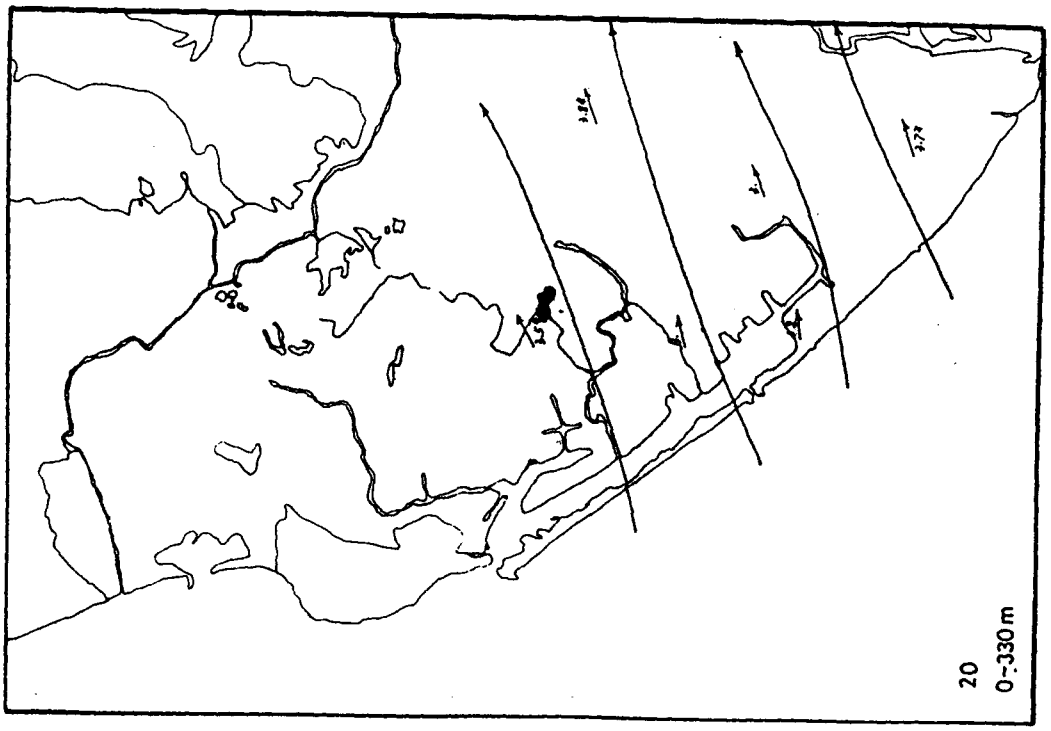
20
0-330m

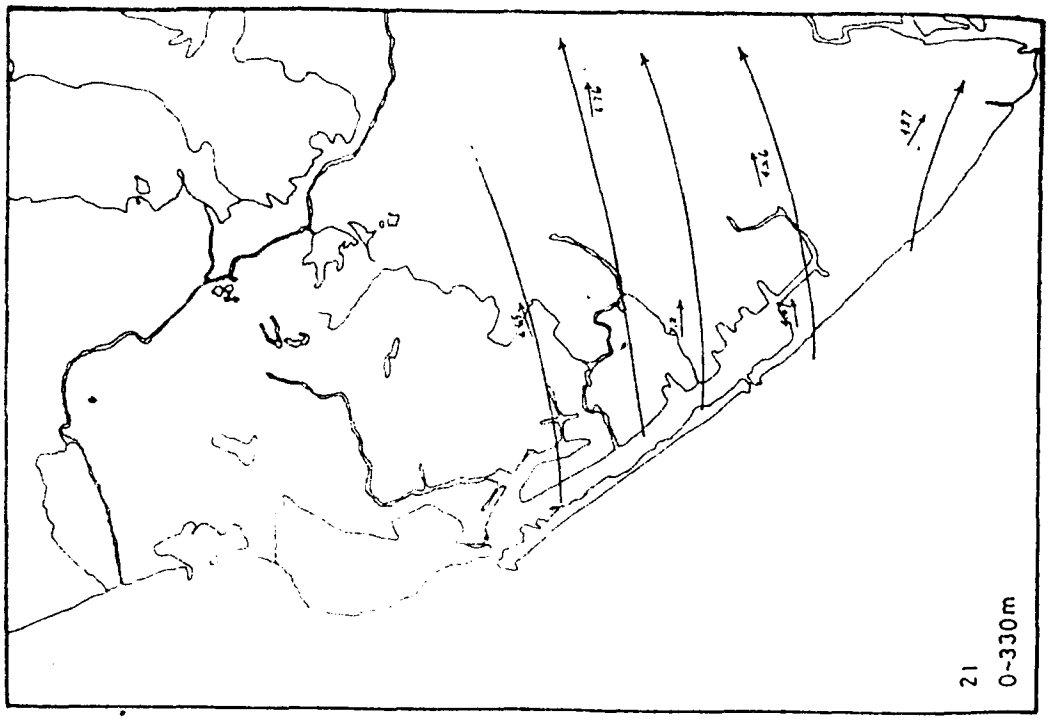
21
0-330m

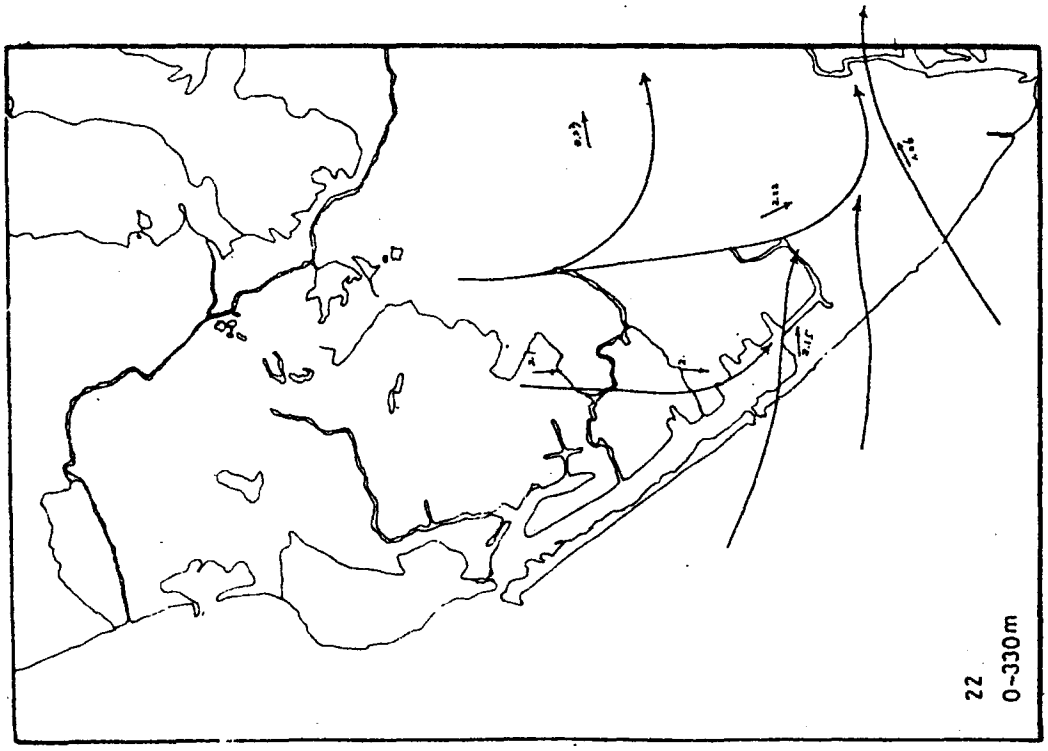
22
0-330m

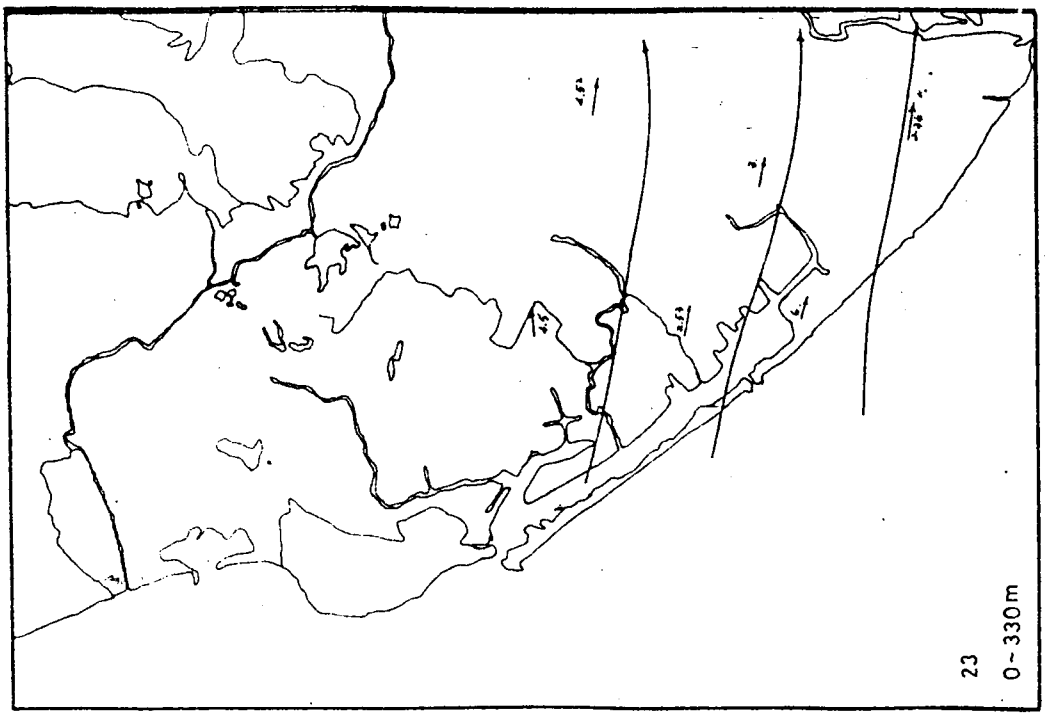
23
0 - 330 m

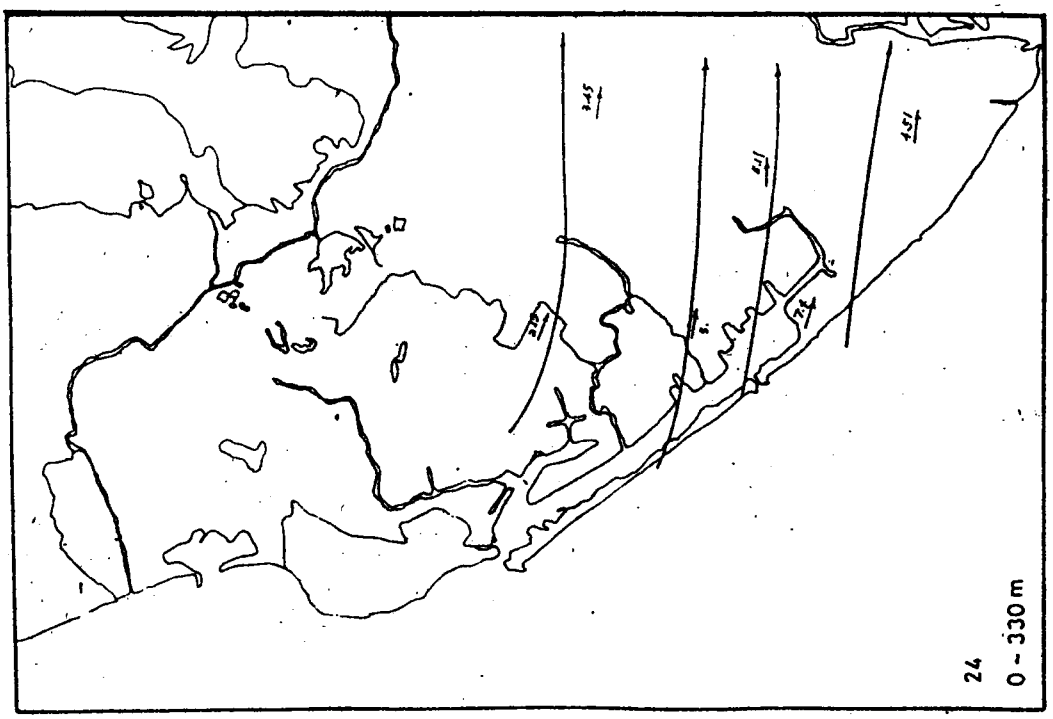
24
0 - 330 m

APPENDIX C - 2 The wind field of Kaohsiung area
(Run 1 - Run 24 , 330 - 660m)

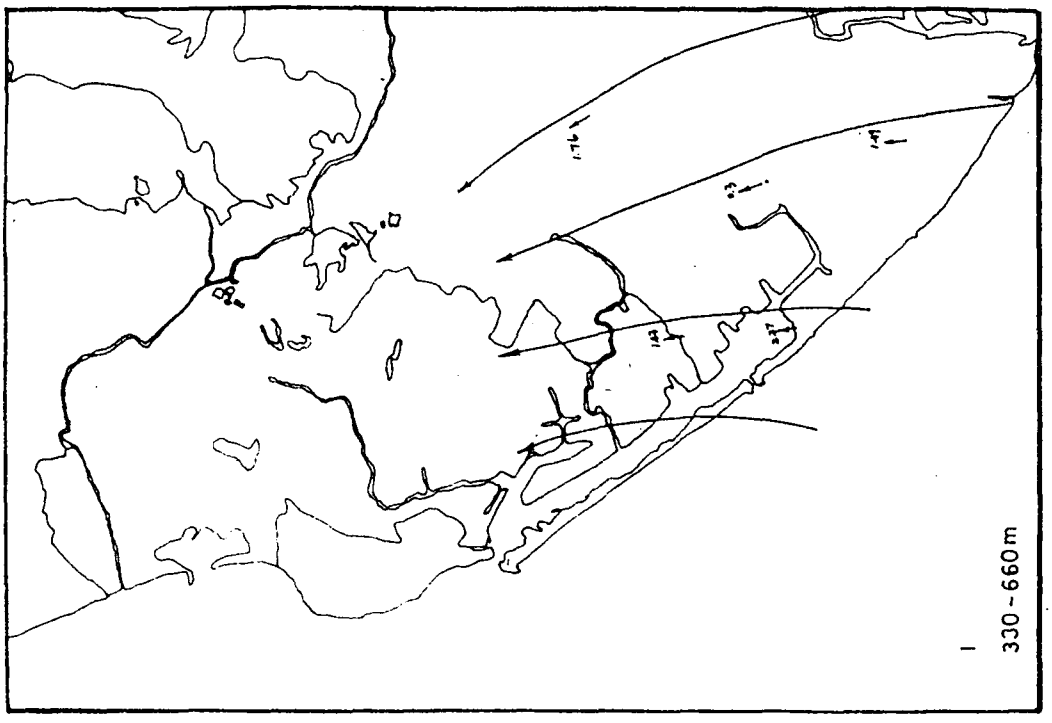

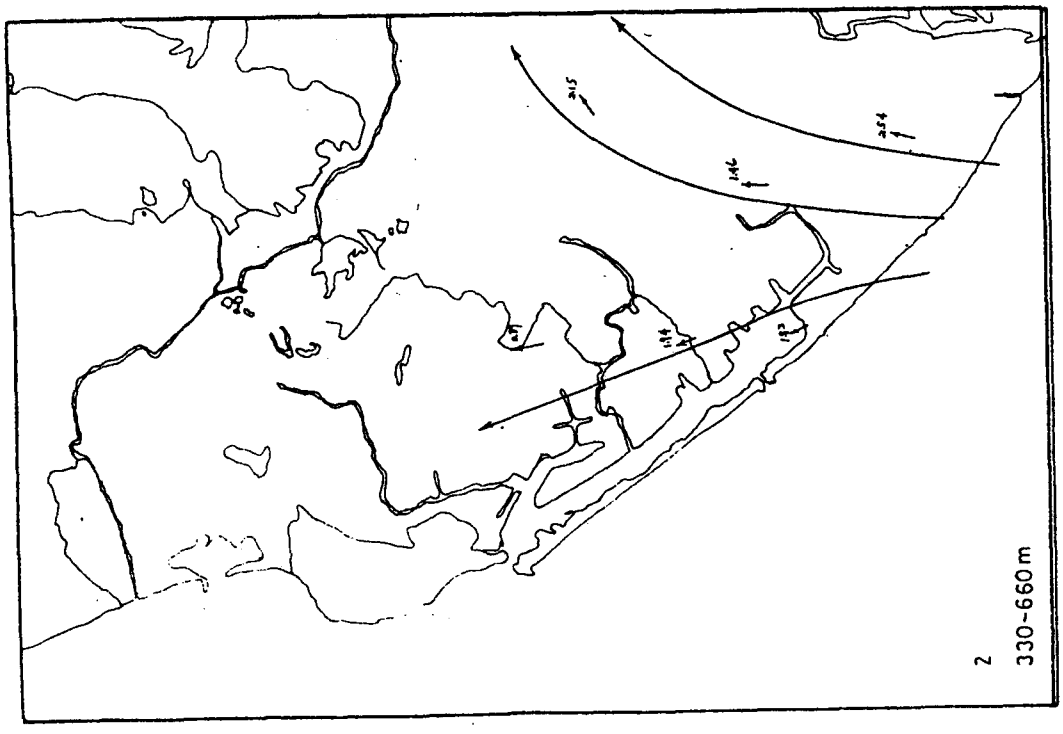

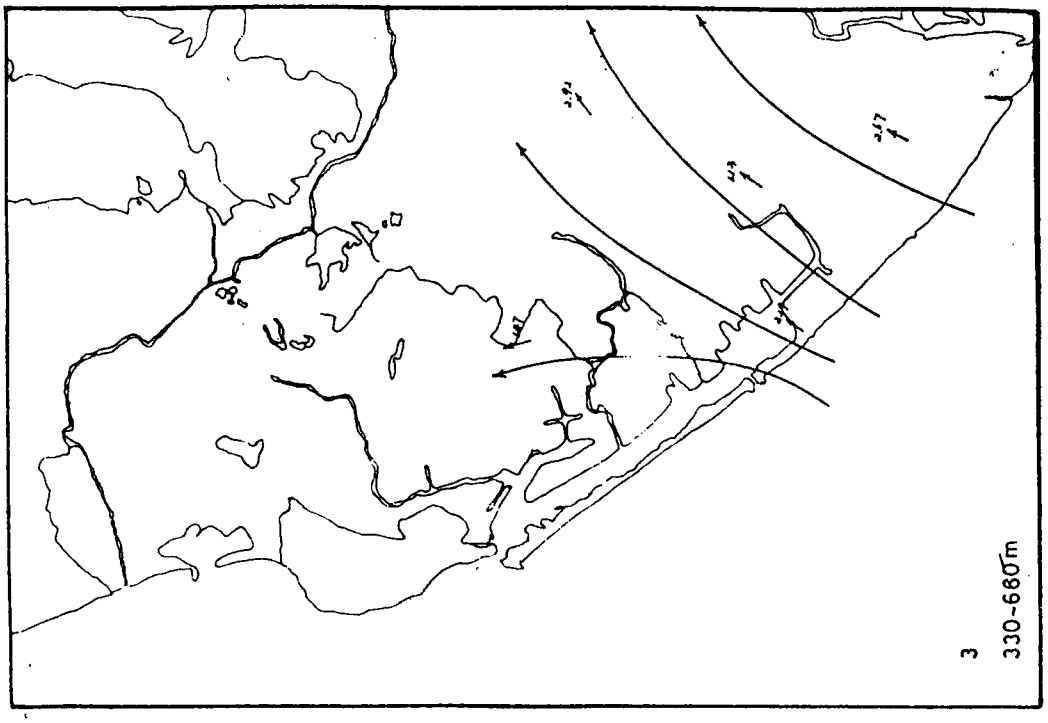
3
330-660m

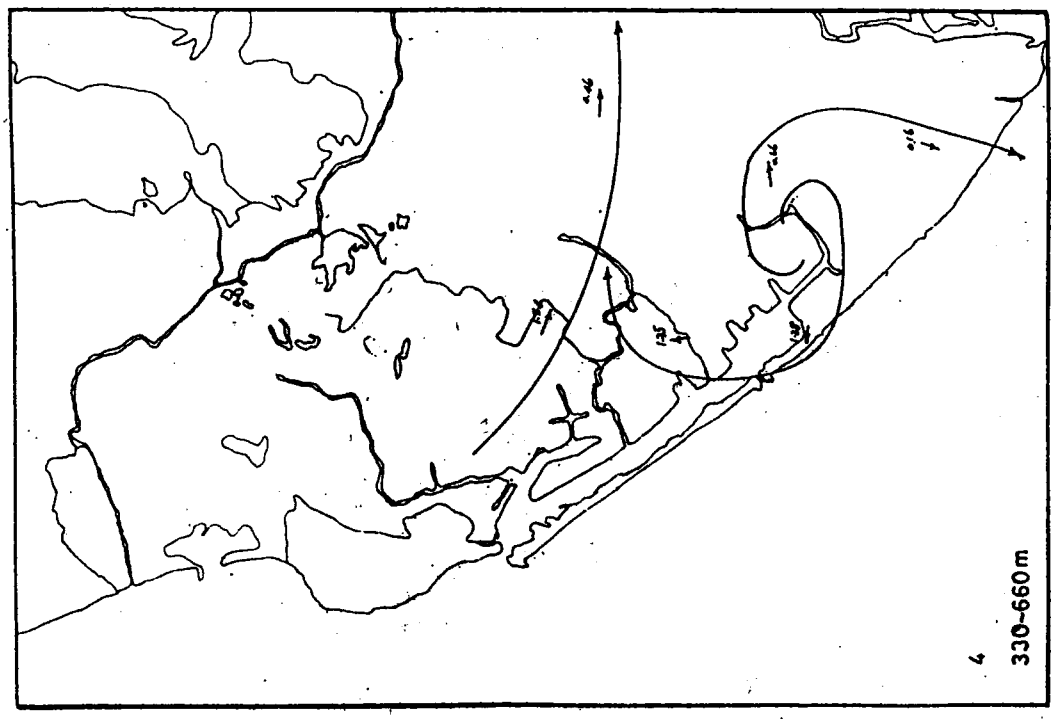
4
330-660m

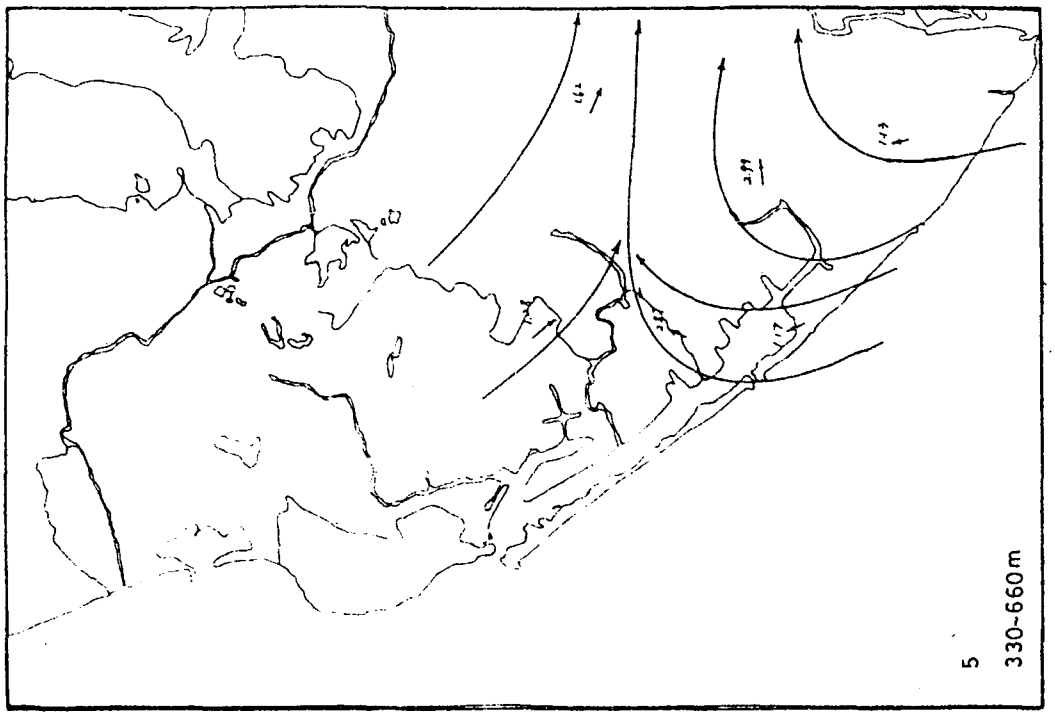
5
330-660m

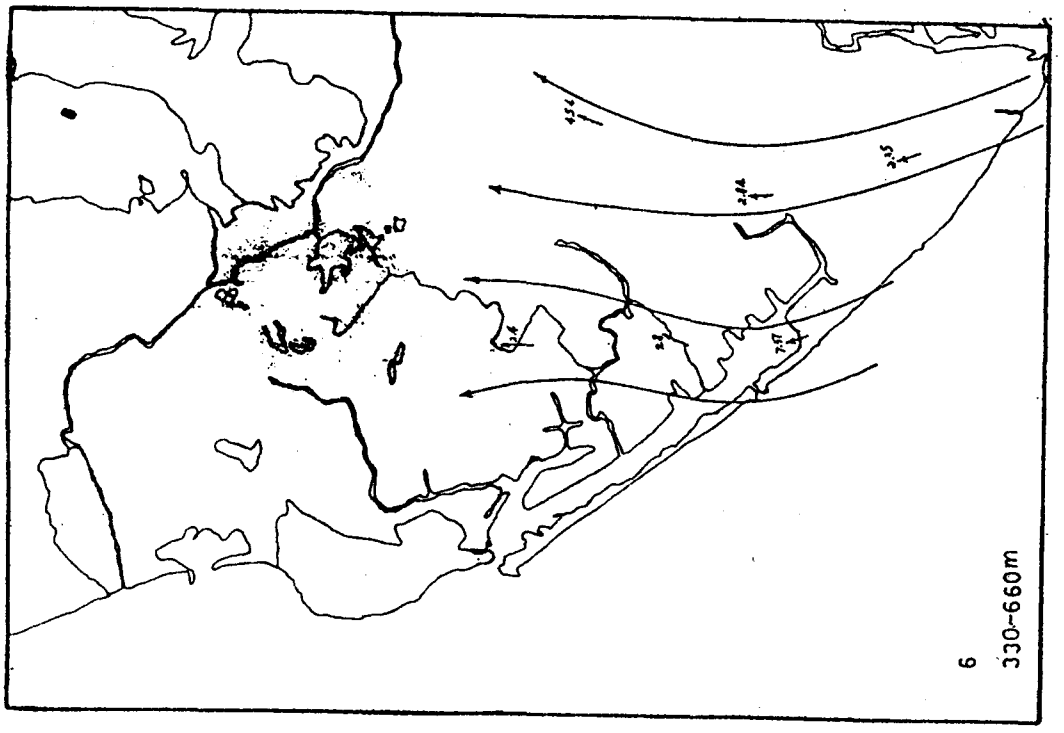
6
330-660m

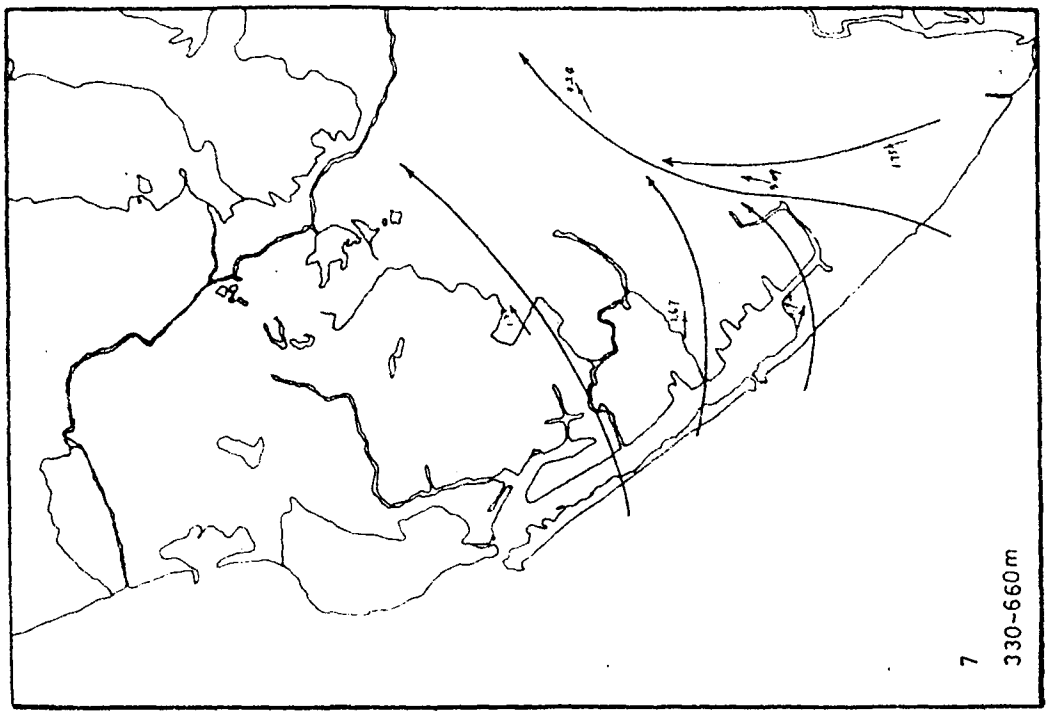
7
330-660m

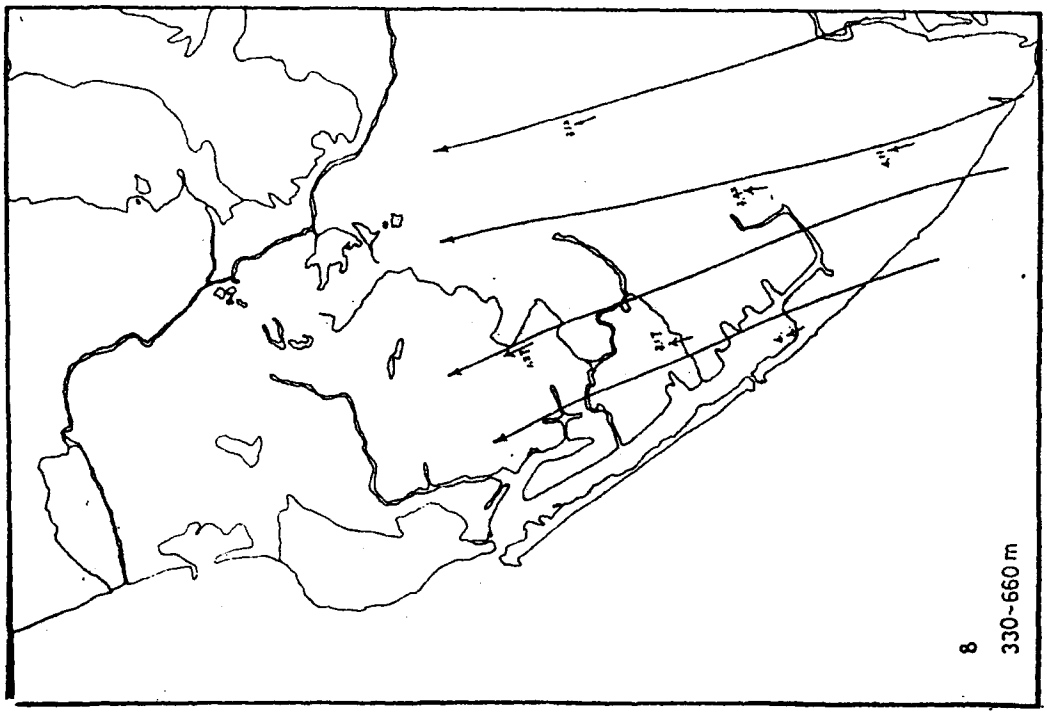
8
330-660m

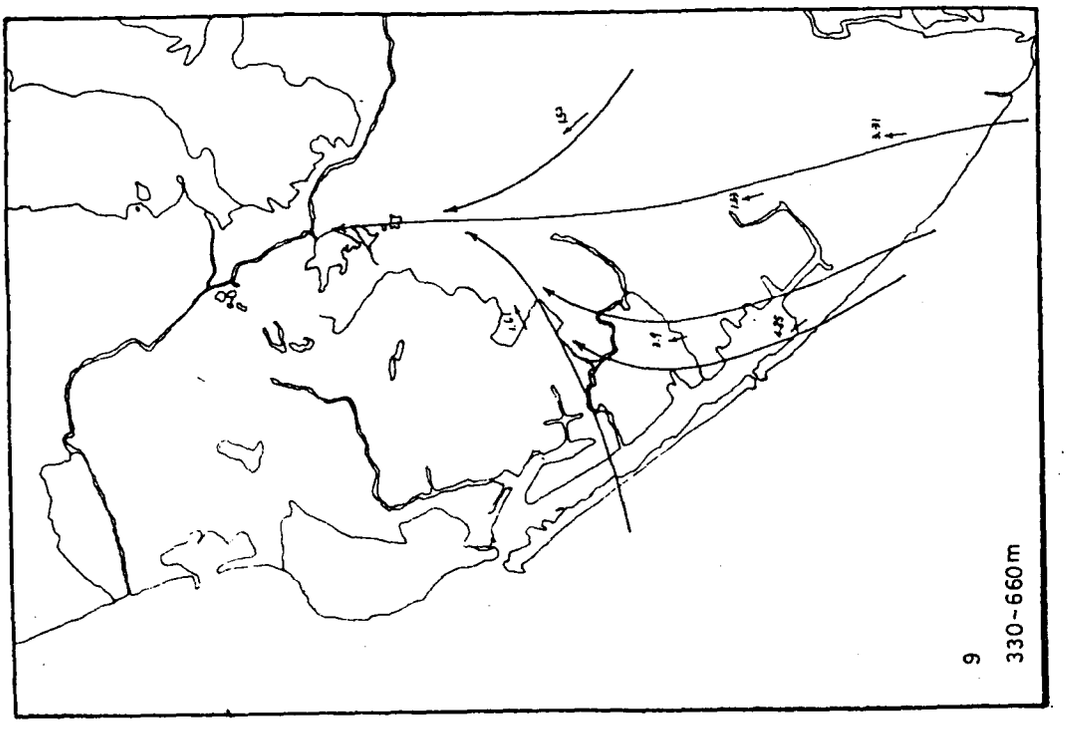
9
330-660m

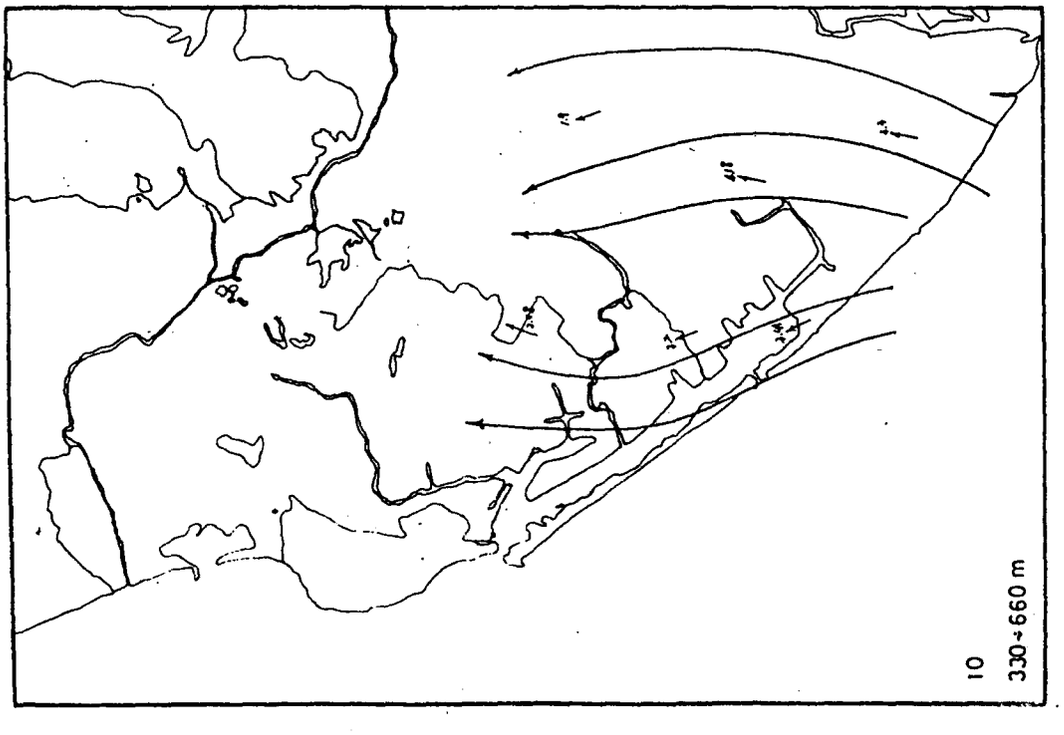
10
330-660 m

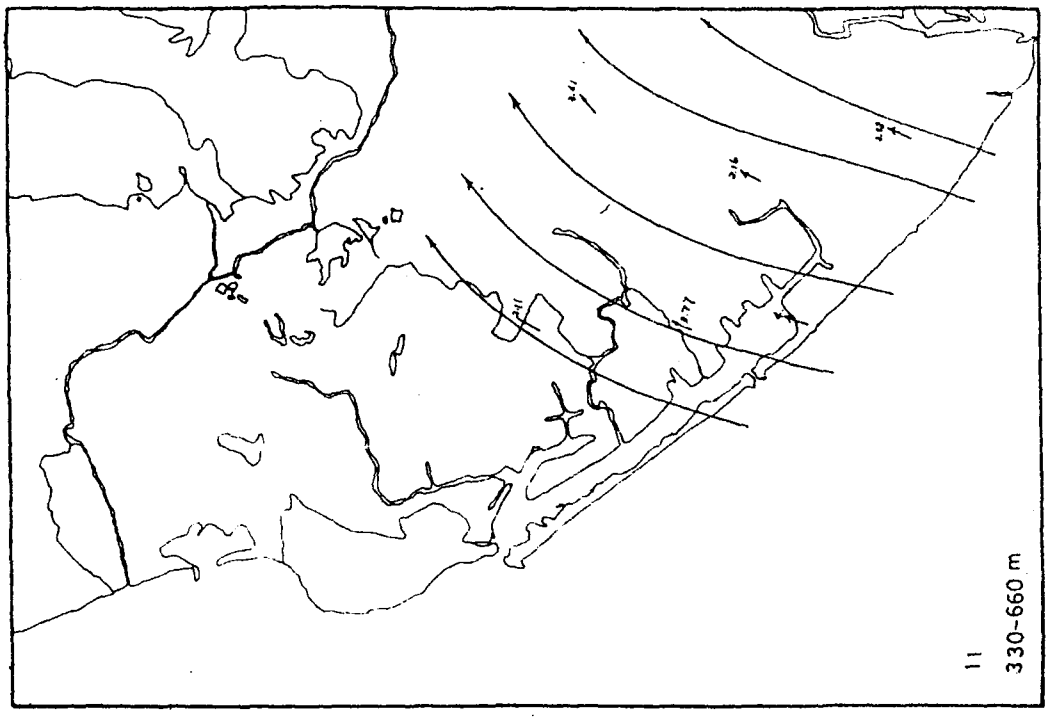
11
330-660 m

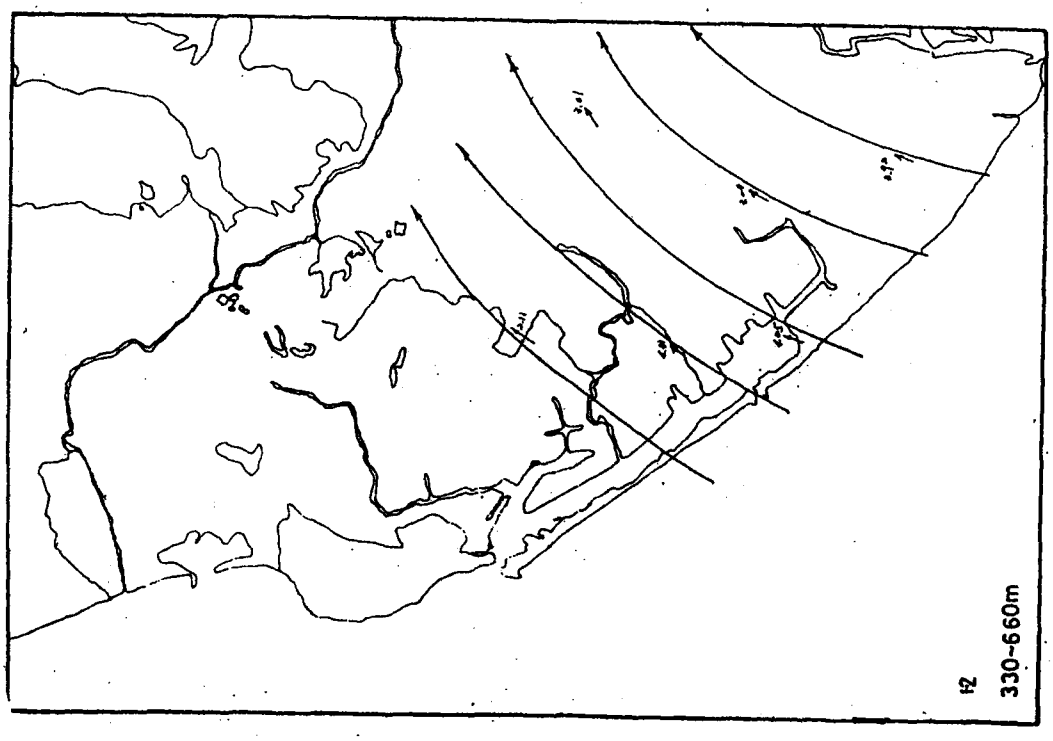
12
330-660m

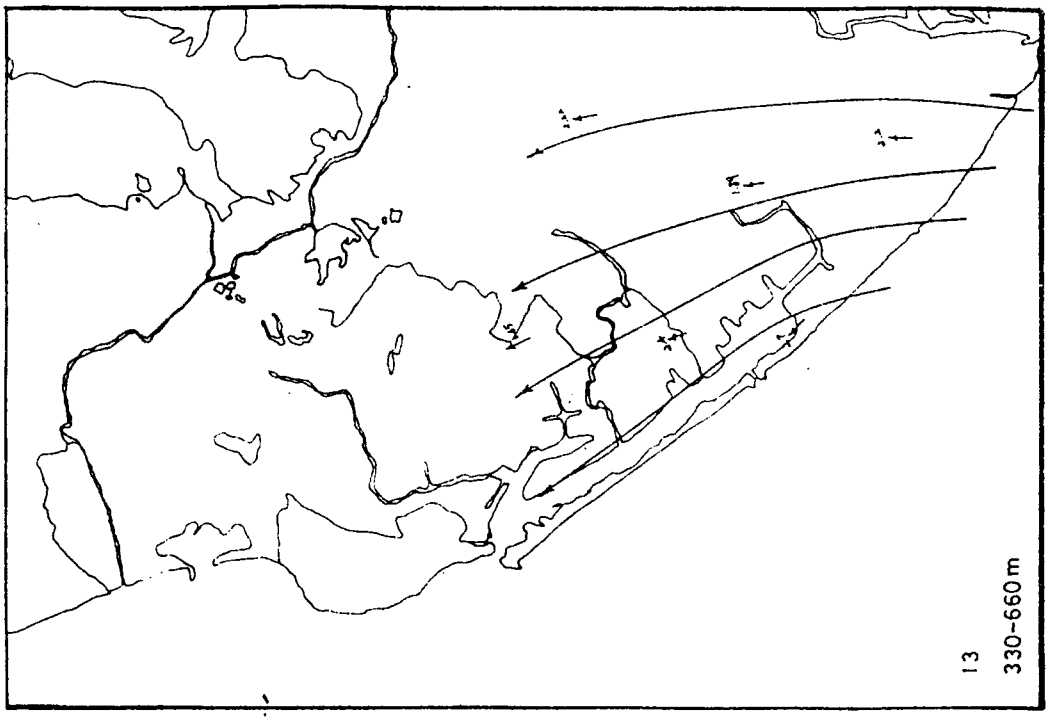
13
330-660m

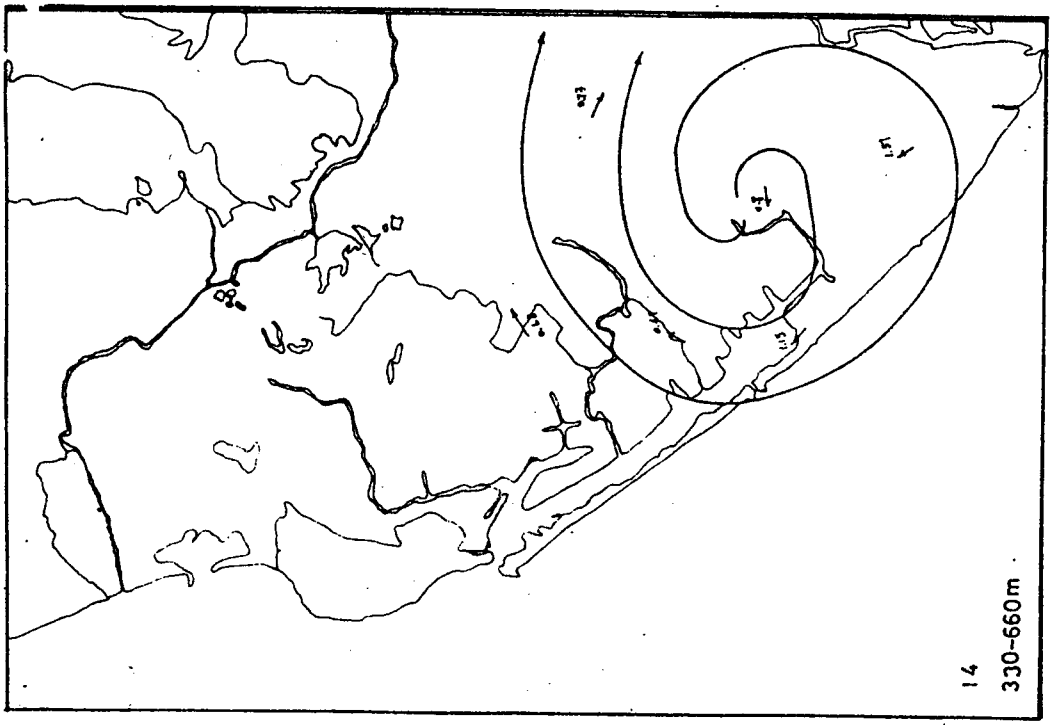
14
330-660m

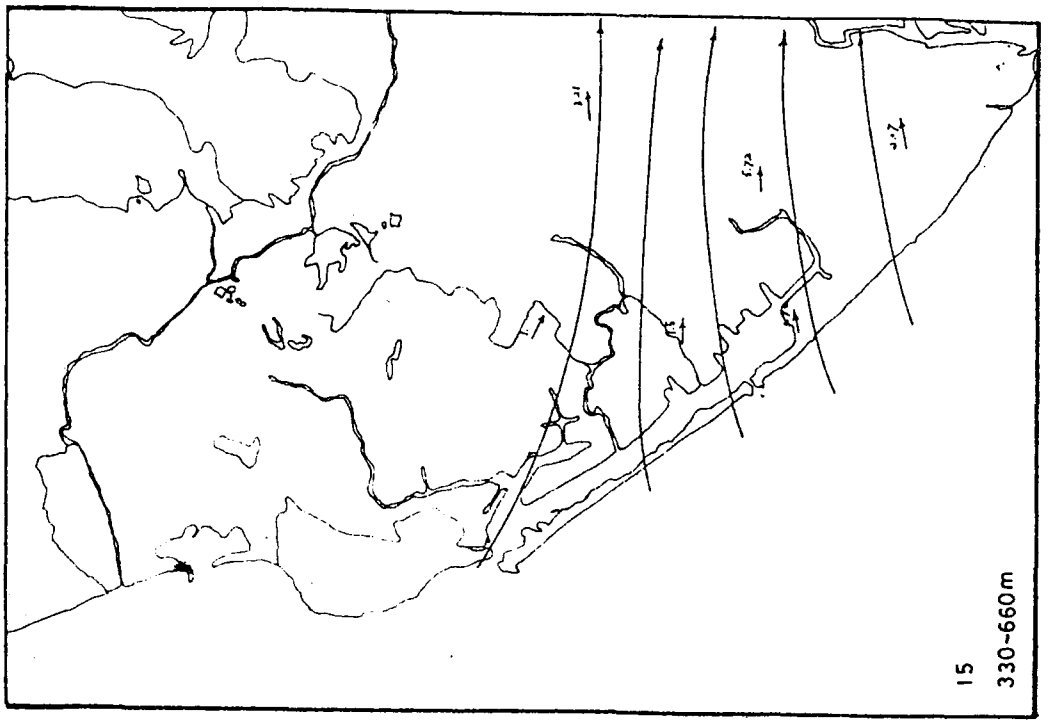
15
330-660m

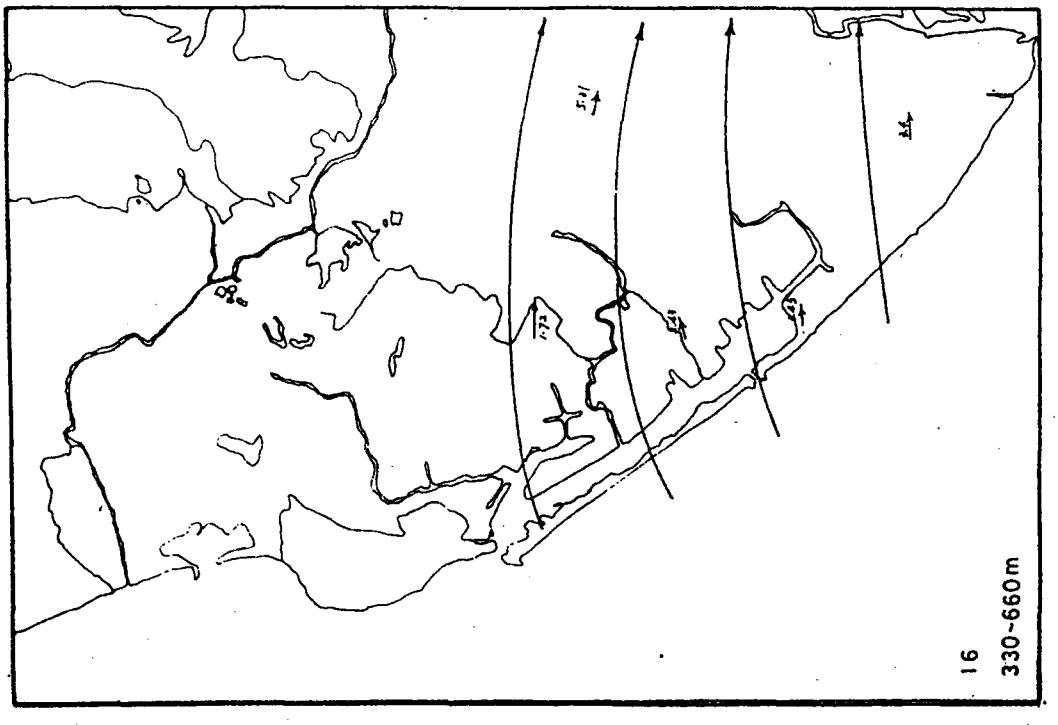
16
330-660m

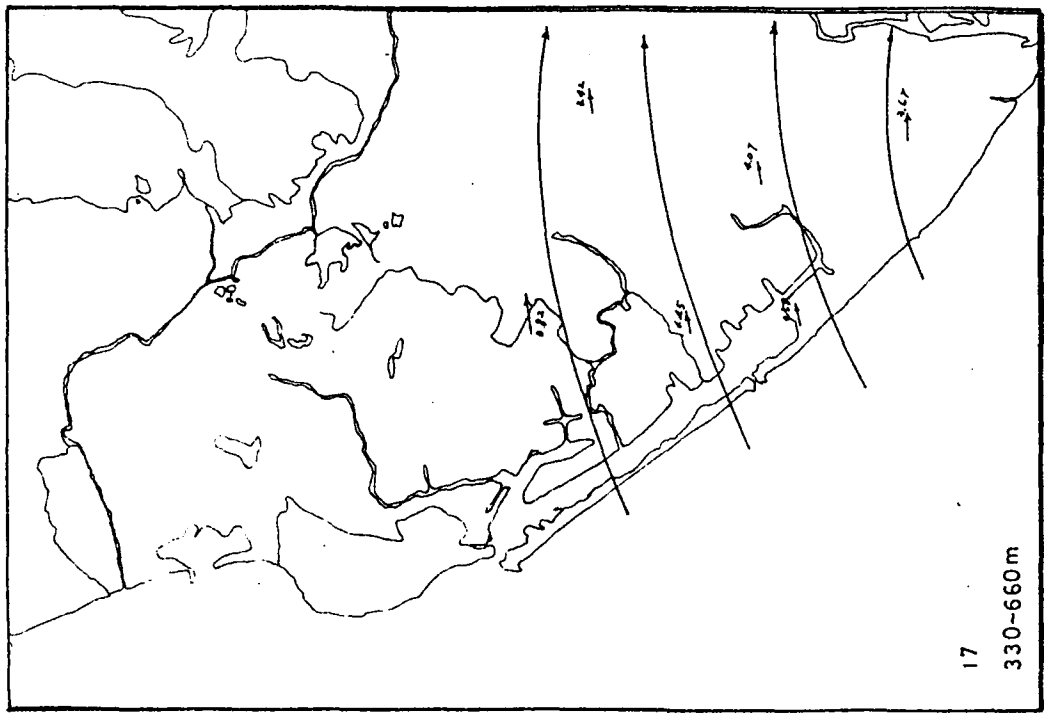
17
330-660m


18
330-660m

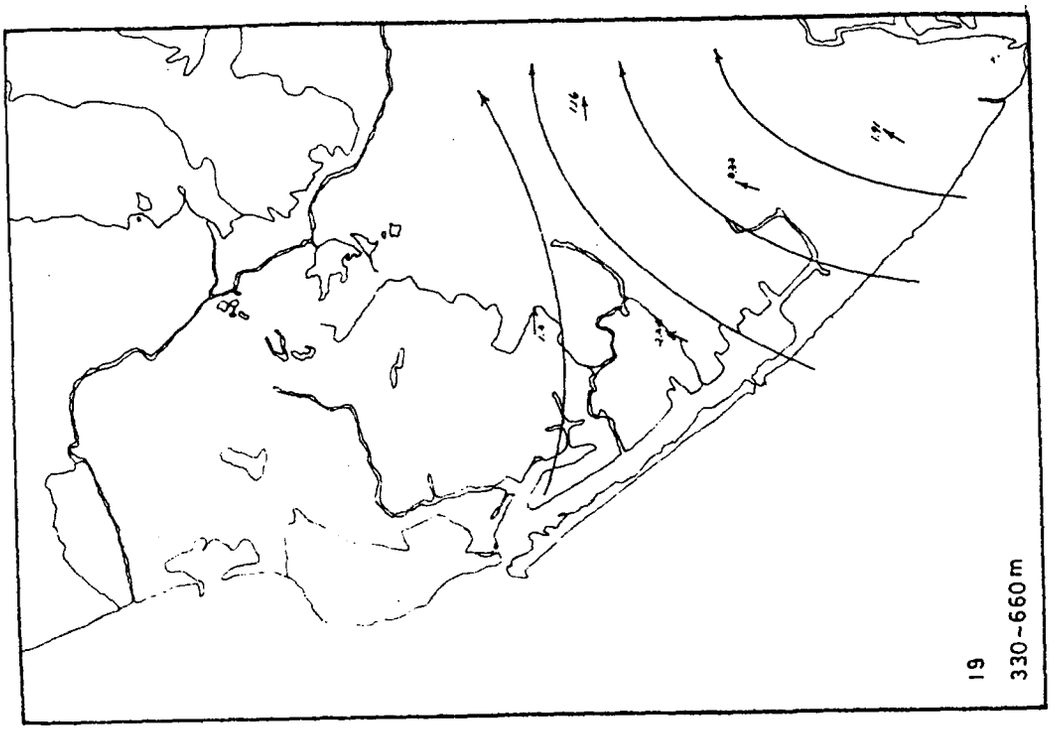
19
330-660m

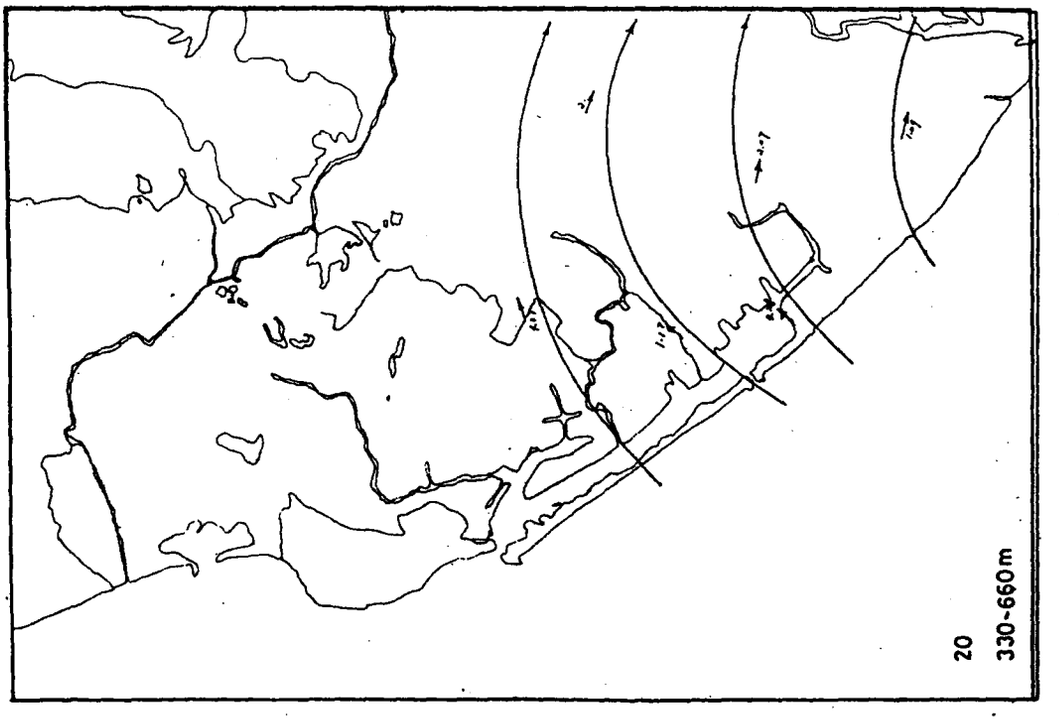
20
330-660m

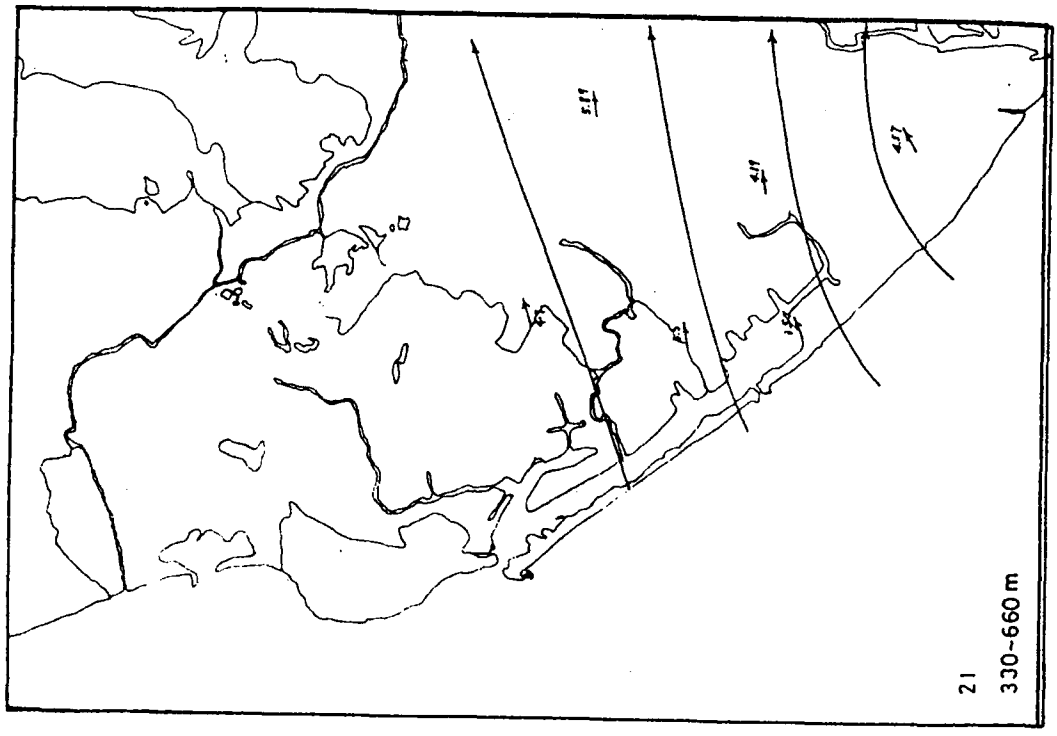
21
330-660 m

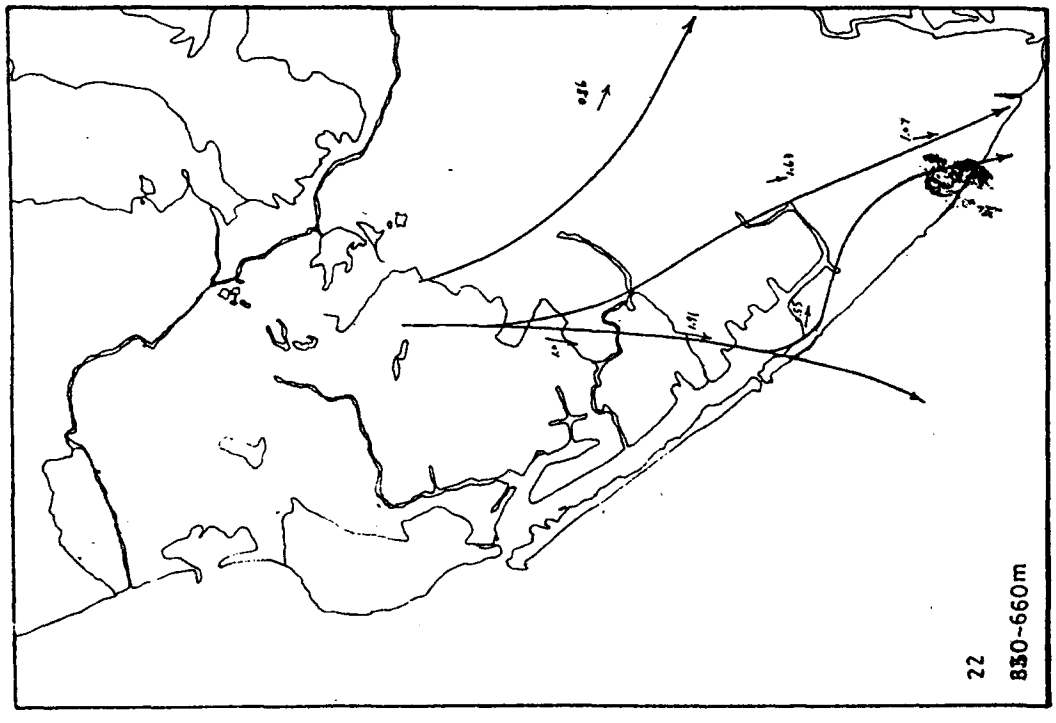
22
330-660m

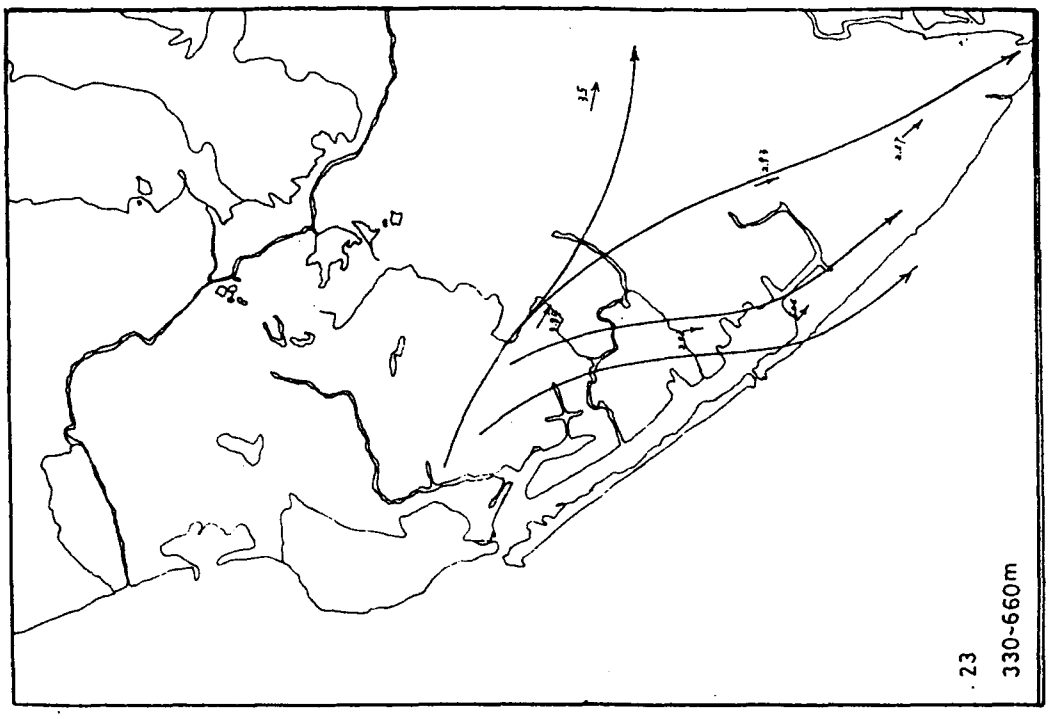
23
330-660m

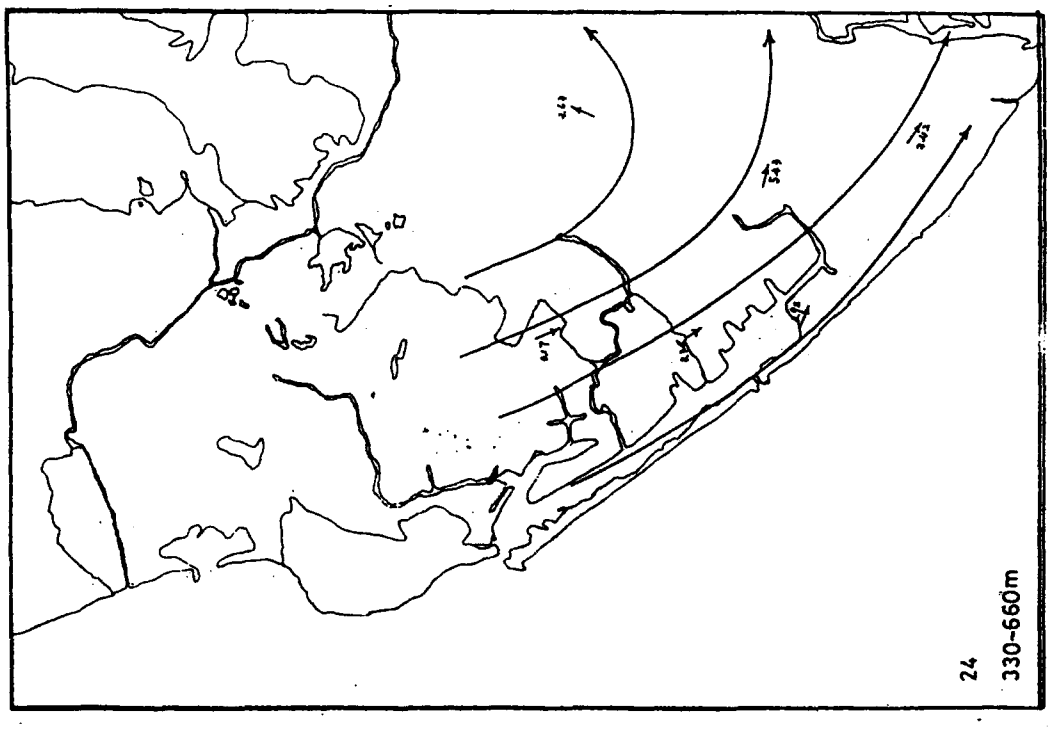
24
330-660m

APPENDIX C - 3 The wind field of Kaohsiung area
(Run 1 - Run 24 , 660 - 1000m)

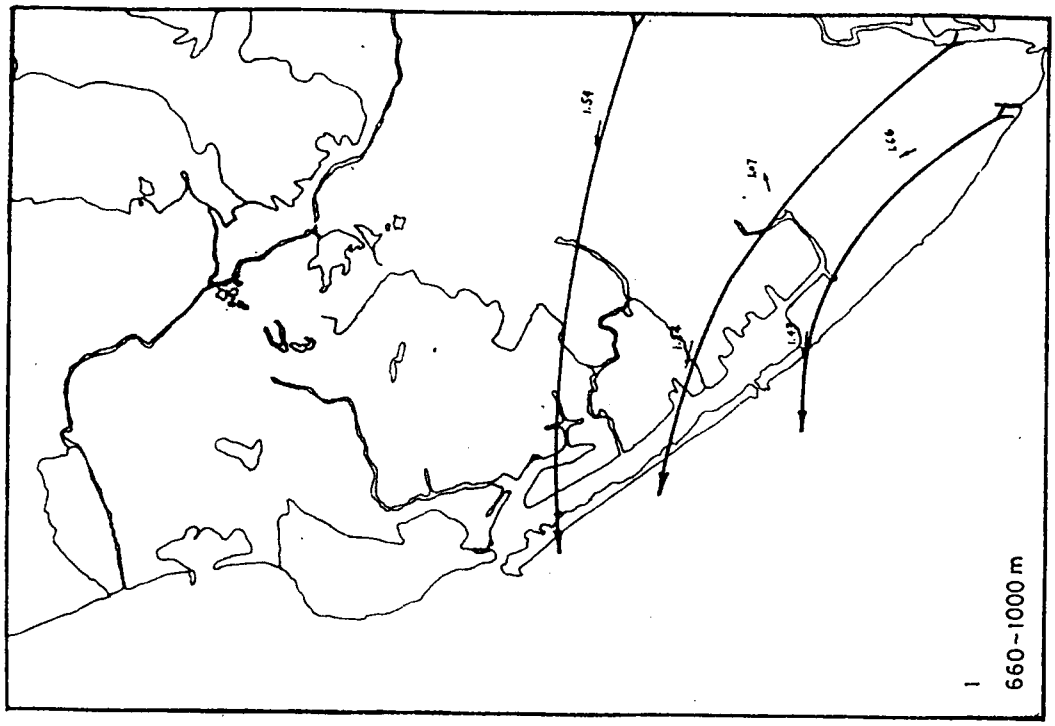

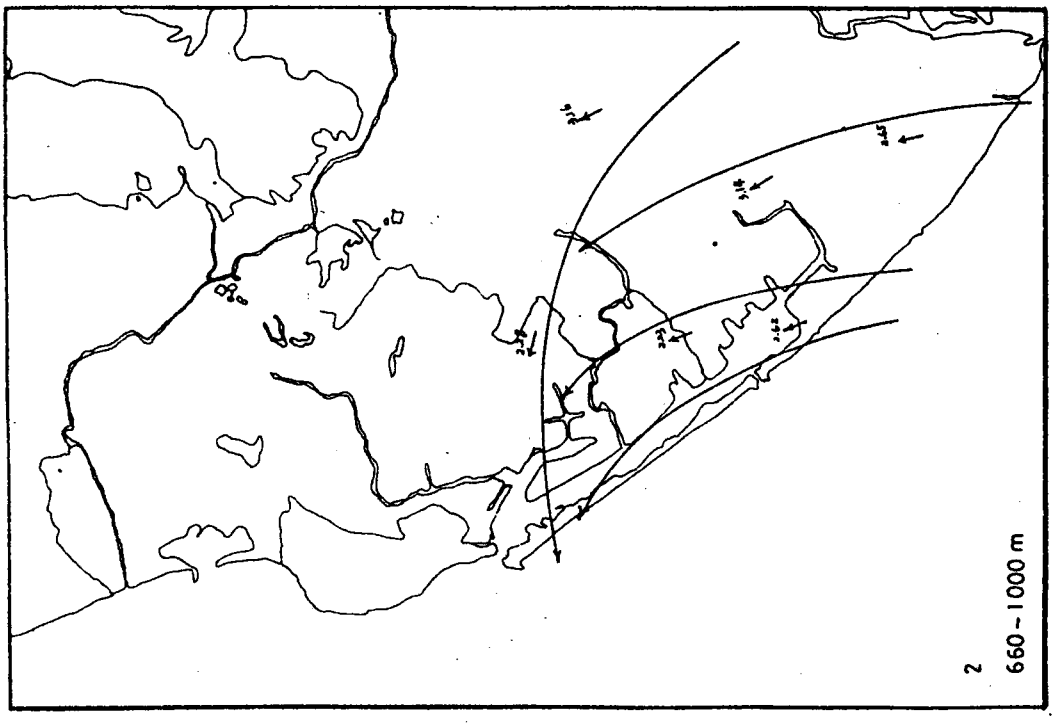

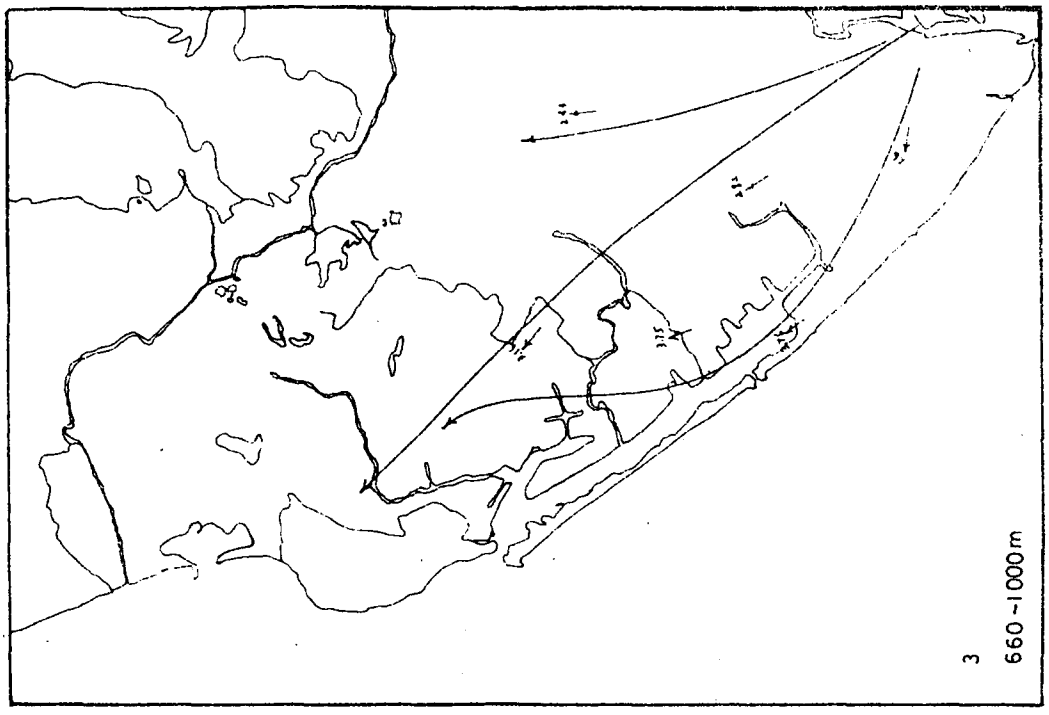
3
660-1000m

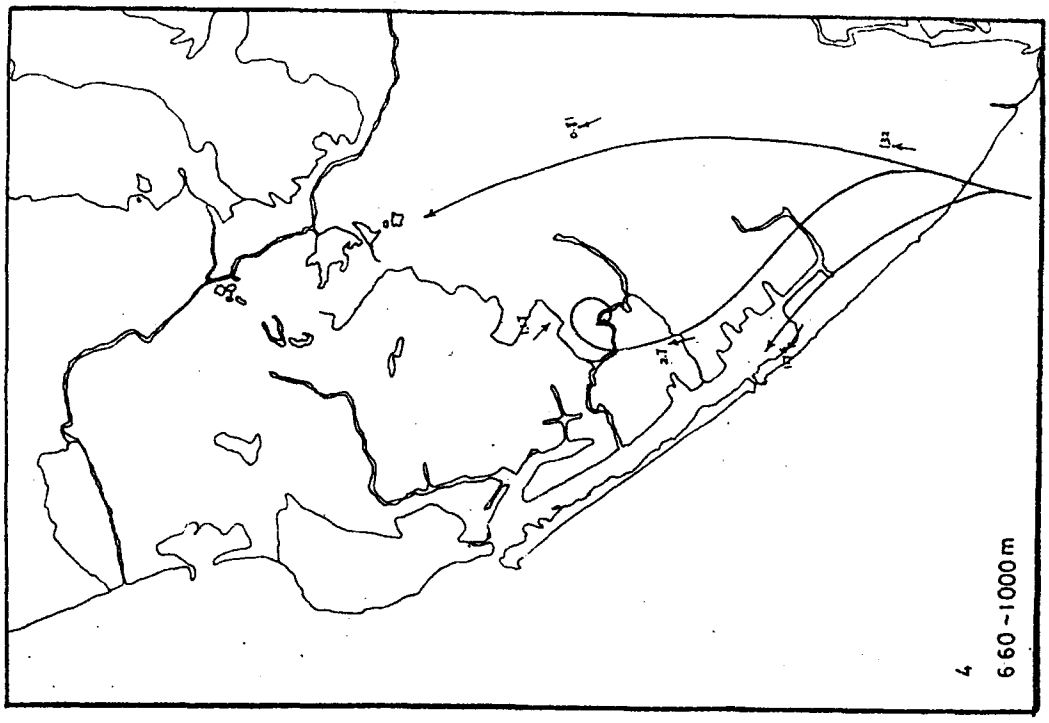
4
660-1000m

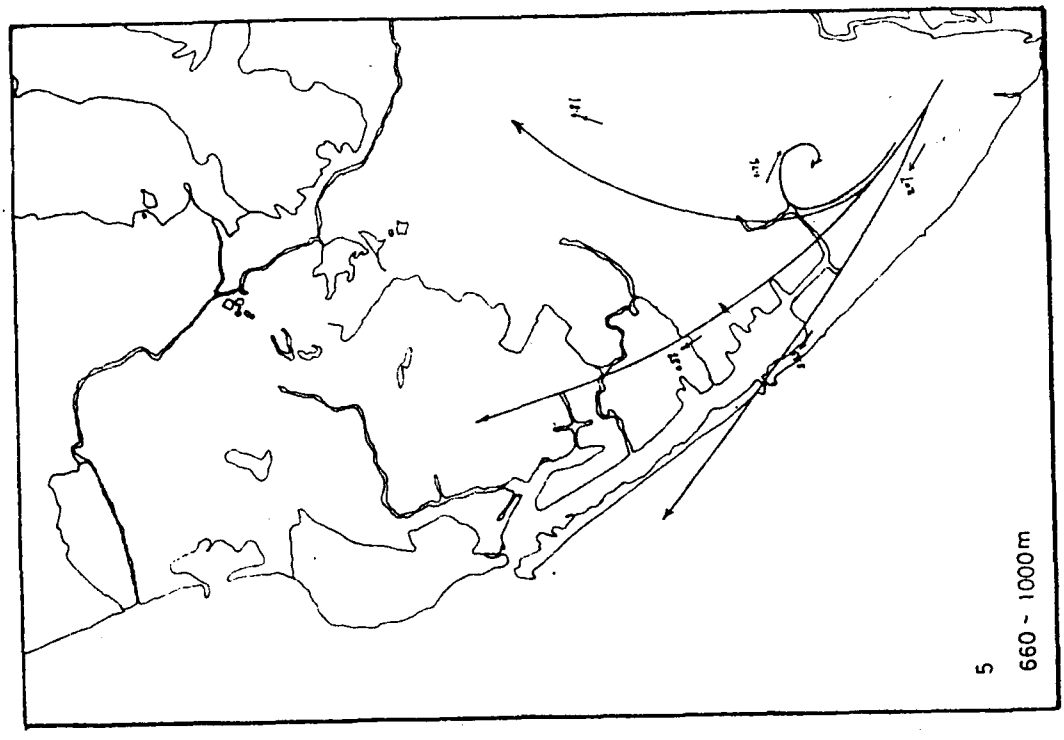
5
660 - 1000m

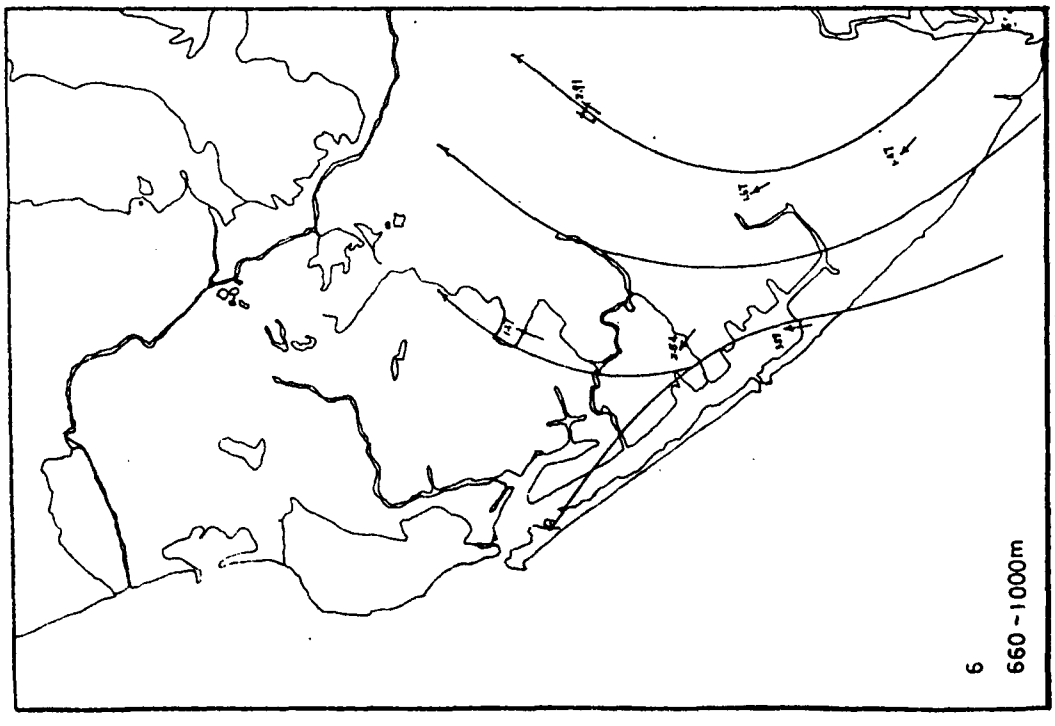
6
660 - 1000m

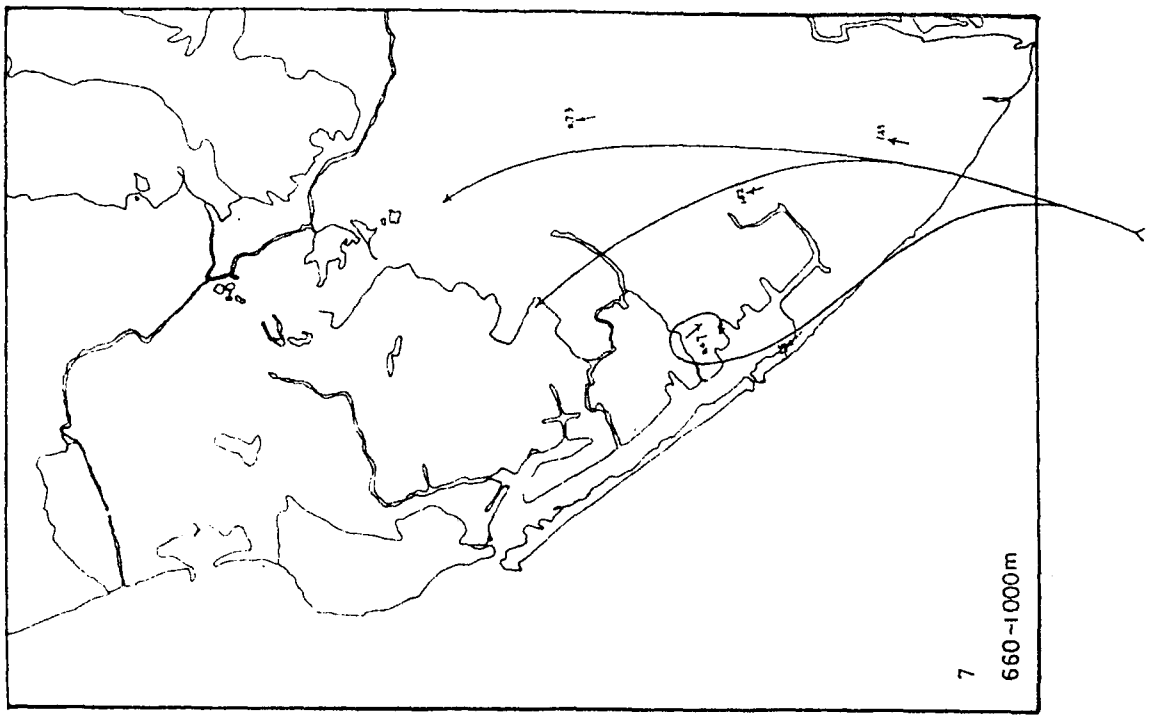
7
660-1000m

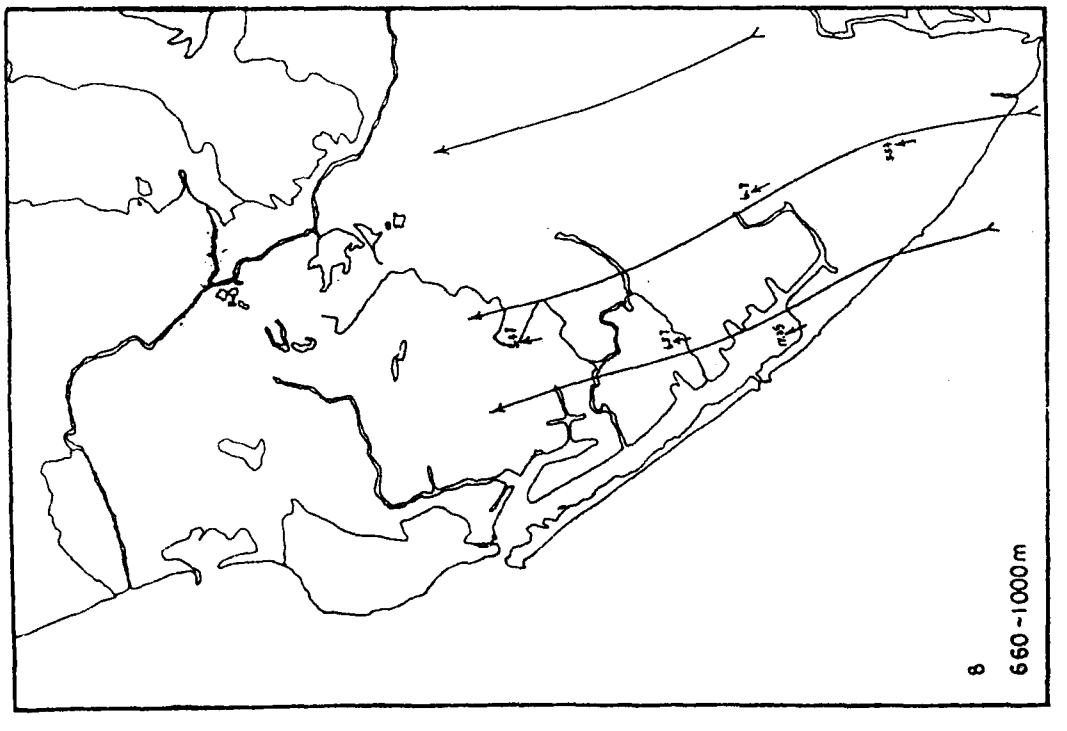
8
660-1000m

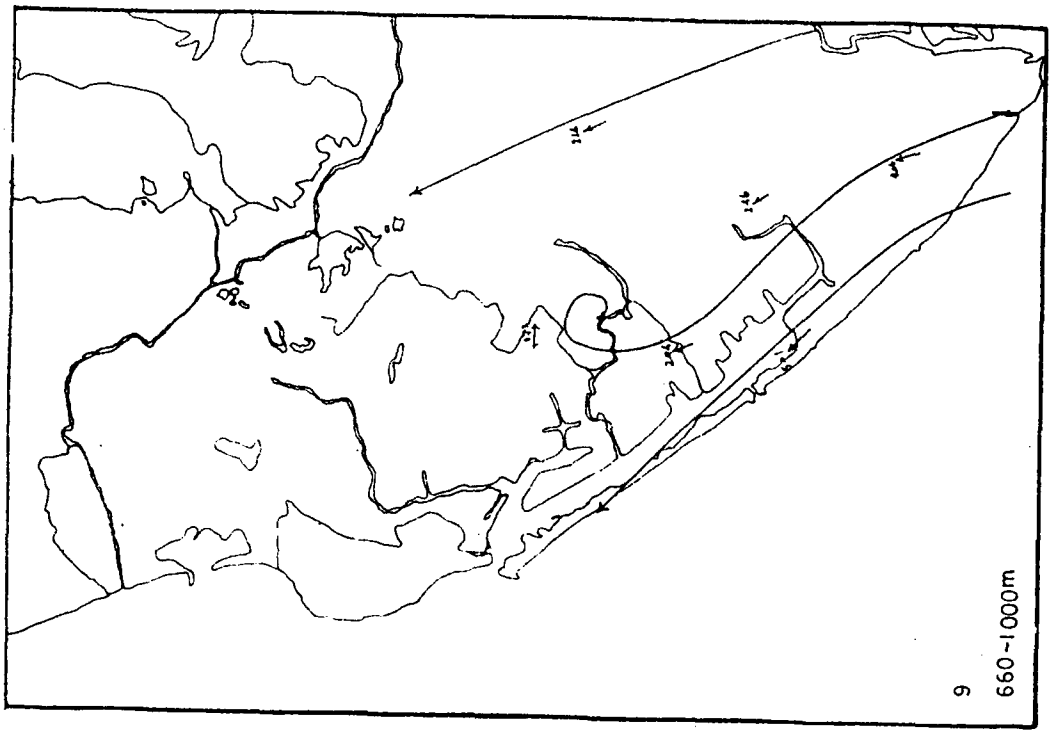
9
660-1000m

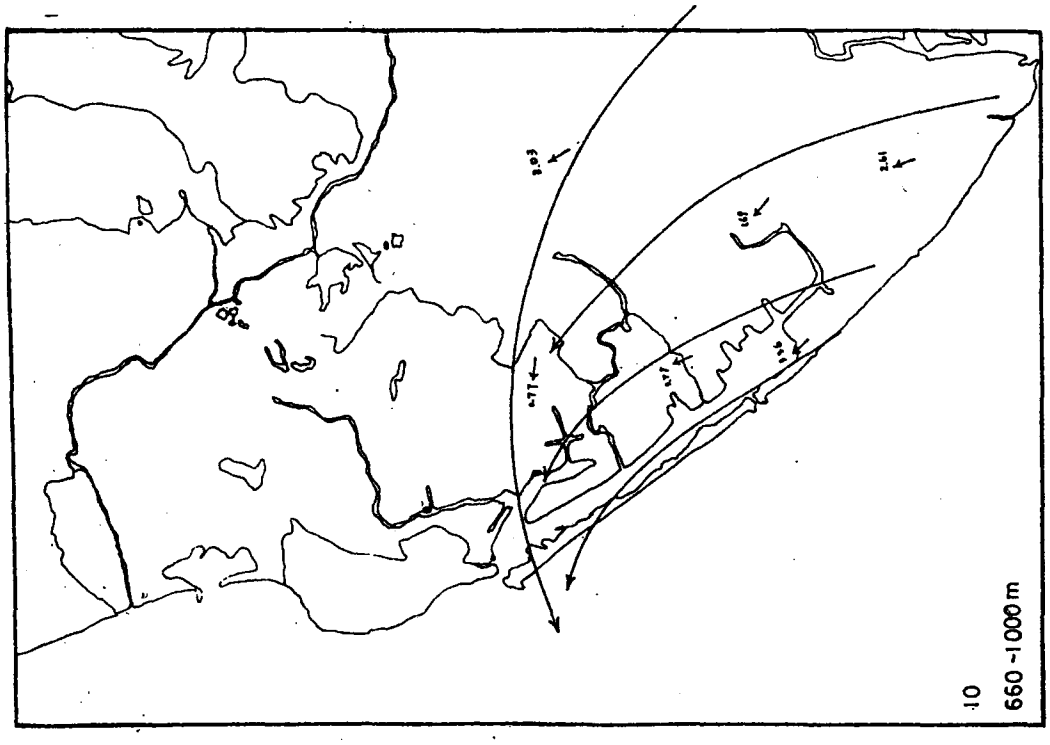
10
660-1000m

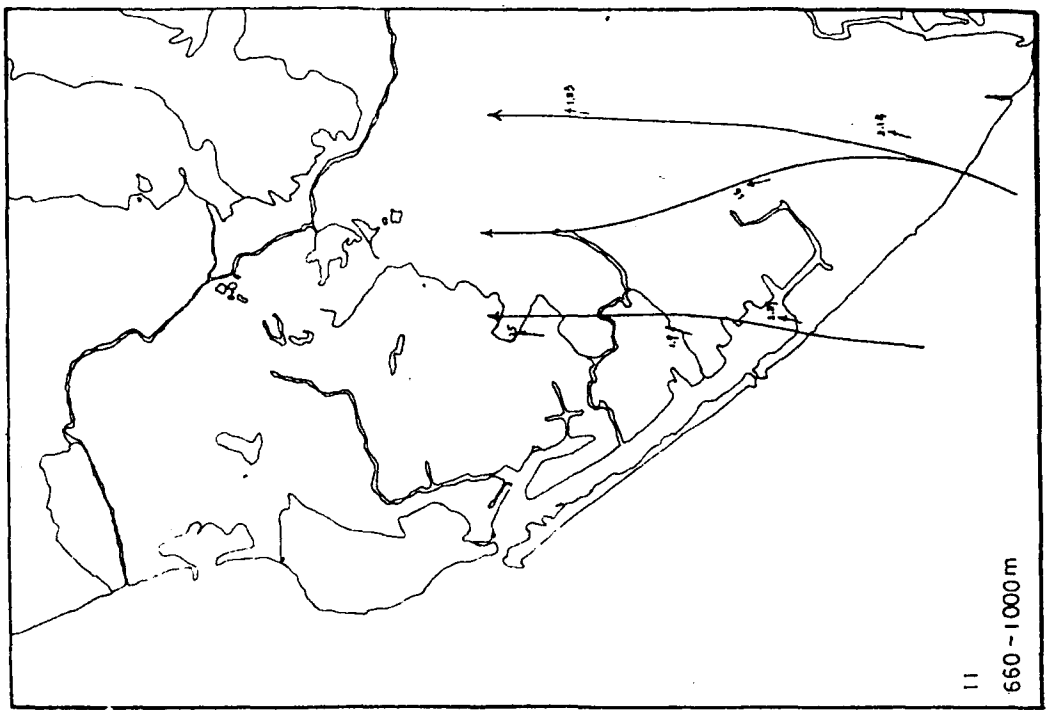
11
660-1000m

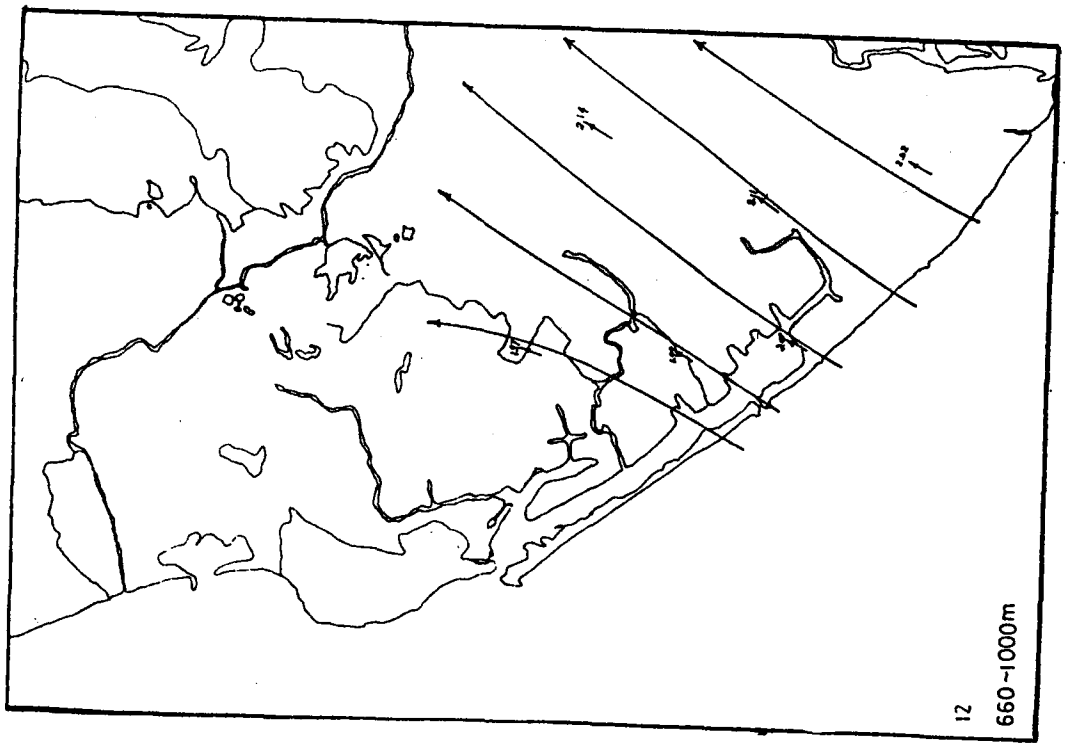
12
660-1000m

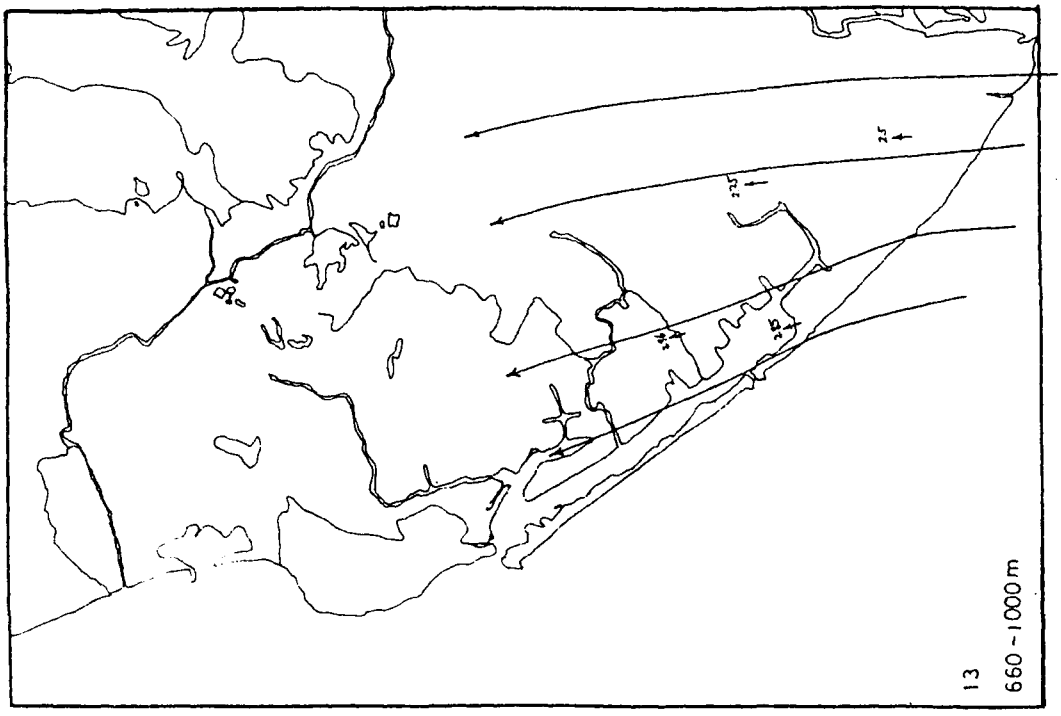
13
660-1000m


14
660-1000m

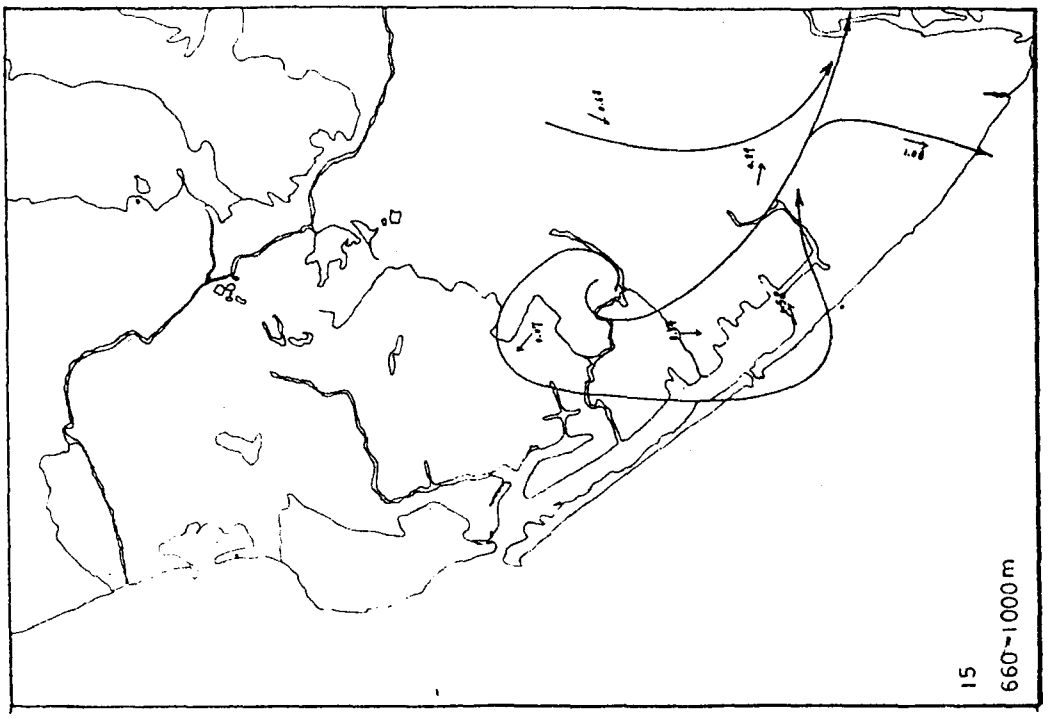
15
660~1000m

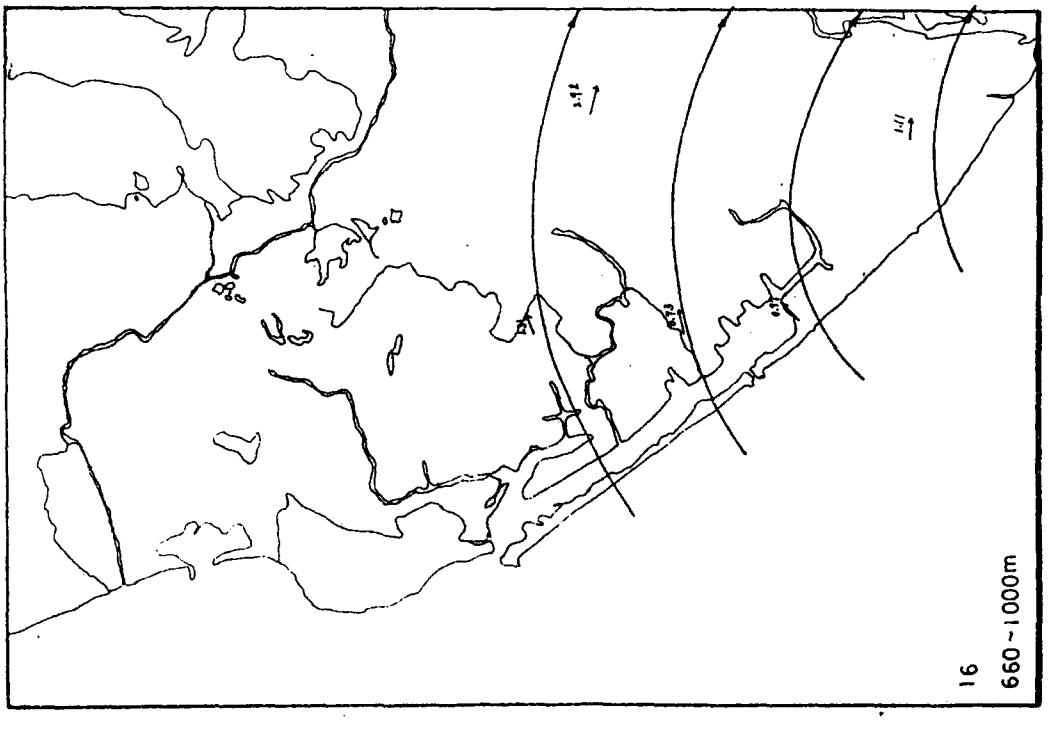
16
660~1000m

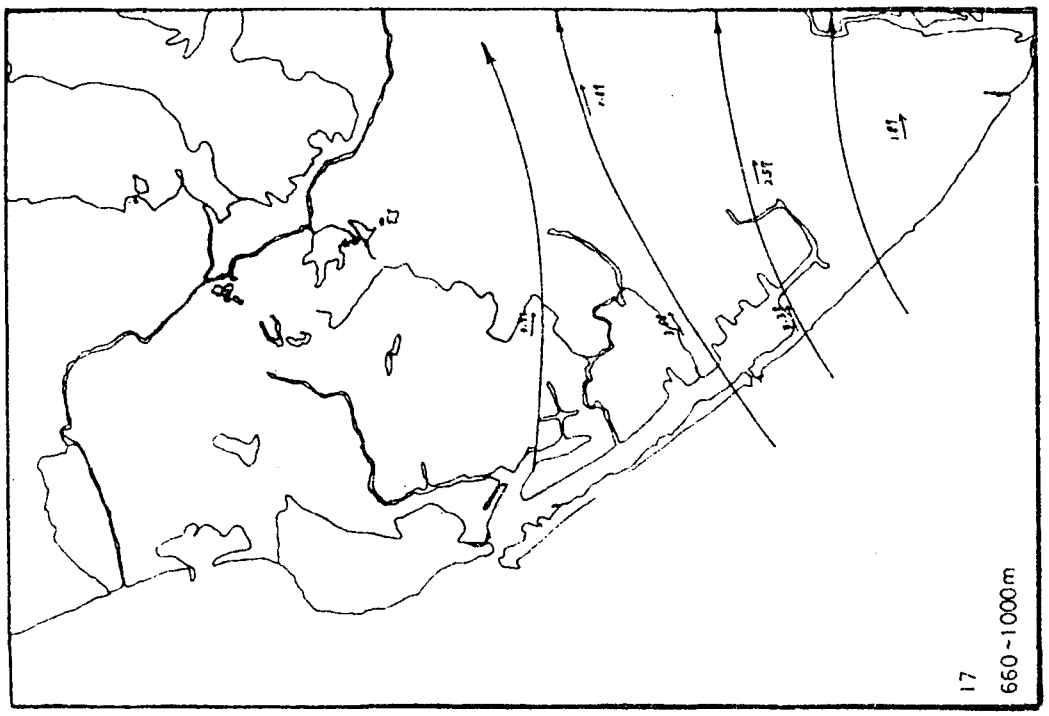
17
660-1000m

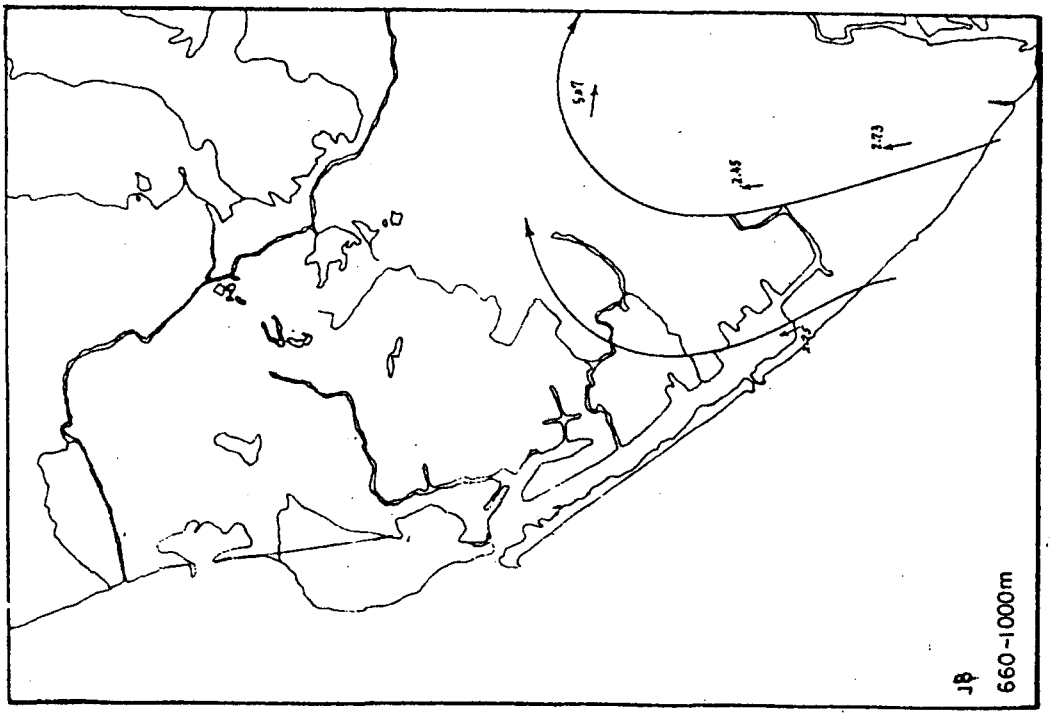
JB
660-1000m

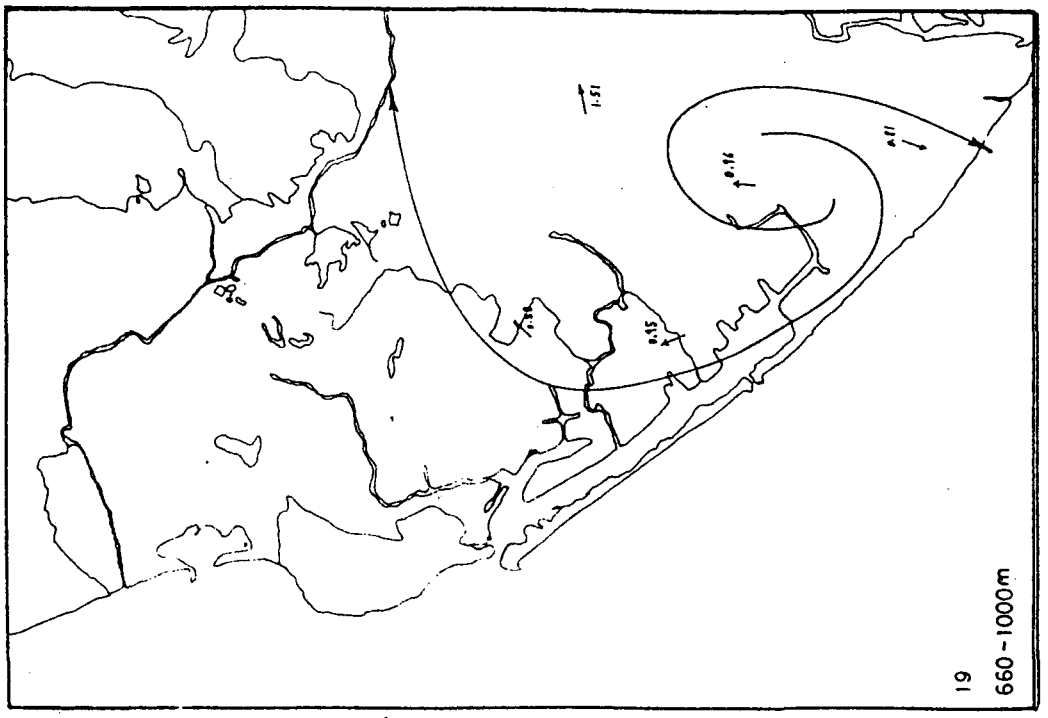
19
660-1000m

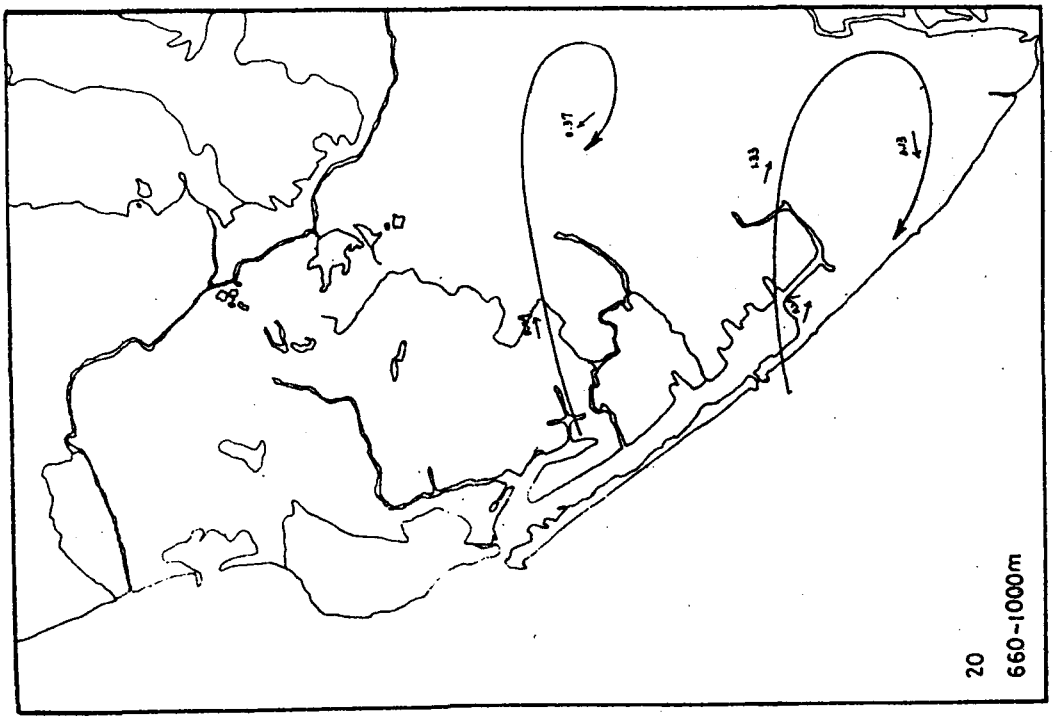
20
660-1000m

21
660-1000m

22
660-1000m

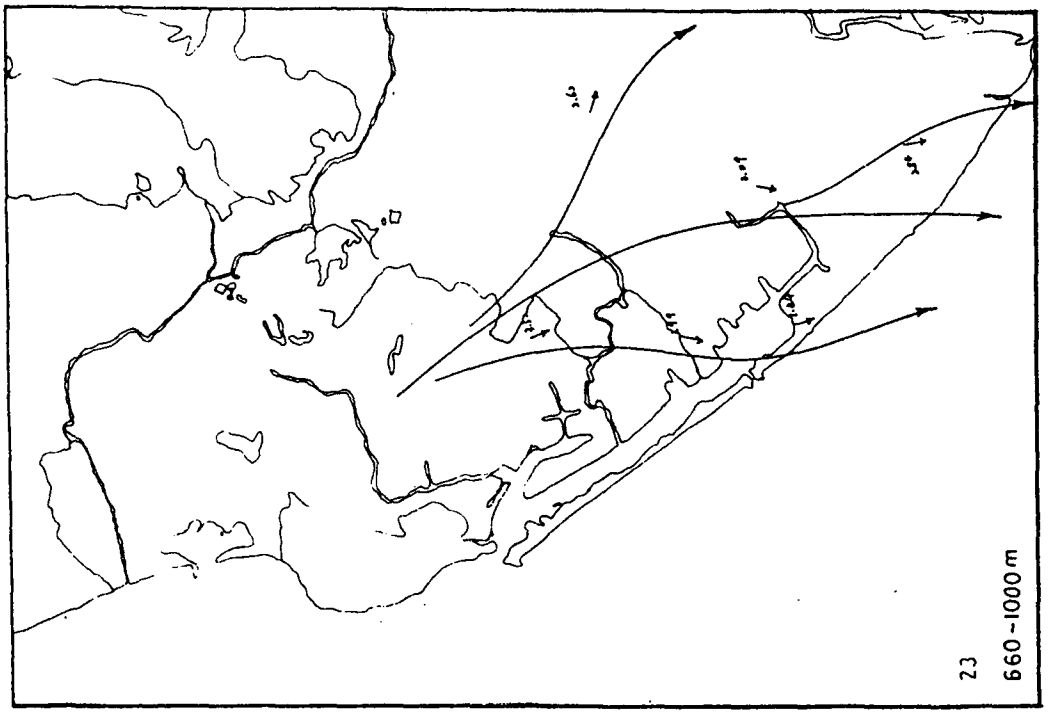
23
660-1000 m

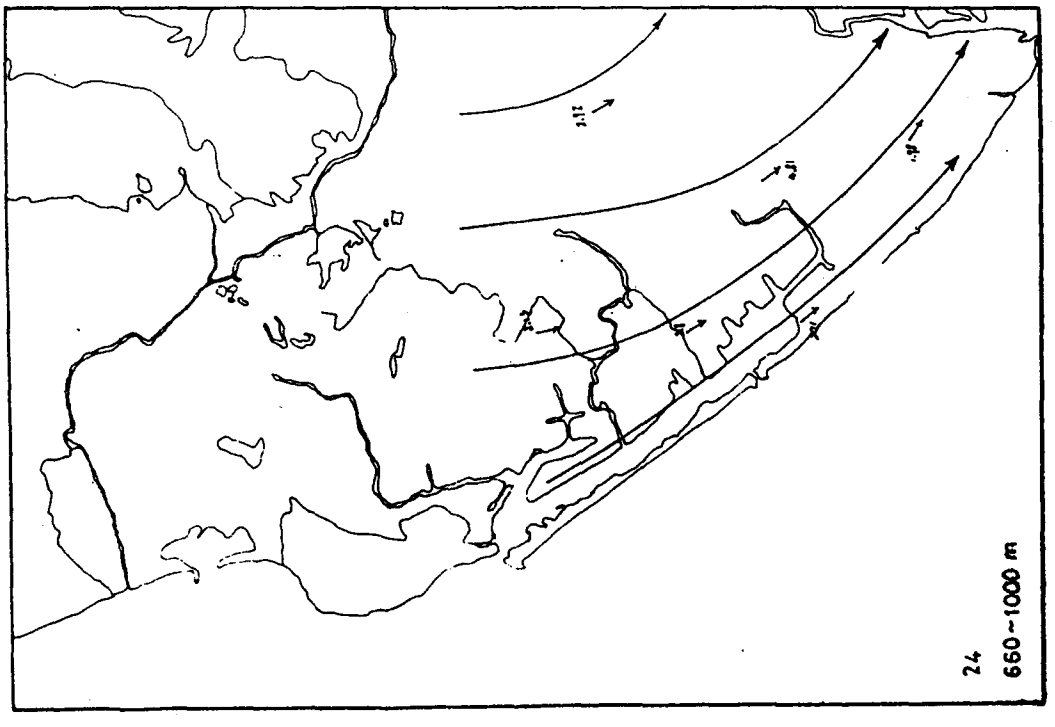
24
660-1000 m

APPENDIX D Temperature profile (Sept. 8 - Sept. 13)

(1) Sept. 8, 1981

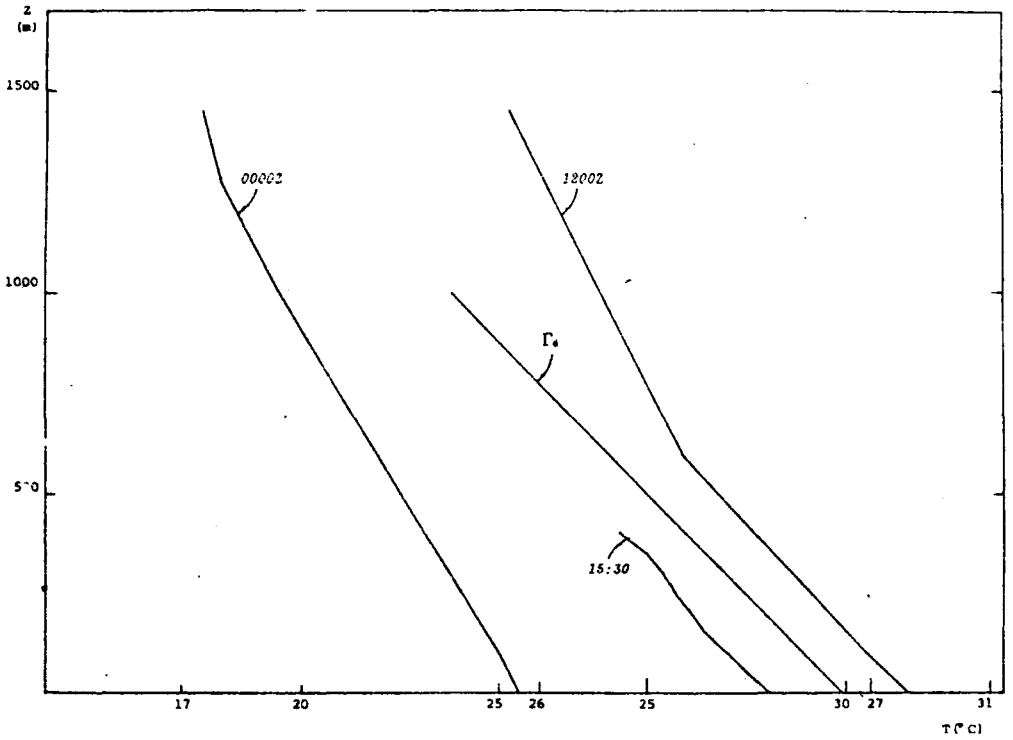

(2) Sept. 9, 1981

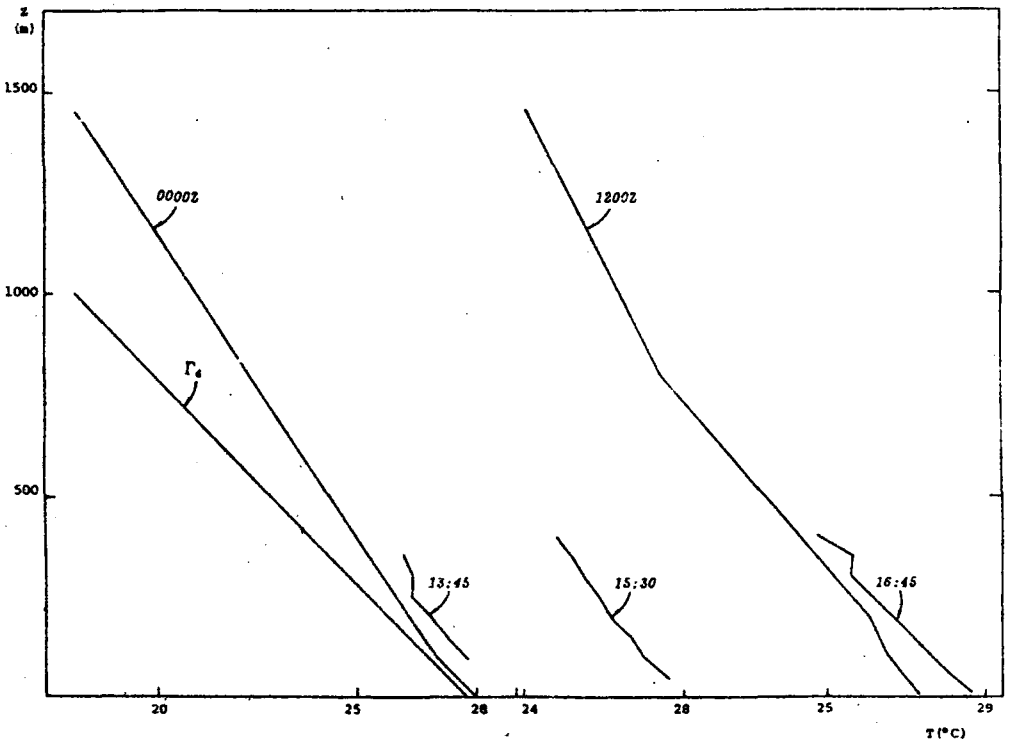

(3) Sept. 10, 1981

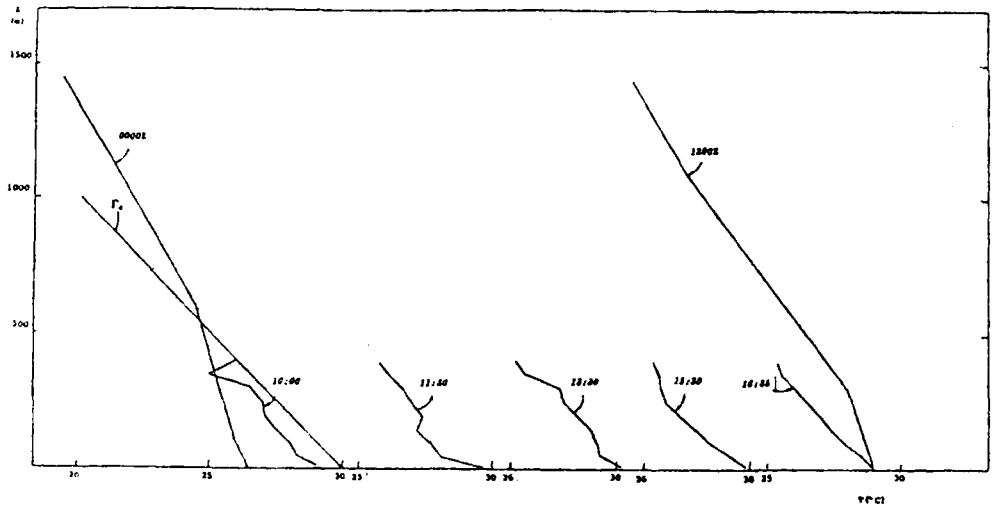

(4) Sept. 11, 1981

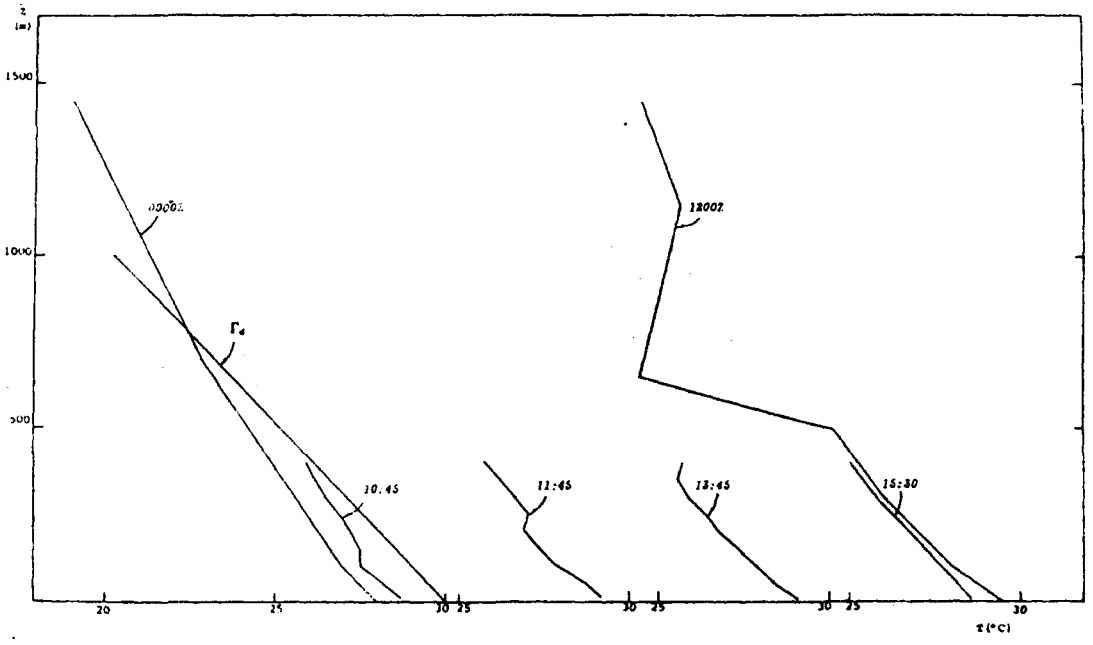

(5) Sept. 12, 1981

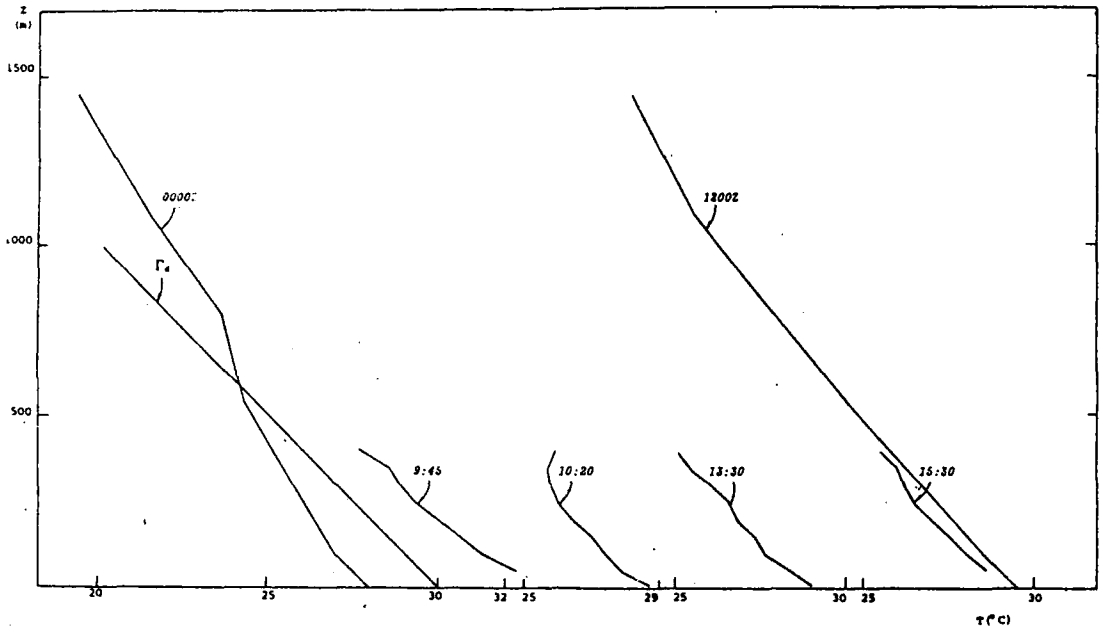

(6) Sept. 13, 1981

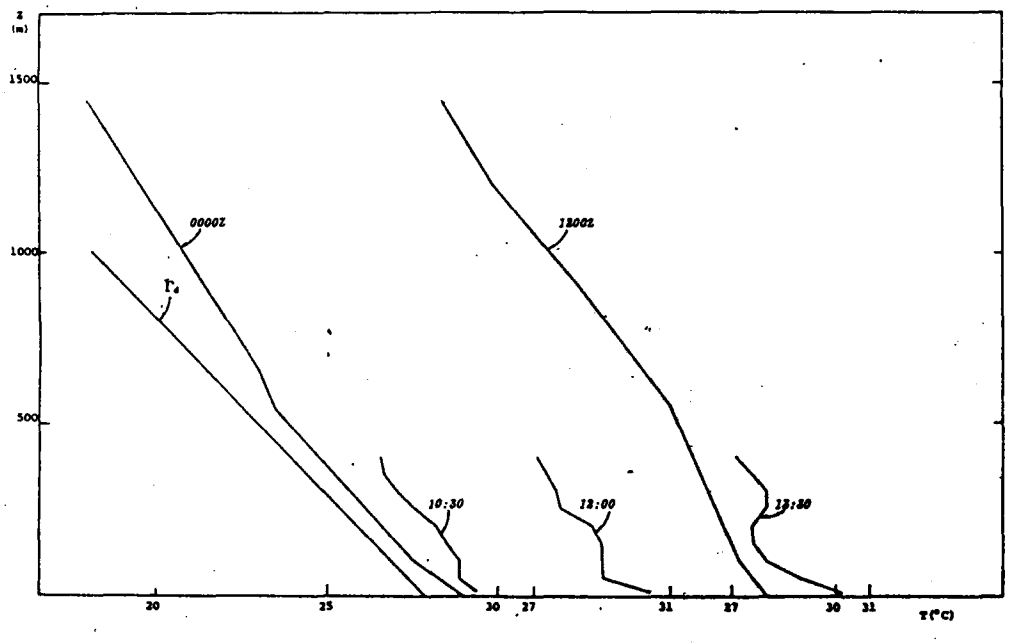

APPENDIX E (1 - 24) : The SF_6 tracer concentration got from experiment in PPt (ND - Non detected, * - without sampling)

1

	1	2	3	4	5	6	7	8	9	10	11	12	13	14	15	16	17	18	19	20	21
A	*	*	*	*	*	*	ND	ND	ND	ND	ND	ND	*	*	*	24	ND	ND	ND	ND	ND
B	*	ND	ND	ND	ND	ND	ND	*	*	*	*	ND	*	ND	*	56	ND	ND	ND	ND	*
C	*	ND	ND	*	ND	ND	ND	ND	ND	ND	7.6	8.5	*	8.5	*	*	ND	ND	ND	ND	ND
D	ND	ND	ND	ND	ND	ND	*	ND	ND	3.4	*	7.5	*	**	*	ND	ND	ND	ND	ND	ND

2

	1	2	3	4	5	6	7	8	9	10	11	12	13	14	15	16	17	18	19	20	21
A	*	*	*	*	*	*	ND	ND	ND	ND	*	ND	*	*	*	ND	ND	ND	ND	ND	ND
B	*	ND	ND	ND	ND	ND	ND	2	6	3	24	48	*	*	*	25	1	ND	ND	ND	ND
C	*	ND	ND	0.6	0.6	0.6	1.8	16	12	11	28	44	*	*	*	*	0.6	ND	1.3	ND	ND
D	ND	0.6	ND	ND	*	0.6	4.1	1.8	1.8	1.3	*	1.3	*	*	*	ND	ND	ND	ND	ND	*

3

	1	2	3	4	5	6	7	8	9	10	11	12	13	14	15	16	17	18	19	20	21
A	*	*	*	*	*	*	ND	ND	ND	ND	*	ND	*	*	*	ND	ND	ND	ND	ND	ND
B	*	ND	ND	ND	ND	ND	ND	ND	ND	ND	5.3	12	*	*	*	19	ND	ND	ND	ND	ND
C	ND	ND	ND	ND	ND	ND	ND	4.1	5.9	5.9	5.3	4.4	*	*	*	*	ND	ND	ND	ND	ND
D	0.6	ND	ND	2.9	5.2	0.6	13	1.2	0.6	ND	*	ND	*	*	*	ND	ND	ND	ND	ND	ND

4

	1	2	3	4	5	6	7	8	9	10	11	12	13	14	15	16	17	18	19	20	21
A	*	*	*	*	*	*	*	ND	ND	ND	*	ND	*	*	*	2.9	4.1	3.5	1.8	ND	ND
B	*	ND	ND	ND	ND	ND	ND	ND	ND	ND	ND	ND	*	*	*	12	14	12	8.2	6.5	6.2
C	*	ND	ND	ND	ND	ND	ND	ND	ND	2.9	4.1	11	*	*	*	*	78	96	24	4.1	20
D	ND	ND	ND	ND	*	ND	ND	ND	ND	ND	*	ND	*	*	*	3.7	2.9	7.1	6.6	4.1	*

5

	1	2	3	4	5	6	7	8	9	10	11	12	13	14	15	16	17	18	19	20	21
A	*	*	*	*	*	*	ND	ND	ND	63	*	98	*	*	*	ND	ND	ND	ND	ND	ND
B	*	ND	ND	ND	ND	ND	27	32	ND	4.1	20	ND	*	*	*	2.9	7.4	5.6	2.7	4.1	4.4
C	*	1.5	1.5	ND	1.1	ND	ND	7.1	11	6.6	35	11	*	*	*	*	1.1	1.1	0.8	ND	8.4
D	ND	ND	ND	ND	ND	ND	1.1	0.6	2.9	4.3	*	11	*	**	*	8	2.9	3.6	4.3	4.1	*

6

	1	2	3	4	5	6	7	8	9	10	11	12	13	14	15	16	17	18	19	20	21
A	*	*	*	*	*	*	ND	ND	ND	ND	*	ND	*	**	*	ND	ND	ND	ND	ND	ND
B	*	ND	ND	ND	ND	ND	2.9	9.7	ND	ND	ND	ND	*	*	*	4.1	ND	4.7	5.0	2.1	4.7
C	*	ND	ND	ND	ND	ND	ND	ND	1.1	1.8	2.3	1.3	*	4	*	*	ND	3.0	ND	ND	7.5
D	ND	ND	ND	ND	ND	ND	ND	ND	ND	ND	*	ND	*	*	*	3.4	2.1	2.5	2.9	2.9	*

7

	1	2	3	4	5	6	7	8	9	10	11	12	13	14	15	16	17	18	19	20	21
A	*	*	*	*	*	*	3.5	7.9	11	14	*	7.9	*	*	*	14	11	2.1	27	9.4	ND
B	*	ND	7.6	3.2	ND	ND	ND	ND	ND	2.4	ND	ND	*	*	*	6.2	4.4	3.5	3.2	2.4	5.3
C	*	1.8	ND	ND	14	0.6	ND	ND	ND	ND	ND	1.8	*	*	*	*	ND	5.2	6.7	23	13
D	1.3	1.8	ND	2.9	1.1	13	ND	ND	1.8	ND	**	1.3	*	*	*	5.8	3.6	4.3	2	7.1	*

8

	1	2	3	4	5	6	7	8	9	10	11	12	13	14	15	16	17	18	19	20	21
A	*	*	*	*	*	*	2.7	ND	ND	ND	*	ND	*	*	*	11	14	9.7	19	24	35
B	*	7.4	8.9	4.4	2.9	2.9	ND	10	ND	ND	ND	ND	*	*	*	15	ND	1.5	5.3	2.7	4.1
C	*	11	27	7.5	5.7	7.5	1.8	1.8	ND	ND	6.4	11	*	*	*	*	8.7	*	7.5	52	19
D	11	35	81	48	19	12	2.9	5.2	30	15	*	11	*	*	*	9.8	9.1	8	9.8	13	*

9

	1	2	3	4	5	6	7	8	9	10	11	12	13	14	15	16	17	18	19	20	21
A	*	*	*	*	*	*	280	320	210	4.4	*	ND	*	*	*	ND	ND	ND	ND	ND	ND
B	*	ND	ND	7.4	60	69	140	61	2.7	ND	ND	ND	*	*	*	6.8	ND	2.9	2.9	5.9	ND
C	*	ND	7.5	76	36	111	64	9.1	ND	4	4.5	6.9	*	*	*	*	7.5	6.1	2.2	4	7.5
D	6.6	5.4	20	27	13	21	24	25	26	22	*	9.2	*	*	*	12.2	12.2	7.6	7.5	6.2	*

10

	1	2	3	4	5	6	7	8	9	10	11	12	13	14	15	16	17	18	19	20	21
A	*	*	*	*	*	*	ND	7.1	24	65	*	ND	*	*	*	ND	ND	ND	ND	ND	ND
B	*	ND	5.9	ND	ND	5	5.9	18	15	75	ND	ND	*	*	*	5.9	ND	ND	2.9	ND	ND
C	*	3.1	ND	0.6	3.1	5.7	49	204	172	37	3.6	4	*	*	*	*	8.4	11	7.1	3.5	16
D	5.7	2.2	5.7	3.1	3.6	44	36	73	63	7.1	*	13	*	*	*	4	2.6	11	5.7	8.4	*

11

	1	2	3	4	5	6	7	8	9	10	11	12	13	14	15	16	17	18	19	20	21
A	*	*	*	*	*	*	ND	ND	ND	ND	*	ND	*	*	*	ND	ND	ND	ND	ND	ND
B	*	ND	ND	ND	ND	ND	ND	2.4	ND	35	120	ND	*	*	*	2.9	2.9	7.6	5	2.9	6.8
C	*	ND	ND	ND	ND	ND	0.8	15	106	154	1.3	2.2	*	*	*	*	11	10	4.5	8.2	7.2
D	*	ND	0.6	4	1.2	0.6	0.6	4.3	50	72	**	0.8	*	*	*	7.5	8.4	6.1	ND	7.9	*

12

	1	2	3	4	5	6	7	8	9	10	11	12	13	14	15	16	17	18	19	20	21
A	*	*	*	*	*	*	2	ND	ND	120	*	ND	*	*	*	ND	2.6	3	ND	ND	ND
B	*	ND	ND	ND	7.6	3.8	ND	3.8	ND	3.8	3.8	3.2	*	*	*	ND	ND	13	14	ND	6.5
C	*	ND	7.5	ND	ND	0.6	0.6	8.4	12.4	21	0.6	1.3	*	*	*	*	7.5	10	ND	3.3	3.6
D	4.7	ND	0.6	2.2	2.2	0.6	1.3	11	7.5	4	*	5.7	*	*	*	3.3	9.8	7.7	6.8	7.7	*

13

	1	2	3	4	5	6	7	8	9	10	11	12	13	14	15	16	17	18	19	20	21
A	*	*	*	*	*	*	21.5	ND	ND	ND	*	ND	*	*	*	ND	ND	ND	ND	ND	ND
B	*	*	ND	ND	35.3	51.9	171.5	120.6	ND	ND	*	ND	*	3.5	*	ND	ND	ND	ND	ND	ND
C	*	ND	1.9	99	159	69	46	51	41	7.5	0.6	0.6	*	ND	*	*	ND	ND	ND	ND	*
D	*	ND	ND	ND	ND	1.3	ND	ND	ND	1.3	*	0.6	*	ND	*	ND	ND	ND	ND	ND	*

14

	1	2	3	4	5	6	7	8	9	10	11	12	13	14	15	16	17	18	19	20	21
A	*	*	*	*	*	*	ND	ND	ND	ND	*	ND	*	*	*	ND	ND	ND	ND	ND	ND
B	*	*	ND	ND	ND	ND	ND	ND	ND	ND	ND	ND	*	ND	*	ND	ND	ND	ND	ND	ND
C	*	ND	ND	1.3	4.5	1.3	6.6	42	32	5.7	0.6	0.6	*	0.6	*	*	ND	ND	ND	*	
D	*	ND	ND	0.6	2.2	8.4	7.1	7.5	4.3	2.2	*	1.3	*	ND	*	0.6	ND	ND	ND	ND	

15

	1	2	3	4	5	6	7	8	9	10	11	12	13	14	15	16	17	18	19	20	21
A	*	*	*	*	*	*	ND	ND	ND	ND	*	ND	*	*	*	ND	ND	ND	ND	ND	ND
B	*	*	ND	ND	ND	ND	ND	ND	ND	ND	ND	ND	*	ND	*	ND	ND	ND	ND	ND	ND
C	*	ND	ND	ND	ND	ND	ND	ND	ND	ND	ND	ND	*	ND	*	*	ND	ND	ND	*	*
D	*	ND	*	ND	ND	ND	ND	ND	ND	ND	*	ND	*	5.6	*	ND	ND	ND	ND	ND	*

	1	2	3	4	5	6	7	8	9	10	11	12	13	14	15	16	17	18	19	20	21
A	*	*	*	*	*	*	ND	ND	ND	ND	*	ND	*	*	*	ND	ND	ND	ND	ND	ND
B	*	*	ND	ND	ND	ND	ND	ND	ND	ND	ND	ND	*	ND	*	ND	ND	ND	ND	ND	ND
C	*	ND	ND	ND	ND	ND	ND	ND	ND	ND	1.9	6.6	*	*	*	*	ND	ND	ND	ND	*
D	*	ND	ND	ND	ND	ND	ND	ND	ND	ND	*	0.6	*	0.6	*	ND	ND	ND	ND	ND	*

	1	2	3	4	5	6	7	8	9	10	11	12	13	14	15	16	17	18	19	20	21
A	*	*	*	*	*	*	2.2	3	3.8	ND	*	0.6	*	*	*	ND	ND	ND	ND	ND	ND
B	*	*	0.2	ND	ND	ND	ND	ND	ND	0.6	0.6	0.6	*	4.0	*	ND	ND	ND	ND	ND	ND
C	*	ND	ND	ND	ND	ND	ND	ND	ND	11	0.6	1.9	*	ND	*	*	ND	ND	ND	ND	*
D	*	ND	ND	0.8	0.8	ND	ND	ND	ND	0.6	*	1.8	*	0.6	*	ND	ND	ND	ND	ND	*

	1	2	3	4	5	6	7	8	9	10	11	12	13	14	15	16	17	18	19	20	21
A	*	*	*	*	*	*	ND	ND	ND	ND	*	ND	*	*	*	ND	ND	ND	ND	ND	ND
B	*	*	0.6	ND	ND	ND	0.6	7.9	24	26	82	152	*	5.7	*	ND	ND	ND	ND	ND	ND
C	*	0.6	ND	ND	ND	ND	2.2	2.2	3.1	4	63	*	*	2.2	*	*	0.6	0.6	ND	0.8	*
D	*	ND	ND	ND	ND	ND	ND	ND	ND	ND	*	ND	*	ND	*	ND	ND	ND	ND	0.6	*

	1	2	3	4	5	6	7	8	9	10	11	12	13	14	15	16	17	18	19	20	21
A	*	*	*	*	*	*	ND	ND	ND	ND	*	ND	*	*	*	ND	4.1	28	ND	ND	ND
B	*	ND	ND	ND	ND	ND	ND	ND	ND	ND	87	90.2	*	69.7	*	ND	ND	ND	ND	ND	ND
C	*	ND	ND	ND	1.3	0.6	4.0	37.4	43	92.6	85.5	80	*	1.3	*	*	0.6	ND	ND	ND	*
D	*	ND	ND	ND	3.1	9.2	2.9	25	45	42	*	83	*	2.8	*	0.6	0.6	ND	0.6	ND	*

	1	2	3	4	5	6	7	8	9	10	11	12	13	14	15	16	17	18	19	20	21
A	*	*	*	*	*	*	ND	ND	ND	ND	*	ND	*	*	*	ND	ND	ND	ND	ND	ND
B	*	*	ND	ND	ND	ND	ND	ND	ND	ND	ND	ND	*	ND	*	ND	ND	ND	ND	ND	ND
C	*	ND	ND	0.6	ND	0.6	ND	0.6	ND	1.4	2.2	2.9	*	4.3	*	*	0.6	0.6	ND	0.6	*
D	*	ND	ND	0.8	ND	0.8	ND	ND	ND	0.8	*	5.7	*	0.8	*	ND	ND	0.6	ND	ND	*

	1	2	3	4	5	6	7	8	9	10	11	12	13	14	15	16	17	18	19	20	21
A	*	*	*	*	*	*	ND	ND	ND	ND	*	65	*	*	*	ND	ND	ND	ND	ND	ND
B	*	*	ND	ND	ND	ND	ND	ND	ND	4.1	180	41	*	ND	*	ND	ND	ND	ND	ND	ND
C	*	0.8	0.6	ND	0.8	ND	1.4	16	17	67	93	87	*	0.6	*	*	0.6	0.6	ND	ND	*
D	*	ND	ND	ND	ND	ND	ND	ND	ND	ND	*	5.7	*	ND	*	ND	ND	ND	ND	ND	*

	1	2	3	4	5	6	7	8	9	10	11	12	13	14	15	16	17	18	19	20	21
A	*	*	*	*	*	*	ND	ND	ND	ND	*	ND	*	*	*	51	113	ND	ND	ND	ND
B	*	*	ND	ND	ND	ND	ND	ND	ND	ND	ND	ND	*	ND	*	ND	ND	ND	ND	ND	ND
C	*	ND	ND	ND	ND	ND	ND	0.6	ND	ND	ND	ND	*	31.2	*	*	16.3	8.4	ND	1.4	*
D		0.6	ND	ND	ND	ND	ND	ND	ND	ND	*	0.6	*	5.7	*	23	11.5	3.6	0.6	ND	*

	1	2	3	4	5	6	7	8	9	10	11	12	13	14	15	16	17	18	19	20	21
A	*	*	*	*	*	*	ND	ND	ND	ND	ND	ND	*	*	*	ND	ND	ND	ND	ND	ND
B	*	*	ND	ND	ND	ND	ND	ND	ND	ND	ND	ND	*	ND	*	ND	ND	ND	ND	ND	ND
C	*	ND	ND	ND	ND	0.6	ND	0.6	ND	0.6	ND	0.8	*	1.9	*	*	2.8	26.3	1	0.8	*
D	*	ND	ND	10	ND	0.6	0.6	ND	0.6	ND	*	ND	*	7.5	*	58	3.3	1	0.8	ND	*

	1	2	3	4	5	6	7	8	9	10	11	12	13	14	15	16	17	18	19	20	21
A	*	*	*	*	*	*	ND	ND	ND	ND	*	ND	*	*	*	ND	ND	ND	ND	ND	ND
B	*	*	ND	ND	ND	ND	ND	ND	ND	2.5	ND	ND	*	ND	*	ND	ND	ND	4.3	ND	ND
C	*	0.6	ND	ND	ND	ND	ND	ND	ND	ND	ND	ND	*	ND	*	*	ND	ND	5.4	3.1	
D	*	ND	ND	ND	ND	3.1	ND	ND	ND	ND	*	ND	*	ND	*	ND	ND	9.8	ND	ND	*

APPENDIX F (1 - 24) : The isopleth of SF_6 concentration (PPt)

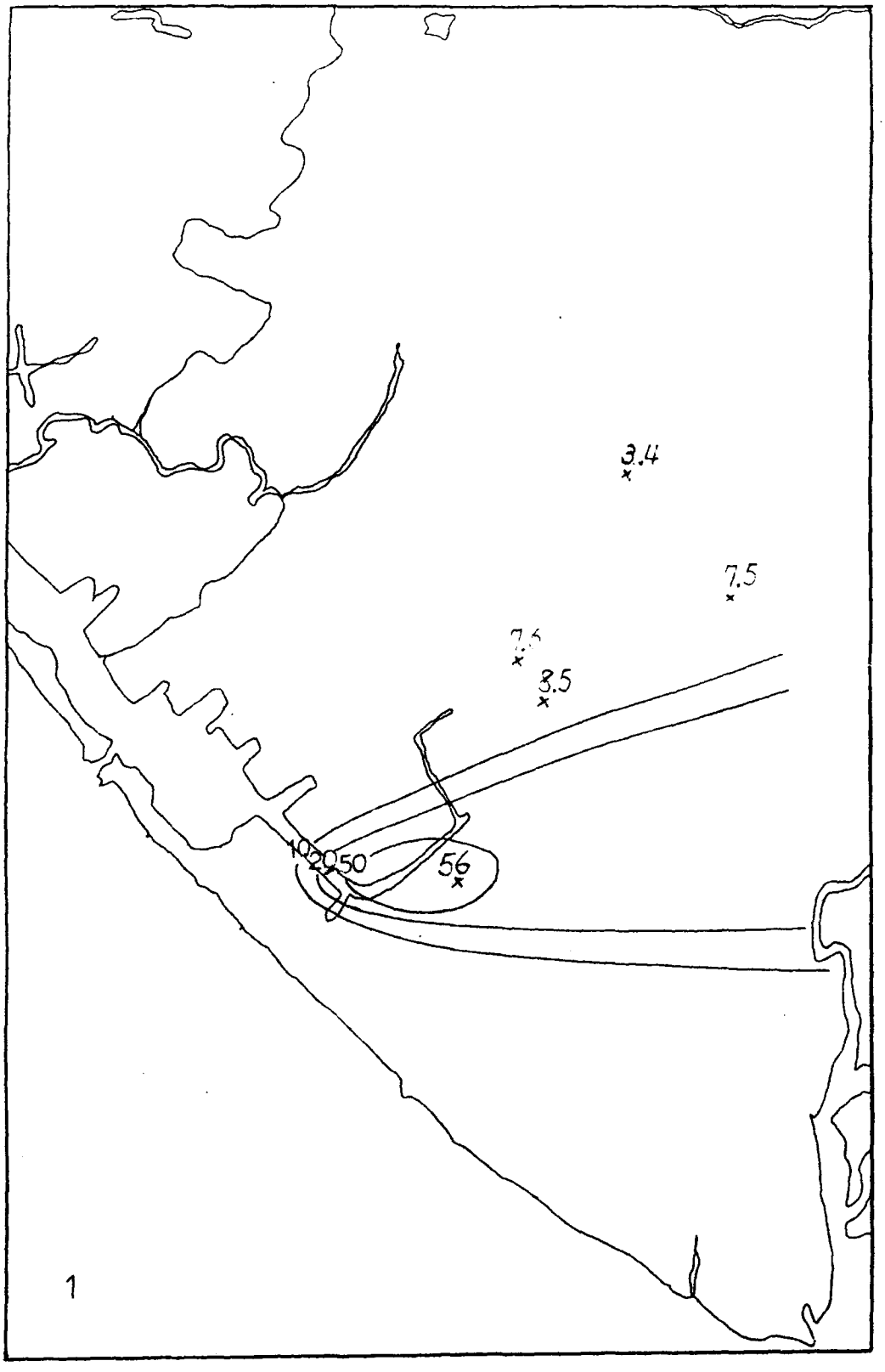

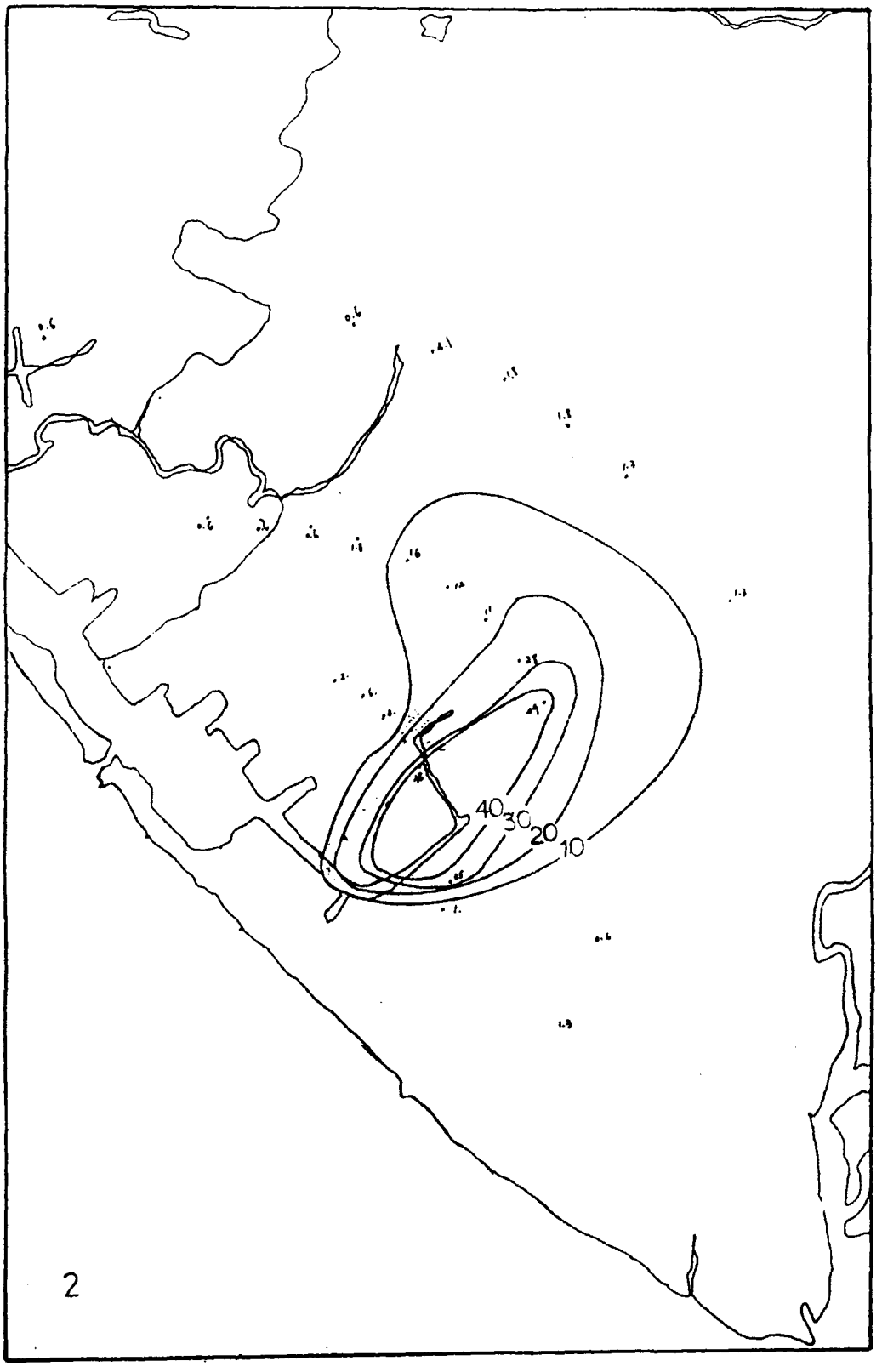
40
30
20
10
2

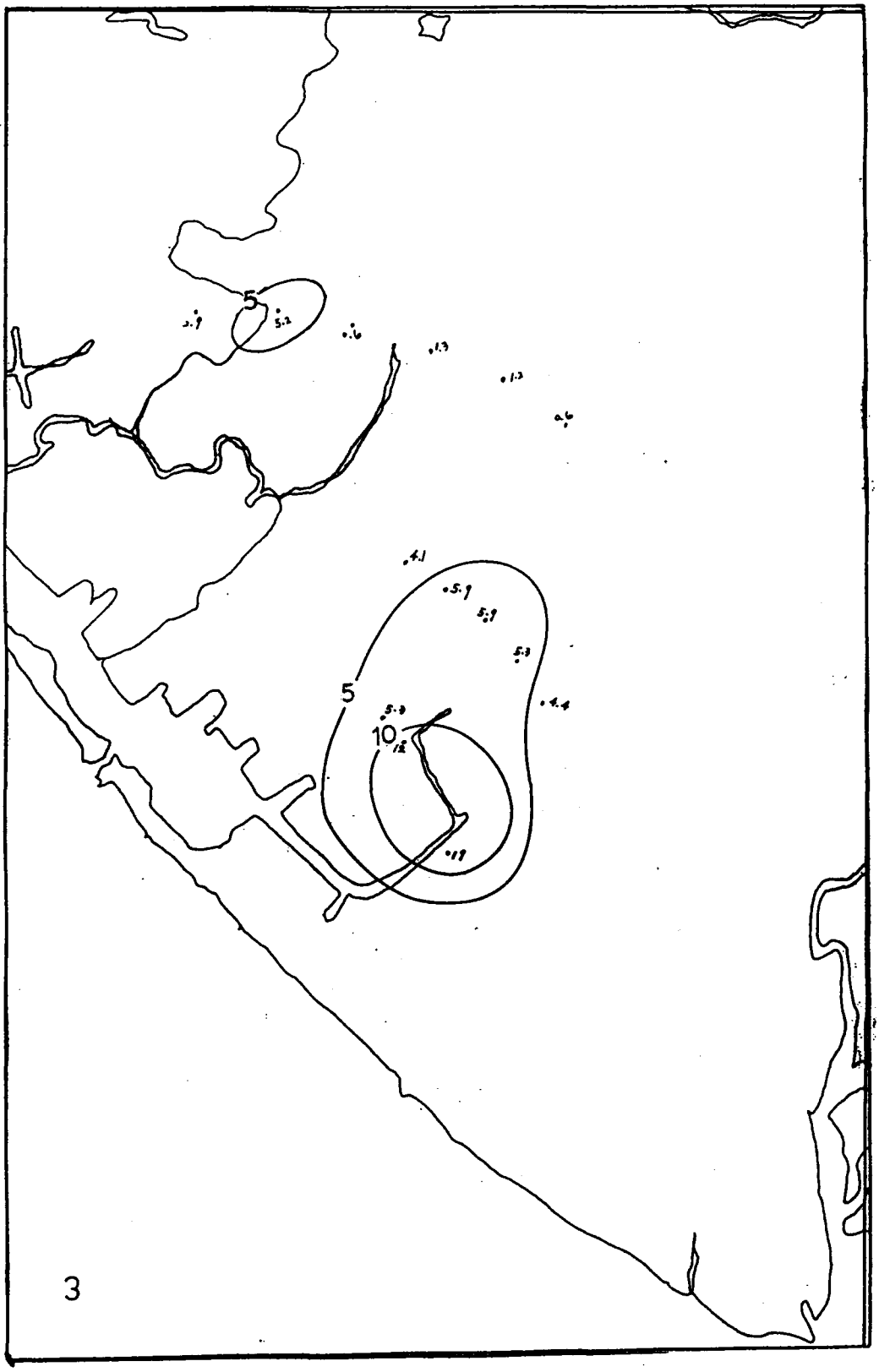
5
5
10
3

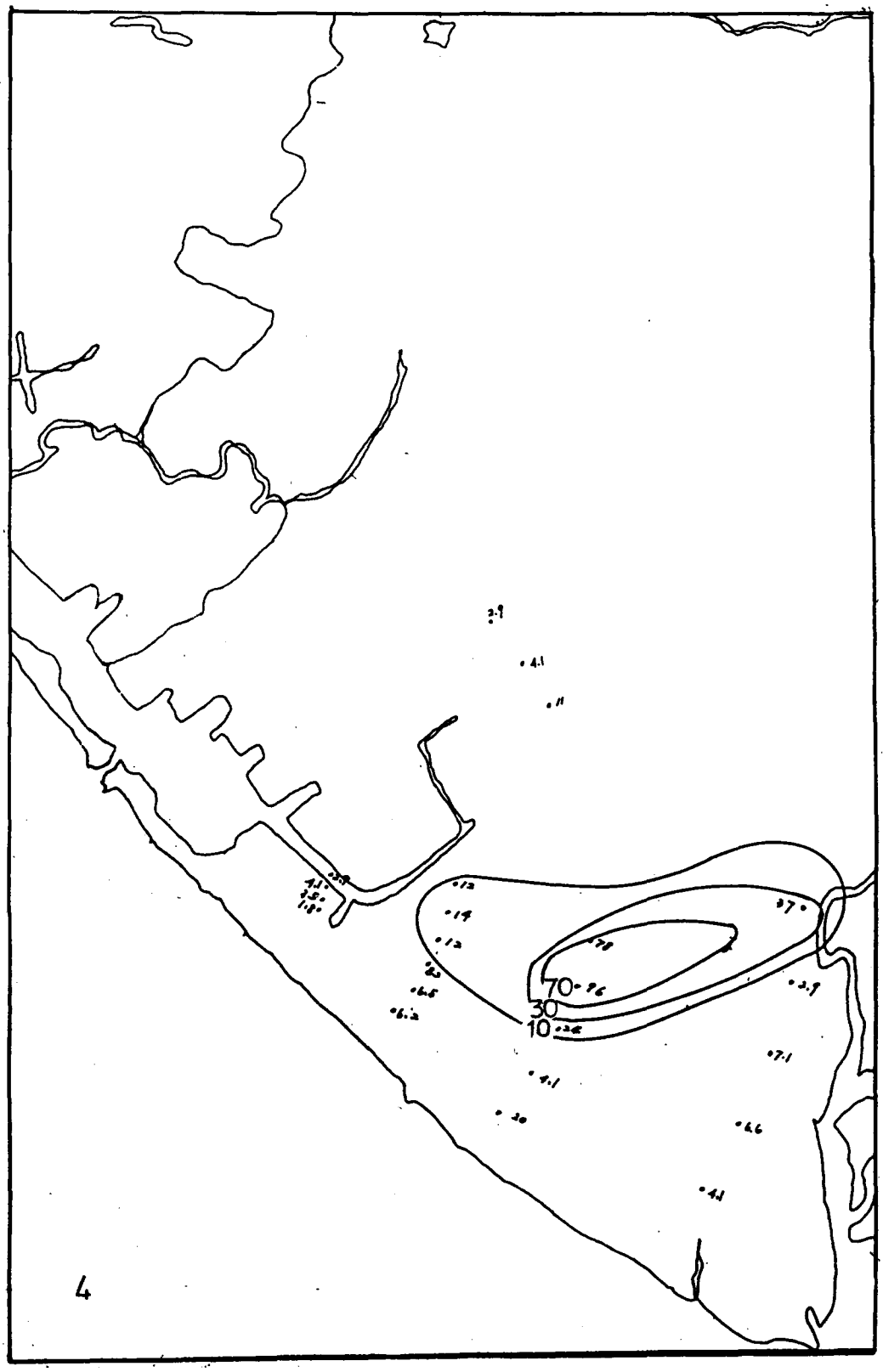
70
30
10
4

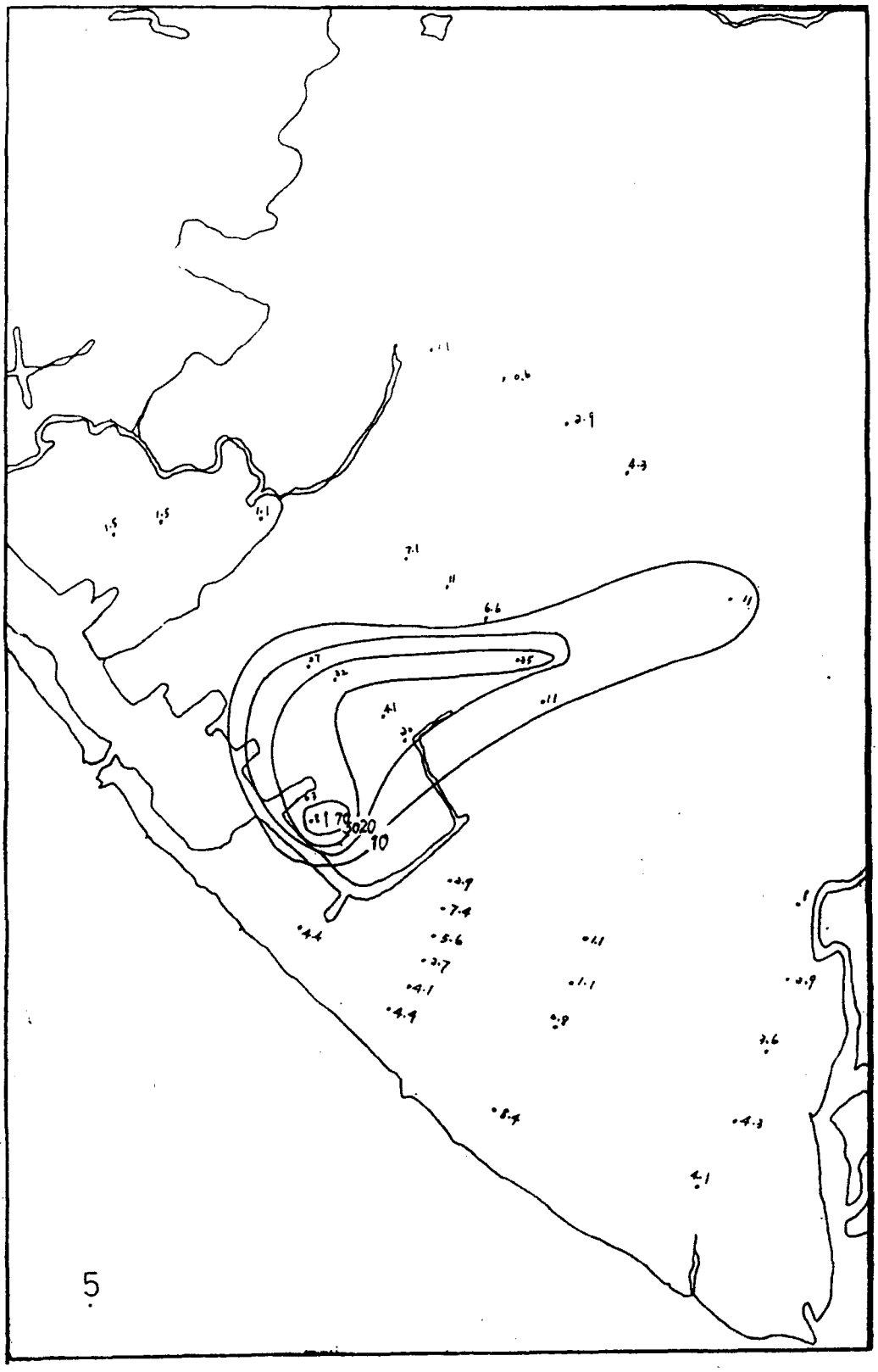
70
30
20
10
5

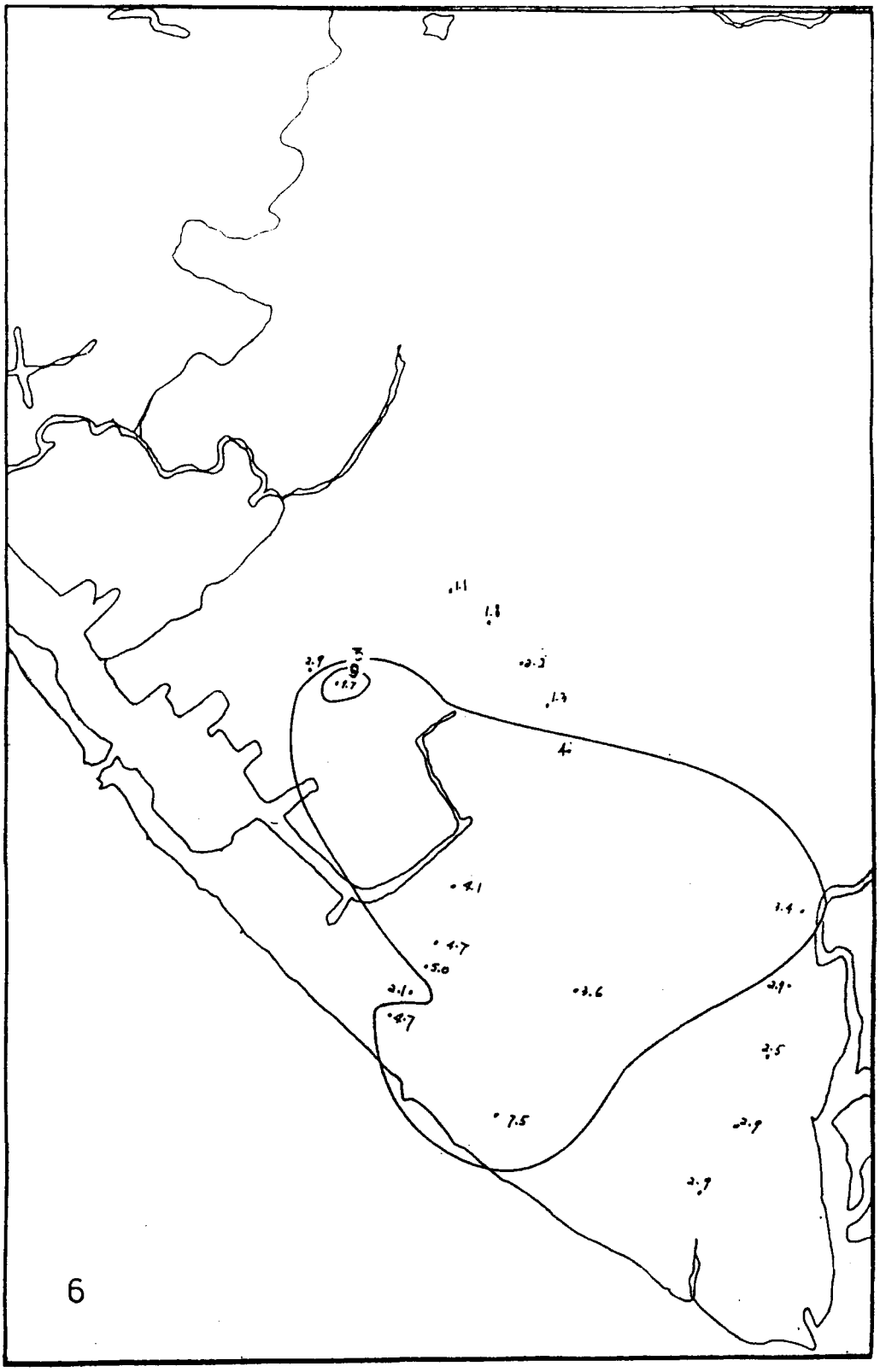
6

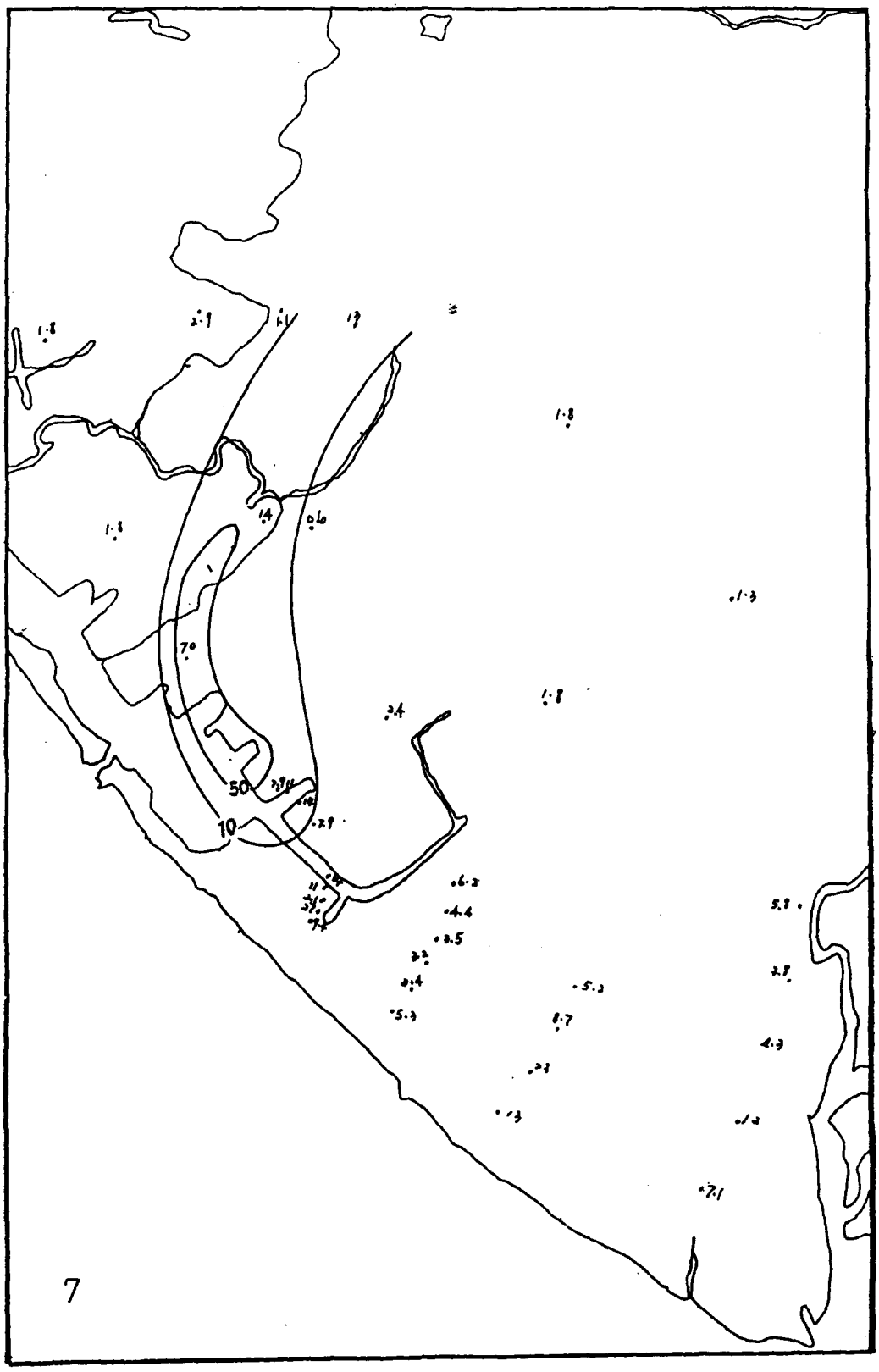
50
10
7

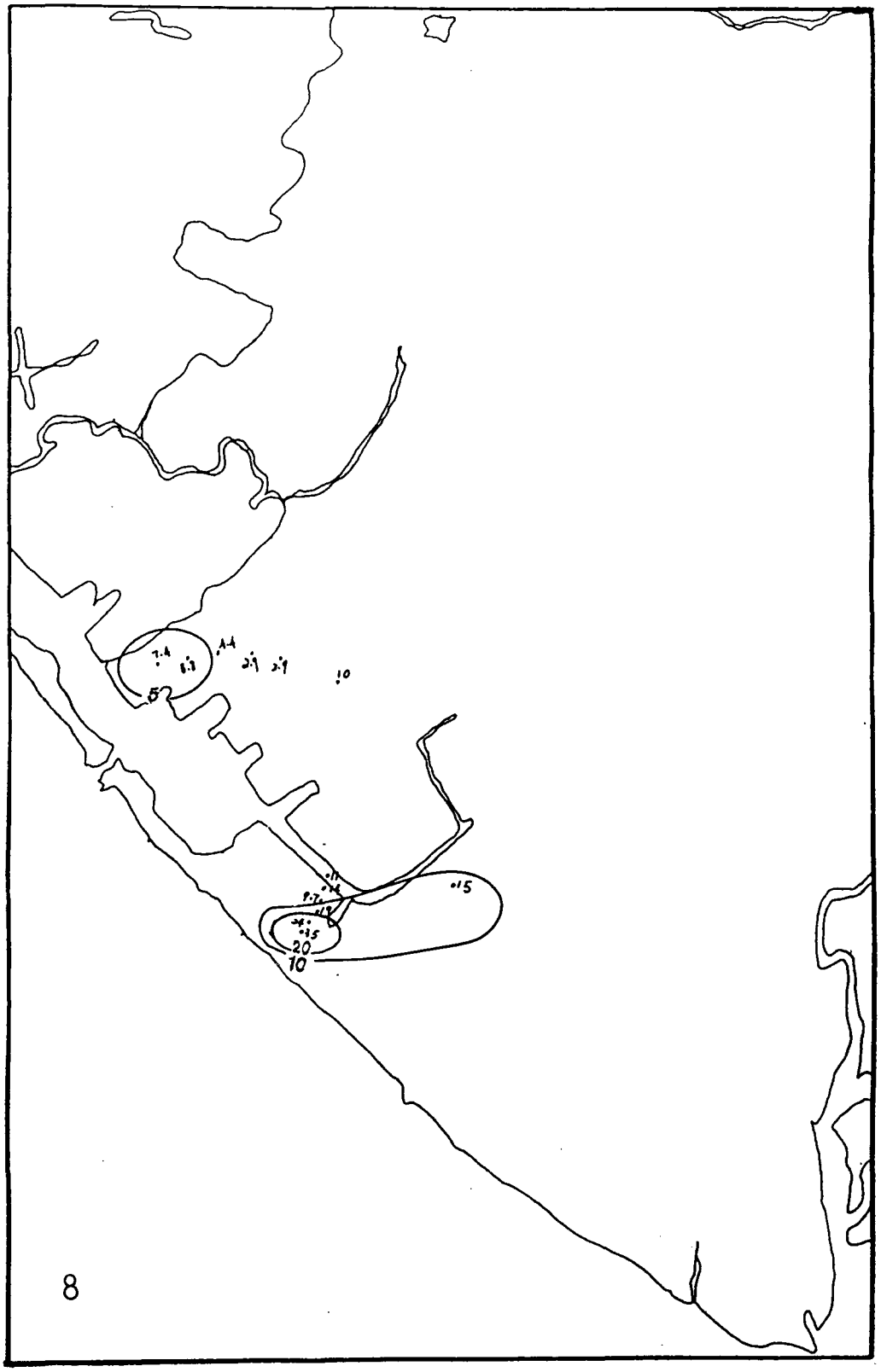
.5
.10
.15
.20
.10
8

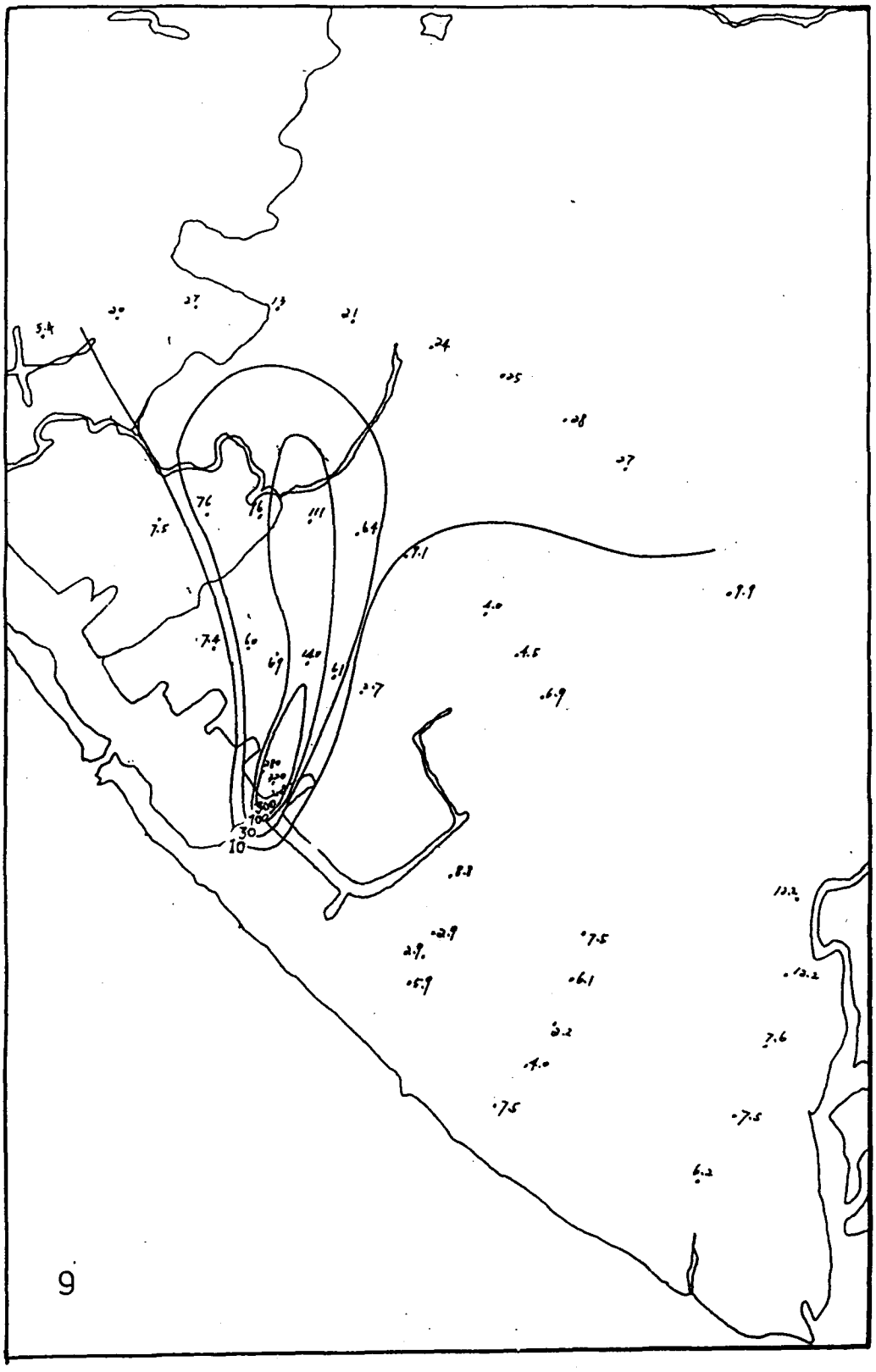
9

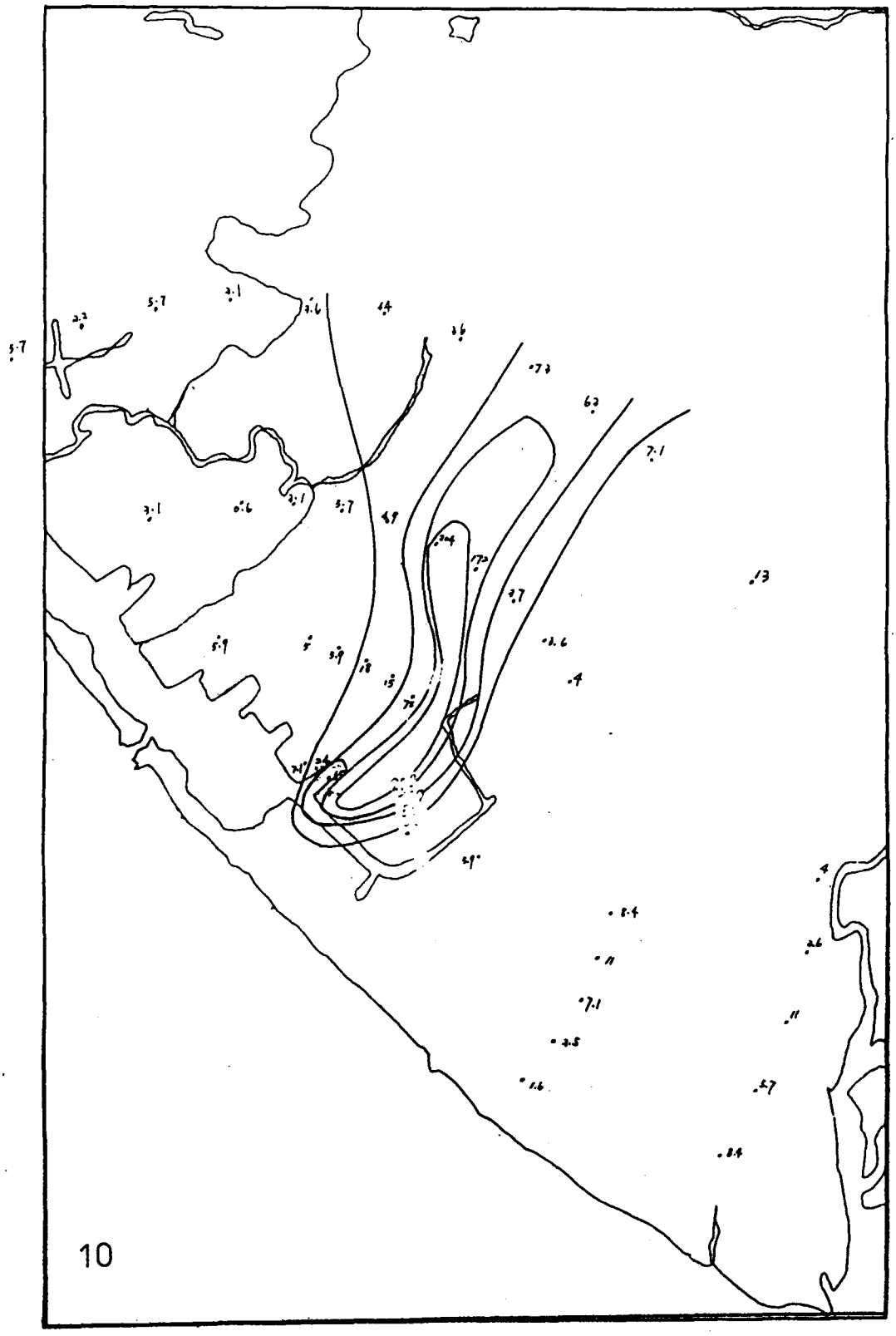
10

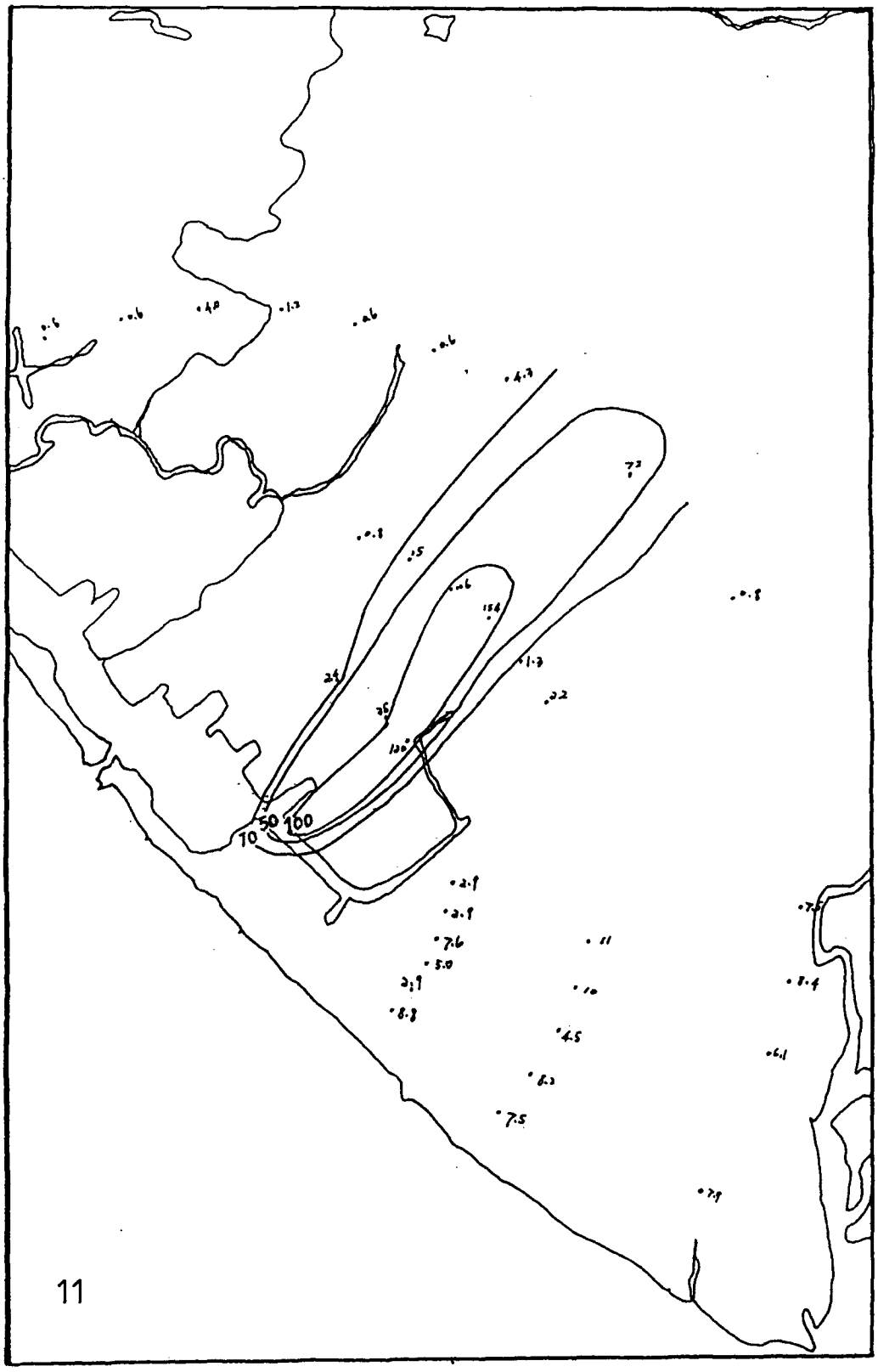
70
50
100
11

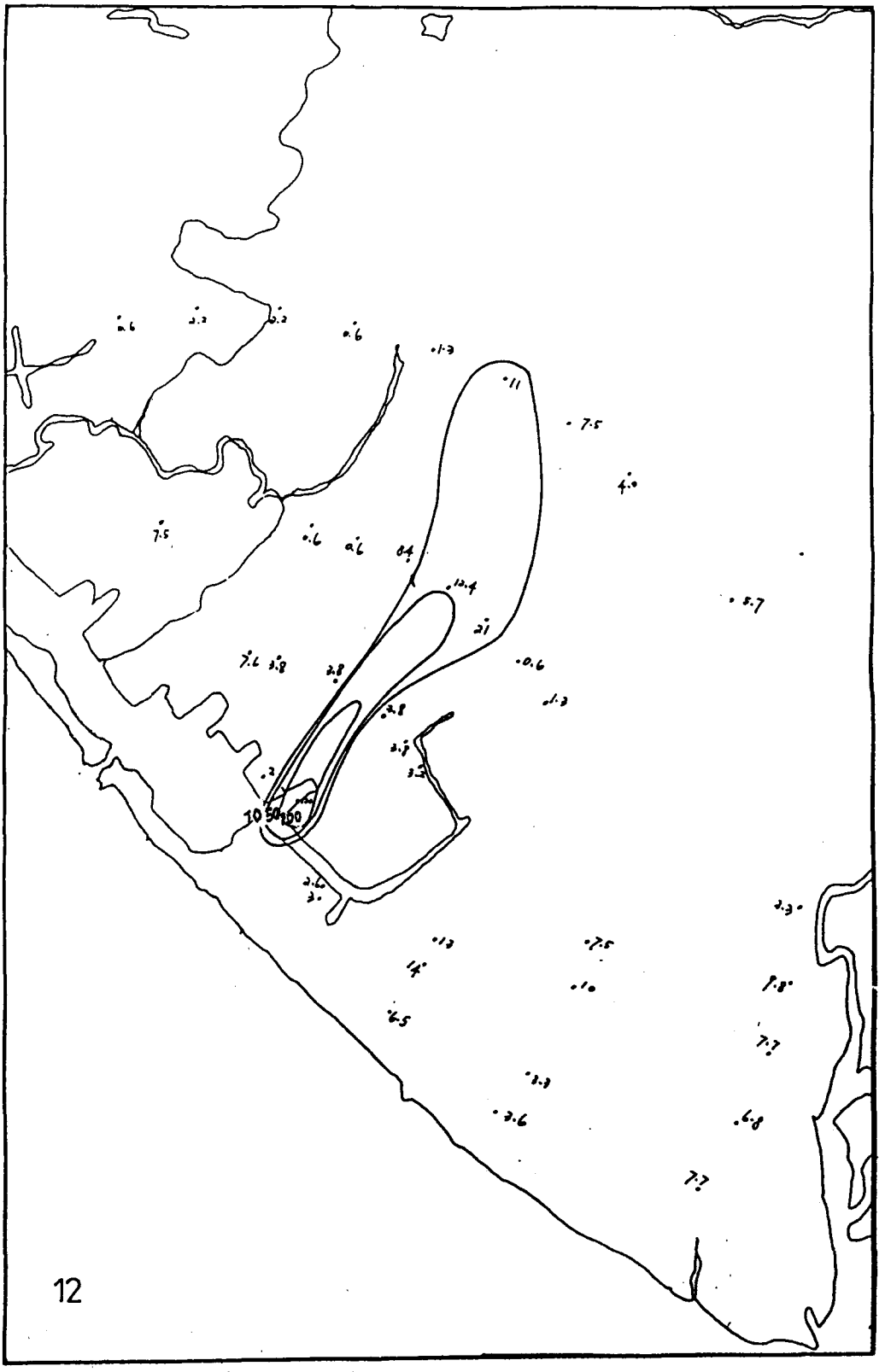
12

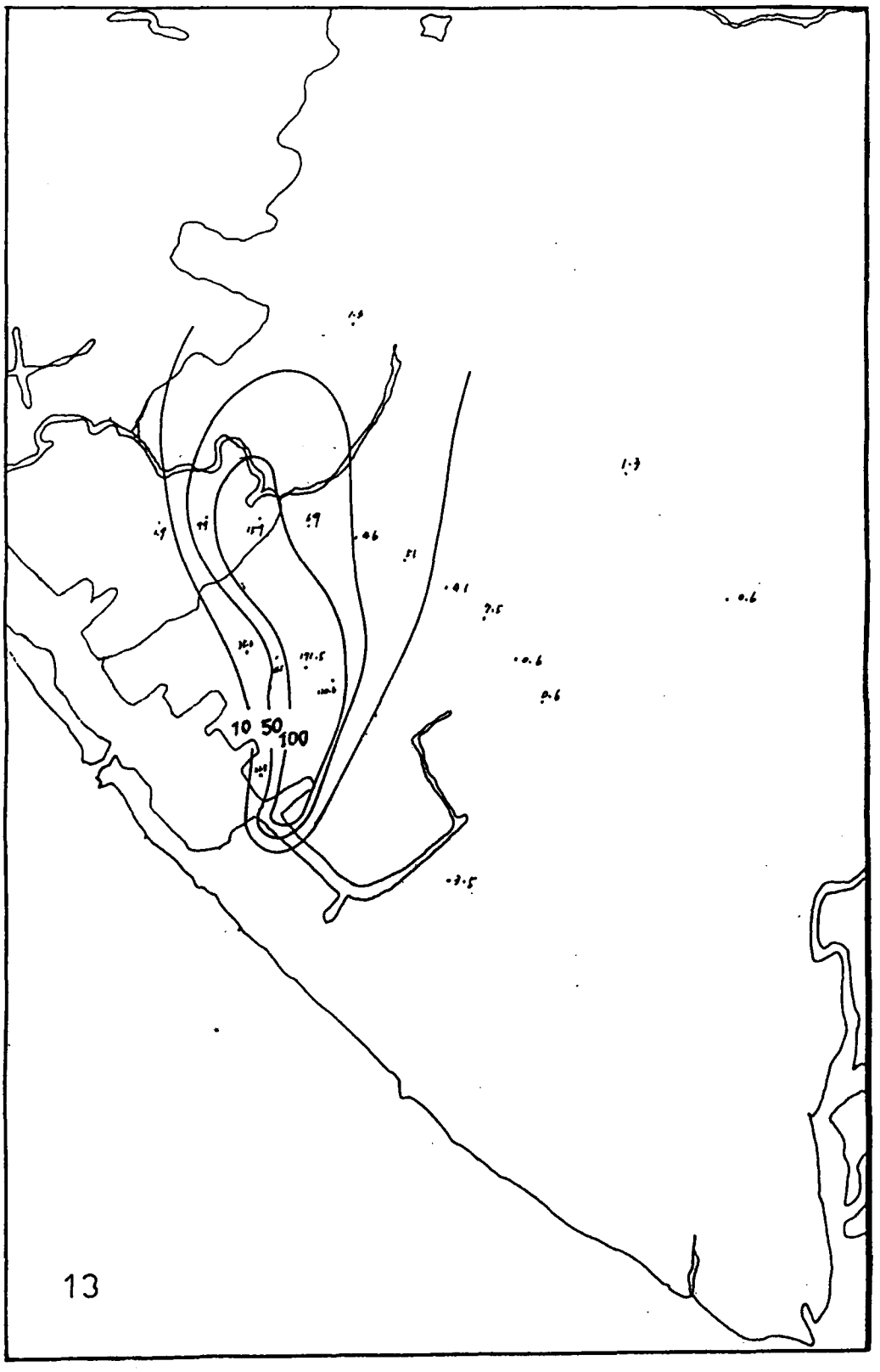
10 50 100
13

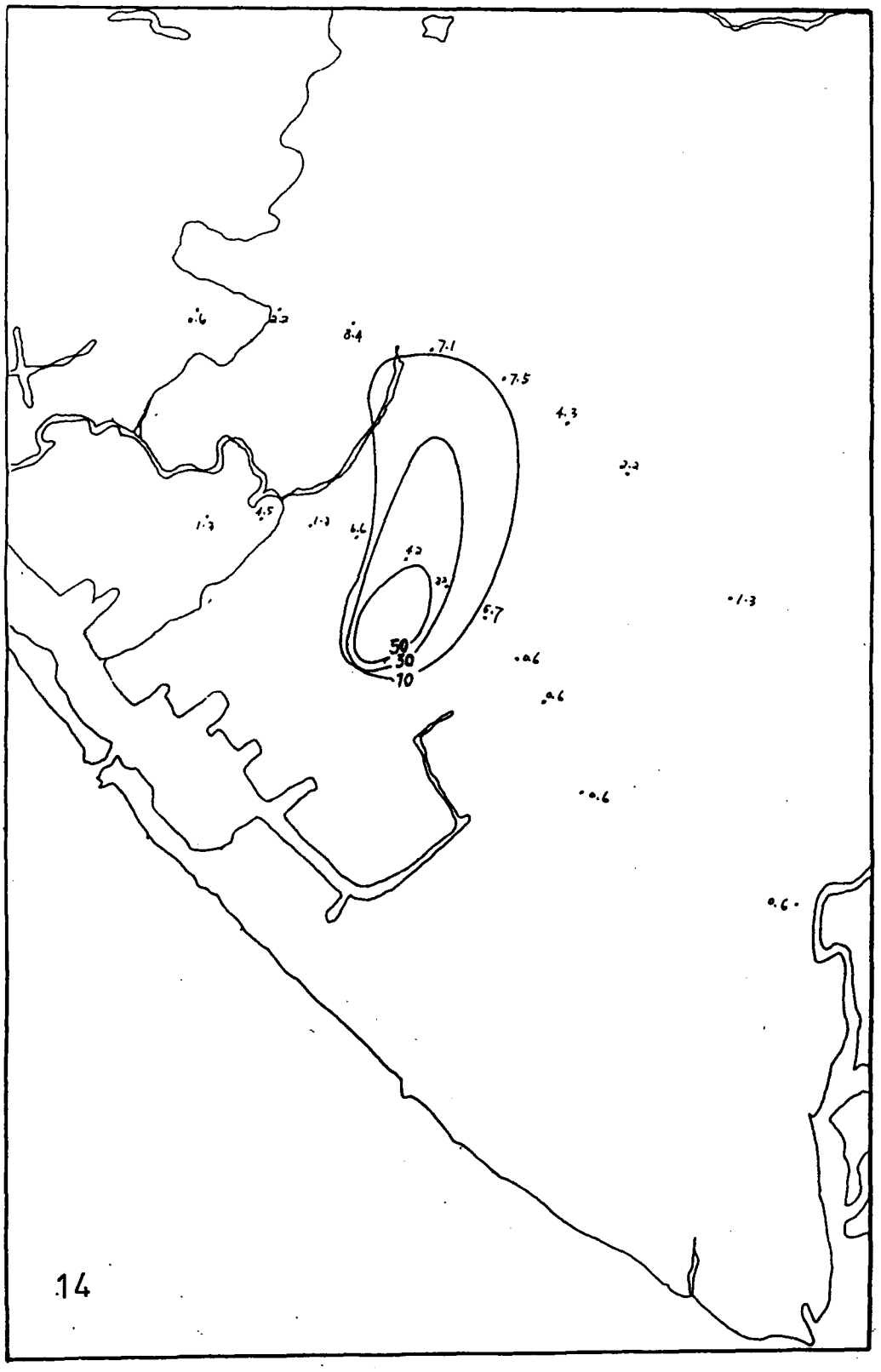
.6
8.4
7.1
7.5
4.3
2.2
1.3
4.5
1.3
4.4
4.2
3.2
5.7
50
30
10
.6
.6
.6
.6
1.3
14

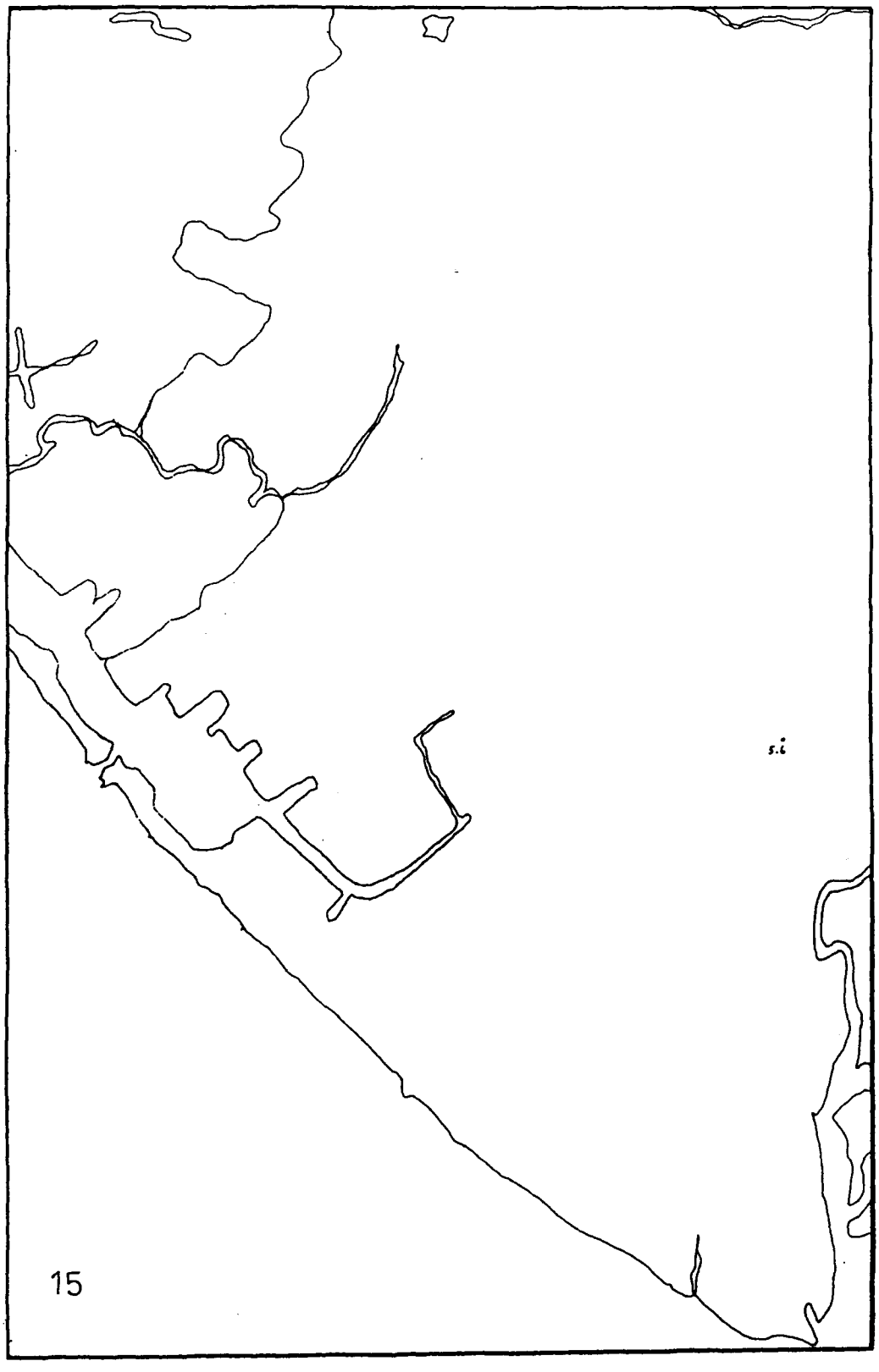
15

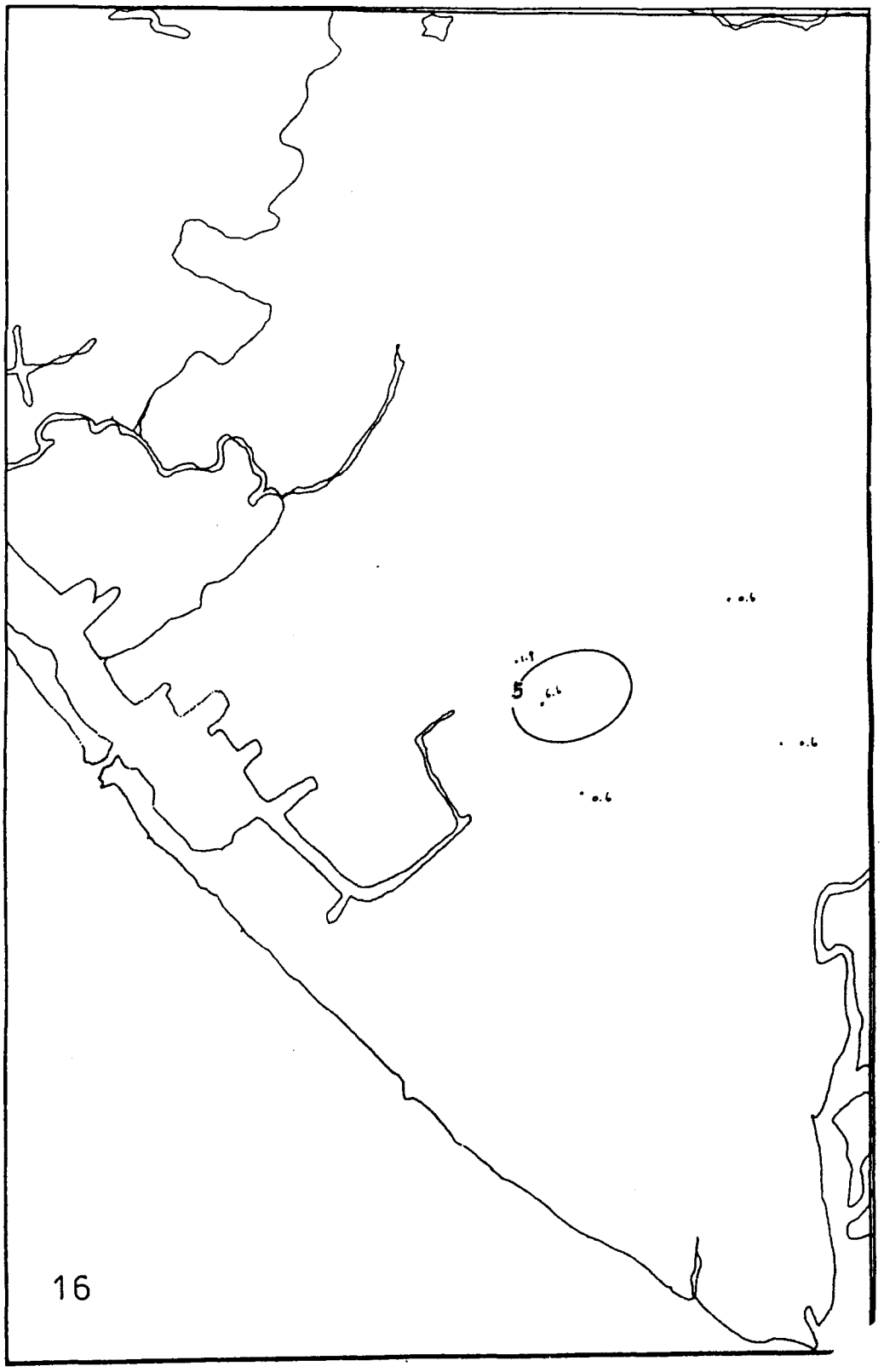
5
16

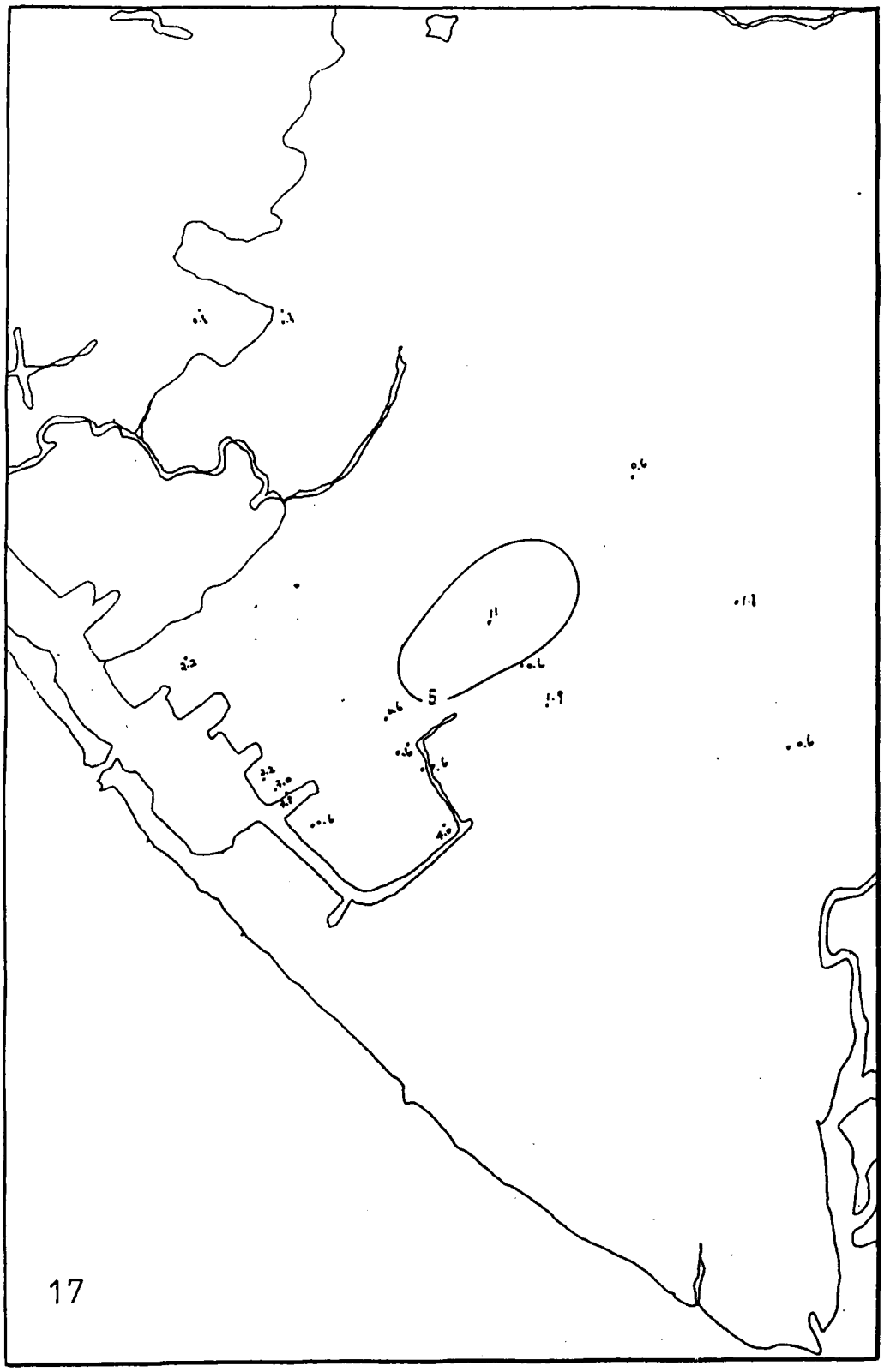
5
17

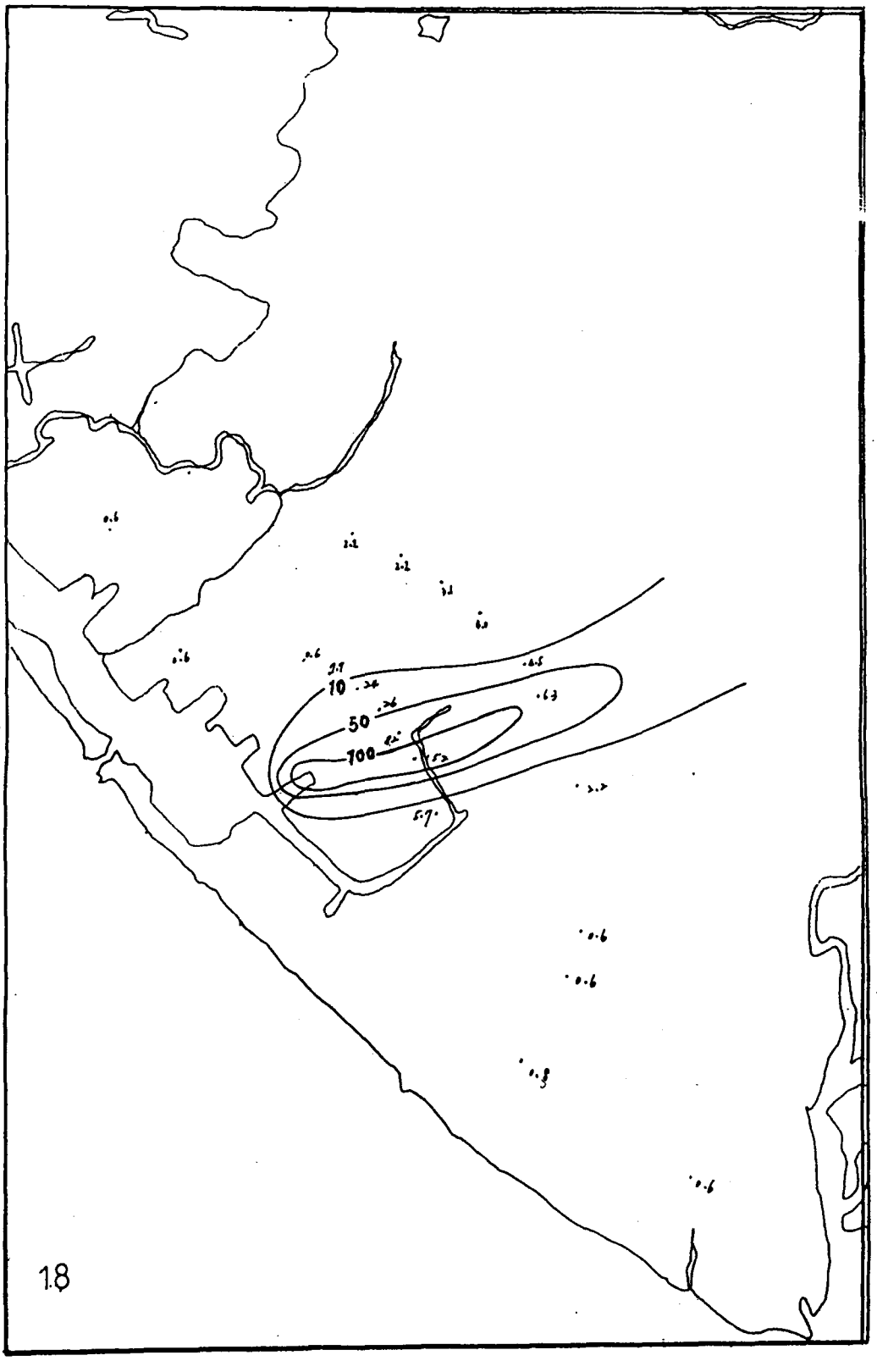
10
50
100
1.8

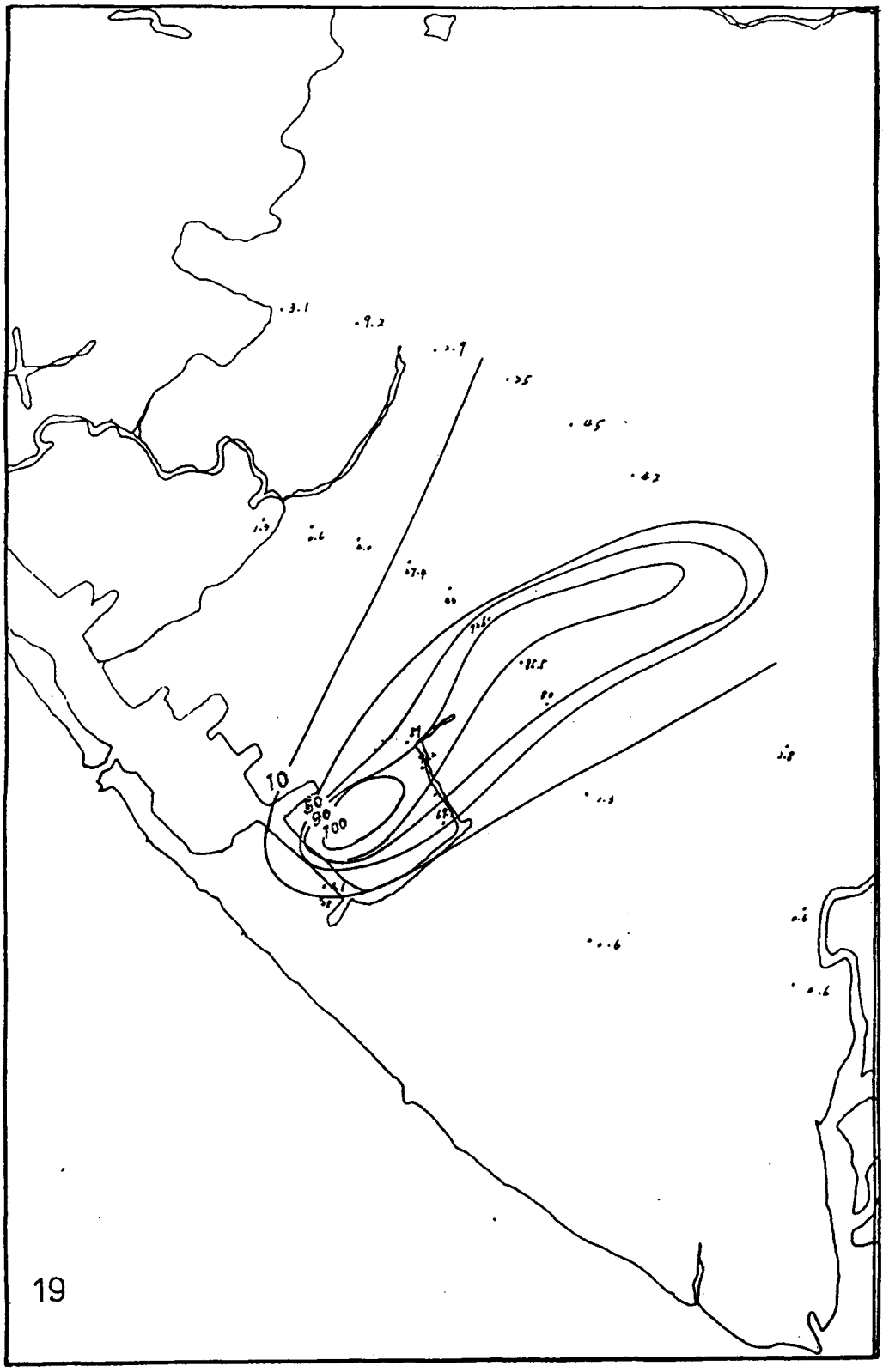
10
50
90
100
19

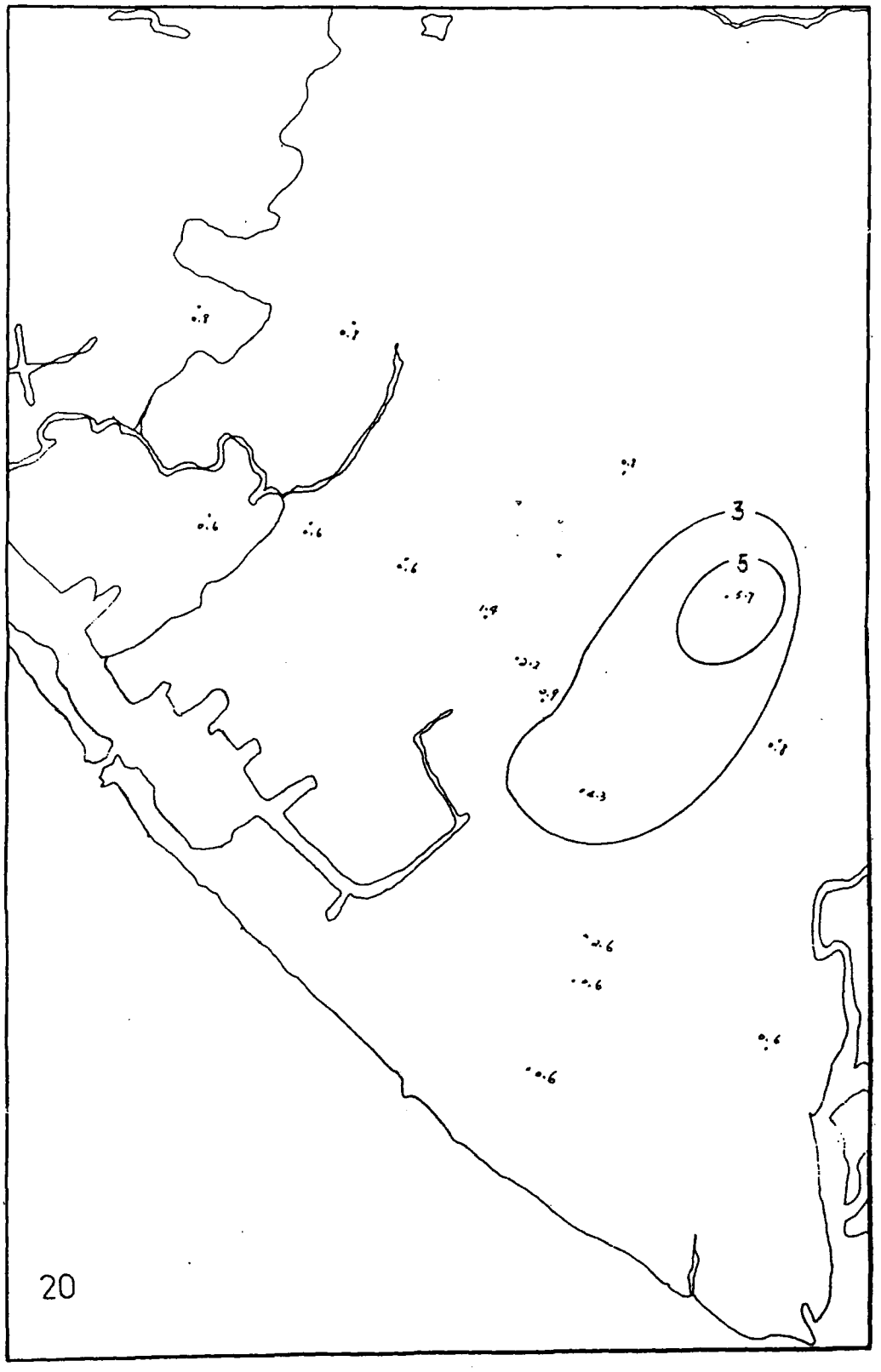
3
5
20

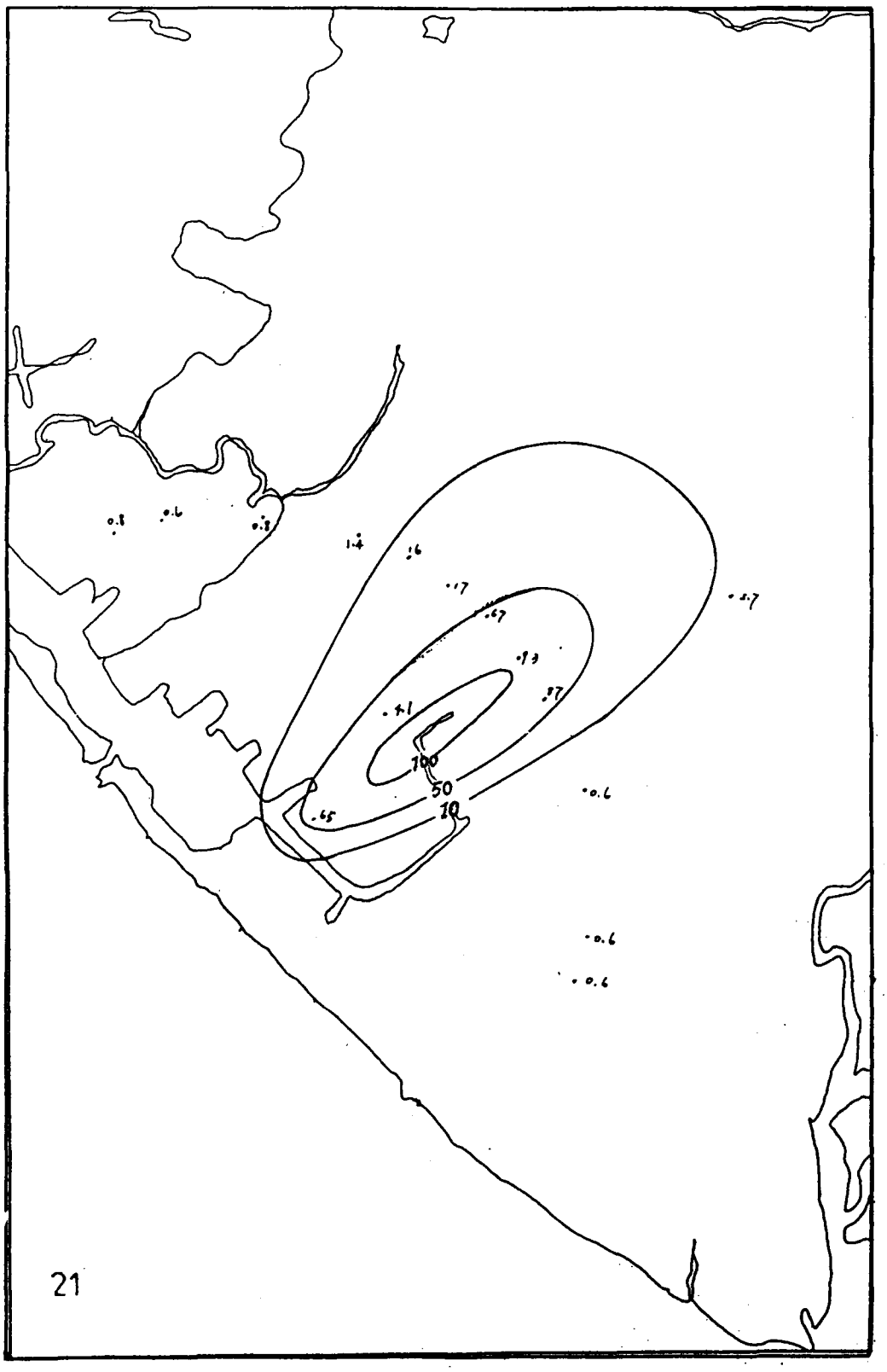
100
50
10
21

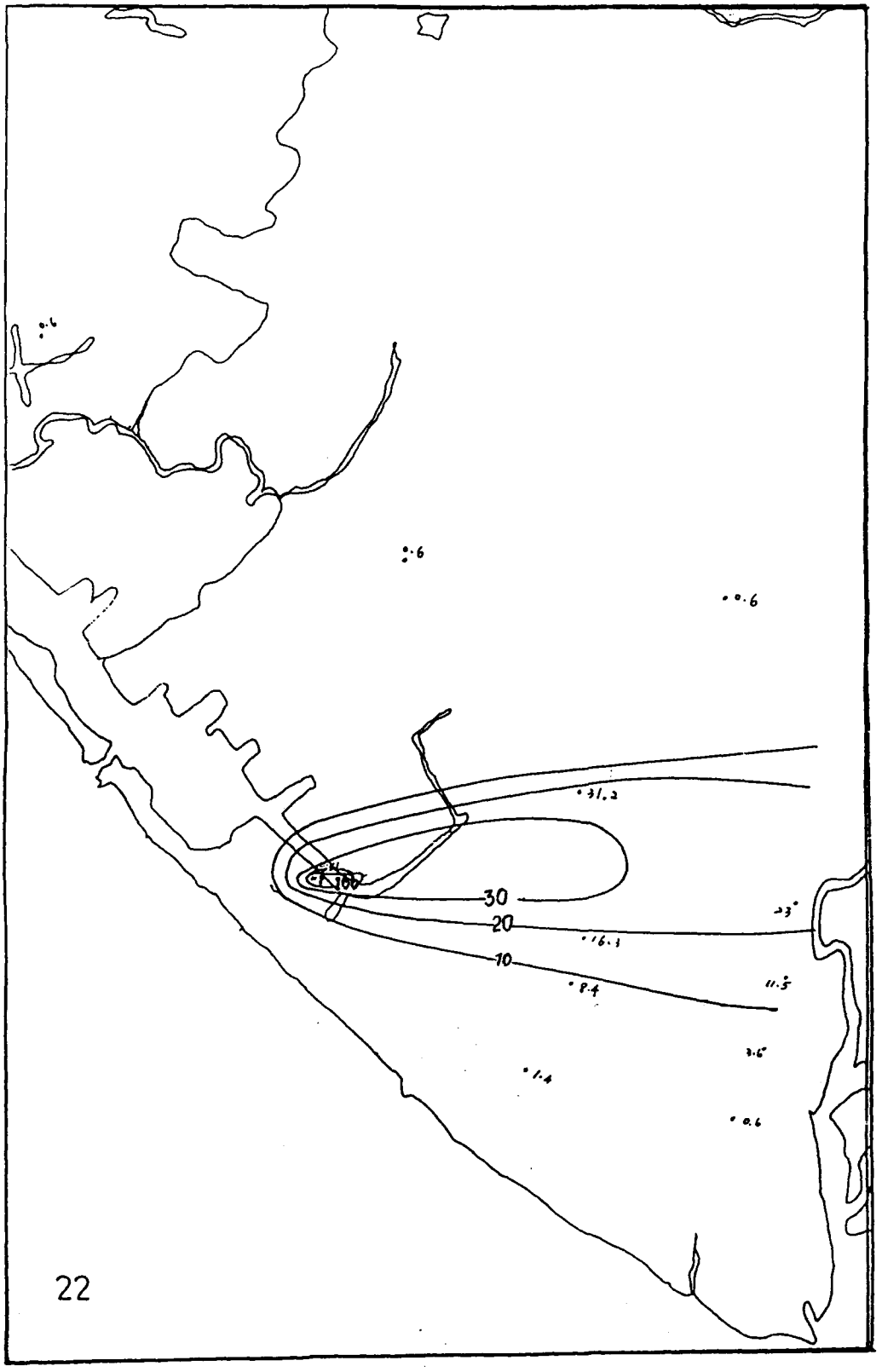
100
30
20
10
22

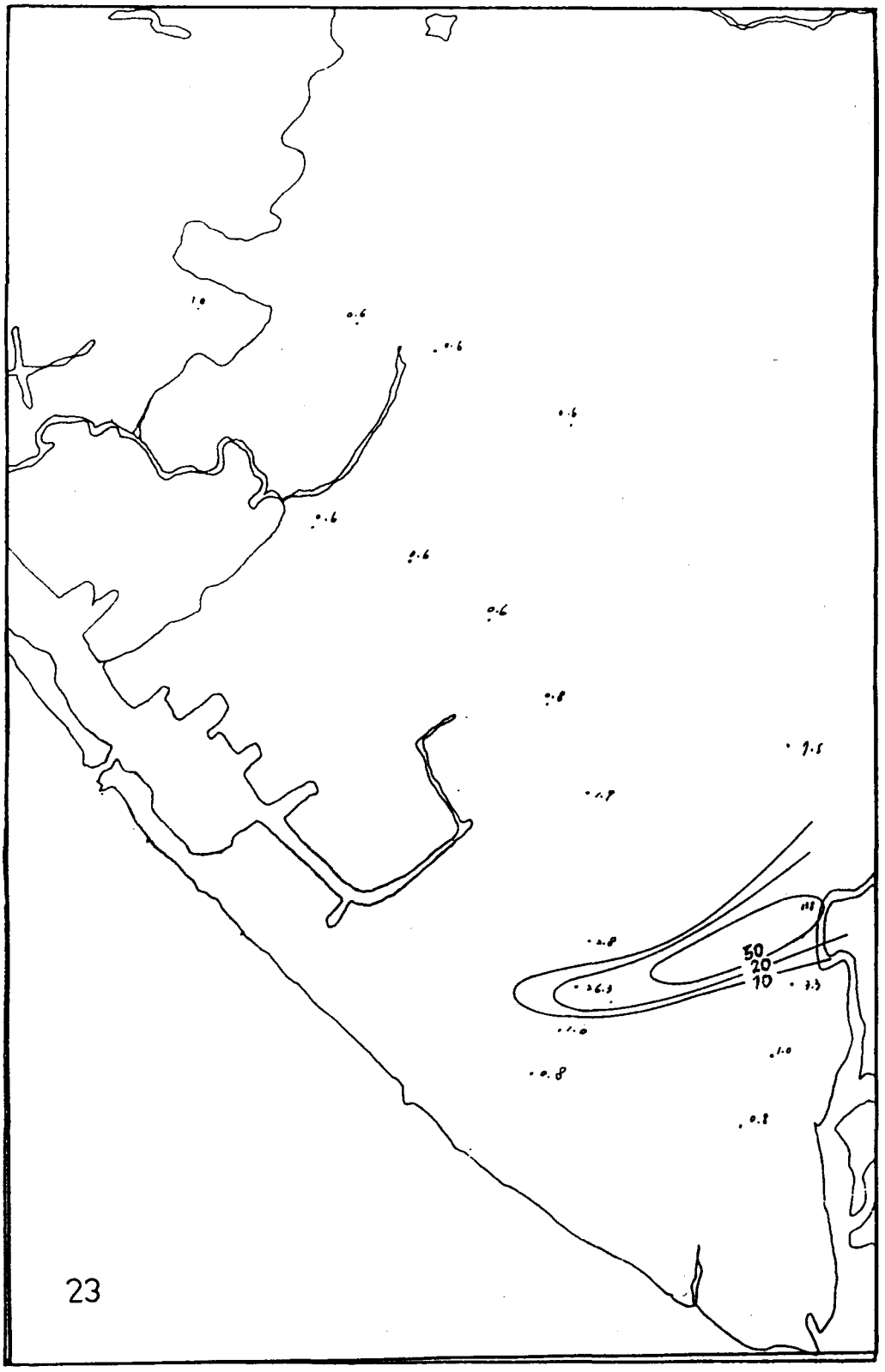
50
20
10
23

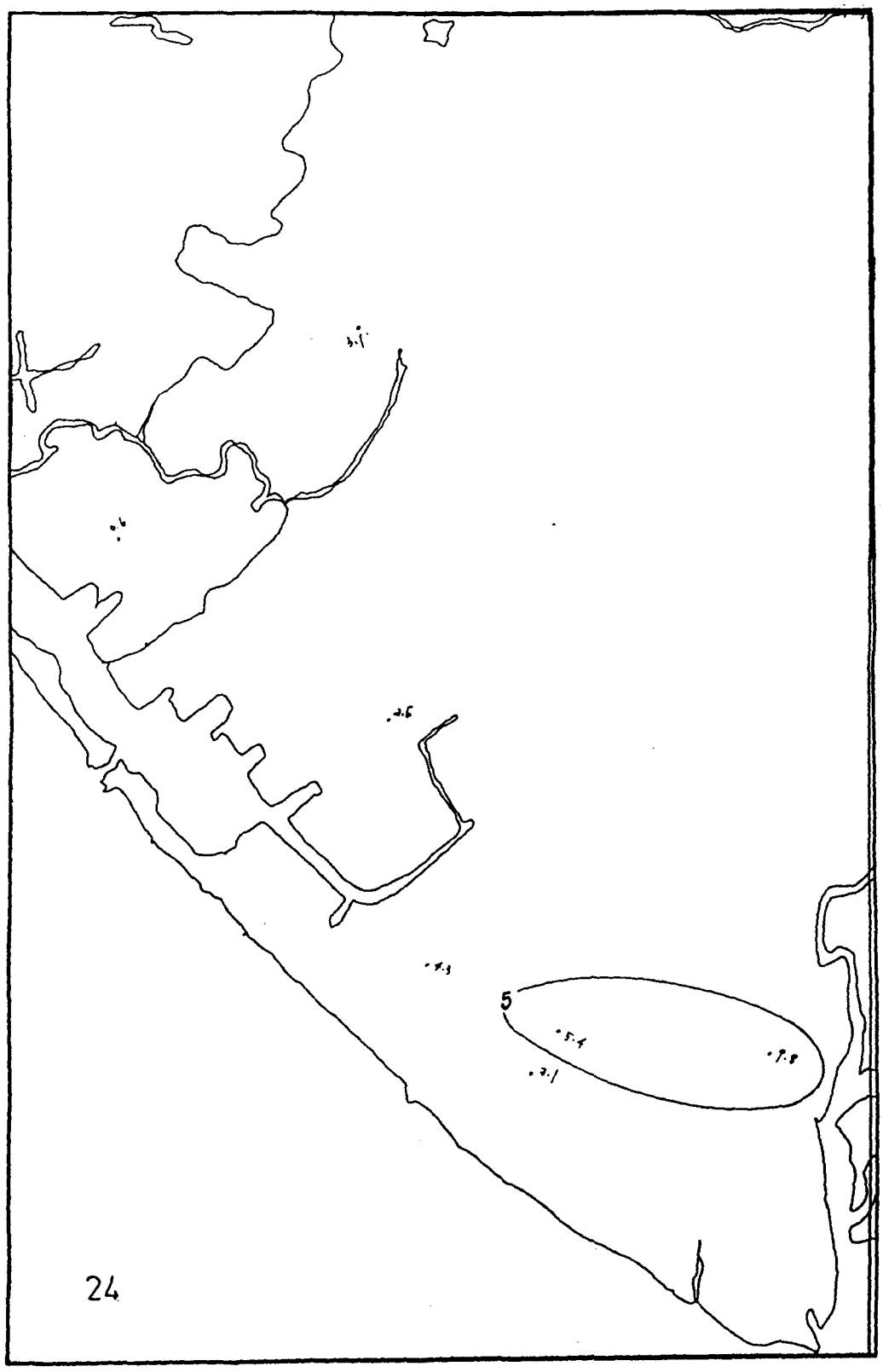
5
24

APPENDIX G Texas climatological model

References: Porter, R. A. and Christiansen, J. H., "Two Efficient Gaussian Plume Models Developed at the Texas Air Control Board." Proceedings of the 7th NATO/CCMS International Technical Meeting on Air Pollution Modeling, Airlie House, Va., September, 1976.

Christiansen, J. H. and Porter, R. A., Users Guide to the Texas Climatological Model, Texas Air Control Board, Austin Texas, May, 1976.

Abstract: The TCM is a climatological model that predicts long-term arithmetic mean concentrations of nonreactive pollutants from point sources and area sources.

Equations:

Area sources are handled by an algorithm proposed by Gifford and Hanna[7]. The concentration due to area sources is given by

$$x_A = FQ/U$$

where x_A = concentration ($\mu g/m^3$)

Q = area source emission rate in the vicinity of the receptor ($\mu g/s\text{-}m^2$)

U = mean ground-level wind speed (m/s)

F = a dimensionless constant

Gifford and Hanna have suggested a value of F = 50 for SO_2 and 225 for total suspended particulate (TSP). The area emission rate, Q, is determined by averaging the emissions in the area source square containing the receptor and in the neighboring squares. The extent of the region around each receptor to use for emission rate averaging is an input parameter.

The TCM uses steady-state Gaussian plume point source logic, with the crosswind distribution averaged across 22.5° azimuthal sectors. The only meteorological input required for area source calculations is the mean wind speed, but the point source calculations require a meteorological joint frequency function with sixteen 22.5° wind sectors, six wind speed classes (0-3, 4-6, 7-10, 11-16, 17-21, and > 21 knots), and six stability classes (Turner classes A, B, C, D (day), D (night), and E plus F).

The basic equation is:

$$\chi = Q_i \sum_{m=1}^{6} (K(x,H,m)\phi(k,m)/U_m)\cdot(\text{decay term})$$

where $K(x,H,m) = (32\times10^6/[(2\pi)^{3/2}\sigma_z])\exp(-H_i^2/2\sigma_z^2)$

(K is precalculated for 20 distances, 9 effective source heights, and six stability classes)

U_m is a wind speed characteristic of an entire stability class, and is computed in the model by the equation:

$$U_m = \left[\sum_{k=1}^{16}\sum_{\ell=1}^{6}\phi(k,\ell,m)\right]\left[\sum_{k=1}^{16}\sum_{\ell=1}^{6}\phi(k,\ell,m)/U_\ell\right]^{-1}$$

with χ = concentration, $\mu g/m^3$

k = the wind sector index appropriate to source i at the receptor

ℓ = wind speed class index

m = stability class index

ϕ = meteorological joint frequency function

Q_i = emission rate of source i, g/s

H_i = effective height of source i, m

σ_z = standard deviation of vertical Gaussian concentration distribution, m

$T_{1/2}$ = half-life for first-order pollutand decay, s

U_ℓ = central wind speed of class ℓ, m/s

x = downwind distance, m

a. Source-Receptor Relationship

Arbitrary location for each point source
Unlimited number of sources
Arbitrary location and square grid width for each area source
The model will allocate area sources into a uniform square grid
Receptor location is arbitrary grid (max. 50 x 50)
Release heights for point sources
The area source algorithm (Gifford-Hanna) does not consider height of release
Receptors are at ground level
No terrain difference between sources and receptors

b. Emission Rate

All sources have a single average emission rate for the averaging time period (i.e., month, season, year)

c. Chemical Composition

One, two, or three inert pollutants are treated simultaneously

d. Plume Behavior

Plume rise calculated according to Briggs[9] neutral/unstable equation
Effective stack heights less than 10 meters are considered 10 meters
Effective stack heights greater than 300 meters are considered 300 meters
No plume rise for area sources
Down-wash and fumigation not considered

e. Horizontal Wind Field

Climatological approach
16 wind directions
Mean wind speed calculated for each stability class from the joint frequency function of stability, wind direction, and wind speed
Wind speed corrected for physical stack height (same as CDM)

f. Vertical Wind Speed

Assumed equal to zero.

g. Horizontal Dispersion

Assumed to be uniform within each 22.5 degree sector (same as CDM)

h. Vertical Dispersion

Gaussian plume
6 stability classes (Pasquill-Gifford-Turner) A, B, C, D-Day, D-Night, E and F
No provision for variation in surface roughness

i. Chemistry/Reaction Mechanism

Exponential decay according to user input half-life (same as CDM)

j. Physical Removal

Same as i above

k. Background

Background may be entered by calibration coefficient for each pollutant

l. Boundary Conditions

Perfect reflection assumed at ground
Mixing height not considered

m. Emission and Meteorological Correlation

Emissions not varied

n. Validation/Correlation

Model is self-calibrating with input of field receptor observations
High correlation achieved for areas dominated by point sources
Poorer correlations have been shown where area sources are dominant

o. Output

Arithmetic mean concentration for the averaging time of the climatological input and emission data (one month to one year)
Any combination of the following outputs are available:
(1) Listing of concentration for an arbitrarily spaced square grid of up to 50 by 50 elements
(2) A print plot of the grid concentrations
(3) Punched card output for isopleth maping (same as CDM)
(4) A listing of the five high contributors to the concentration (by % concentration) at each grid point

p. Computer Requirements

Digital computer required
Core requirements are moderate

q. Limitations

Flat terrain, relatively constant emissions
Use not recommended where area sources dominate

APPENDIX H (1 - 24) : The isopleth of SF_6 concentration calculated by TCM

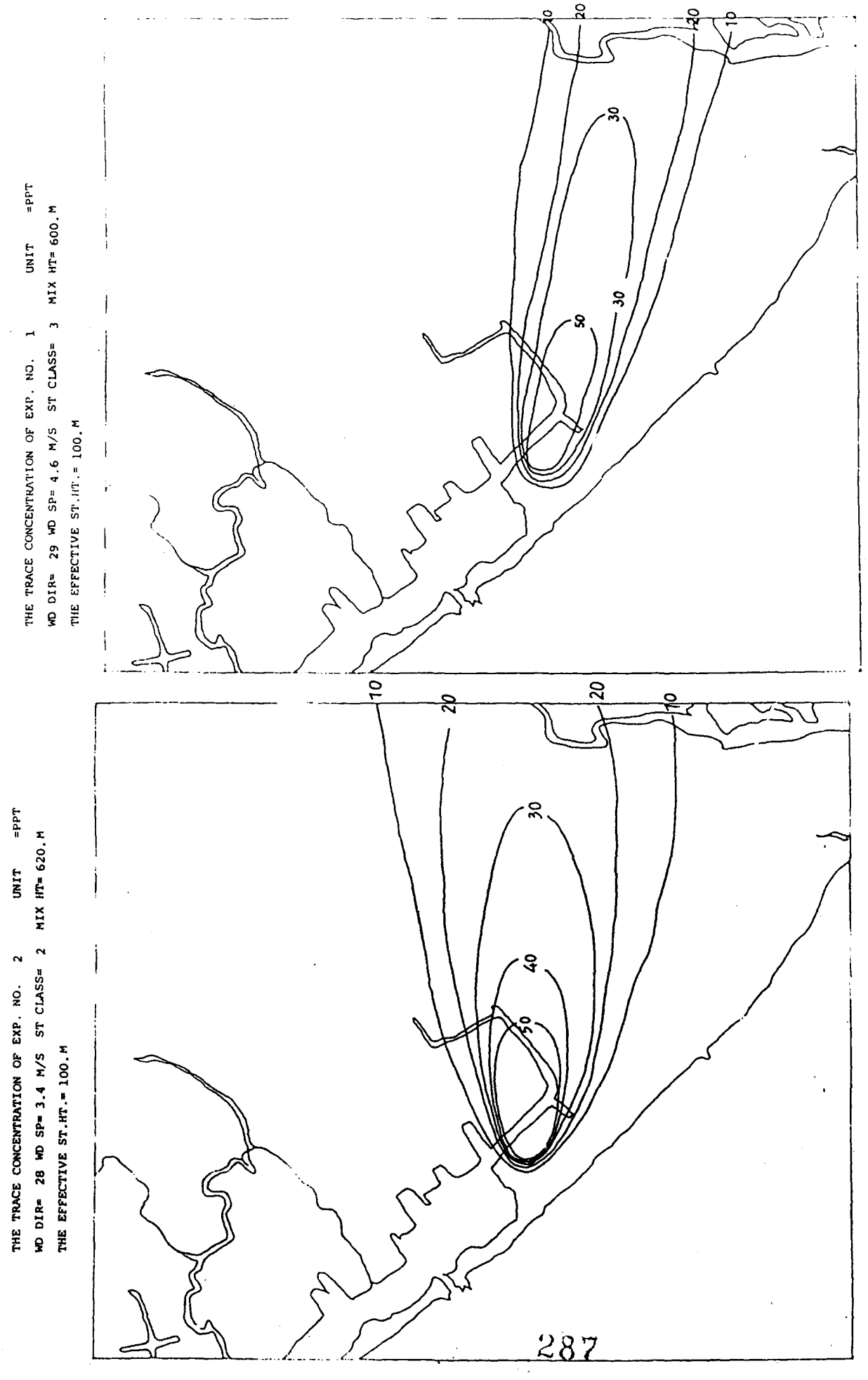

THE TRACE CONCENTRATION OF EXP. NO. 4 UNIT =PPT
WD DIR= 29 WD SP= 3.6 M/S ST CLASS= 3 MIX HT= 250.M
THE EFFECTIVE ST.HT.= 100.M

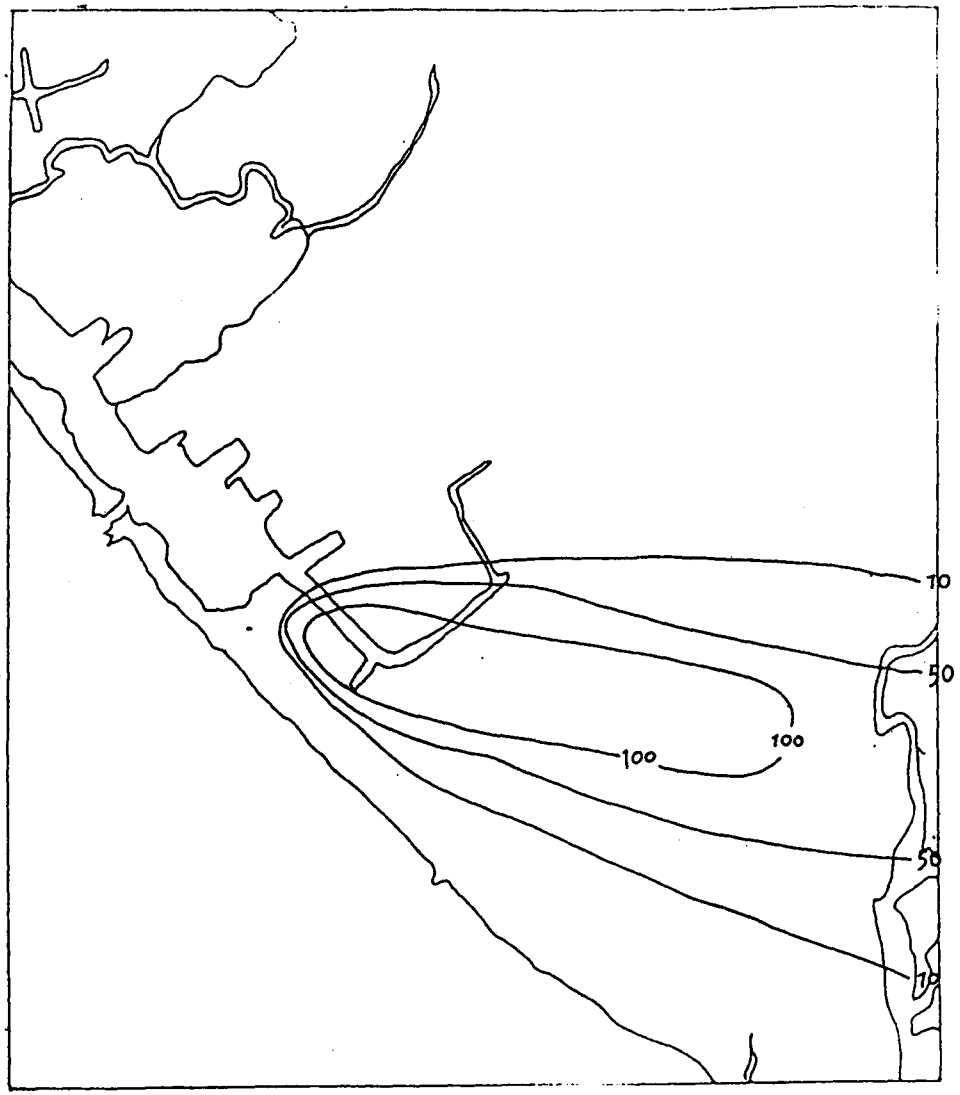

THE TRACE CONCENTRATION OF EXP. NO. 3 UNIT =PPT
WD DIR= 29 WD SP= 3.6 M/S ST CLASS= 2 MIX HT= 710.M
THE EFFECTIVE ST.HT.= 100.M

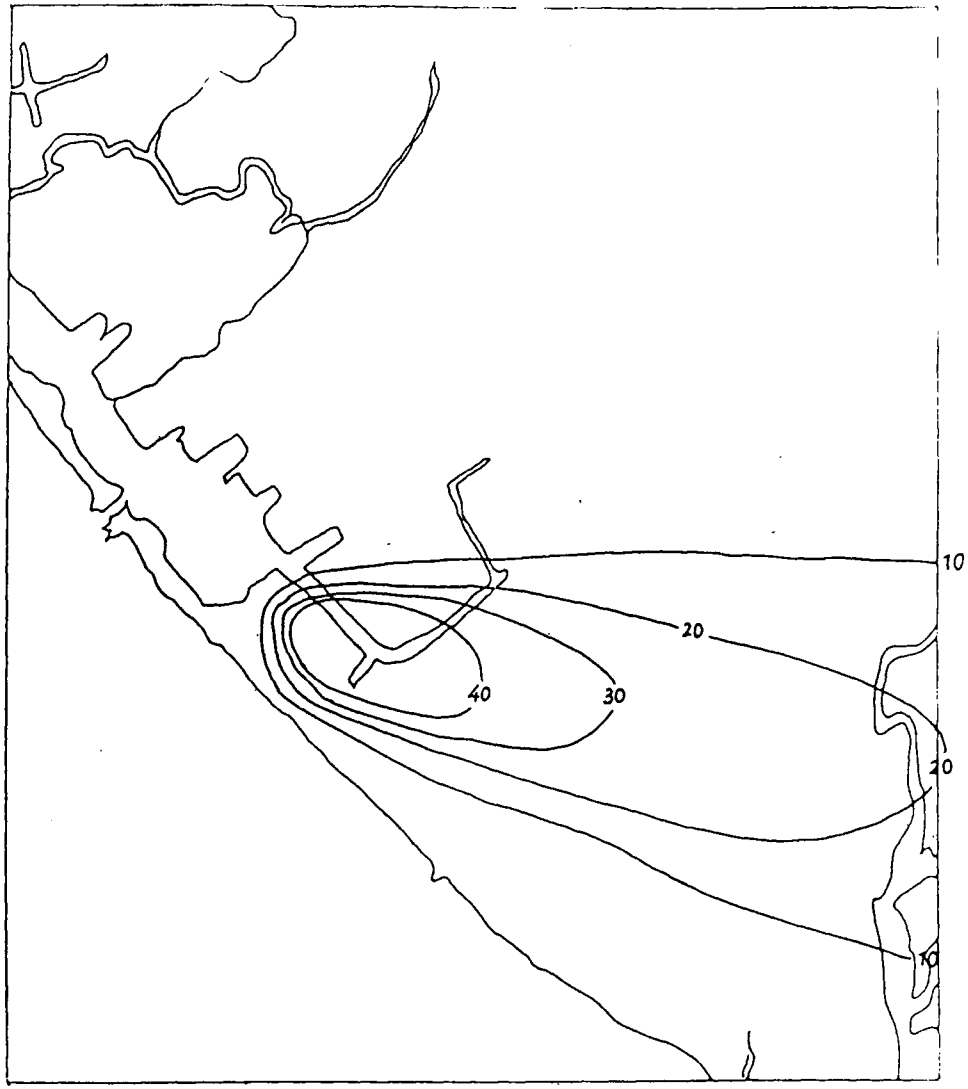

THE TRACE CONCENTRATION OF EXP. NO. 6 UNIT =PPT

WD DIR= 20 WD SP= 2.8 M/S ST CLASS= 3 MIX HT= 200.M

THE EFFECTIVE ST.HT.= 473.M

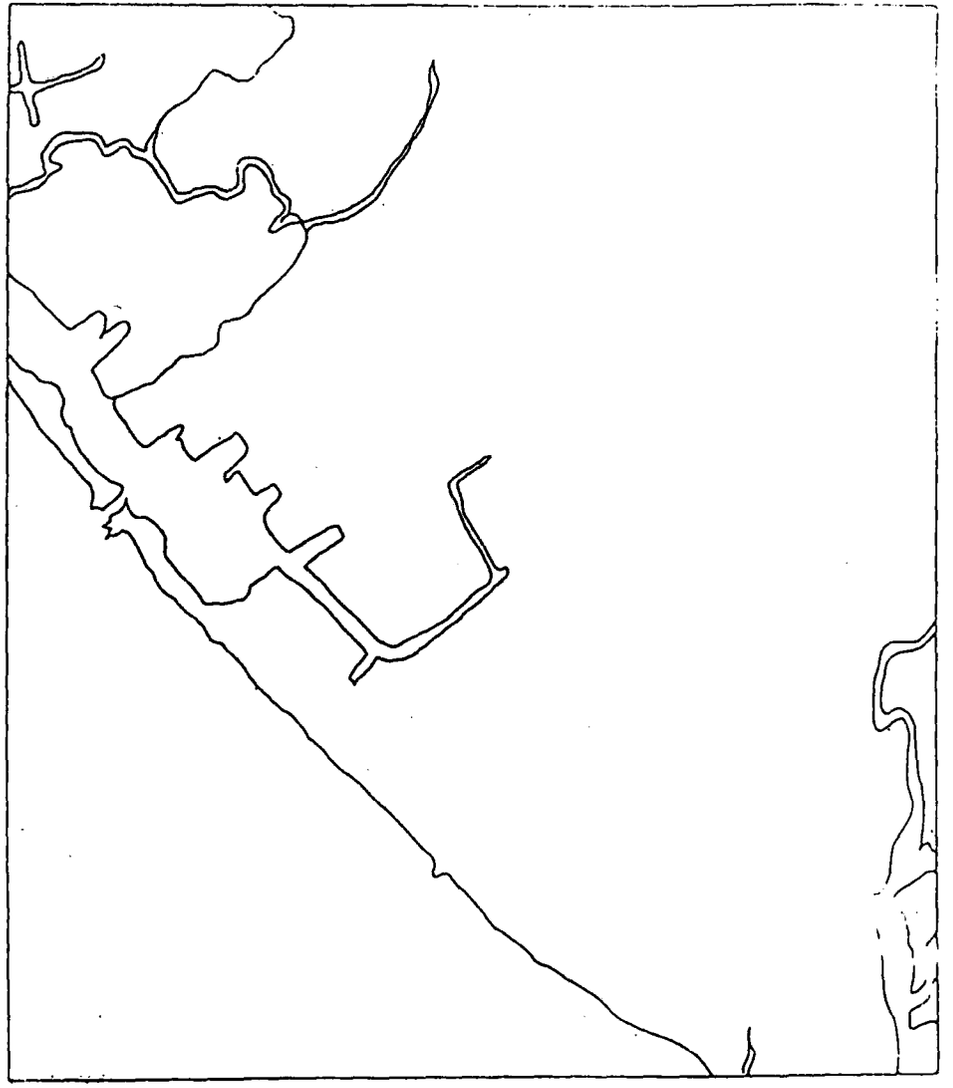

THE TRACE CONCENTRATION OF EXP. NO. 5 UNIT =PPT

WD DIR= 28 WD SP= 3.6 M/S ST CLASS= 3 MIX HT= 300.M

THE EFFECTIVE ST.HT.= 397.M

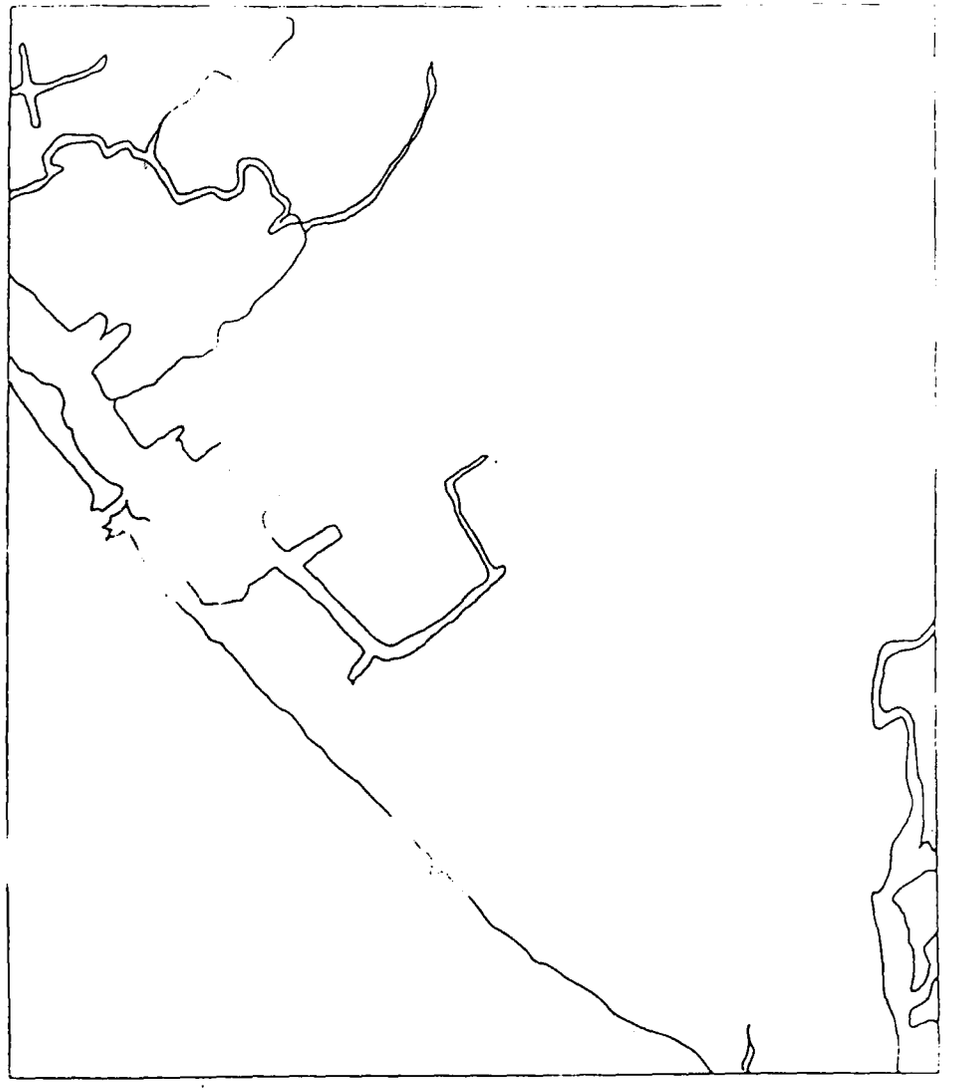

THE TRACE CONCENTRATION OF EXP. NO. 8 UNIT =PPT
WD DIR= 26 WD SP= 0.3 M/S ST CLASS= 2 MIX HT= 500.M
THE EFFECTIVE ST.HT.=3729.M

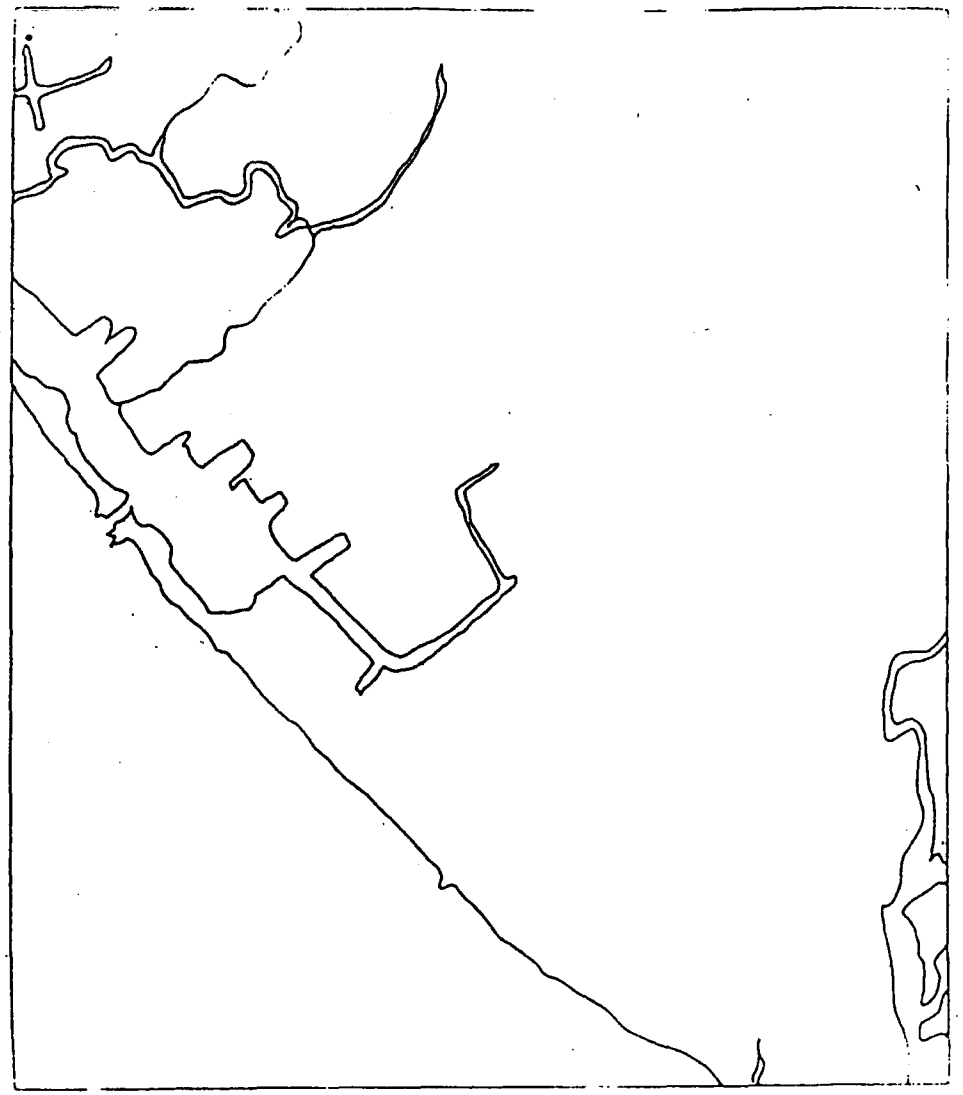

THE TRACE CONCENTRATION OF EXP. NO. 7 UNIT =PPT
WD DIR= 19 WD SP= 2.5 M/S ST CLASS= 3 MIX HT= 200.M
THE EFFECTIVE ST.HT.= 100.M

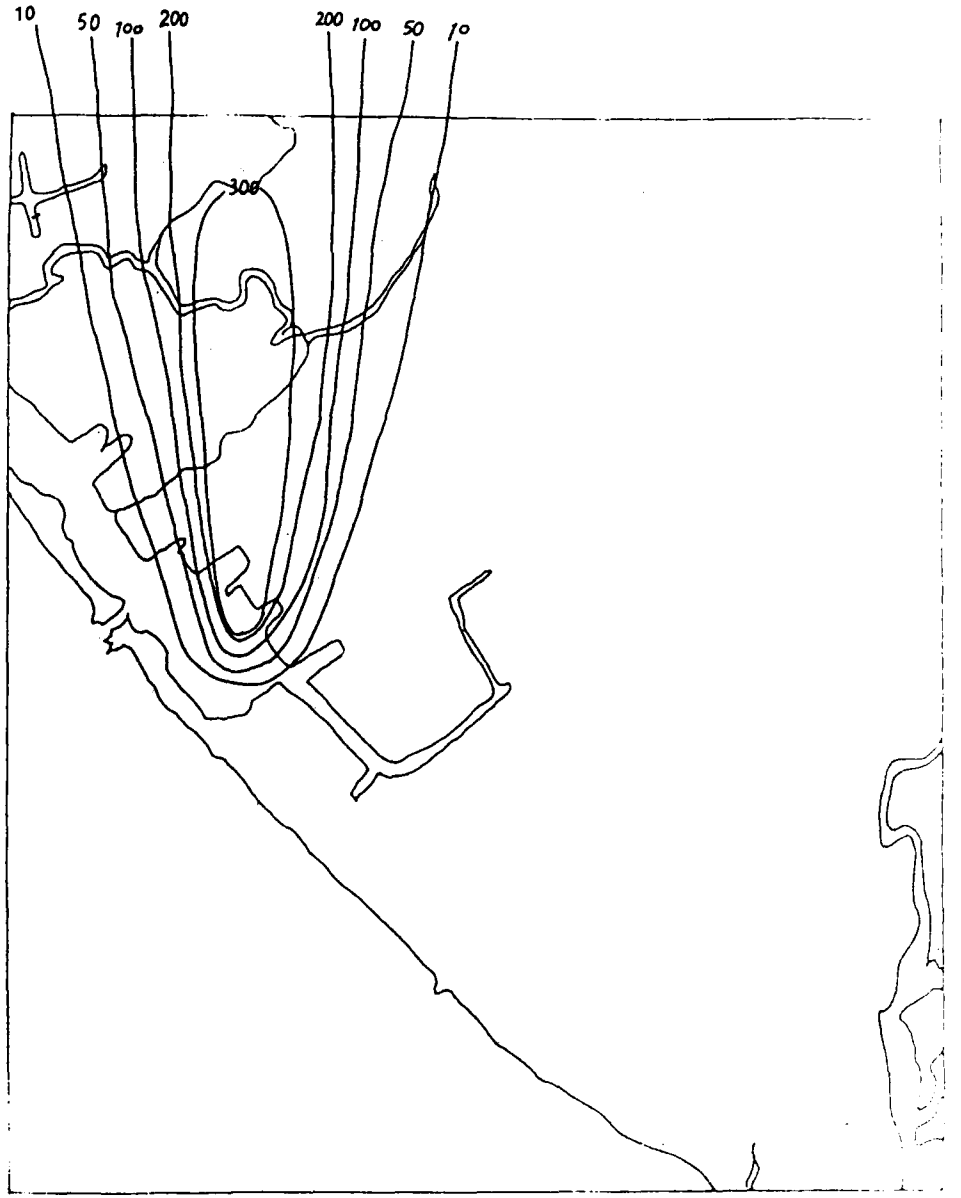

THE TRACE CONCENTRATION OF EXP. NO. 10 UNIT =PPT

WD DIR= 23 WD SP= 3.3 M/S ST CLASS= 3 MIX HT= 600. M

THE EFFECTIVE ST.HT.= 100. M

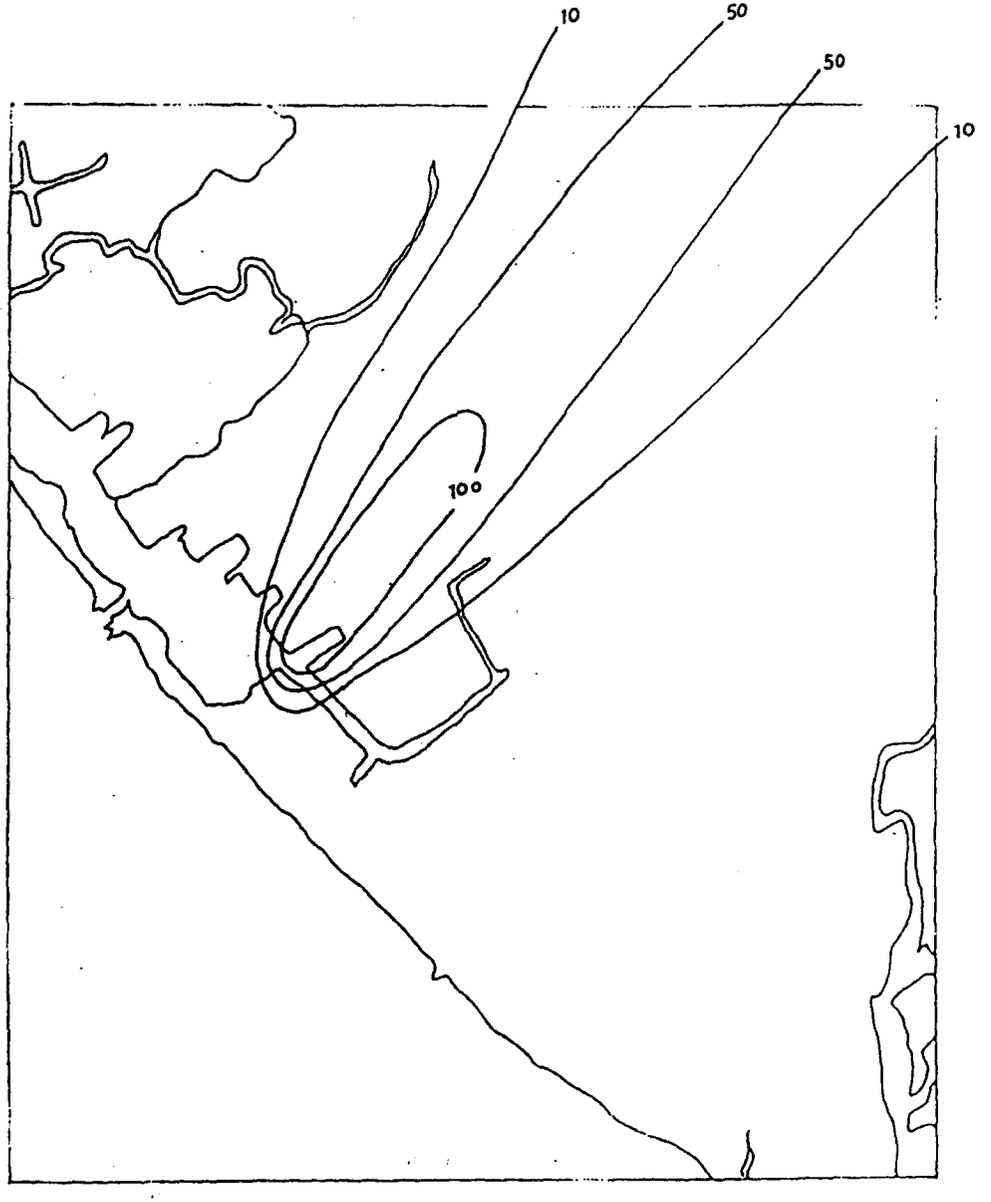

THE TRACE CONCENTRATION OF EXP. NO. 9 UNIT =PPT

WD DIR= 26 WD SP= 2.7 M/S ST CLASS= 3 MIX HT= 450. M

THE EFFECTIVE ST.HT.= 100. M

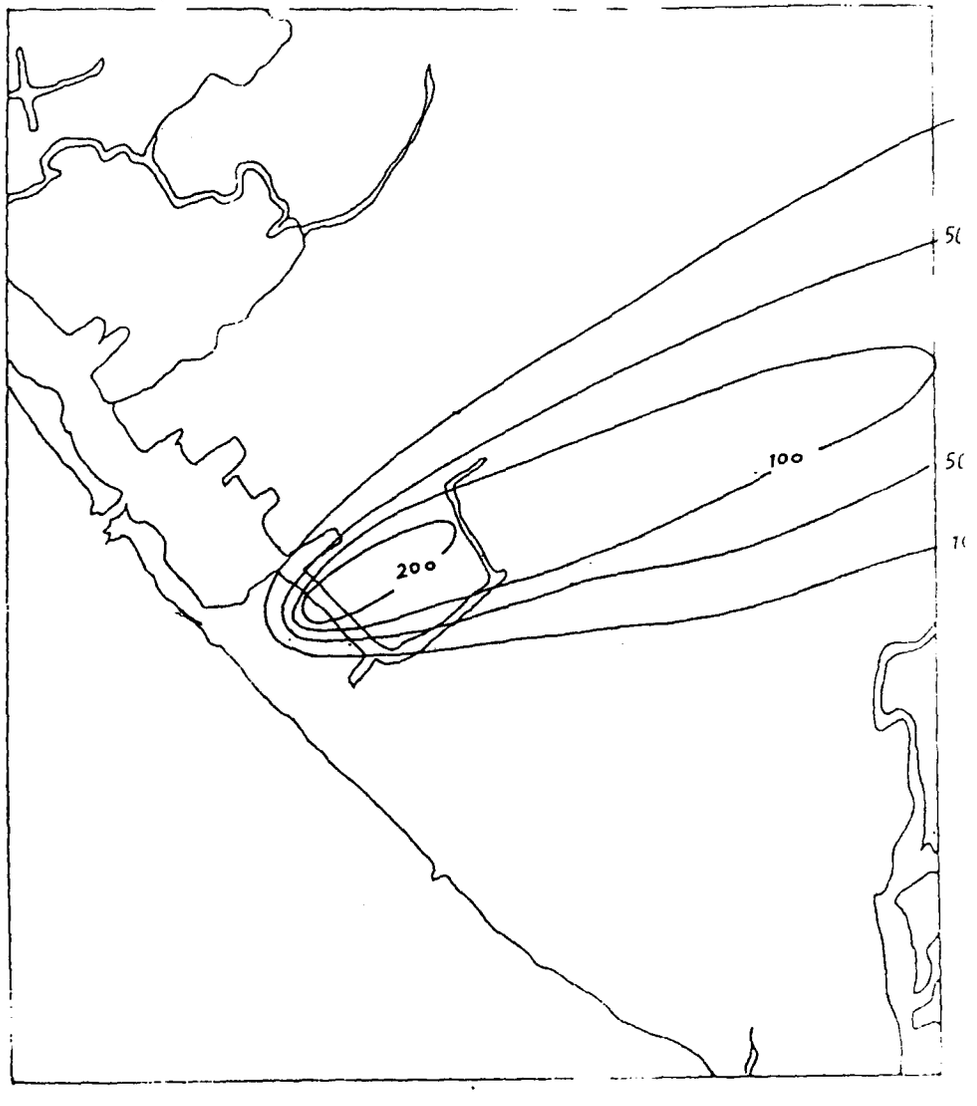

THE TRACE CONCENTRATION OF EXP. NO. 12 UNIT = PPT
WD DIR= 24 WD SP= 4.1 M/S ST CLASS= 3 MIX HT= 200. M
THE EFFECTIVE ST.HT.= 100. M

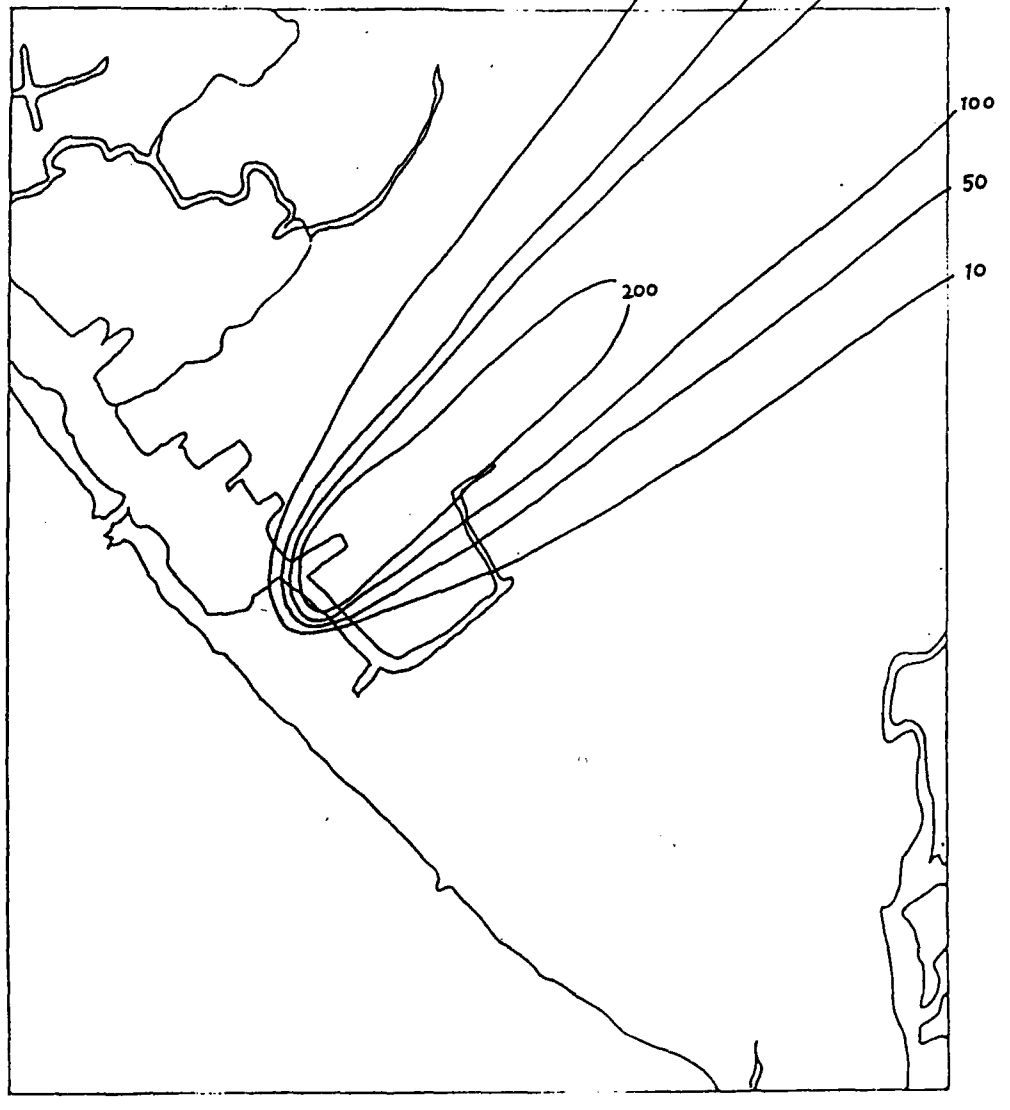

THE TRACE CONCENTRATION OF EXP. NO. 11 UNIT = PPT
WD DIR= 24. WD SP= 2.6 M/S ST CLASS= 3 MIX HT= 580. M
THE EFFECTIVE ST.HT.= 100. M

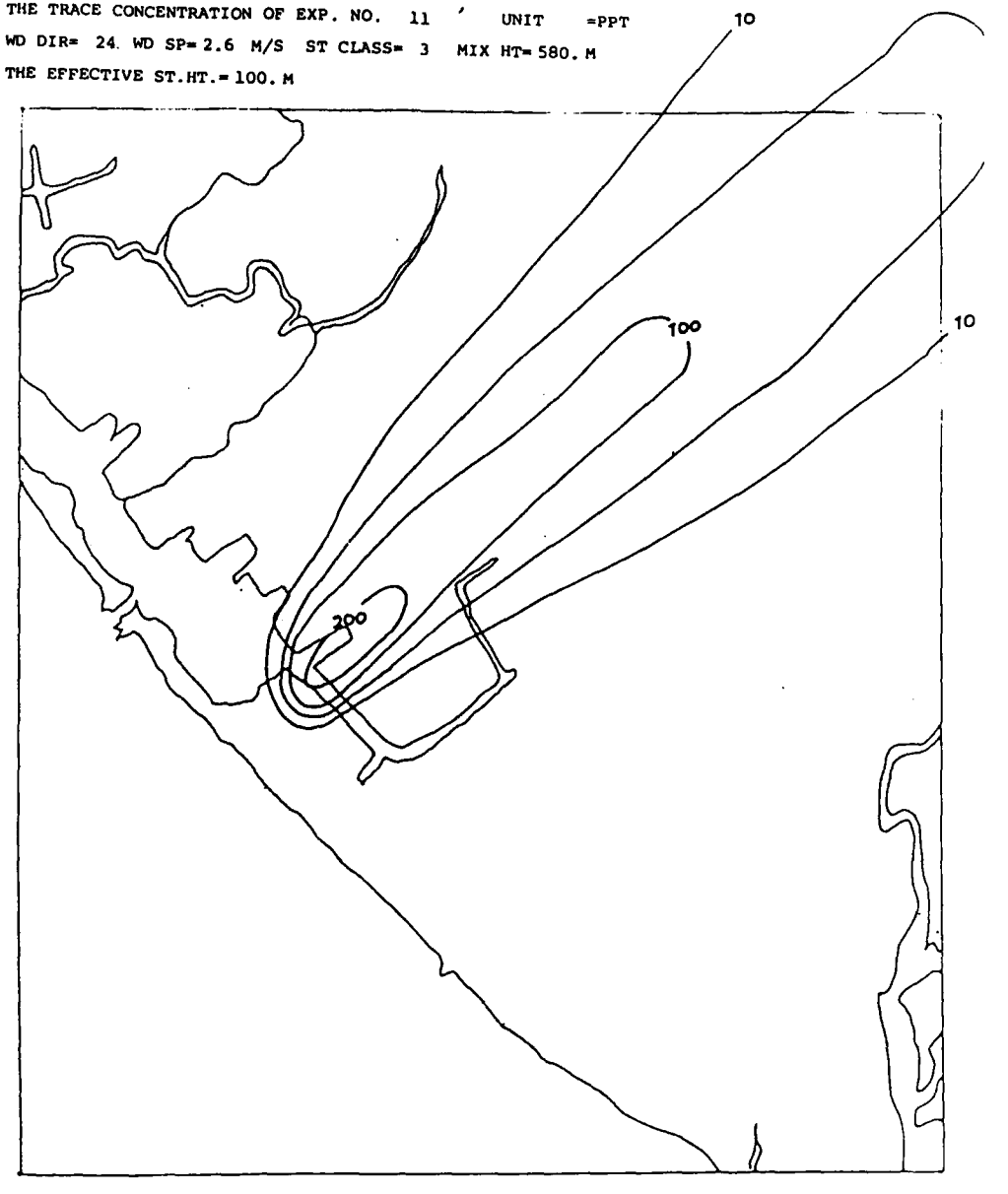

THE TRACE CONCENTRATION OF EXP. NO. 14 UNIT =PPT
WD DIR= 21 WD SP= 3.0 M/S ST CLASS= 2 MIX HT= 700.M
THE EFFECTIVE ST.HT.= 487.M

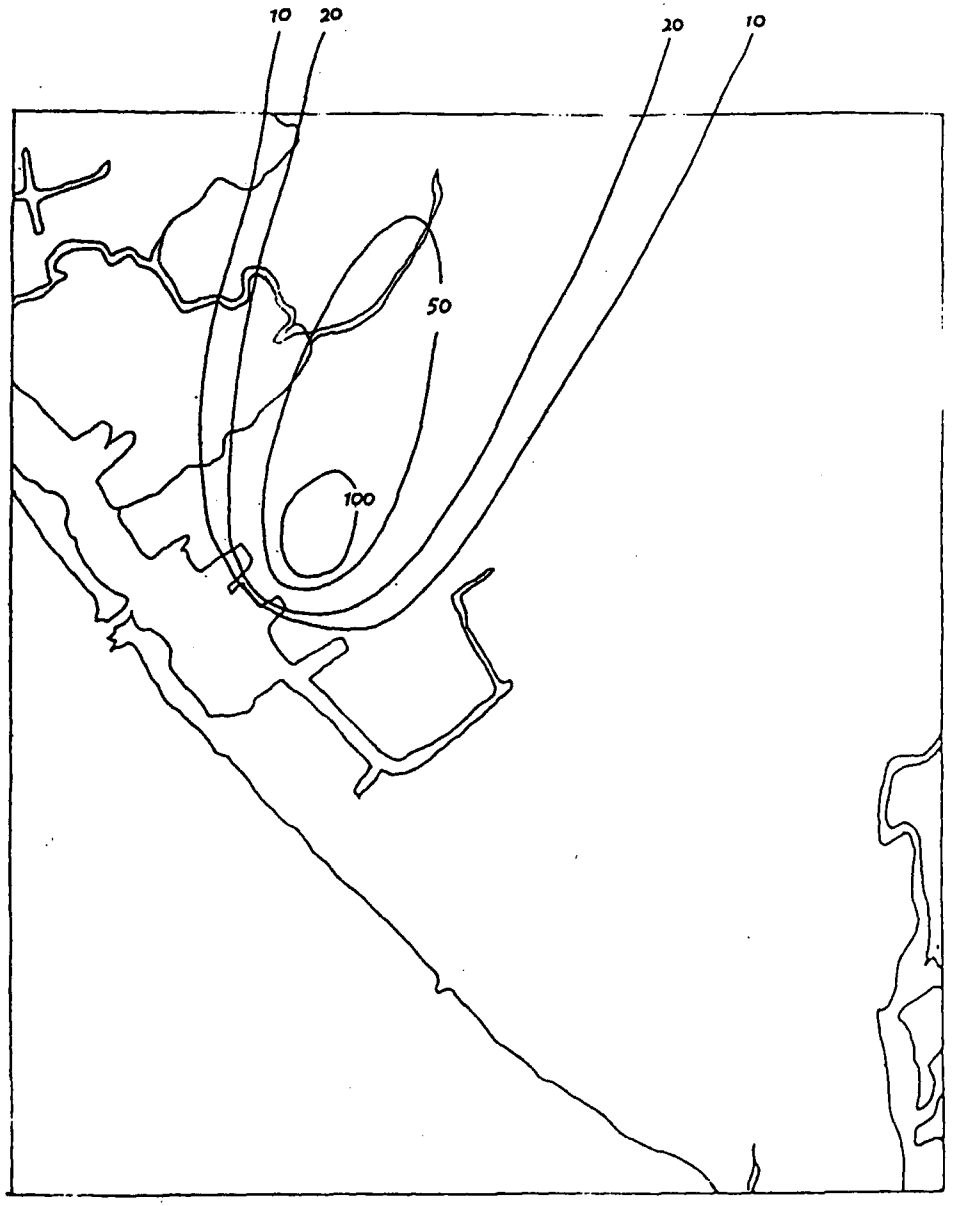

THE TRACE CONCENTRATION OF EXP. NO. 13 UNIT =PPT
WD DIR= 18 WD SP= 3.3 M/S ST CLASS= 2 MIX HT= 700.M
THE EFFECTIVE ST.HT.= 100.M

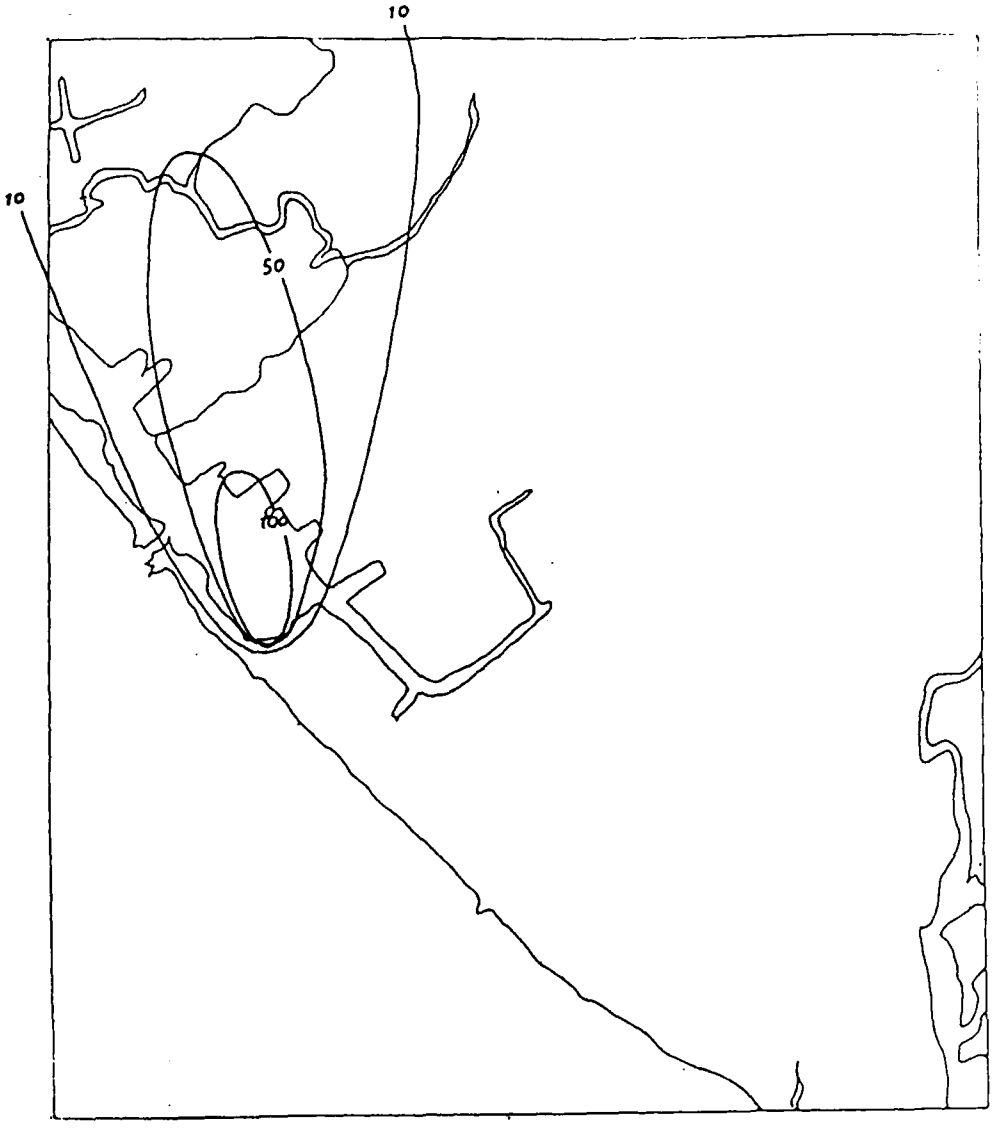

THE TRACE CONCENTRATION OF EXP. NO. 16 UNIT =PPT
WD DIR= 28 WD SP= 3.9 M/S ST CLASS= 3 MIX HT= 650.M
THE EFFECTIVE ST.HT.= 372.M

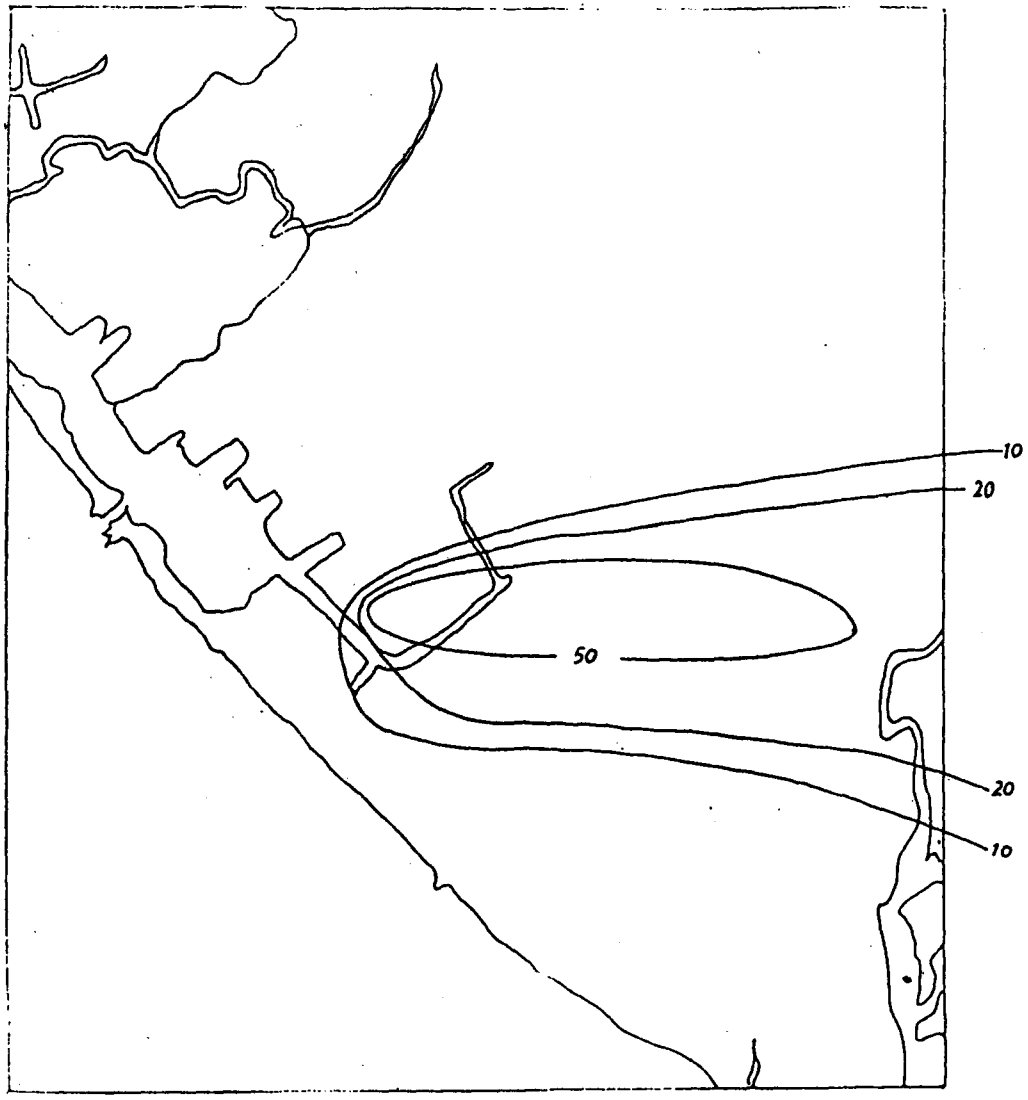

THE TRACE CONCENTRATION OF EXP. NO. 15 UNIT =PPT
WD DIR= 28 WD SP= 4.6 M/S ST CLASS= 3 MIX HT= 800.M
THE EFFECTIVE ST.HT.= 100.M

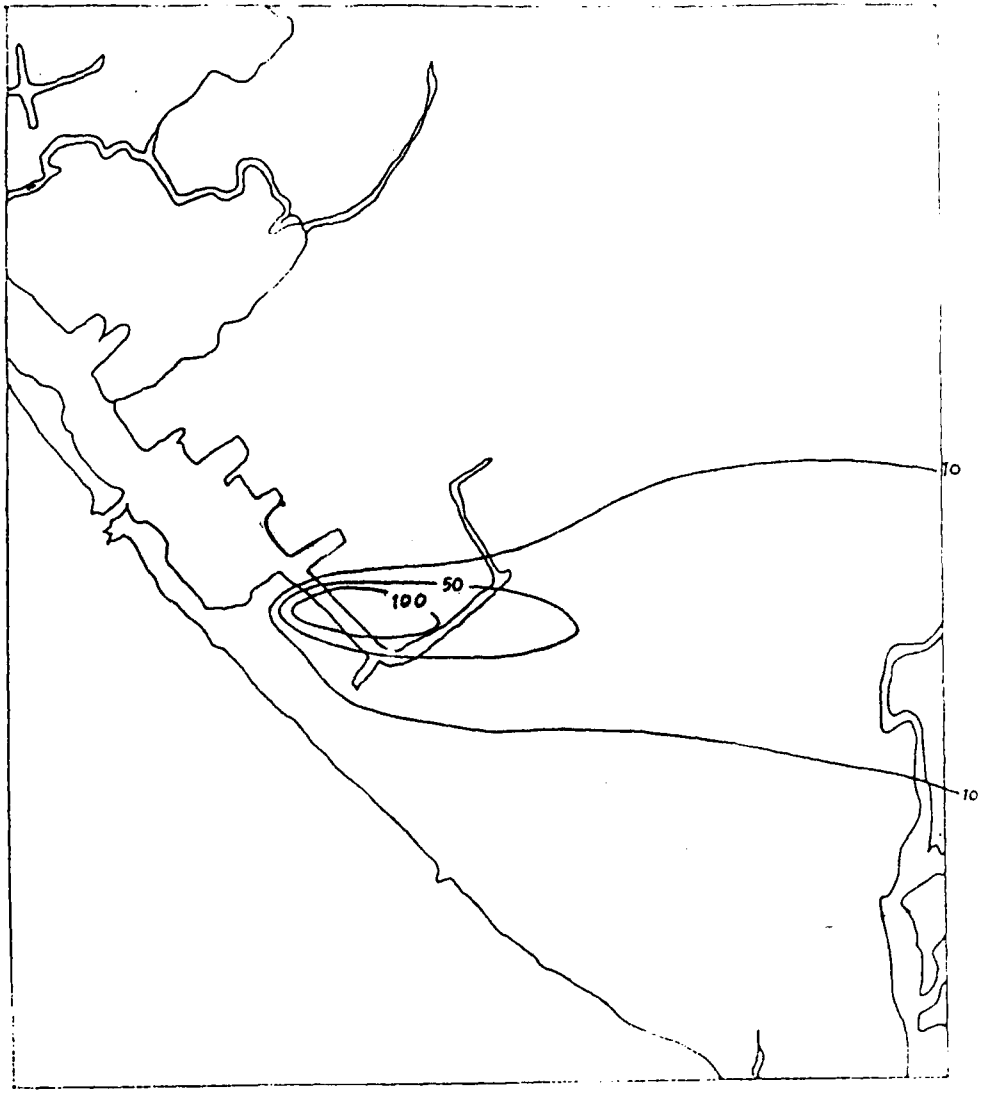

THE TRACE CONCENTRATION OF EXP. NO. 18 UNIT =PPT
WD DIR= 28 WD SP= 1.4 M/S ST CLASS= 3 MIX HT= 350.M
THE EFFECTIVE ST.HT.= 100.M

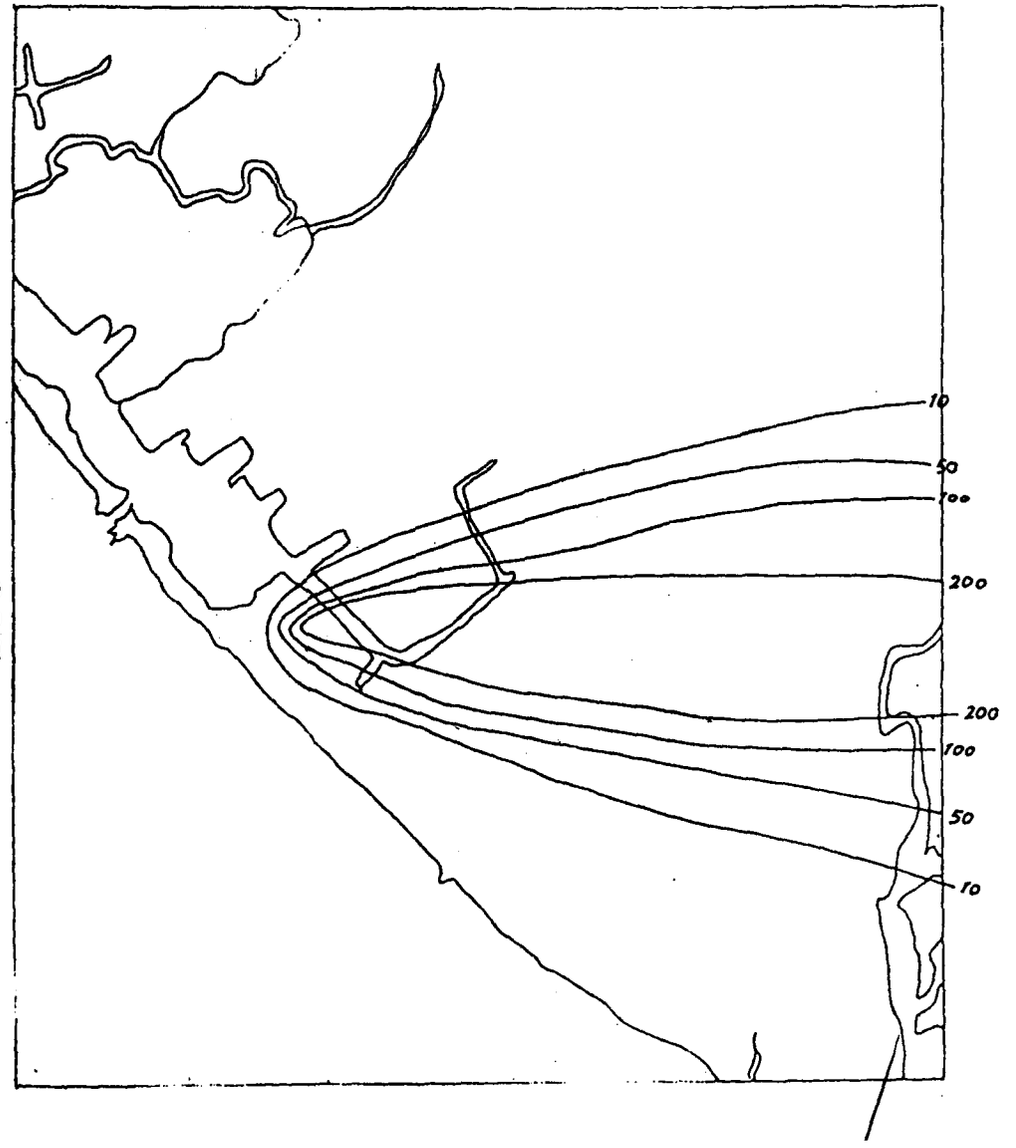

THE TRACE CONCENTRATION OF EXP. NO. 17 UNIT =PPT
WD DIR= 28 WD SP= 3.9 M/S ST CLASS= 3 MIX HT= 500.M
THE EFFECTIVE ST.HT.= 100.M

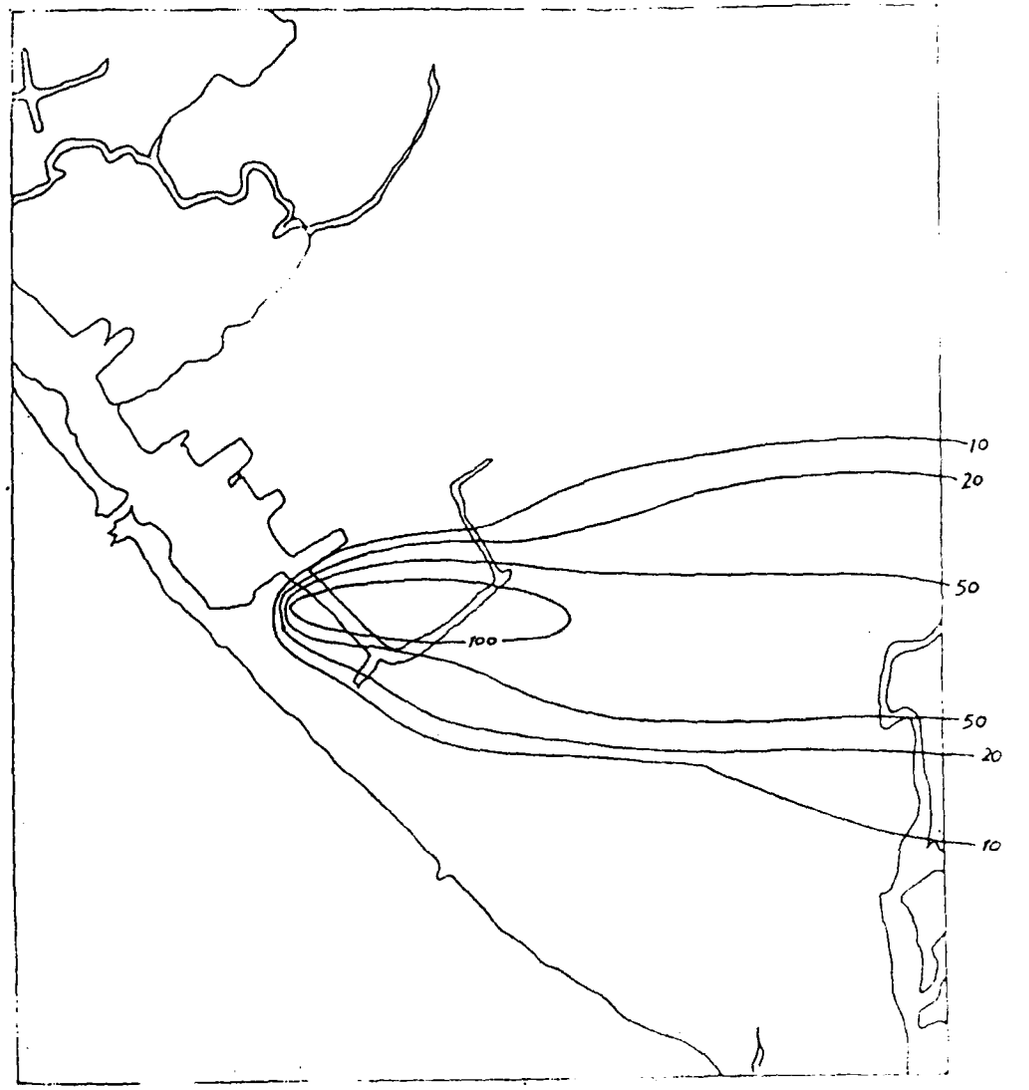

THE TRACE CONCENTRATION OF EXP. NO. 20 UNIT =PPT
WD DIR= 27 WD SP= 4.8 M/S ST CLASS= 3 MIX HT= 610.M
THE EFFECTIVE ST.HT.= 100.M

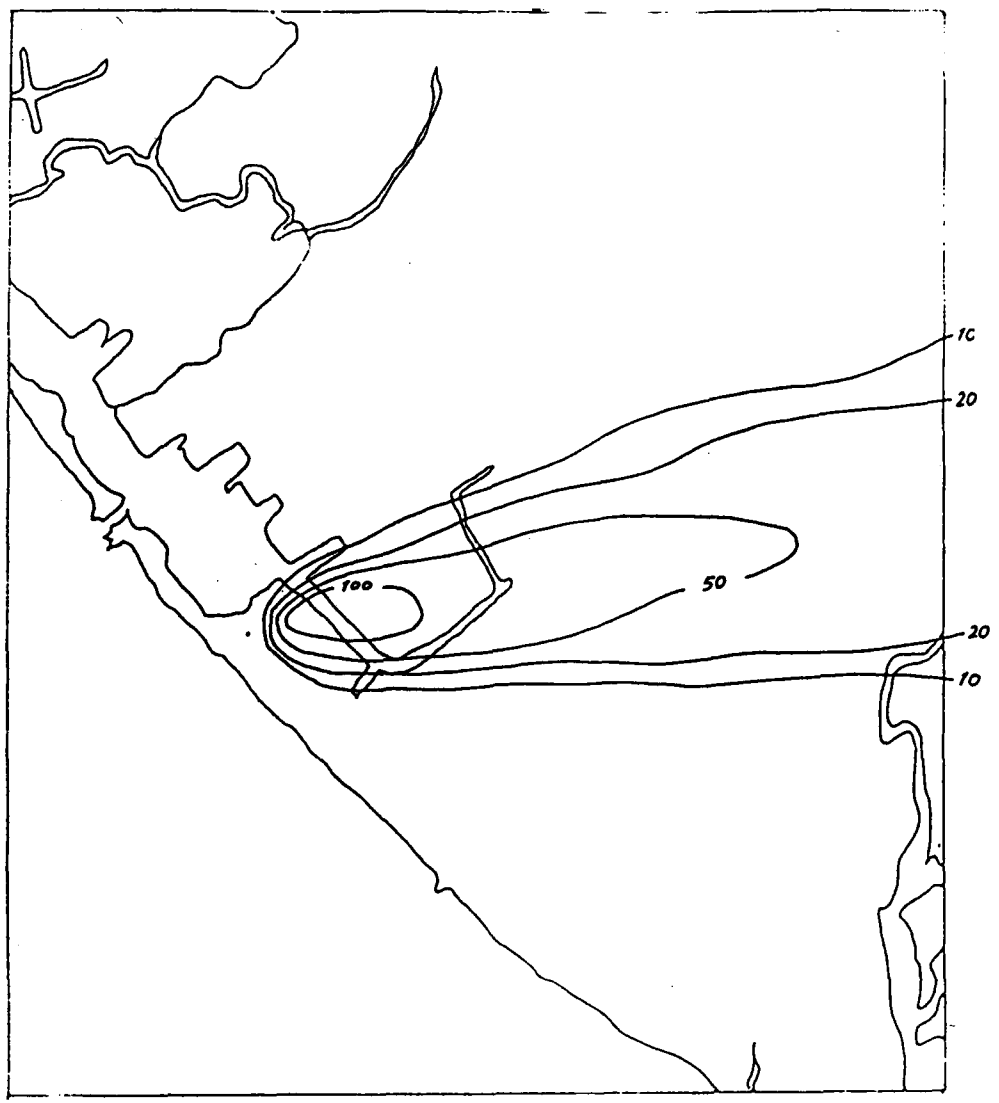

THE TRACE CONCENTRATION OF EXP. NO. 19 UNIT =PPT
WD DIR= 27 WD SP= 3.1 M/S ST CLASS= 2 MIX HT= 550.M
THE EFFECTIVE ST.HT.= 480.M

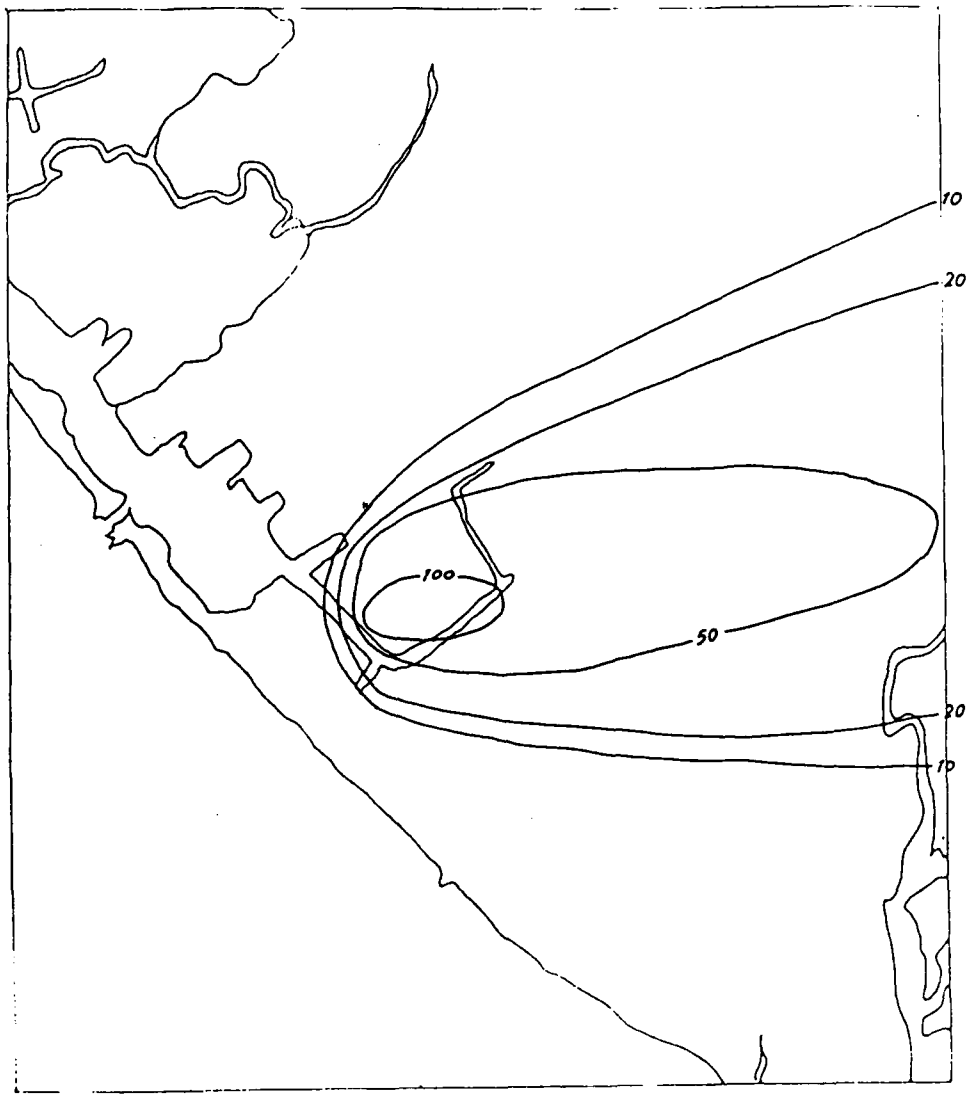

THE TRACE CONCENTRATION OF EXP. NO. 22 UNIT =PPT
WD DIR= 29 WD SP= 3.0 M/S ST CLASS= 1 MIX HT= 800.M
THE EFFECTIVE ST.HT.= 100.M

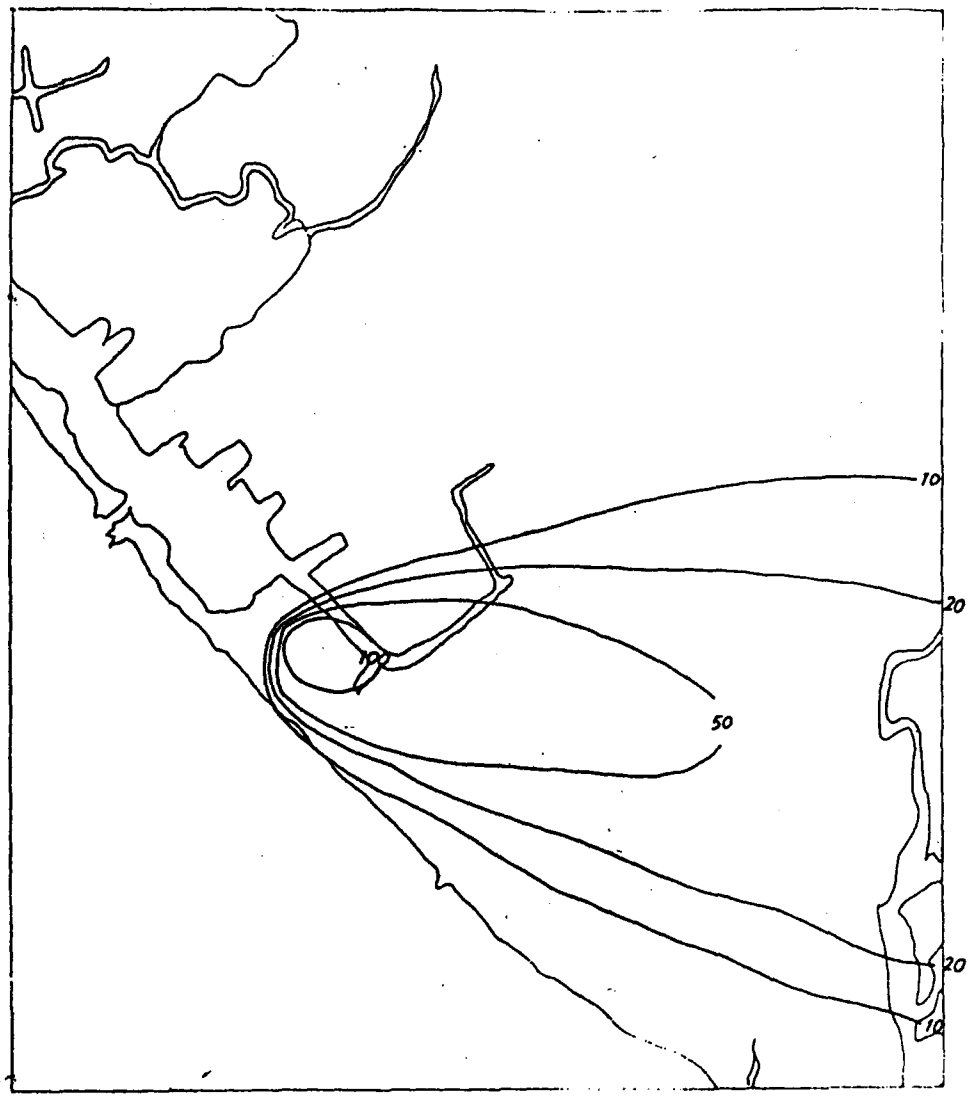

THE TRACE CONCENTRATION OF EXP. NO. 21 UNIT =PPT
WD DIR= 27 WD SP= 4.6 M/S ST CLASS= 3 MIX HT= 620.M
THE EFFECTIVE ST.HT.= 337.M

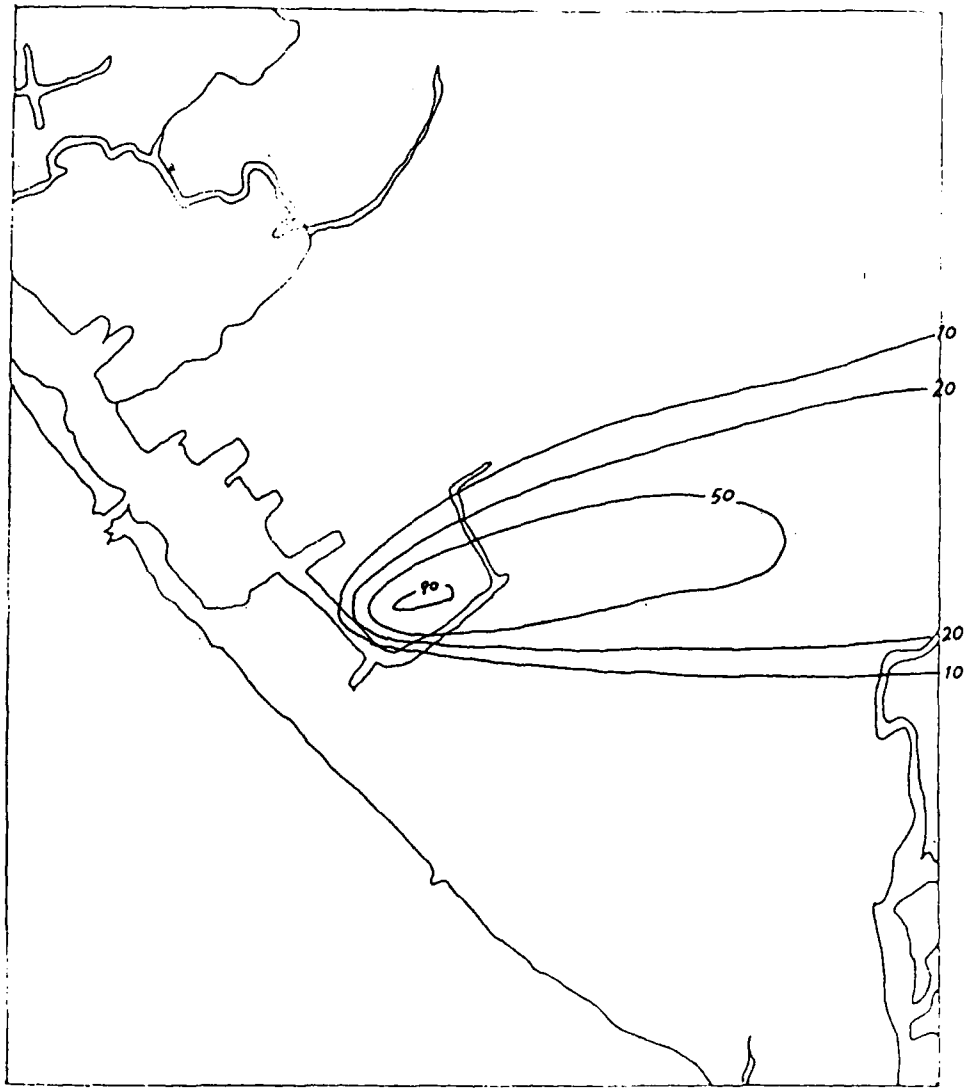

THE TRACE CONCENTRATION OF EXP. NO. 24 UNIT =PPT
WD DIR= 31 WD SP= 8.4 M/S ST CLASS= 3 MIX HT= 400.M
THE EFFECTIVE ST.HT.= 245.M

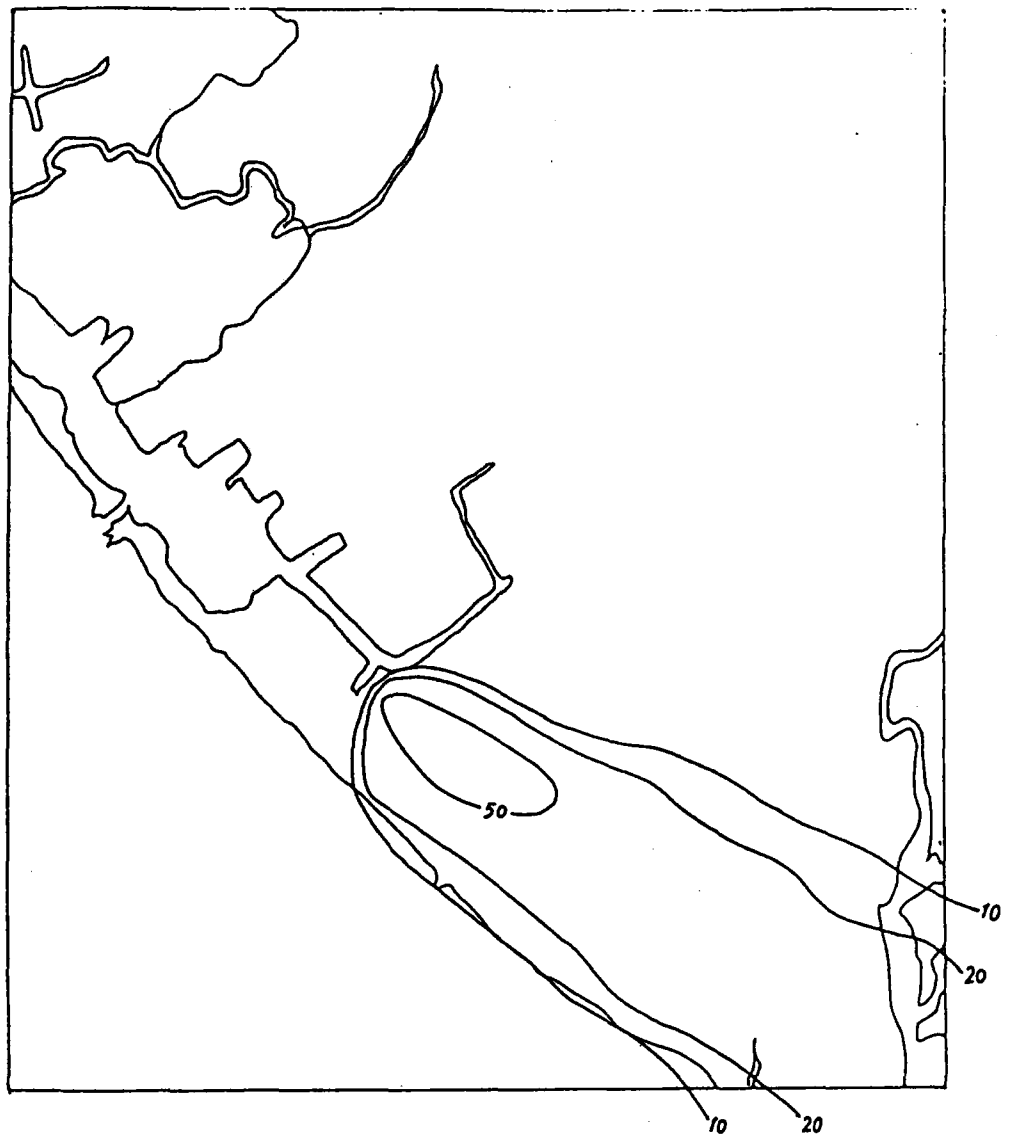

THE TRACE CONCENTRATION OF EXP. NO. 23 UNIT =PPT
WD DIR= 31 WD SP= 6.0 M/S ST CLASS= 3 MIX HT=1000.M
THE EFFECTIVE ST.HT.= 289.M

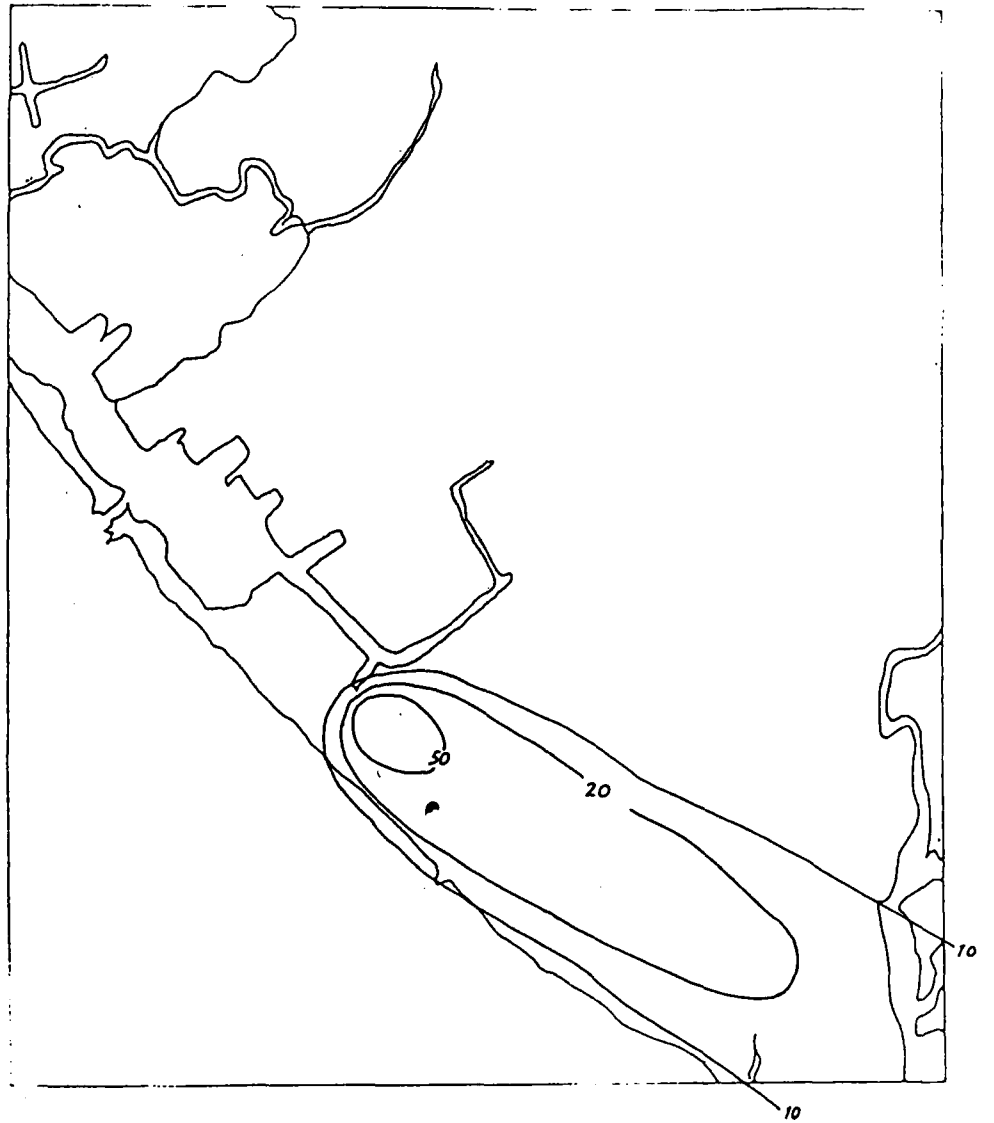

APPENDIX I GAUSSIAN- Plume multiple source air quality algorithm (RAM)

Reference: Turner, D. B., and J. H. Novak, "User's Guide for RAM." Environmental Protection Agency, Research Triangle Park, North Carolina 27711, 1978.

Abstract: RAM is a steady state Gaussian plume model for estimating concentrations of relatively stable pollutants for averaging times from an hour to a day from point and area sources. Level or gently rolling terrain is assumed. Calculations are performed for each hour. Both rural and urban versions are available.

Equations:

The area source contributions are determined using the narrow-plume hypothesis similar to applications by Gifford and Hanna[7] Contribution. Contribution from a single upwind area source

$$x_A = \frac{q}{u} \int_{x_1}^{x_2} f \, dx \qquad \text{integral evaluated numerically}$$

x_1, x_2 = points of intersection of ray from receptor through area source in question

q = emission rate per unit area of the area source ($g/s\text{-}m^2$)

u = mean wind speed (m/s)

For stable conditions: $f = \frac{1}{\sqrt{2\pi}\,\sigma_z} g_2$

$$x_{point} = \frac{Q}{2\pi u\, \sigma_y\, \sigma_z} g_1 g_2$$

For neutral or unstable conditions, $\sigma_z \leq 1.6L$: $f = \frac{1}{\sqrt{2\pi}\,\sigma_z} g_3$

$$x_{point} = \frac{Q}{2\pi u\, \sigma_y\, \sigma_z} g_1 g_3$$

For neutral or unstable conditions, $\sigma_z > 1.6L$: $f = \frac{1}{L}$

$$\chi_{point} = \frac{Q}{\sqrt{2\pi}\, u L\, \sigma_y}\, g_1$$

In which

$$g_1 = \exp\left[-\frac{1}{2}\left(\frac{y}{\sigma_y}\right)^2\right]$$

$$g_2 = \exp\left[-\frac{1}{2}\left(\frac{z-H}{\sigma_z}\right)^2\right] + \exp\left[-\frac{1}{2}\left(\frac{z+H}{\sigma_z}\right)^2\right]$$

$$g_3 = \sum_{n=-\infty}^{+\infty}\left\{\exp\left[-\frac{1}{2}\left(\frac{z-H+2nL}{\sigma_z}\right)^2\right] + \exp\left[-\frac{1}{2}\left(\frac{z+H+2nL}{\sigma_z}\right)^2\right]\right\}$$

a. Source-Receptor Relationship

Arbitrary location for point sources
Receptors may be
(1) arbitrarily located
(2) internally located near individual source maxima
(3) on a program-generated hexagonal grid to give good coverage to a user-specified portion of the region of interest
Receptors all at same height above (or at) ground
Flat terrain assumed
Unique stack height for each point source
User may specify up to three effective release heights for area sources, each assumed appropriate for a 5 m/sec wind speed. Value used for any given area source must be one of these three
Unique separation for each source-receptor pair

b. Emission Rate

Unique, constant emission rate for each point, area source
Area source treatment-
Narrow plume approximation
Area source used as input; not subdivided into uniform elements
Arbitrary emission heights input by user

Areas must be squares; side lengths = integer multiples of a basic unit
Effective emission height = that appropriate for 5 m/s wind
Area source contributions obtained by numerical integration along upwind distance of narrow-plume approximation formulae for contribution from area source with given effective release height

c. Chemical Composition

Treats a single inert pollutant

d. Plume Behavior

Briggs[8,9,10] plume rise formulas
Does not treat fumigations or downwash
If plume height exceeds mixing height, ground level concentration is assumed zero

e. Horizontal Wind Field

Uses user-supplied hourly wind speeds
Uses user-supplied hourly wind directions (nearest 10°), internally modified by addition of a random integer value between -4° and +5°
Wind speeds corrected for release height based on power law variation, different exponents for different stability classes, reference height = 10 meters
Constant, uniform (steady-state) wind assumed within each hour

f. Vertical Wind Speed

Assumed equal to zero.

g. Horizontal Dispersion

Semi-empirical/Gaussian plume
Hourly stability class determined internally by Turner[2] procedure, six classes used
Dispersion coefficients from McElroy and Pooler[3] (urban) or Turner[6] (rural). No further adjustments made for variations in surface roughness or transport time

h. Vertical Dispersion

Semi-empirical/Gaussian plume
Hourly stability class determined internally
Dispersion coefficients from McElroy and Pooler[3] (urban) or Turner[5] (rural). No further adjustments made for variations in surface roughness

i. Chemistry/Reaction Mechanism

Exponential decay, user-input half-life

j. Physical Removal

Exponential decay, user-input half-life

k. Background

Not treated

l. Boundary Conditions

Lower boundary: perfect reflection
Upper boundary: perfect reflection
Neutral and unstable conditions
  Multiple reflections numerically accounted for by summation of series until σ_z = 1.6 times mixing height
  Uniform mixing assumed in vertical thereafter
Stable conditions: there is no upper boundary
Mixing height for a given hour is obtained by suitable interpolation using data from soundings taken twice a day
Interpolation technique dependent on mode of operation (urban or rural) and calculated stability class for the hour in question as well as the stability class for the hour just preceding sunrise

m. Emission and Meteorological Correlation

User supplies hourly values of wind speed, wind direction, mixing height and other meteorological variables required for determination of stability class and plume rise

n. Validation/Calibration

No calibration option provided
Limited experience with validation or comparison with observed data

o. Output

Hourly and average (up to 24 hours) concentrations at each receptor
Limited individual source contribution list
Cumulative frequency distribution based on 24-hour averages and up to 1 year of data at a limited number of receptors

p. Computer Requirements

Digital computer required
Core requirements are moderate

q. Limitations

Flat or gently rolling terrain